LMSC-HSV TR F312203

Phase I

Definition of the

Laser Atmospheric Wind Sounder (LAWS)

Contract NAS8-37590

DR-19 Final Study Report

Volume II

Final Report

APRIL 1990

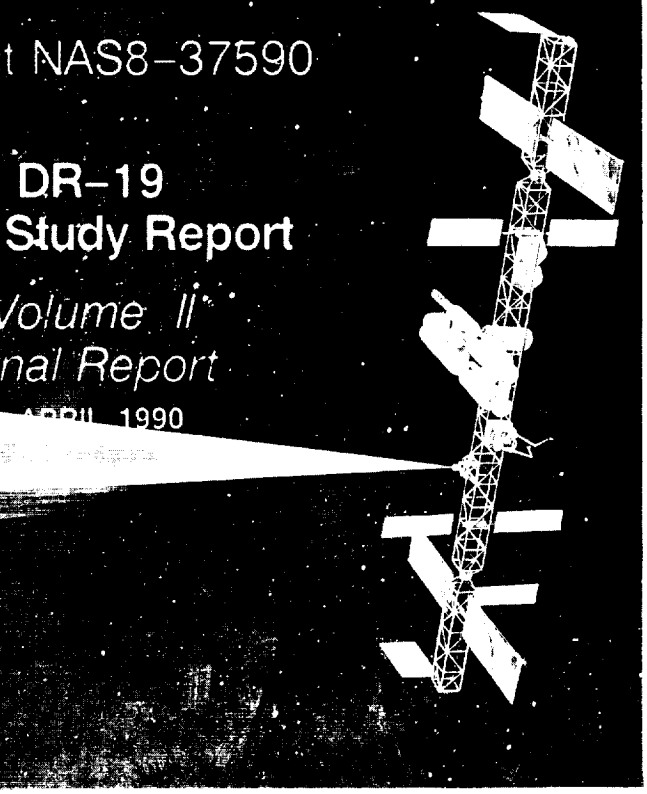

Prepared for:

GEORGE C. MARSHALL SPACE FLIGHT CENTER
MARSHALL SPACE FLIGHT CENTER, AL 35812

DR-19

Final Study Report (Phase I)

for

Laser Atmospheric Wind Sounder (LAWS)

Volume II Final Report

Submitted in Partial Fulfillment of

Contract NAS8-37590

April 1990

Prepared for:

GEORGE C. MARSHALL SPACE FLIGHT CENTER
MARSHALL SPACE FLIGHT CENTER, AL 35812

Submitted by:

Lockheed
Missiles & Space Company, Inc.
4800 Bradford Blvd., Huntsville, AL 35807

W.E. Jones, Project Manager
LAWS Project Office
Lockheed - Huntsville

FOREWORD

This document presents the final results of the 12-month Phase I effort for the Laser Atmospheric Wind Sounder (LAWS). This work was performed for the Marshall Space Flight Center (MSFC) by Lockheed Missiles & Space Company, Inc., Huntsville, Alabama, under Contract NAS8-37590. The study was conducted under the direction of R.G. Beranek, NASA Program Manager, PS02. The period of performance was 24 March 1989 to 23 March 1990.

The complete Phase I final reports consist of the following three volumes:

Volume I	Executive Summary
Volume II	Final Report
Volume III	Program Cost Estimates.

Subcontractors contributing to this effort are Avco Research Laboratory, Inc., GEC Avionics Ltd., and Itek Optical Systems.

TABLE OF CONTENTS

TABLE OF CONTENTS (Concluded)

LIST OF ILLUSTRATIONS

LIST OF ILLUSTRATIONS (Continued)

LIST OF ILLUSTRATIONS (Continued)

LIST OF ILLUSTRATIONS (Continued)

LIST OF ILLUSTRATIONS (Continued)

LIST OF ILLUSTRATIONS (Concluded)

LIST OF TABLES

LIST OF TABLES (Concluded)

LIST OF ACRONYMS AND ABBREVIATIONS

A/D	Analog-to-digital
ARL	Avco Research Laboratory
ARTS	Automated Requirements Traceability System
ASE	Airborne Support Equipment
ATP	Authority to proceed
BPLO	Backward-propagated local oscillator
BW	Bandwidth
CDR	Critical Design Review
CEI	Contract End Item
CER	Cost Estimating Relationship
CI	Configuration Inspection
CMT	Cadmium Mercury Telluride
CW	Continuous wave
DCR	Design Certification Review
DR	Data Requirements
EMC	Electromagnetic compatibility
EMI	Electromagnetic interference
E/N	Electric field/number density
EOS	Earth Observing System
EVA	Extravehicular activity
FFT	Fast Fourier transform
FRR	Flight Readiness Review
GPS	Global Positioning System
GRM	Gaussian reflectivity mirror
GSE	Ground support equipment

LIST OF ACRONYMS AND ABBREVIATIONS (Continued)

HST	Hubble Space Telescope
IRAD	Independent Research & Development
JPOP	Japanese Polar Orbiting Platform
LAWS	Laser Atmospheric Wind Sounder
LIMP	Laser induced medium perturbation
LIS	LAWS Integrated System
LMSC	Lockheed Missiles & Space Company, Inc.
LO	Local oscillator
LRR	Launch Readiness Review
MO	Master Ooscillator
MOPA	Master oscillator/power amplifier
MSFC	Marshall Space Flight Center
MSS	Marconi Space Systems
NASA	National Aeronautics and Space Administration
NASDA	Japanese National Space Development Agency
$\mathbf{N_{eq}}$	Equivalent Fresnel
NHB	NASA Handbook
NOAA/WPL	National Oceanic and Atmospheric Administration/ Wave Propagation Laboratory
OMV	Orbital Maneuvering Review
ORR	Orbital Readiness Review
ORU	Orbital Replacement Unit
OVE	Orbital Verification and Evaluation
PDR	Preliminary Design Review
PFN	Pulse forming network
PIA	Payload interface adapter
PIE	Photo initiated impulse enhanced

LIST OF ACRONYMS AND ABBREVIATIONS (Concluded)

PO	Power oscillator
POP	Polar Orbiting Platform
POPA	Power oscillator/power amplifier
PRF	Pulse repetition frequency
PRR	Program Requirements Review
PZT	Piezo-electro translator
RFP	Request for Proposal
RSRE	Royal Signal and Radar Establishment
SIA	Surface interface adaptor
SLM	Single longitudinal mode
S/N, SNR	Signal-to-noise ratio
SOW	Satement of Work
SSE	Space support equipment
SSF	Space Station Freeedom
STI	Spectra Technology Inc.
STM	Single transverse mode
TE	Transverse excitation
TEA	Transversely excited atmospheric
TOF	Turn-over frequency
ULE	Ultra low expansion glass
URM	Uniform relfectivity mirror
V-T	Vibration-translation
WBS	Work Breakdown Structure
YAG	Ytrium aluminum garnet

INTRODUCTION

This report summarizes and documents the results of the 12-month Phase I work effort. The objective of Phase I was to establish the conceptional definition of the Laser Atmospheric Wind Sounder (LAWS) sensor system, including accommodations analyses to ensure compatibility with the Space Station Freedom (SSF) and the EOS Polar Orbiting Platform (POP). Various concepts were investigated with trade studies performed to select the configuration to be carried forward to the Phase II Preliminary Design Definition. Appendix A contains a summary of the LAWS system and subsystem trade studies that were performed leading to the baseline design configuration.

The overall objective of the LAWS Project is to define, design, and implement an operational space based facility, LAWS, for accurate measurement of earth wind profiles. The objectives of Phases I and II are to define an optimum configuration through systematic trades and analyses, to perform preliminary design of this configuration, and to prepare a systems plan for Phase C/D and to define those tasks required to achieve Phase C/D objectives.

Phase I addressed three major areas: (1) requirements definition; (2) instrument concepts and configurations; and (3) performance analysis. For the LAWS instrument concepts and configurations, the issues which press the technological state of the art are reliable detector lifetime and laser performance and lifetime. Lag angle compensation, pointing accuracy, satellite navigation, and telescope design are significant technical issues, but they are considered to be currently state of the art. The primary issues for performance analysis concern interaction with the atmosphere in terms of backscatter and attenuation, wind variance, and cloud blockage. The Phase I tasks were formulated to address these significant technical issues and demonstrate the technical feasibility of the LAWS concept. Primary emphasis was placed on analysis/trade and identification of candidate concepts. Promising configurations were evaluated for performance, sensitivities, risks, and budgetary costs.

Lockheed's baseline LAWS configuration is presented. This system configuration is comprised of six basic subsystems: optics, laser, receiver/processor, command/control/communication, electrical power and mechanical. Our baseline configuration meets all resource budget requirements for the POP and SSF as stated in the SOW Guidelines and Assumptions. Both expendable launch vehicles, such as the Japanese H-II and/or Titan, and the Space Shuttle (STS) can be used as payload carriers. LAWS orbital servicing and maintenance activities can be accomplished by incorporating design features developed

and verified on the Lockheed Hubble Space Telescope vehicle, the first satellite designed for on-orbit maintenance.

Lockheed has two laser contractors on our LAWS team, Avco Research Laboratory and GEC Avionics Limited. Either candidate laser concept can be integrated into our baseline design with minimum system impact.

SECTION 1. BACKGROUND LITERATURE REVIEW

A literature review was conducted of previous studies related to space-based operations of a Doppler lidar in order to determine applicability to the Laser Atmospheric Wind Sounder (LAWS). At the Baseline Requirements Review, we presented a summary of previous studies which are applicable to the Space Station Freedom (SSF) and/or Earth Observation System (EOS) Polar Orbiting Platform (POP) LAWS operations. Areas requiring further examination were identified.

A summary of this literature review is presented in the following figures. Figure 1-1 summarizes the review for all LAWS subsystems, and Figures 1-2 through 1-7 summarize the review for the individual subsystems. Figure 1-8 summarizes the review for systems analysis and performance modeling. In each case, a matrix is developed which identifies previous studies across the top and categories of investigation in the left column. The cross reference indicates whether or not the studies are applicable to the SSF, POP, or both. As indicated, we found no areas in which the literature could be applied directly to LAWS without re-examination.

LEGEND

APPLICABLE TO POP	P
APPLICABLE TO SS	S
APPLICABLE TO BOTH	B

CATEGORIES	NOAA WPL-37 1978	NOAA WPL-63 1980	LMSC WIND SAT 1981	MSFC FEASIBILITY 1982	RCA FEASIBILITY 1983	BAKER/COURAN WORKSHOP 1985	BAKER/CURRAN PROCEED. 1985	MSFC SCALE 1987	CURRAN LAWS 1987	POLAR PLATFORM ACCOM. 1988	SS ATTACHED PAYLOAD 1988	LAWS SS ACCOMODATIONS 1988
LASER SUBSYSTEM	B	B	B	B	B			B	B			
RECEIVER-PROCESSOR SUBSYSTEM	B	B	B	B	B			B	B			S
OPTICAL SUBSYSTEM	B	B	B	B	B			B	B			
MECHANICAL & SUPPORT SUBSYSTEM			B	B	B			B	B	P	S	S
ELECT. POWER DIST. SUBSYSTEM			B	B	B			B		P	S	S
COMMAND, CONTROL, COMM. SUBSYSTEM			B	B	B			B	B	P	S	S
SYSTEMS ANALYSIS/PERFORMANCE	B	B	B	B	B	B	B	B	B			S

PREVIOUS STUDY

NOTE: ALL IDENTIFIED AREAS REQUIRE RE-EXAMINATION FOR FURTHER STUDY

Figure 1-1. Literature Review Summary for all LAWS Subsystems

LEGEND

APPLICABLE TO POP	P
APPLICABLE TO SS	S
APPLICABLE TO BOTH	B

CATEGORIES	NOAA WPL-37 1978	NOAA WPL-63 1980	LMSC WIND SAT 1981	MSFC FEASIBILITY 1982	RCA FEASIBILITY 1983	BAKER/COURAN WORKSHOP 1985	BAKER/CURRAN PROCEED. 1985	MSFC SCALE 1987	CURRAN LAWS 1987	POLAR PLATFORM ACCOM. 1988	SS ATTACHED PAYLOAD 1988	LAWS SS ACCOMODATIONS 1988
LASER SUBSYSTEM	B	B	B	B	B			B	B			
OPTICAL CAVITY ASSEMBLY	B	B	B	B	B			B	B			
POWER SUPPLY ASSEMBLY	B	B	B		B			B	B			
HIGH VOLTAGE PULSE FORMING NETWORK			B		B			B				
ELECTRODE ASSEMBLY			B		B			B				
GAS CIRCULATION ASSEMBLY	B	B	B	B	B			B	B			
GAS MAKEUP ASSEMBLY			B	B	B			B	B			
LASER STABILITY CONTROL NETWORK			B		B			B				

PREVIOUS STUDY

Figure 1-2. Literature Review Summary for LAWS Laser Subsystem

LEGEND

APPLICABLE TO POP	P
APPLICABLE TO SS	S
APPLICABLE TO BOTH	B

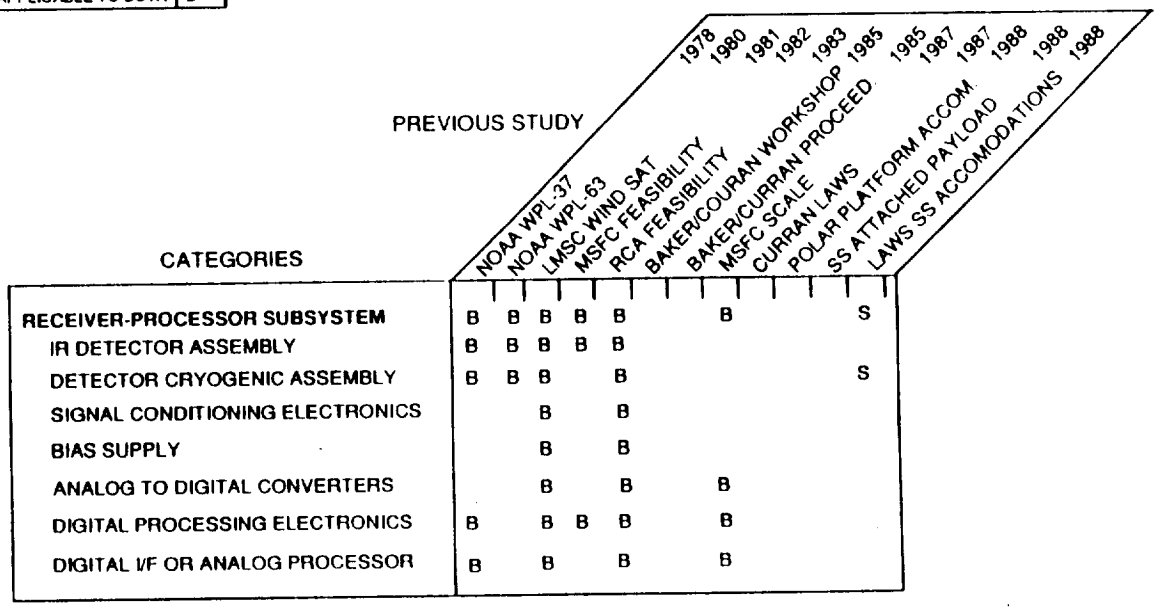

Figure 1-3. Literature Review Summary for LAWS Receiver-Processor Subsystem

LEGEND

APPLICABLE TO POP	P
APPLICABLE TO SS	S
APPLICABLE TO BOTH	B

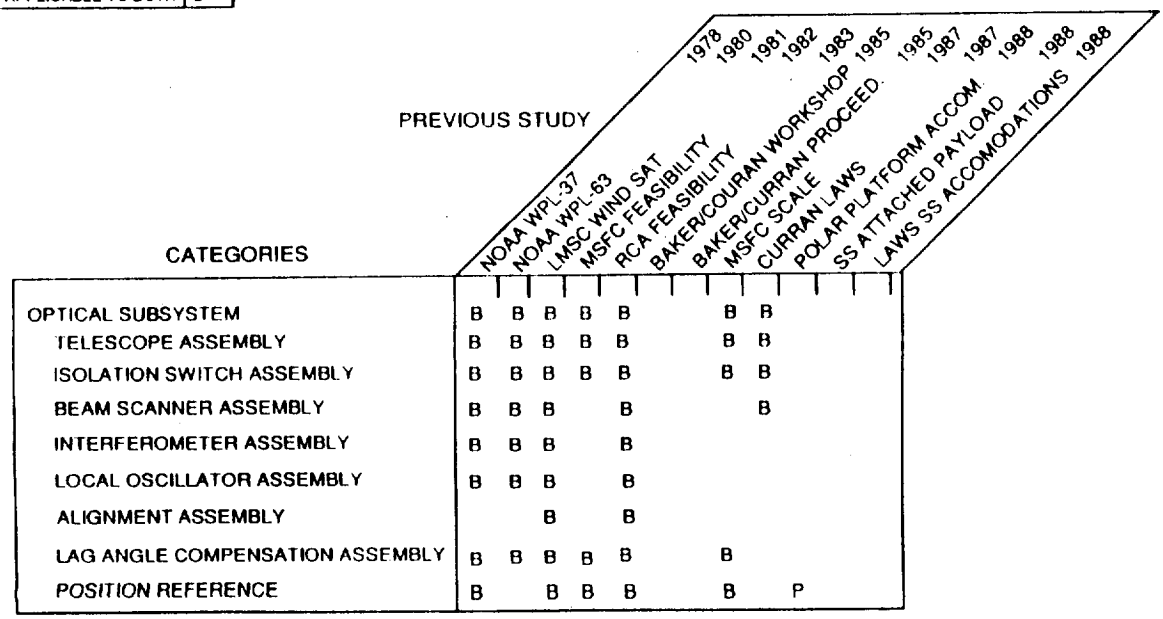

Figure 1-4. Literature Review Summary for LAWS Optical Subsystem

LEGEND

APPLICABLE TO POP	P
APPLICABLE TO SS	S
APPLICABLE TO BOTH	B

CATEGORIES	NOAA WPL-37 1978	NOAA WPL-63 1980	LMSC WIND SAT 1981	MSFC FEASIBILITY 1982	RCA FEASIBILITY 1983	BAKER/COURAN WORKSHOP 1985	BAKER/CURRAN PROCEED. 1985	MSFC SCALE 1987	CURRAN LAWS 1987	POLAR PLATFORM ACCOM 1988	SS ATTACHED PAYLOAD 1988	LAWS SS ACCOMODATIONS 1988
	PREVIOUS STUDY											
MECHANICAL & SUPPORT SUBSYSTEM	B	B	B			B	B	P	S	S		
PLATFORM INTERFACE STRUCTURES		B				B	B	P	S	S		
SUPPORT STRUCTURES	B	B	B			B	B	P	S	S		
GIMBAL ASSEMBLY	B	B	B				B	P	S	S		
THERMAL CONTROL SYSTEM	B	B	B			B	B	P	S	S		
VIBRATION DAMPING/ISOLATION SYSTEM	B		B					P	S	S		
ORBITAL REPLACEMENT UNITS (ORUs)								p	S	S		

Figure 1-5. Literature Review Summary for LAWS Mechanical and Support Subsystem

LEGEND

APPLICABLE TO POP	P
APPLICABLE TO SS	S
APPLICABLE TO BOTH	B

CATEGORIES	NOAA WPL-37 1978	NOAA WPL-63 1980	LMSC WIND SAT 1981	MSFC FEASIBILITY 1982	RCA FEASIBILITY 1983	BAKER/COURAN WORKSHOP 1985	BAKER/CURRAN PROCEED. 1985	MSFC SCALE 1987	CURRAN LAWS 1987	POLAR PLATFORM ACCOM 1988	SS ATTACHED PAYLOAD 1988	LAWS SS ACCOMODATIONS 1988
	PREVIOUS STUDY											
ELECTRICAL POWER DISTRIBUTION SUBSYS	B	B	B			B		p	S	S		
PLATFORM POWER INTERFACE	B	B	B			B		p	S	S		
POWER CONDITIONING ELECTRONICS			B			B			S	S		
CIRCUIT PROTECTION										S		
DISTRIBUTION NETWORK			B			B			S			
EMERGENCY POWER OPTION			B									

Figure 1-6. Literature Review Summary for LAWS Electrical Power Distribution Subsystem

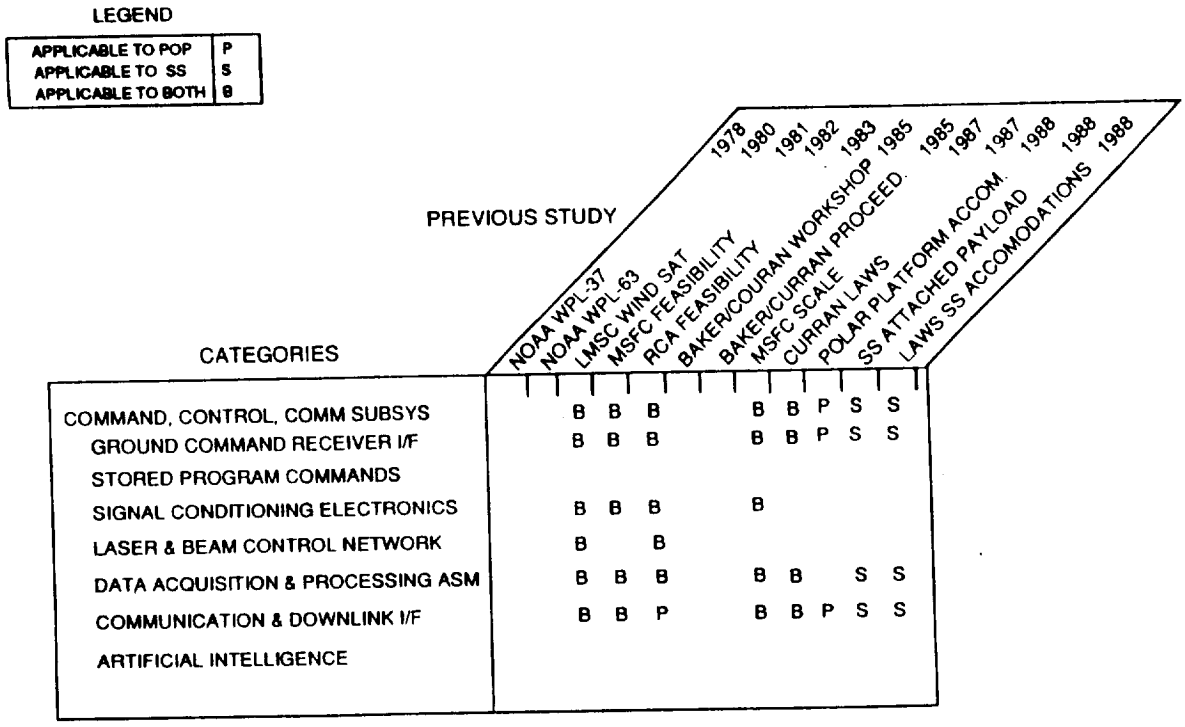

Figure 1-7. Literature Review Summary for LAWS Command/Control/Communication Subsystem

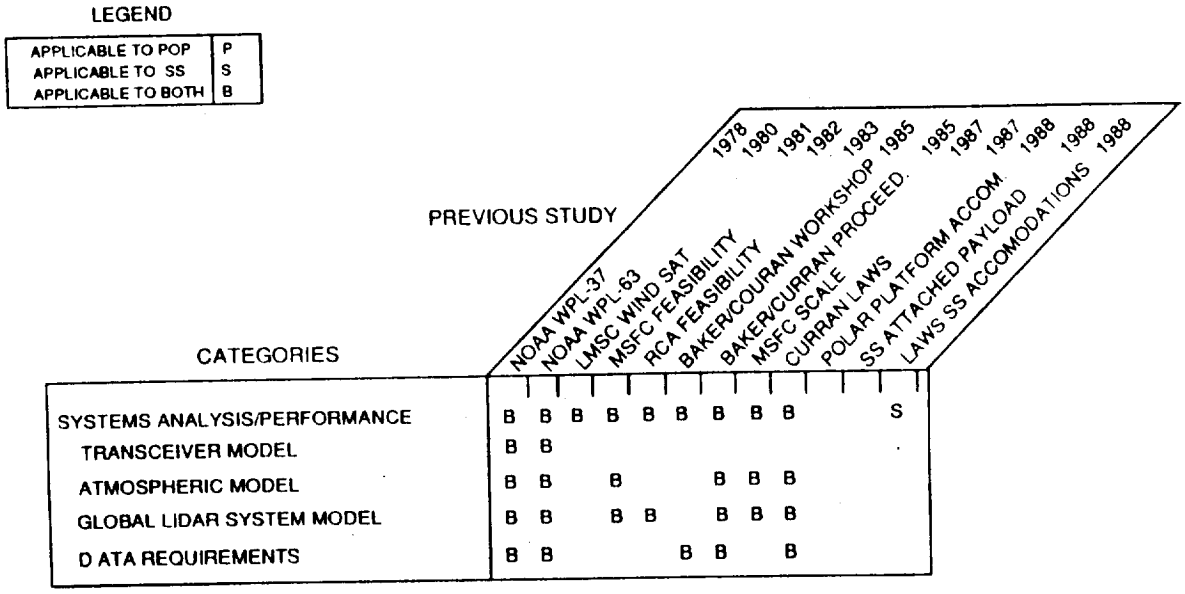

Figure 1-8. Literature Review Summary for LAWS System Analysis and Performance Modeling

SECTION 2. REQUIREMENTS DEFINITION

Operational elements of the LAWS System Conceptual Configuration are shown in Figure 2-1. It is understood that the Japanese Polar Orbiting Platform (JPOP), upon which the LAWS Instrument is to be installed, may be launched into a sun synchronous, retrograde polar orbit with an inclination angle of 98.7 deg and an altitude of 824 km above mean sea level. Under these conditions, the platform, moving in a nearly circular orbit with an eccentricity of 0.001, will have an orbital velocity of 7.45 km/sec and will make a complete orbit in 101 min. During this time, the earth will rotate approximately 25.4 deg.

Alternative orbital altitudes have also been considered as a result of trade studies conducted to evaluate the effects of reduced altitude upon such considerations as laser pulse power, signal-to-noise ratio (SNR) values, average electrical power, etc. For example, at an altitude of 705 km, analysis shows an orbital velocity of 7.51 km/sec with an orbital period of 98.9 min.

After satisfactory orbit conditions are achieved and verified, the LAWS Instrument will be unlatched from its stowed launch configuration. An initial checkout will be conducted to verify the correct response of the LAWS Instrument to ground commanded test routines. Accurate orientation of the platform and the Instrument will also be verified. Command and data transmission and reception through satellite communication relay links will also be exercised for proper operation. Ground tracking station measurements will be needed during the first few orbits for calibration of the orbital parameter values. Calibration of these parameters should be checked periodically for continued accurate operation of the LAWS Instrument. The updated values will be compared with orbital positions of the JPOP computed from data provided by the Global Positioning System (GPS). These data are required for computation of the correct earth coordinates and velocity values associated with each of these measured wind vector components.

2.1 LAWS PROJECT HIERARCHY

The LAWS Project, managed by NASA-MSFC, includes tasks associated with the development of the LAWS Flight Experiment, JPOP launch vehicle interface, JPOP interface, STS Orbiter interface, Space Station interface, and ground facilities. These tasks are shown in Figure 2-2 as Level 1 tasks. The LAWS Instrument, system support equipment, and operations are shown in this figure as System Level 2 tasks.

2.2 LAWS INSTRUMENT REQUIREMENTS

Hardware elements of the LAWS Instrument are shown in Figure 2-3. Subsystems listed as Level 3 elements under the LAWS Instrument are the Laser; Optics; Receiver/

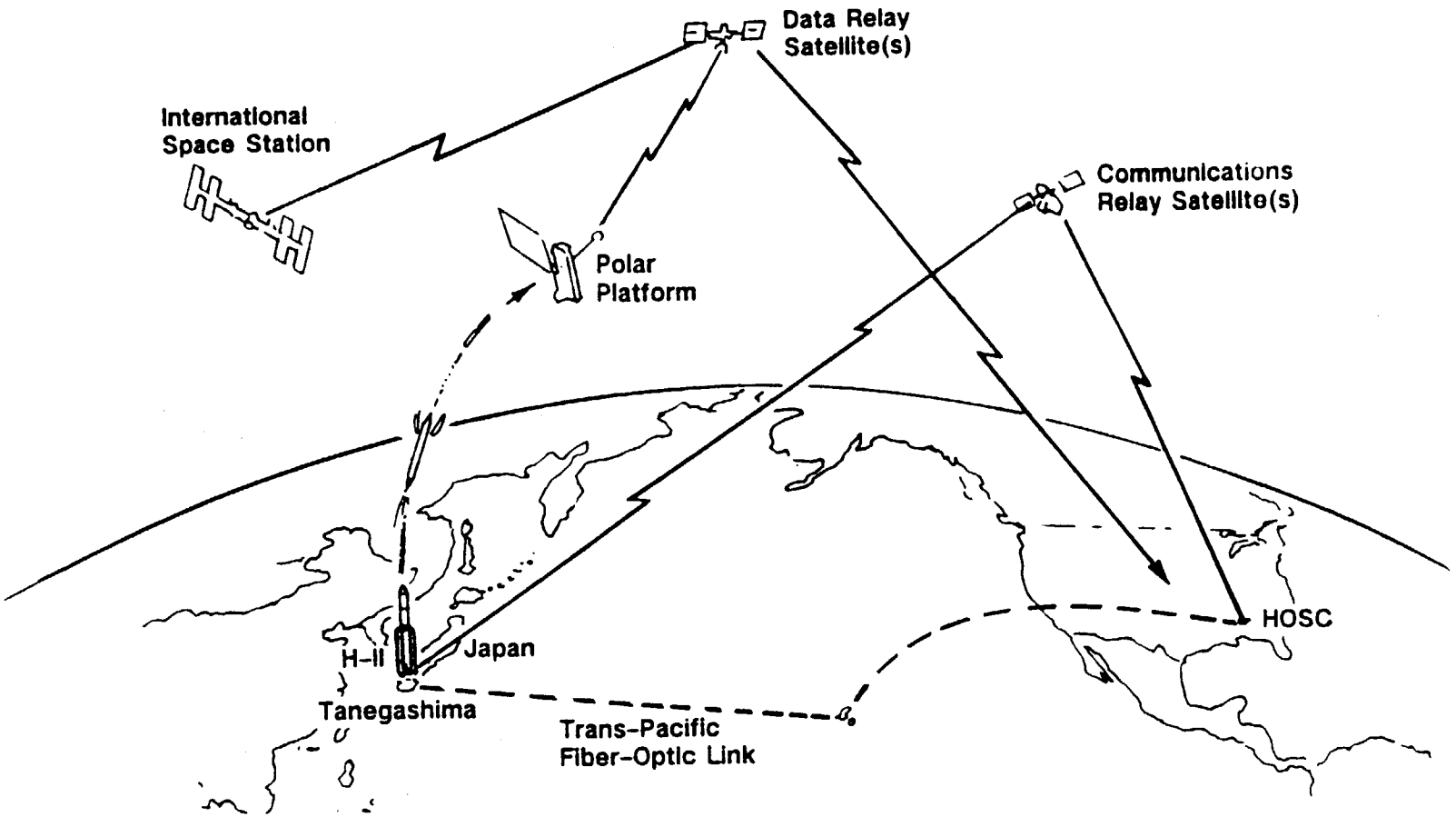

Figure 2-1. LAWS System Concept

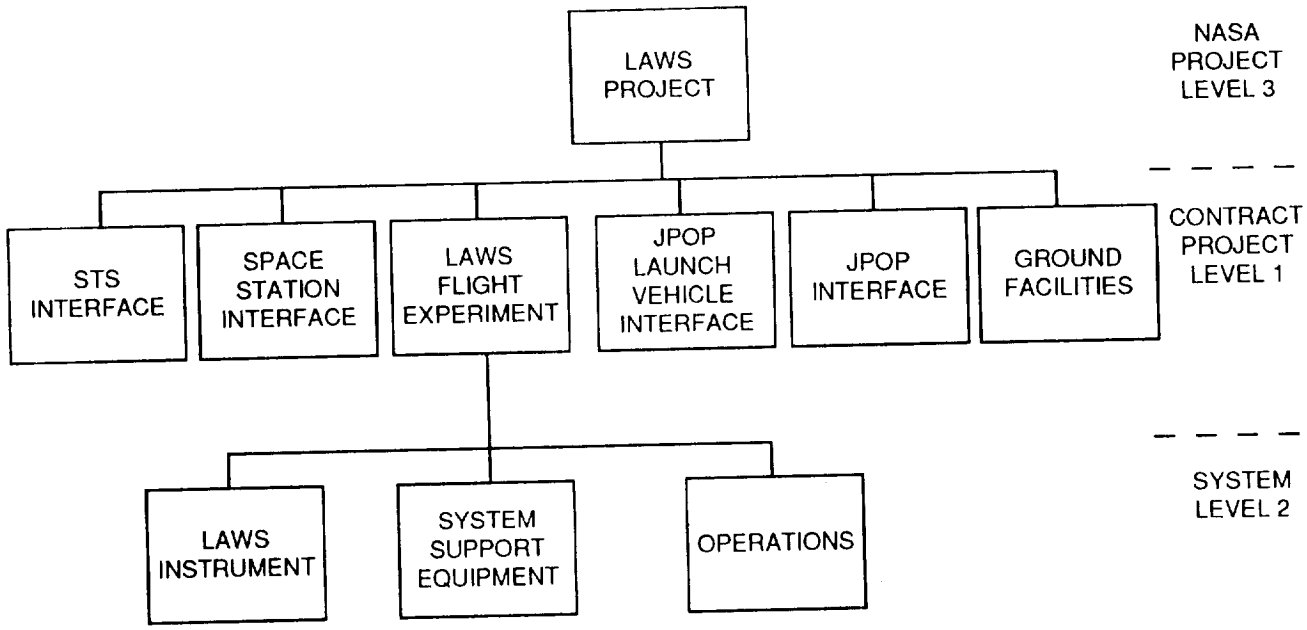

Figure 2-2. Flight Experiment Hierarchy

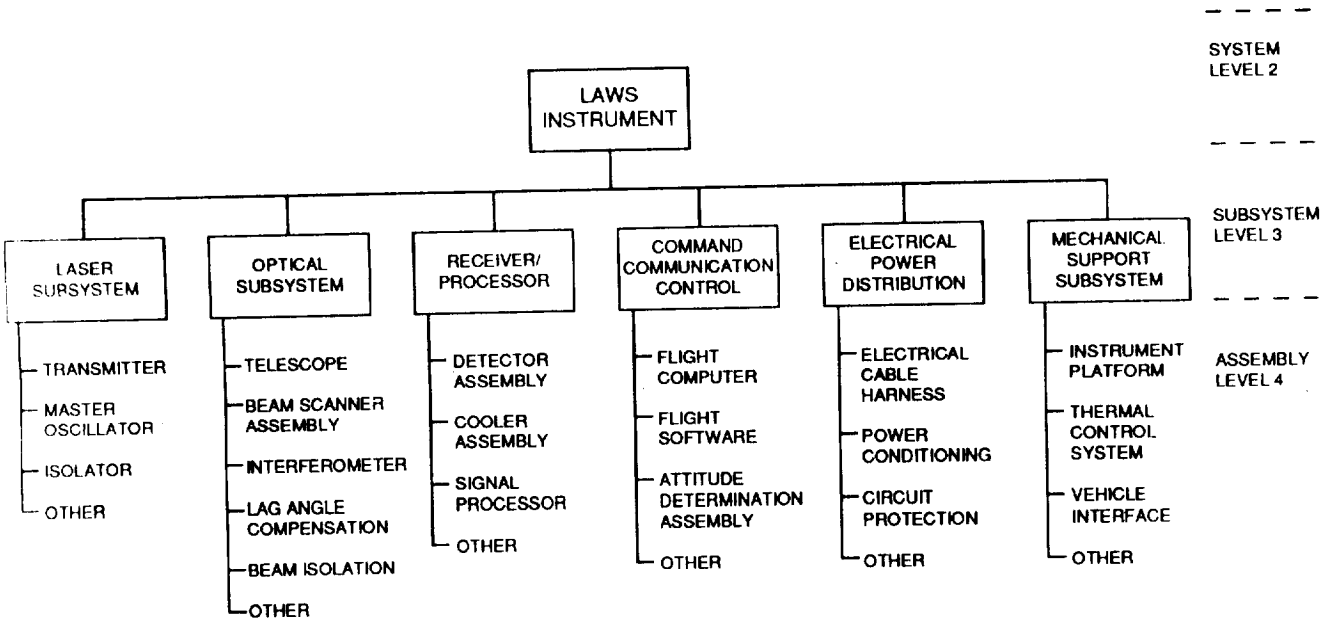

Figure 2-3. LAWS Instrument Hierarchy

Processor; Command, Control, and Communication; Mechanical Support, and Electrical Power Distribution. Requirements for the LAWS Instrument start with Level 2 system performance requirements and flow down to more detailed Level 3 and Level 4 requirements.

Each requirement, when first identified and formally stated, is given a unique identification number as shown in Table 2-1. These requirements can then be selected or sorted into any desired order by use of these numbers. Level numbers, corresponding to the levels shown in Figure 2-3, are assigned to each of the requirements. A classification is given to state the purpose of each requirement, e.g., PF for performance, SC for system configuration, SP for support, etc. Each requirement is allocated to either the entire LAWS System, or to a specific element of the system. The status indicates that a requirement is either Given, Derived, or Pending. "Given" indicates that the requirement was given in the NASA Statement of Work (SOW) or has been approved by NASA as the accepted requirement. "Derived" indicates that a lower level requirement has been established to implement a higher level approved requirement. "Pending" indicates that a recommendation has been presented to NASA to change an existing requirement based upon the results of a trade study, but that the recommended change has not yet been approved. "Pending" is also used to indicate that a trade study is currently being conducted but has not yet been completed. The notes in Table 2-1 provide additional details concerning requirements with a status of Pending. The source of each requirement, such as a SOW paragraph number, is given in the last column.

The LAWS Instrument configuration recommended by Lockheed meets all the strawman requirements set forth by NASA in the NSA8-37590 SOW. Recommended changes to a few of these requirements are shown in Figure 2-4. Based upon the results of trade studies and performance analysis, the performance enhancements provided clearly justify the changes with little impact on cost, weight, power, and reliability. The circled letters by the Lockheed LAWS System requirements identify the recommended changes. The performance requirements affected by these changes are identified in the last two columns of Figure 2-4.

These requirements are entered and maintained in the LAWS Automated Requirements Traceability System (ARTS) data base. This data base is set up to accept new requirements for the LAWS Instrument as they are developed and will allow different types of specifications to be assembled from the requirements contained. Requirements for system support equipment and for operations will also be developed, expanded, and entered into the ARTS data base.

Table 2-1 LAWS System Requirements (1 of 4)

Req. Ident.	Level	Class	Requirements	Alloc	Status	Source
LAWS0010	2	PF	The LAWS Instrument, operating from earth orbiting platforms, shall measure aerosol motions to continuously update global-scale wind profiles for selected altitude levels of the troposphere.	SYSTEM	GIVEN	SOW 1.2
LAWS0190	2	PF	The LAWS Instrument shall be designed to provide continuous on-orbit operations.	SYSTEM	GIVEN	SOW 4.0 (6)
LAWS0030	2	PF	The LAWS Instrument generates pulses of laser energy, which are directed through a rotating telescope to scan the atmosphere. A fraction of the incident radiation is backscattered by natural aerosols suspended in the atmosphere. This backscattered radiation is collected, detected, and range gated for altitude determination. Since the aerosols are moving relative to the transmitter, the backscattered radiation is Doppler shifted from the transmitter frequency by an amount proportional to the line-of-sight component of the aerosol relative velocity. The motion of the air may be found by processing this data to remove the effects of the spacecraft motion and earth rotation motions. Since this technique measures only the line-of-sight velocity component, scan techniques and processing algorithms are employed to obtain the desired horizontal wind vectors. The combination of beam scanning and spacecraft motion allows the same region to be seen from different aspect angles. These line-of-sight measurements are then weighted, taking into account such parameters as signal-to-noise, intershot spacing, and line-of-sight angles. The weighted values are then combined to produce velocity vectors for the selected regions of the atmosphere.	SYSTEM	GIVEN	SOW 1.2
LAWS0110	2	SC	The LAWS Instrument shall provide compatible interfaces for the accomodation of all elements with the boost vehicles, orbital platforms, and orbital operations. Modification of existing systems to support LAWS shall not be required.	SYSTEM	GIVEN	SOW 4.0 (3)(4)
LAWS0120	2	SC	The LAWS Instrument shall be compatible with the Japanese Polar Orbiting Platform (JPOP) and Space Station Freedom for installation and operation.	SYSTEM	GIVEN	SOW 4.0 (1)
LAWS 0170	2	SP	~~Servicing shall be accomplished by use of a Flight Teleoperator System (FTS) or other emerging robotic services for LAWS Instruments installed on Polar Orbiting~~ Platforms.	SYSTEM	PENDING NOTE 1	SOW 4.0 (5)

rec laws sys req 1-4

(1) SOW system requirements indicated POP servicing via FTS or other emerging remote robotic services. NASA EOS studies have since determined cost savings by development of expendable POP platforms and instruments. Deletion of the subject POP servicing requirement is recommended.

Table 2-1 LAWS System Requirements (2 of 4)

Req. Ident.	Level	Class	Requirements	Alloc	Status	Source
LAWS0130	2	SC	The mass of the LAWS Instrument, when configured for deployment on the Japanese Polar Orbiting Platform (JPOP), shall not exceed 800 kilograms (kg).	SYSTEM	GIVEN	SOW 4.0 (2)
LAWS0140	2	SC	The LAWS Instrument, as configured for the Japanese Polar Orbiting Platform (JPOP), shall not require more than 3 kw (three kilowatts) of electrical power.	ELECTRICAL	PENDING NOTE 2	SOW 4.0 (2)
LAWS0150	2	SC	The LAWS Instrument shall be compatible with the selected Expendable Launch Vehicles (ELVs) and the NSTS Space Shuttle Orbiter.	SYSTEM	GIVEN	SOW 4.0 (3)
LAWS0160	2	SP	Servicing and maintenance of the LAWS Instrument will be accomplished by use of a Flight Teleoperator System (FTS) and by Extravehicular Activity (EVA) capability planned for the Space Station.	SYSTEM	GIVEN	SOW 4.0 (5)
LAWS0020	2	SC	The LAWS Instrument shall consist of a laser energy source, a scanning transmit and receive telescope, a detector, a signal processing subsystem, and supporting mechanical, electrical, and control subsystems.	SYSTEM	GIVEN	SOW 1.2
LAWS0590	2	SC	The LAWS Instrument shall employ a coherent lidar as the means of obtaining data samples for use in the determination of atmospheric winds.	LASER	GIVEN	SOW 1.2 SOW 4.0 (7)
LAWS0580	3	SC	The LAWS Instrument shall employ a pulsed transmitter operating at CO_2 wavelengths.	LASER	GIVEN	SOW 1.2 SOW 4.0 (7)
LAWS0600	4	SC	The LAWS Instrument laser shall operate at a wavelength of 9.11×10^{6} meter.	LASER	PENDING NOTE 3	SOW 4.0 (7)

rec laws sys req 1-4

(2) According to SOW guidelines " the electrical power constraint is 3.0 kilowats". At the LAWS Concept Review, NASDA provided a preliminary indication that only 2 kw may be available for LAWS. Our baseline configuration has thus reduced the LAWS power requirement to 2.5 kw average for an 800 km orbit and to 1.9 kw average for a 705 km orbit. We thus recommend the available power specification to be altered for consistancy with available platform average power.

(3) The SOW "Presently envisioned baseline" is 9.11 micrometer wavelength operation. According to record, this was chosen for three purposes: a) minimal attenuation b) enhanced backscatter coefficient and c) reasonable for gas laser design. Wavelength of 11.2 micrometers is recommended as an alternate to be considered during Phase II for the following reasons: a) similar attenuation values (reference LL Firepond considerations), b) higher probability of building a succesful long life laser (i.e., no potential O^{16} contamination) and c) very little difference in measured backscattered coefficients (reference NOAA data presented at Configuration Review).

Table 2-1 LAWS System Requirements (3 of 4)

Req. Ident.	Level	Class	Requirements	Alloc	Status	Source
LAWS0210	4	SC	The LAWS Instrument laser output energy shall not be less than 10 Joules/pulse.	LASER	PENDING NOTE 4	SOW 4.0 (7)
LAWS0040	4	SC	The LAWS Instrument laser shall have a Pulse Repetition Frequency (PRF) which is adjustable from one to ten Hertz (Hz) i.e., minimum of 100 ms between shots.	LASER	PENDING NOTE 5	SOW 1.2 SOW 4.0 (7)
LAWS0610	4	SC	The LAWS Instrument laser pulse width shall be 3 microseconds.	LASER	PENDING NOTE 6	SOW 4.0 (7)
LAWS0220	4	PF	The LAWS Instrument lidar shall have an overall efficiency, defined as the ratio of laser output power to total power drawn by the lidar from the platform, of not less than five percent (5%).	LASER	GIVEN	SOW 4.0 (7)
LAWS0180	4	PF	The LAWS Instrument shall have an operational lifetime of not less than 1×10^9 (one billion) pulses or "shots" of laser energy.	LASER	GIVEN	SOW 4.0 (6)
LAWS0620	4	SC	The LAWS Instrument telescope shall have an aperture diameter of not less than 1.5 meters.	OPTICS	PENDING NOTE 7	SOW 4.0 (7)
LAWS0640	4	SC	The LAWS Instrument telescope elevation angle shall be remotely settable and shall include settings of 35°, 45°, and 55 degrees with respect to the nadir.	OPTICS	PENDING NOTE 8	SOW 4.0 (7)

rec laws sys req 1-4

(4) Higher energy pulses from the laser are highly beneficial in providing data from lower backscatter (ß) regions of the globe and thus greatly increases global coverage from LAWS as demonstrated in section ___. "Not less than 20 J/pulse" is recommended in place of "not less than 10 J/pulse." This is well within the projected state-of-the-art and weight constraints and expands the LAWS coverage area into weaker ß regions.

(5) Shot Managment with fire upon command is recommended over firing at a continuous PRF. 100 ms minimum time between shots is a readily achievable baseline with no maximum time specified. This controls the data to global areas of interest and optimizes scientific data.

(6) Final pulse width has not yet been selected with 1 to 3 microseconds baselined. Final selection will impact laser efficiency, velocity and range resolution, and number of independent detection samples associated with each lidar shot.

(7) Larger apertures are highly beneficial in providing data from lower backscatter (ß) regions of the globe and thus increases global coverage from LAWS as demonstrated in section ___. "Not less than 1.67 m" is recommended in place of "not less than 1.5m". This is well within the projected state-of-the-art and weight constraints.

(8) The SOW "Presently envisioned baseline" was a 45 degree off nadir (elevation angle). The science team listed 35, 45, and 55 degrees as highly desirable at the Configuration Review. These selectable angles are incorporated into the configuration baseline.

Table 2-1 LAWS System Requirements (4 of 4)

Req. Ident.	Level	Class	Requirements	Alloc	Status	Source
LAWS0630	4	SC	The LAWS Instrument scan rate shall be 6 revolutions per minute (RPM).	OPTICS	PENDING NOTE 9	SOW 4.0 (7)
LAWS0050	2	PF	LAWS Instrument data, collected by successive measurements at different orbital positions, shall provide wind profiles when processed.	RECEIVER/ PROC	GIVEN	SOW 4.0 (6) SOW 1.2
LAWS0100	2	PF	The LAWS Instrument receiver shall detect 9.11 x 10^{-6} meter wavelength laser energy backscattered from aerosol particales dispersed in varying amounts in the global troposphere. The backscatter coefficients of the atmosphere at typical CO_2 wavelengths range from 1 x 10^{-11} /m sr to 1 x 10^{-7} /m sr. The lower backscatter values are typically observed over remote ocean areas and at higher altitudes.	RECEIVER/ PROC	PENDING NOTE 10	SOW 1.3 SOW 4.0 (7)
LAWS0080	2	PF	The LAWS Instrument shall provide data with a horizontal resolution of 100 x 100 kilometers.	SYSTEM	GIVEN	SOW 1.2 SOW 4.0 (6)
LAWS0090	2	PF	The LAWS Instrument shall provide data which will permit the computation of horizontal wind vectors with an accuracy of +/- 1 (one) meter per second (m/s) at lower altitudes, and +/- 5 m/s in the upper troposphere.	PROC	GIVEN	SOW 1.2 SOW 4.0 (6)
LAWS0060	2	PF	The LAWS Instrument shall provide data over the altitude range from zero (0) to twenty (20) kilometers (km) above the surface of the earth.	PROC	GIVEN	SOW 1.2
LAWS0070	2	PF	The LAWS Instrument shall provide data with a vertical resolution of one (1) kilometer.	PROC	GIVEN	SOW 1.2 SOW 4.0 (6)
LAWS0230	2	PF	Manage availabe shot and optimize their distribution pattern	SYSTEM	GIVEN	SOW 1.3
LAWS0240	2	PF	Operate min. of 3 years with a goal of 5 years	SYSTEM	DERIVED	SOW 4.0 (6)

rec laws sys req 1-4

(9) The SOW "Presently envisioned baseline" was 6 RPM scan rate. Scan rate of 6.6 RPM is required for the baseline 100 x 100 km grid as discussed in section ___ and is recommended for the configuration baseline.

(10) See Footnot (3).

NASA Strawman LAWS System	Lockheed LAWS System
Coherent Lidar • Pulsed Transmitter (CO_2) • 9.11 μm Wavelength • 3 μsec Pulse Length • 10 Hz PRF • 10 Joules/Pulse • 5% Wallplug Efficiency • 10^9 Shots Lifetime **Telescope** • 1.5 m Aperture • 6 rpm Scan Rate • 45 deg Nadir Angle	**Coherent Lidar** • Pulsed Transmitter (CO_2) • 9.11 μm Wavelength (11.2 μm being Considered) (A) • 1 μsec - 3 μsec (B) • 1 - 10 Hz on Demand (C) • 20 Joules/Pulse (D) • 5% Wallplug Efficiency • 10^9 Shots Lifetime **Telescope** • 1.67 m Aperture (E) • 6.6 rpm (F) • 35, 45, 55 deg Nadir Angles (G)

LAWS - 10

NASA Strawman Requirements	Lockheed Design Meets or Exceeds Requirements	Specification Impact
• Global Wind Measurements commensurate with coverage	With variable scan angle, can adjust scan in orbit for optimal coverage and sensitivity	(G)
• Horizontal Resolution of 100 x 100 km	With pulse upon demand, can adjust laser firing for optimal coverage	(C)
	6.7 rpm provides approx. 1.5 pulses per 100 km swath as satellite passes over	(F)
• Vertical Resolution of 1 km	1 to 3 μsec pulse provides a vertical resolution of approx. 200 to 600 m. Pulse length to be refined during Phase II.	(B)
• Horizontal Wind Vector +/- 1 m/s in lower and +/- 5 m/s in upper troposphere	A function of pulse length, atmospheric decorrelation and system sensitivity. 1 to 3 μsec pulse length is commensurate with velocity accuracy requirement. Higher energy (20 J) and larger aperture (1.67 m) enhances sensitivity and therefore accuracy.	(A) (D) (E)
• Operational Lifetime of 10^9 shots	Meets requirements. Fire upon demand extends operational lifetime in years on orbit by judicial placement of shots.	(C)
• Serviceability	Meets requirements. Takes advantage of HST derived experience. Likely not required for JPOP.	
• 800 kg wt budget	Meets requirement.	
• 3 kW power budget	Operates with 2.5 kW average power from 800 km orbit or 2 kW from 705 km orbit.	(C) (D) (E) (G)
• Shot mgmt to optimize Distribut. Pattern	Fire upon demand provides optimal shot management.	(C)
• $\beta = 10^{-11}$ to 10^{-7} /m SR	Larger aperture, higher energy enhances sensitivity to lower values of β.	(A) (E)

LAWS-11

Figure 2-4. Lockheed Design Enhances LAWS System Requirements

SECTION 3. EVALUATION AND SELECTION CRITERIA

The overall approach to evaluation and selection of appropriate candidates has been presented in the Evaluation and Selection Criteria Plan, DR-18. Ultimately, the performance index given in that plan will be used to determine LAWS performance and to support detailed trade studies. The performance index is an index of the quality of wind velocity data measured over the life of the instrument. For Phase I studies, several more basic parameters can be used as performance indices in order to perform concept and configuration selection. These performance indices are primarily related to accuracy in the line-of-sight velocity measurement and to data coverage. They are used in analyses with appropriate parts of the LAWS Integrated System Performance Model, described in DR-18. Optimization of those parameters will necessarily result in the optimization of the overall performance index given in DR-18. Different parameters are appropriate for the different trade studies which support concept and configuration selection. The parameters used for evaluation are presented in this section, and the rationale for the use of the parameters for each trade study is presented in the discussion of each of the trade studies.

The first performance measure is SNR, which is given by (Ref. 1)

$$SNR = \frac{J\lambda\tau}{h} \left[\beta E_1\right] \left[\eta \frac{D^2}{TSR^2}\right]$$

where
- J = Pulse energy
- λ = Wavelength
- τ = Pulse length
- h = Planck's constant
- β = Backscatter coefficient
- $E1$ = Attenuation factor from the extinction profile
- η = Optic efficiency
- D = Optics diameter
- TSR = Total slant range.

The second performance measure used in the trade studies is σ_r, which is the standard deviation of the error of the measured line-of-sight component of velocity. In general, σ_r is a function of the signal processing technique, for which several forms can be used. For these initial trade studies, two forms of the σ_r equation have been used.

The first is the Cramer-Rao bound for the variance of the mean frequency for laser radar. The Cramer-Rao bound does not estimate LAWS performance, but it is a lower bound on LAWS performance. Because it is not sensitive to particular signal processing techniques, it provides a standard which is useful in comparison studies rather than in the determination of absolute performance estimates. The equation for the Cramer-Rao lower bound has been adapted from Ref. 2 and is given by

$$\sigma_r^2 = \frac{6}{4\pi^2 \tau^2 SNR}\left[\frac{1}{\tau B} + \frac{1}{SNR\, \tau^2 B_{if}^2}\right]$$

where τ = Pulse length
SNR = narrow band signal-to-noise ratio
Bif = IF bandwidth (i.e., narrow band fitter width).

The second form of the σ_r equation is the poly pulse pair equation given in Ref. 1 as

$$\sigma_r = \left[\frac{\lambda\sigma_v}{2\tau}\left(\frac{1}{4\sqrt{\pi}} + \frac{2\rho}{SNR_w} + \frac{1}{8\pi^2 \rho\, SNR_W^2}\right)\right]^{1/2}$$

where σ_v = rms velocity width of received spectrum (assumed to be 1 m/sec for this study)
ρ = $\sigma_v/2$ Vmax
SNRw = $\sqrt{(2\pi)}\ \rho$ SNR
Vmax = velocity span of velocities to be measured.

The σ_r parameter can also be expressed for other signal processing techniques, such as the block filter bank (i.e., fast Fourier transform), auto regressive estimates, and Capon technique estimators. These estimators provide results which lie between the Cramer-Rao lower bound and the poly pulse pair. The results of all the estimates are also sometimes expressed in terms of fractions of estimates for which the error is less than some specified value, typically 1 m/sec.

The use of the Cramer-Rao and the pulse-pair estimators in these trade studies permit identification of the optimal concept for LAWS, although the numbers obtained may not be representative of the actual numbers which LAWS will achieve. Stated alternatively, the optimal concept can be defined, although the performance numbers generated may be different from those which LAWS will produce.

In order to get a good estimate of the velocity estimation values which LAWS will achieve, Lockheed has simulated LAWS signal processing. These results are presented in Section 4.4.8.

The third measure of performance used in these studies is $\sigma r/\sqrt{n}$, where n is the statistical expectation of the number of line-of-sight measurements to be taken in a grid square of 100 km by 100 km. Conceptually, it is the standard deviation of all data taken in a grid square when sr is the standard deviation of one line-of-sight velocity measurement. Alternatively, it may be considered to be the error in a curve fit of data over a limited azimuth range. This measure of performance is used to trade the desirability of a few measurement points of high accuracy versus many measurement points of lower accuracy.

The fourth measure of performance is percentage of coverage under the swath in the tropics for a polar orbit. For the purposes of this study, the tropics are defined as less than 20 deg of latitude. The fifth measure of performance is the percentage of coverage under the swath for the globe for a polar orbit.

One of the measures of performance is knowledge of velocity accuracy, which has been discussed in meetings of the LAWS Science Panel but is not included in this analysis. There is a significant trade between velocity accuracy and knowledge of velocity accuracy. Increased knowledge of velocity accuracy requires parameter selection which causes a degradation in velocity accuracy. Because knowledge of velocity accuracy has only been discussed in the LAWS Science Panel and has not been formulated as an official LAWS requirement, it has not been used as a selection criterion. However, its influence on concept and configuration selection is presented qualitatively in the trade study discussions.

SECTION 4. IDENTIFICATION AND ANALYSIS OF CANDIDATE INSTRUMENT CONCEPTS

4.1 LAWS PRINCIPLES

Several principles of LAWS operation have been defined as a result of the trade studies conducted to support concept selection.. These principles guide both the concept selection and the configuration development. These principles are described below.

The available backscatter for much of the LAWS measurement domain is marginal at best. Backscatter for low altitudes appears to be quite adequate, but backscatter for mid and high altitudes ranges from marginally adequate to inadequate. Therefore, the LAWS design is driven by the requirements to make the best of marginal backscatter, and the concept selected is different from that which would be selected if the backscatter were more than adequate.

The importance of adequate backscatter is illustrated in Figure 4-1, which was taken from Reference 1 with additional data added. The plot shows the standard deviation of measurement error of the line-of-sight component of velocity as a function of wide band SNR for the poly pulse-pair velocity estimator with the Cramer-Rao lower bound added. Because of marginal backscatter, a significant fraction of LAWS operations is on the left side of the plot where small increases in wide band SNR can significantly decrease the measurement error. Therefore, increasing the wide band SNR is of primary importance. Although Figure 4-1 shows the results of one velocity estimator (as well as the Cramer-Rao lower bound), the conclusion is not dependent on the particular velocity estimator selected. All velocity estimators have the characteristic steep slope at low values of signal-to-noise (S/N), although the S/N level at which the steep slope occurs varies.

The choice of S/N equation and, to a greater degree, the choice for the equation for the error in measured line-of-sight component of velocity (σ_r) will affect the performance estimate, but because of the marginal backscatter under any choice of S/N or σ_r equations, such choices will not affect the concept selection.

In late 1989, the GLOBE experiment gathered improved backscatter data at several wavelengths. It is expected that this improved backscatter data will improve the quality of the LAWS performance estimate. While the results of that data collection effort have not been included in this report, it is not expected that the GLOBE data will alter the fact that backscatter data are marginal in much of the LAWS measurement domain.

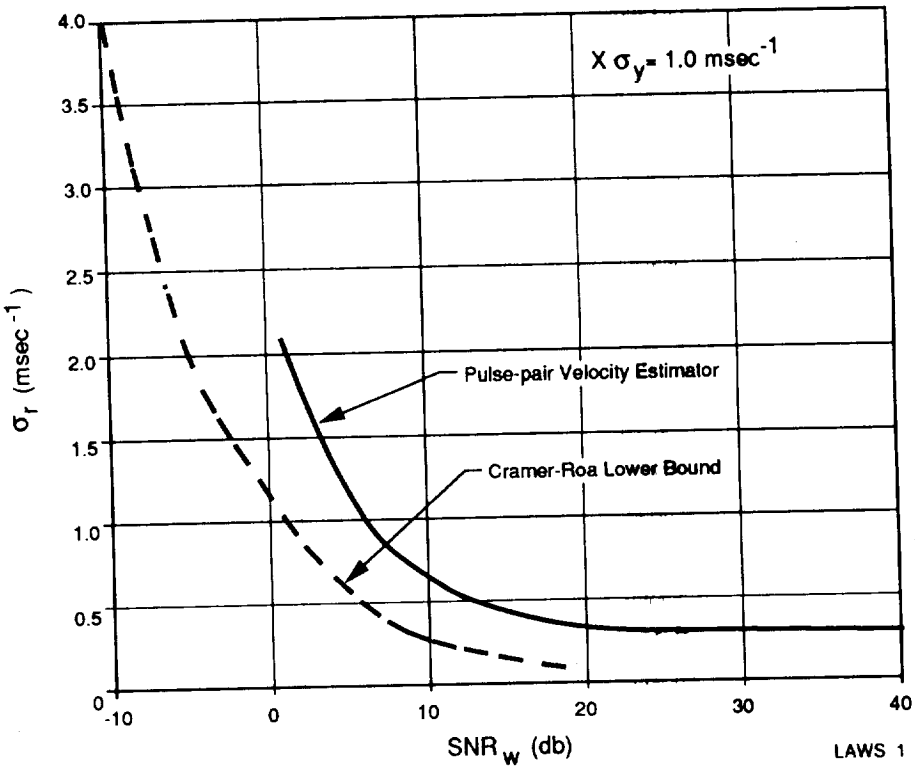

Figure 4-1. Radial Velocity Error as a Function of Wide Band SNR

Therefore, it is expected that the concept presented in this report will not change because of improved data gathered from the GLOBE experiment.

There are two issues which will require significant input from the LAWS Science Panel. The first is the significant trade between data coverage and data quality. Section 4.4.4 shows that as data coverage increases, data quality decreases. The recommendations of the LAWS Science Panel will be required before the optimal point in this trade can be established.

The second issue is the trade between data accuracy and knowledge of data accuracy. Since knowledge of data accuracy has not been formally stated as a LAWS requirement, it will not be addressed in this Phase I report. However, the issue is relevant for future discussions by the LAWS Science Panel.

4.2 LAWS CONCEPT SUMMARY

The Lockheed LAWS baseline concept has been derived from the trade studies which are described below in Section 4.4. Although numbers are given for important system parameters, the concept consists primarily of the principles stated, with the

numbers being those which have been used for a baseline approach. The Lockheed LAWS concept may be summarized as shown below.

- Wavelength = 9.11 μm
- Laser pulse energy should be as large as possible. Nominal value is 20 J per pulse. This is the maximum pulse energy which is currently believed to be achievable with low technical risk. In a power-limited system, the trade between many pulses at low energy per pulse and a few pulses at high energy per pulse favors the latter approach. This conclusion is reached for the condition for which the error in the wind measurement is to be minimized and does not consider knowledge of velocity accuracy. There is some discussion among the LAWS Science Panel that knowledge of velocity accuracy is as important (and perhaps more important) as velocity accuracy. However, since the knowledge of velocity accuracy issue has not been formally addressed in the LAWS requirements, it has not been included as an issue in the formulation of the LAWS concept.
- Optics diameter should be as large as possible within weight constraints. In a weight-limited system, the trade between laser weight (as related to pulse energy) and optics weight (as related to telescope diameter) favors increasing pulse energy at the expense of optics diameter. Nominal optics diameter is 1.67 m.
- Low satellite altitude is preferable to high satellite altitude, although the SOW value of 800 km is retained as the nominal value. Trade studies have shown that complete tropical and global coverage can be obtained at 400 km satellite altitude, and the data quality is better at the lower altitude. A 29 percent improvement in backscatter coefficient measurement is achieved by dropping the orbit from 800 to 705 km for the identical LAWS Instrument parameters.
- The nadir angle has been made selectable between the limits of 35 and 55 deg. This is in keeping with the philosophy of the initial LAWS Instrument as an experiment. Low nadir angles favor better accuracy in line-of-sight velocity measurements because of decreased range from the satellite to the atmosphere. High nadir angles favor better accuracy of horizontal components of wind (given fixed accuracy of the line-of-sight component) and better global coverage. These relationships are very strong. Analytical models of instrument performance are not reliable enough to allow launch of the instrument with a fixed nadir angle. For example, if the instrument were launched with a large nadir angle and the actual received S/N were small, there would be no way to decrease the angle to achieve a better S/N. Conversely, if the instrument were launched with a small nadir angle, and the actual S/N were strong, there would be no way to

increase the angle to achieve better coverage. The selectable nadir angle permits changing of the nadir angle as more operational experience with the instrument is obtained.

- Azimuth controlled pulsing is preferable to laser pulsing at a uniform pulse repetition rate. Azimuth controlled pulsing appears to be practical, but is subject to further investigation. Under azimuth controlled pulsing, the laser is pulsed at selected intersection points of the scan. In a power-limited system, the desirability of high pulse energy drives the average pulse rate down.
- A selectable power usage around the orbit is desirable. The four selectable levels are defined below:
  1. High pulse rate: 3200 W laser power (3800 W instrument power), and pulse rate $\approx$ 8 Hz
  2. Moderate pulse rate: 2000 W laser power (2500 W instrument power), pulse rate $\approx$ 5 Hz
  3. Reduced pulse rate: between 2000 and 300 W laser power
  4. Laser idle rate: 300 W laser power (800 W instrument power), no laser pulsing
- Scan rate $\approx$ 6.7 scans/minute
- Pointing knowledge < 100 μrad (3σ).

4.3 ATTENUATION AND BACKSCATTER PROFILES

The backscatter profile is the most significant parameter affecting LAWS performance. It varies over several orders of magnitude. Because of the importance of backscatter profile, the LAWS Science Team has specified two profiles for use in trade studies: one with and one without cirrus clouds. Figure 4-2 shows the standard attenuation and backscatter profiles. The figure shows both the mean backscatter profile and the 70 percent (mean minus one standard deviation) backscatter profile without cirrus clouds. Profiles with cirrus clouds have been run in our simulations with the effect of enhancing backscatter where the clouds are present.

4.4 SUPPORTING ANALYSES FOR LAWS CONCEPTS

This section presents the supporting trade studies and analyses for the selected LAWS concept presented in Section 4.2. This discussion first presents the issues which affect the accuracy in the line-of-sight velocity component. A performance summary of line-of-sight velocity accuracy is then presented. Issues related to scan rate are presented after the performance summary of line-of-sight velocity. Shot management

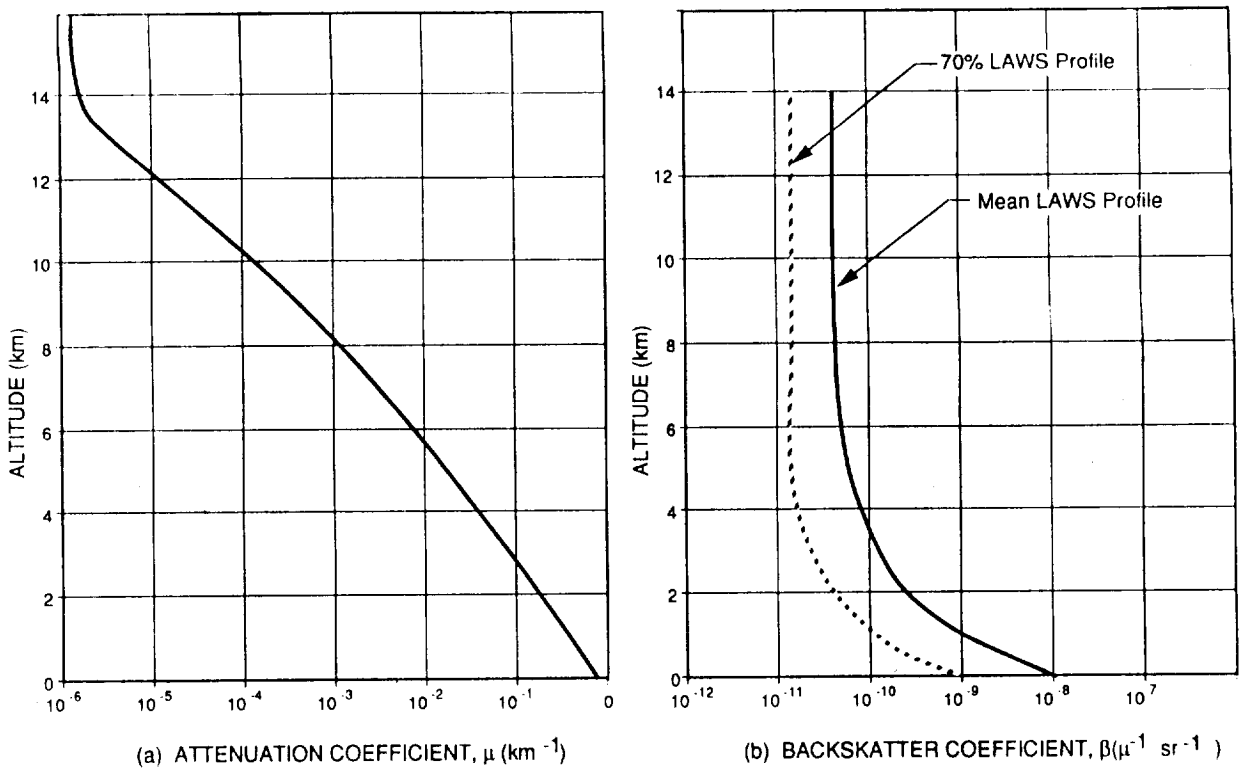

Figure 4-2. Reference Attenuation and Backscatter Coefficients for LAWS

concepts are discussed along with pointing knowledge requirements. Pulse length effects are discussed using a Lockheed developed simulation.

4.4.1 Laser Wavelength

Selection of laser wavelength was based on the following for operation at the specified wavelength:

- Backscatter coefficient
- Atmospheric absorption
- Laser efficiency, lifetime (reliability), and cost.

During previous studies (Refs. 4 through 10), 9.11 micrometers was selected as the wavelength of choice and is also selected by Lockheed as the baseline concept wavelength.

The referenced efforts indicated that the 9.11 micrometer wavelength had potential for a greater backscatter coefficient than the longer wavelengths; this was demonstrated experimentally by Menzies (Ref. 6), who compared 9.25 micrometer data with 10.59 data (see Figure 4-3) and postulated that similar results would hold for 9.11 where little

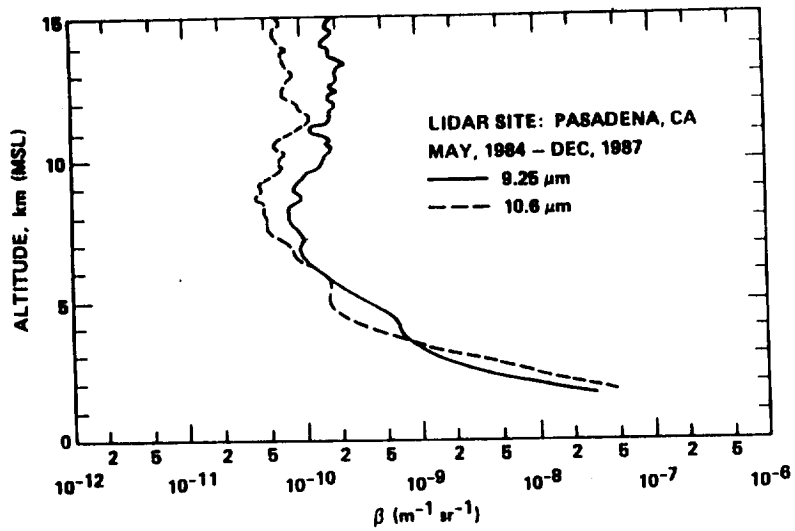

Figure 4-3. JPL Comparison of 9.25 and 10.6 μm Lidar Backscatter Coefficients at Pasadena over Several Years

backscatter data existed. Modeled comparisons indicate 9.11 to be best in the SCALE Study (Ref. 7).

Similarly, atmospheric absorption profiles were calculated for 9.11, 10.59, and 11.19 μm by Murty (Ref. 8), at 9.11 μm by Grant (Ref. 9), and for 9.11, 9.25, and 10.59 μm in Ref. 7. Reference 8 depicts 9.11 superior to 10.59 and 11.19 by over 10 dB between the surface and satellite altitude. Reference 7 depicts 9.11 superior to 9.25 and 10.59 by over 10 dB using the best available codes (LASER) at that time (1987).

Consideration was given to developing an isotopic CO_2 laser to operate at 9.11 μm. Work was initiated under an AFGL/MSFC contract to Spectra Technology Inc. (STI) to develop laser kinetics data for a $^{12}C^{18}O_2$ laser operating at 9.11 μm. Catalyst work was initiated at LRC to develop a long life catalyst suitable for operation at the subject wavelength.

Since this LAWS Phase I effort was initiated, new data is becoming available which can potentially alter the selection of 9.11 μm as the best CO_2 wavelength for LAWS. Data presented by M. Post of NOAA/WPL at the Pasadena Configuration Review (see Figures 4-4 and 4-5) showed very little difference between 9.25 and 10.59 μm in backscatter data with a very limited number of runs; 9.25 μm were slightly better at some altitudes, and 10.59 μm were slightly better at others. Globe pulsed lidar data at

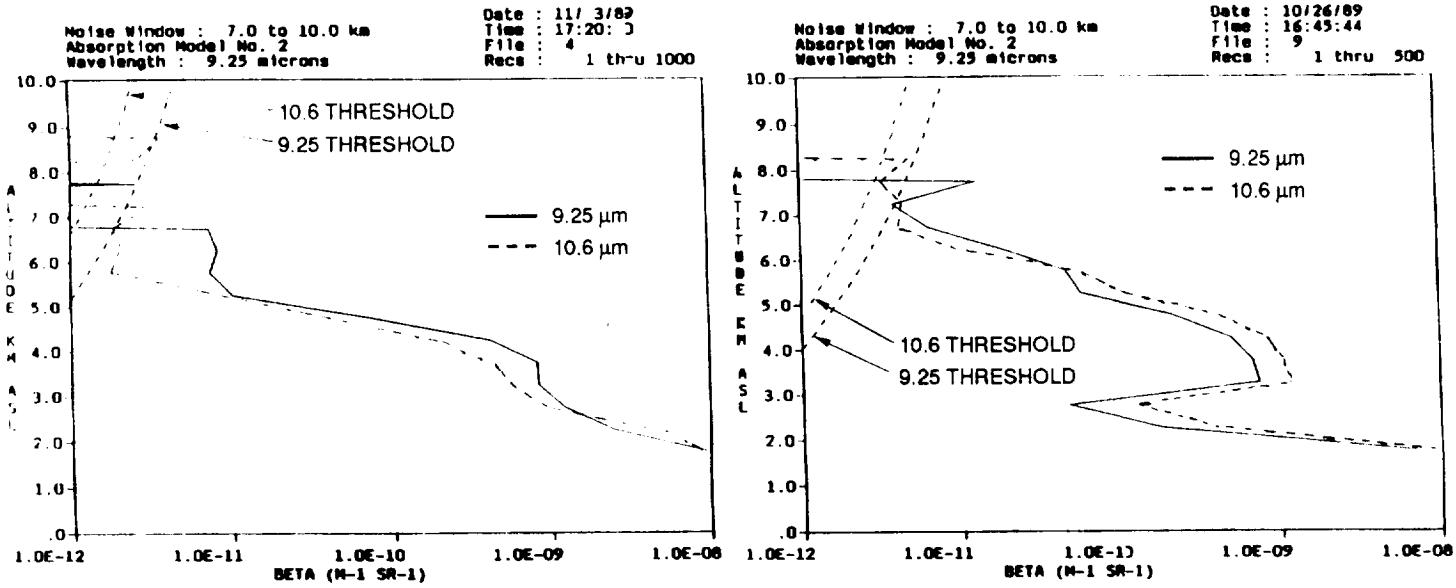

Figure 4-4. NOAA/WPL Comparison of 9.25 and 10.6 Micrometer Lidar Backscatter Coefficients at Moffit Field, California for Two Days' Runs

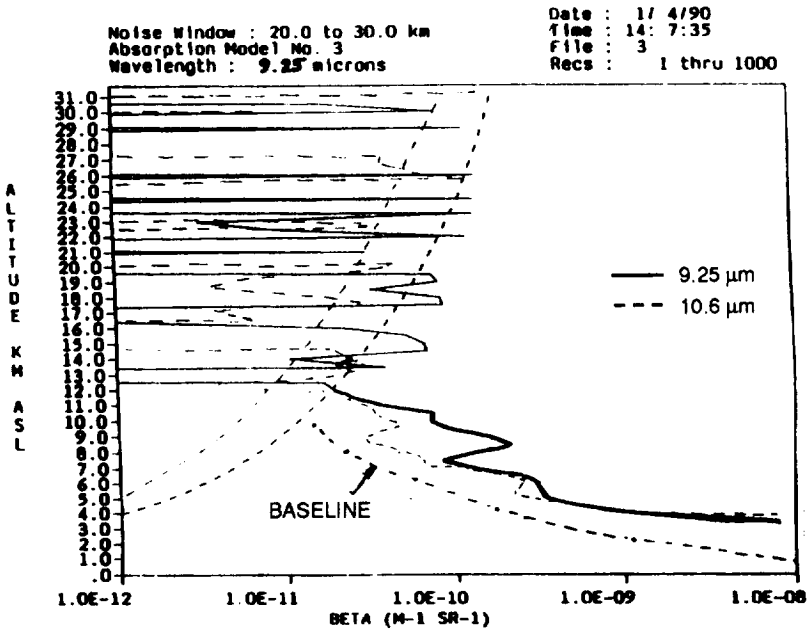

Figure 4-5. NOAA/WPL Comparison of 0.25 and 10.6 Micrometer Lidar Backscatter Coefficients at Boulder, Colorado for a Single Day's Runs

9.25 μm has not yet been analyzed, but may shed light upon the subject. The same is true for the Globe continuous wave lidar data at 9.11 and 10.59 μm.

An extensive study related to the Firepond coherent ladar upgrade was undertaken recently at MIT/LL to pick a wavelength for minimum atmospheric attenuation, good laser operating characteristics, and reasonable gas expense. The wavelength of 11.19 μm was selected as the wavelength of choice for this ground based coherent ladar (in Lexington, MA) designed to Doppler image satellites overhead and to Doppler image sounding rockets launched from Wallops Island, VA, with the ladar aimed at a very low elevation angle.

Water vapor, considered the primary absorber, is certainly less concentrated at Lexington than in the tropics for an overhead ladar firing. However, the near horizontal, low elevation angle firing (aiming for the Wallops launch) will present a case of equal or greater severity as the equatorial 45° LAWS case, since almost all water vapor absorption occurs in the lower 3 to 5 km of the atmosphere.

From the laser design standpoint, the Lockheed team has not yet been provided access to the STI kinetics data for 9.11 μm. Thus we can only speculate about laser efficiency at this wavelength, and we will not do so in this report. Concern is expressed about poisoning of the laser gas mixture from residual $^{16}O_2$ in the walls of the laser, in the muffler material, in the pre-ionizer dielectric, and in the catalyst. While a laser of this type can be kept free of ^{13}C poisoning (for a 11.19 μm $^{13}C^{16}O_2$ isotope laser) by not using carbon in any of the imbedded components, it will be much more difficult to completely eliminate $^{16}O_2$ poisoning without an occasional laser gas purge/refill, since $^{16}O_2$ will initially be present as surface and imbedded oxidation in many laser materials.

In summary, Lockheed has selected 9.11 μm as the baseline concept/configuration wavelength; however, we suggest a wavelength optimization review during Phase II.

4.4.2 Optimal Allocation of Power

The issue related to optimal allocation of power is whether, in a power limited system, power should be allocated to many pulses of low pulse energy or few pulses of high pulse energy. The performance measure is $\sigma_r/\sqrt{n}$, which is a measure of the standard deviation of the average of all data taken in a grid square. Figure 4-6 shows $\sigma_r/\sqrt{n}$ as a function of pulse repetition rate for five selected altitudes for the mean LAWS backscatter profile. Figure 4-6 does not show data above 8 km because the backscatter coefficient does not vary significantly above 8 km. This plot uses the Cramer-Rao lower

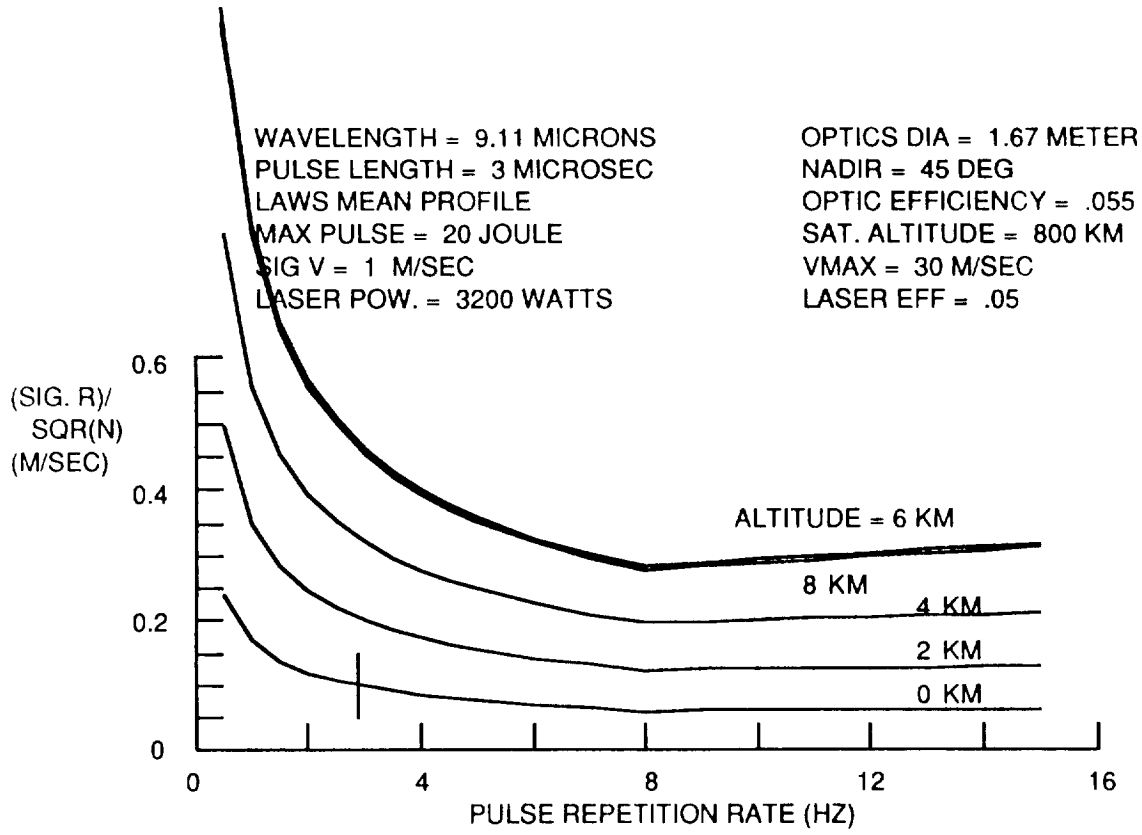

Figure 4-6. Optimal Allocation of Power for 20 J Maximum Laser Pulse Energy (Cramer-Rao Estimator)

coefficient does not vary significantly above 8 km. This plot uses the Cramer-Rao lower bound algorithm, so absolute values are low. The left side of the graph is determined by the limitation on pulse energy (20 joules/pulse in Figure 4-6); $\sigma r/\sqrt{n}$ decreases with increasing pulse repetition rate because of increasing n. The right side of the graph is determined by the limitation on laser power. For good backscatter conditions (i.e., altitude of 0 km in Figure 4-6), increasing the pulse repetition rate is favorable because these data are on the right side of the σr versus S/N curve, as shown in Figure 4-1. Increasing S/N does not decrease σr significantly, but increasing pulse repetition rate increases n. However, for the upper altitudes, increasing pulse repetition rate on the right side of Figure 4-6 decreases S/N, and the increase in n is more than offset by the degradation in σr as S/N decreases. Overall, the optimal pulse repetition rate for the parameters shown is 8 Hz.

Figure 4-7 shows the same information for a pulse energy of 10 J. This set of curves optimizes at a higher pulse rate than the 20 J set of curves. The higher pulse repetition rate will yield a better knowledge of velocity accuracy, but as seen in Figure

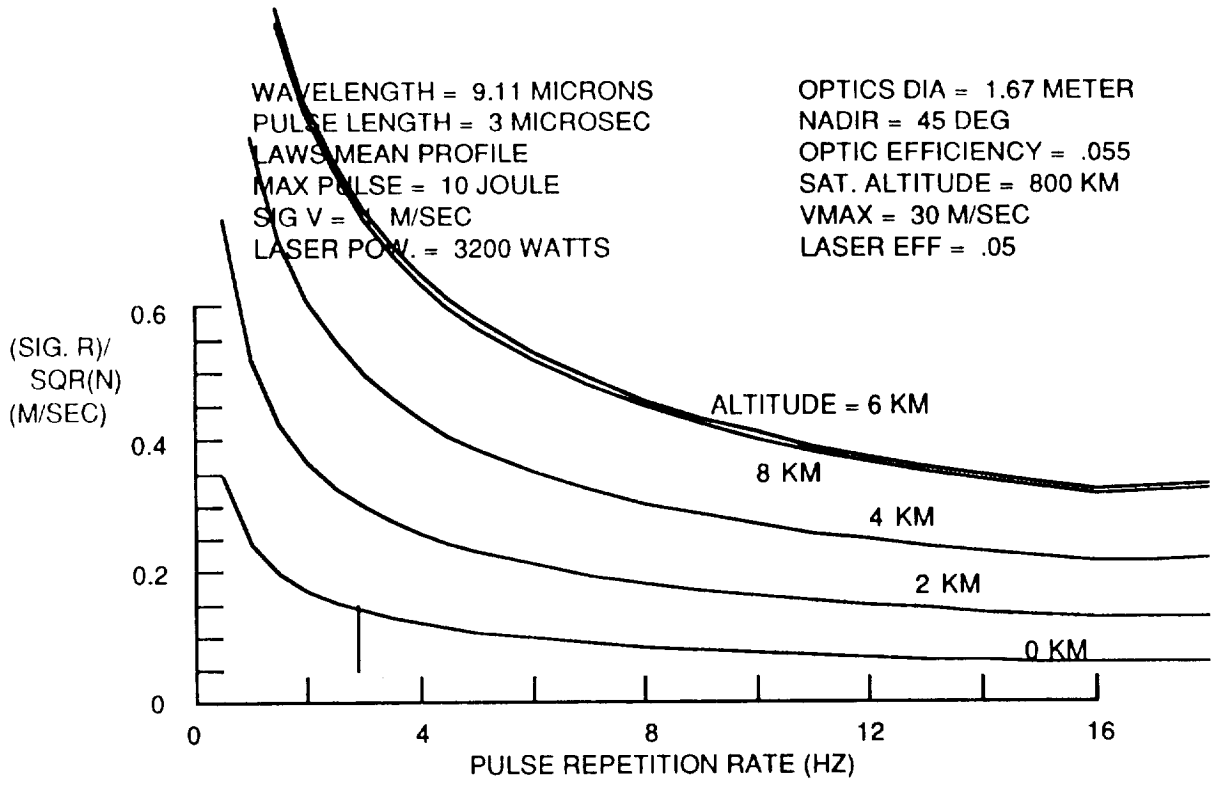

Figure 4-7. Optimal Allocation of Power for 10 J Maximum Laser Pulse Energy (Cramer-Rao Estimator)

4-6, the lower pulse rate gives a better velocity accuracy. The LAWS Science Panel must conduct the quantitative trade to determine how much velocity accuracy can be sacrificed for a better estimate of knowledge of velocity accuracy.

It was desirable to determine if this same conclusion would be valid if an alternative (worst case) velocity estimator were used. Figure 4-8 shows the same information as Figure 4-6, but with the pulse-pair estimator used instead of the Cramer-Rao lower bound. The values of $\sigma r/\sqrt{n}$ have been reduced by an order of magnitude, but the characteristic shape remains the same. Figure 4-9 shows the same information with a pulse energy of 10 J, and Figure 4-10 shows the information with a pulse energy of 30 J.

The desirability of increasing pulse energy is shown in Figure 4-10, which is identical to Figure 4-9, except that the maximum laser pulse energy has been increased to 30 J. The right side of the figure is unchanged, but the left side of the figure has decreased because of the increased pulse energy. For a pulse energy of 30 J, the optimal pulse repetition rate decreases to 5 Hz, and the value of $\sigma r/\sqrt{n}$ is decreased for the upper altitudes. The overall conclusion of this analysis is that increases in pulse energy decrease the optimal value of $\sigma r/\sqrt{n}$ and also decrease the pulse repetition rate at which the

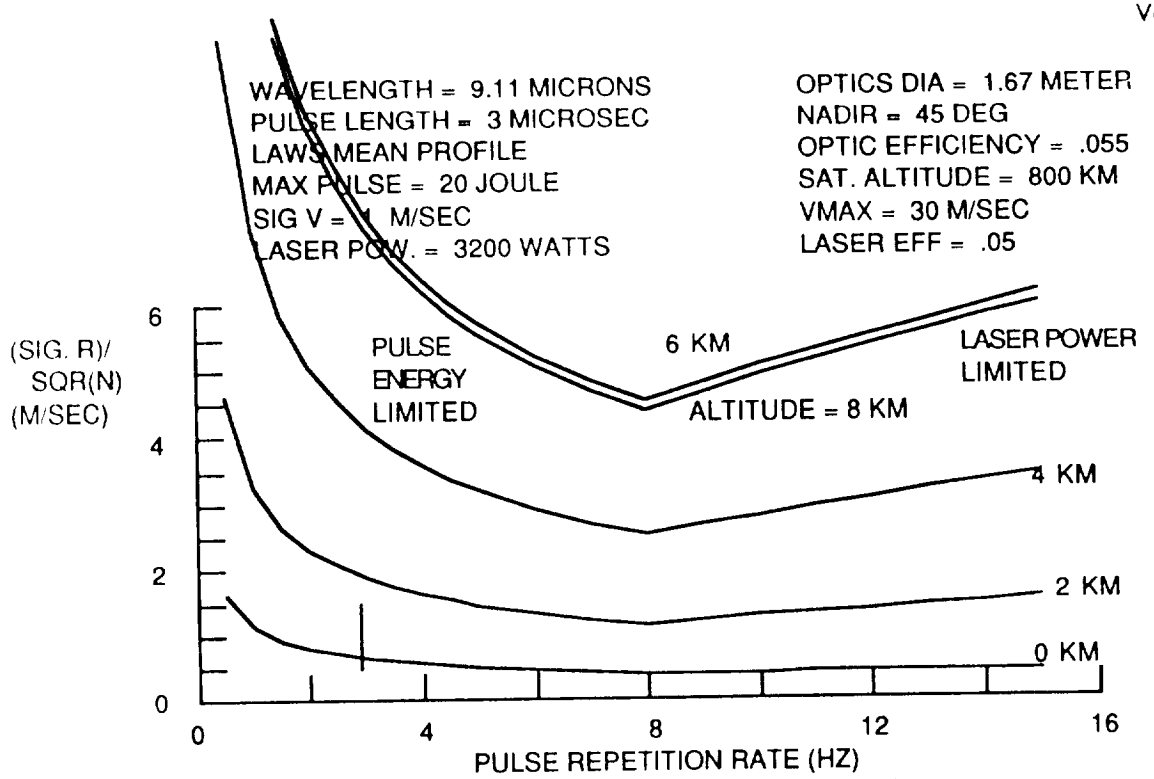

Figure 4-8. Optimal Allocation of Power for 20 J Maximum Laser Pulse Energy (Poly Pulse Pair Estimator)

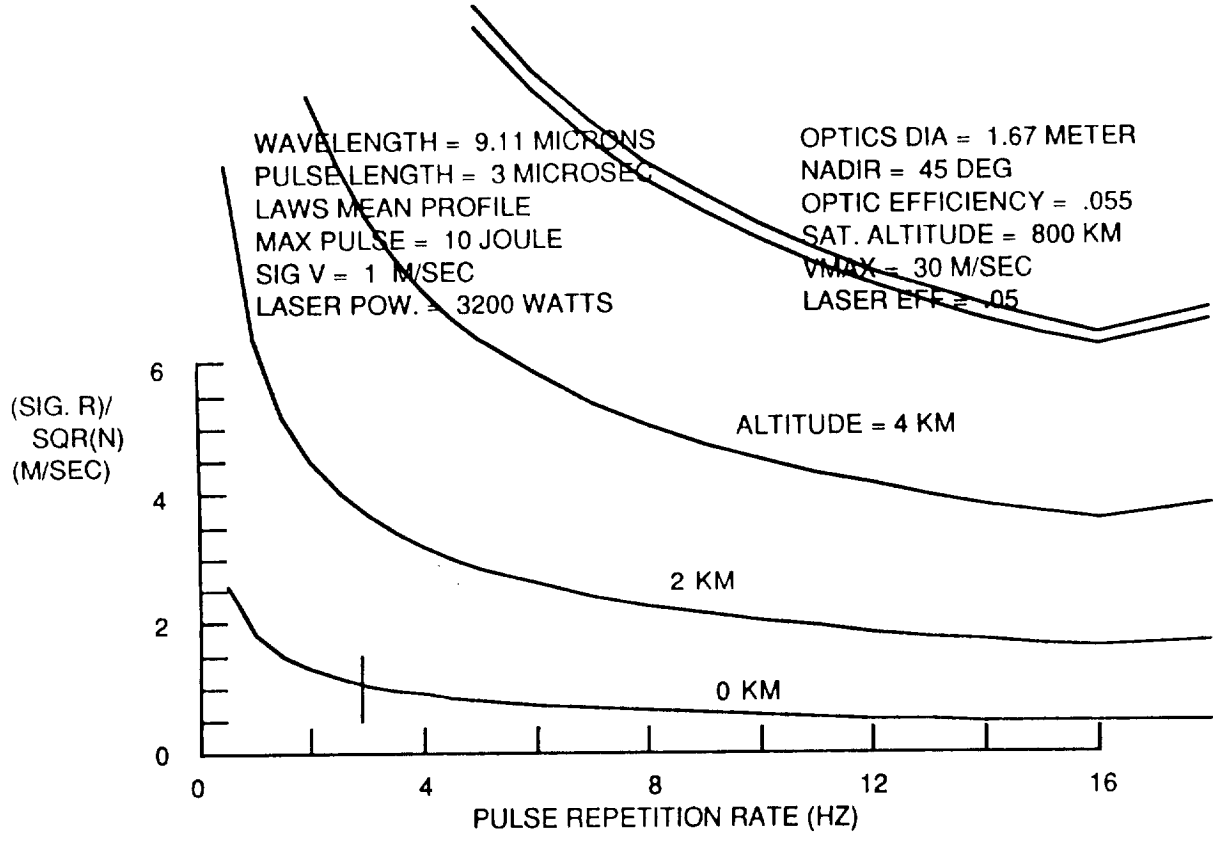

Figure 4-9. Optimal Allocation of Power for 10 J Maximum Laser Pulse Energy (Poly Pulse Pair Estimator)

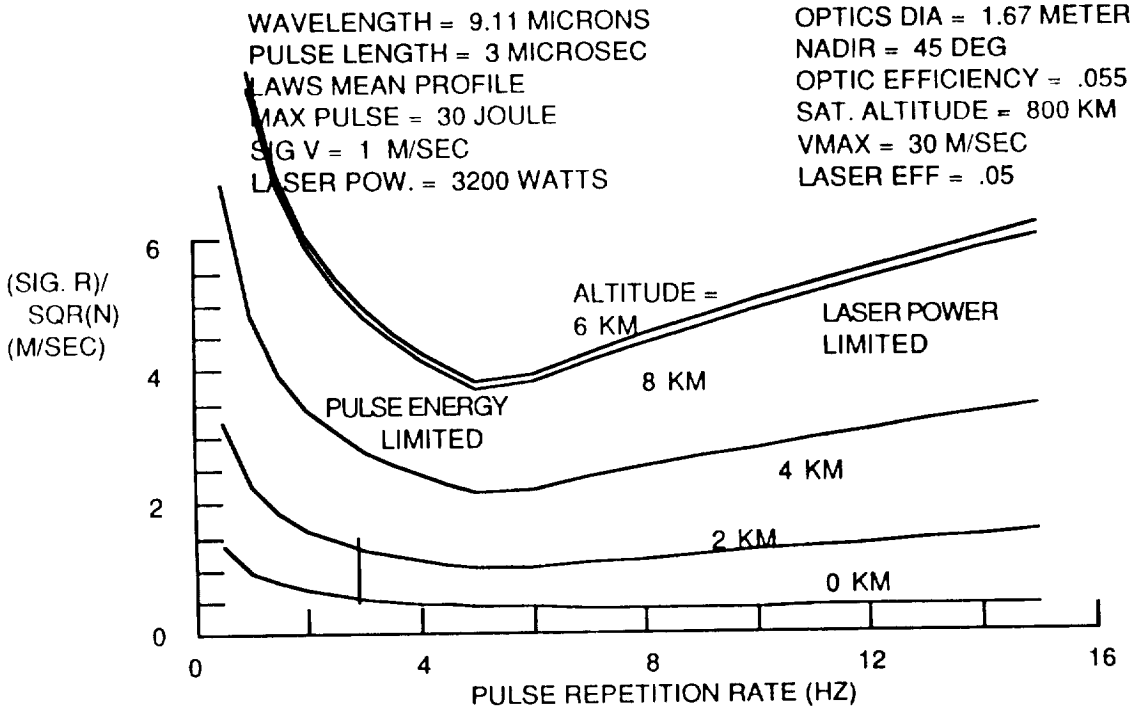

Figure 4-10. Optimal Allocation of Power for 30 J Maximum Laser Pulse Energy (Poly Pulse Pair Estimator)

optimum occurs. Performance is improved by using available power for a few pulses of high pulse energy rather than for many pulses of low pulse energy.

A number of velocity (frequency) estimators are available for LAWS as outlined by Anderson (Ref. 10). These include the pulse-pair estimator used by both NASA-MSFC and NOAA (pulsed coherent lidars) starting in the late seventies and the block matched filter (FFT) estimator used by Lockheed (continuous wave coherent lidars) starting in the early eighties. They also include a number of estimators used for coherent radars and evaluated for lidar by Anderson. Anderson provides a comparison of the effectiveness of these estimators in Figure 4-11 and references these to the Cramer-Rao lower bound. The Cramer-Rao lower bound is a theoretical lower limit on estimator efficiency.

According to Anderson and depicted in the chart, the pulse-pair is an "upper bound," i.e., worst case estimator, with the FFT block matched filter providing a 4.3 dB improvement and the Capon estimator a 6.6 dB improvement for the "50 percent error less than 1 m/sec" criteria. Anderson projects that with forethought a LAWS estimator could be developed which approaches the Cramer-Rao lower bound within a few dB. Lockheed has chosen to depict data processed through both the pulse-pair and Cramer-Rao lower bound estimators in order to bracket the results between the upper and the

Estimator	SNR Required for 50% Errors < 1 m/sec	SNR Required for 75% Errors < 1 m/sec
Pulse-Pair (actual)	-3.9	+0.7
Cramer-Rao bound after Zrnic'	-15.2	-12.9
Block Matched Filter	-8.2	-4.8
Autoregressive least squares form order 10	-9.7	-6.0
Autoregressive least squares form order trimmed	-10.0	-6.4
Capon, order = 12	-10.5	-7.7
Capon AR autocorrelations with order trimming	-10.3	-7.7

Note: *All SNR values are for +25 m/sec Nyquist bandwidth.*

Figure 4-11. Velocity Estimator Performance Summary

lower bounds conveniently provided by these two estimator types. A simulation of a baseline LAWS velocity estimator (i.e., the FFT estimator) is also presented in Section 4.4.8.

4.4.3 Optimal Allocation of Weight

The issue related to optimal allocation of weight is whether in a weight limited system weight should be allocated to the laser to increase pulse energy or should be allocated to the optic system to increase optic diameter. Figure 4-12 shows the laser pulse energy and telescope aperture as functions of mass. Figure 4-12 is drawn so that the sum of laser mass and telescope mass is constant at 400 kg.

Figure 4-13 shows S/N as a function of laser pulse energy for the LAWS mean backscatter profile. Aperture diameter is also shown so that the sum of the laser mass and the telescope mass is constant at 400 kg across Figure 4-13. Figure 4-14 shows similar information where performance is expressed by σ_r for the Cramer-Rao lower bound.

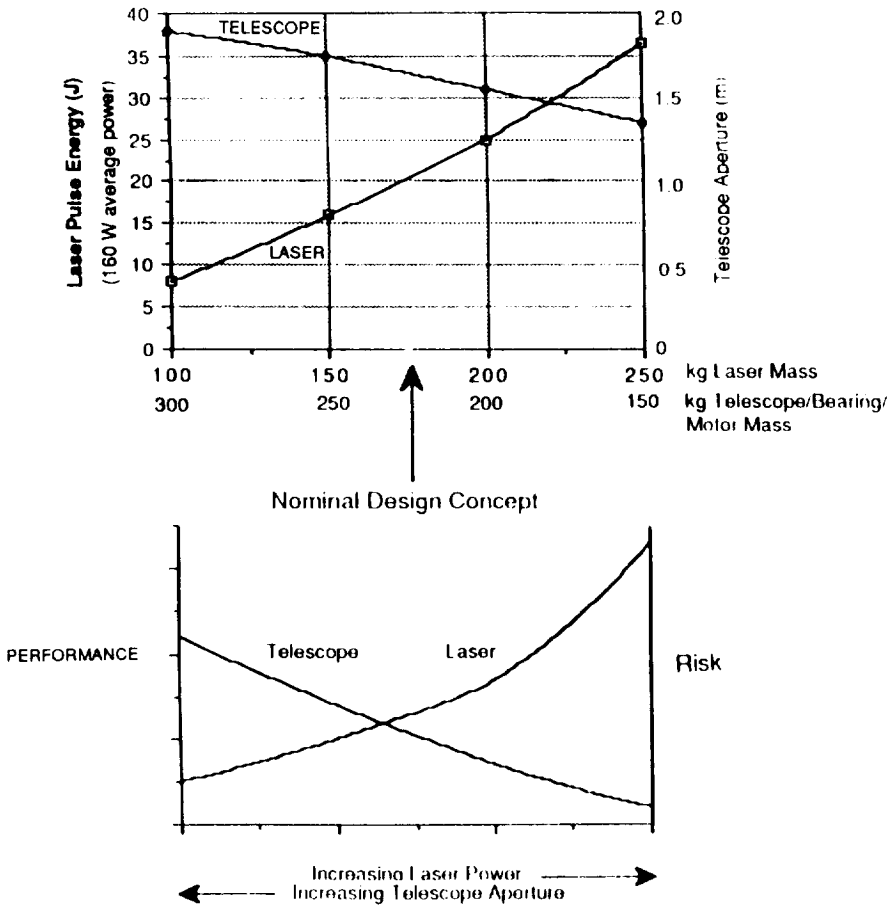

Figure 4-12. 400 kg Combined Laser/Telescope/Motor/Bearing Concept Trades

It is of interest that both optimal allocation of power and optimal allocation of weight favor a high laser pulse energy. There is no fundamental reason why this should be true, but it is fortuitous that both optimization studies yield the same result.

4.4.4 Data Quality Versus Data Coverage

As described in a previous section on LAWS principles, there is a significant trade between data coverage and data accuracy. Increasing satellite altitude gives better data coverage but decreases data accuracy. This trade is shown in Figure 4-15, which shows S/N as a function of percent of tropical coverage for a polar orbit. High backscatter is achieved by setting the measurement altitude to 1 km for the mean LAWS backscatter profile. Tropical coverage is defined by a combination of satellite altitude and nadir angle, and Figure 4-15 shows the combinations by which specific levels of tropical coverage can be achieved. Figure 4-15 shows satellite altitudes from 400 to 800 km and nadir angles from 30 deg to greater than 60 deg. The selection of an optimum along the

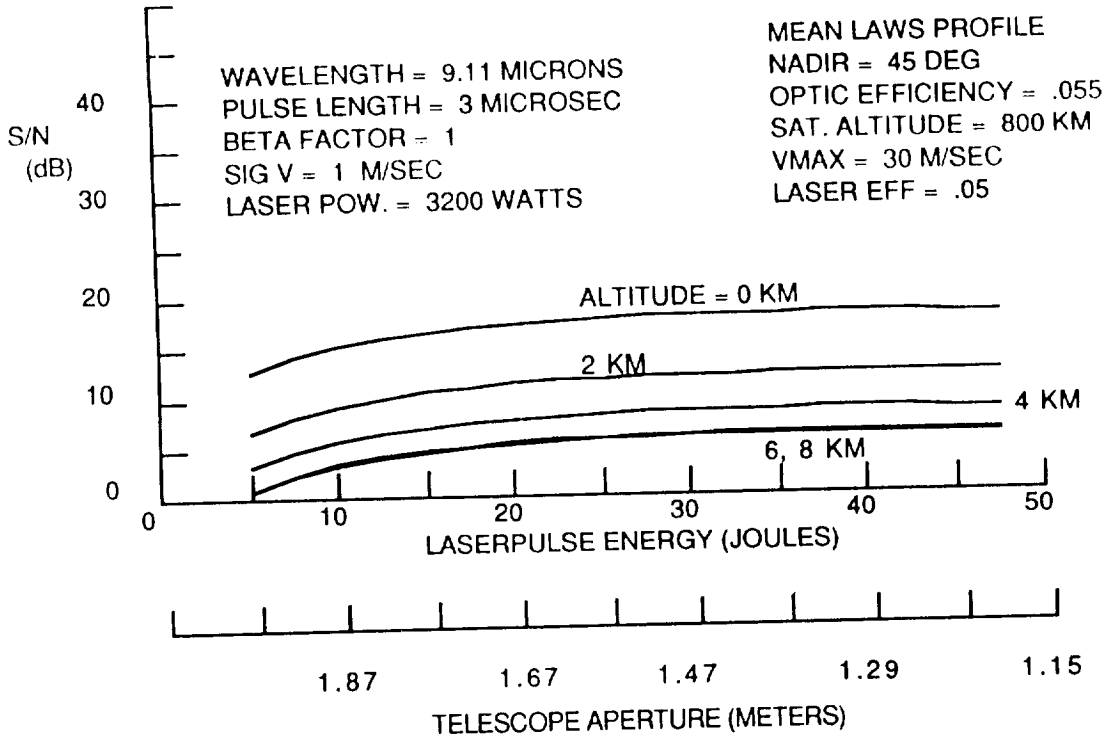

Figure 4-13. Optimal Allocation of Weight for a 400 kg Sum of Laser Mass and Telescope Mass

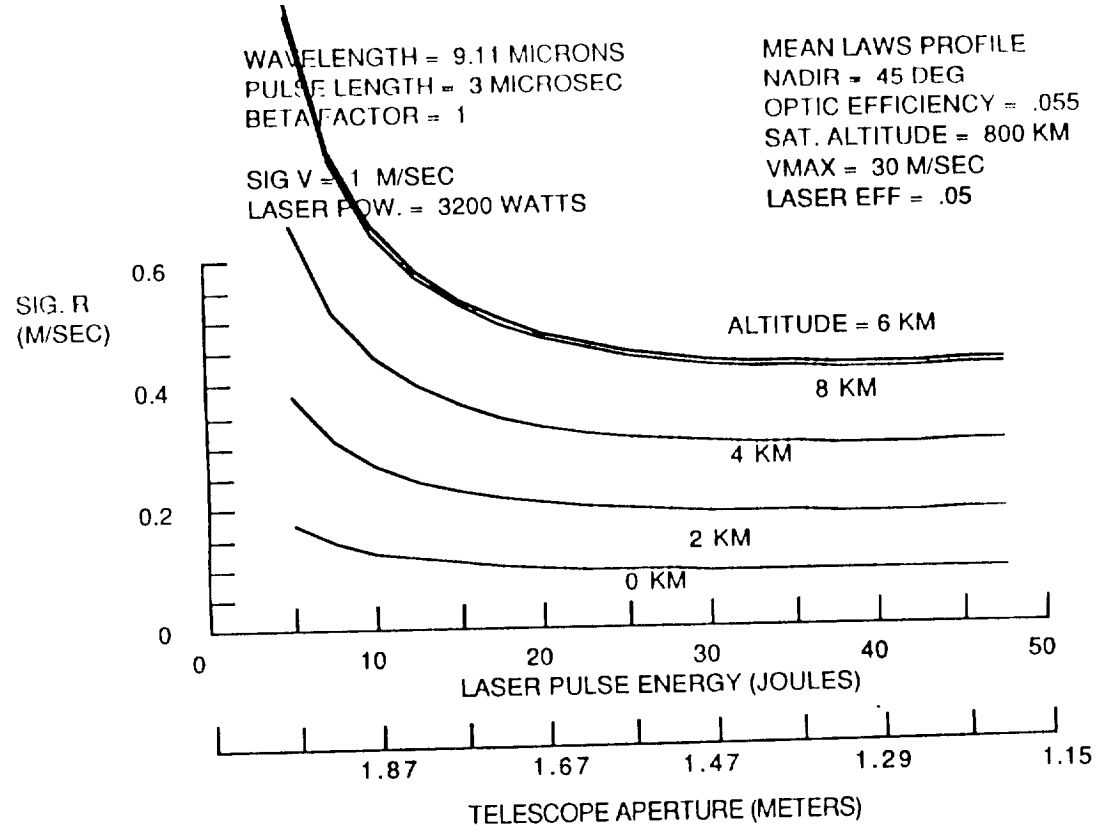

Figure 4-14. Optimal Allocation of Weight as Expressed by σ_r Using Cramer-Rao Velocity Resolution Estimator (400 kg Mass)

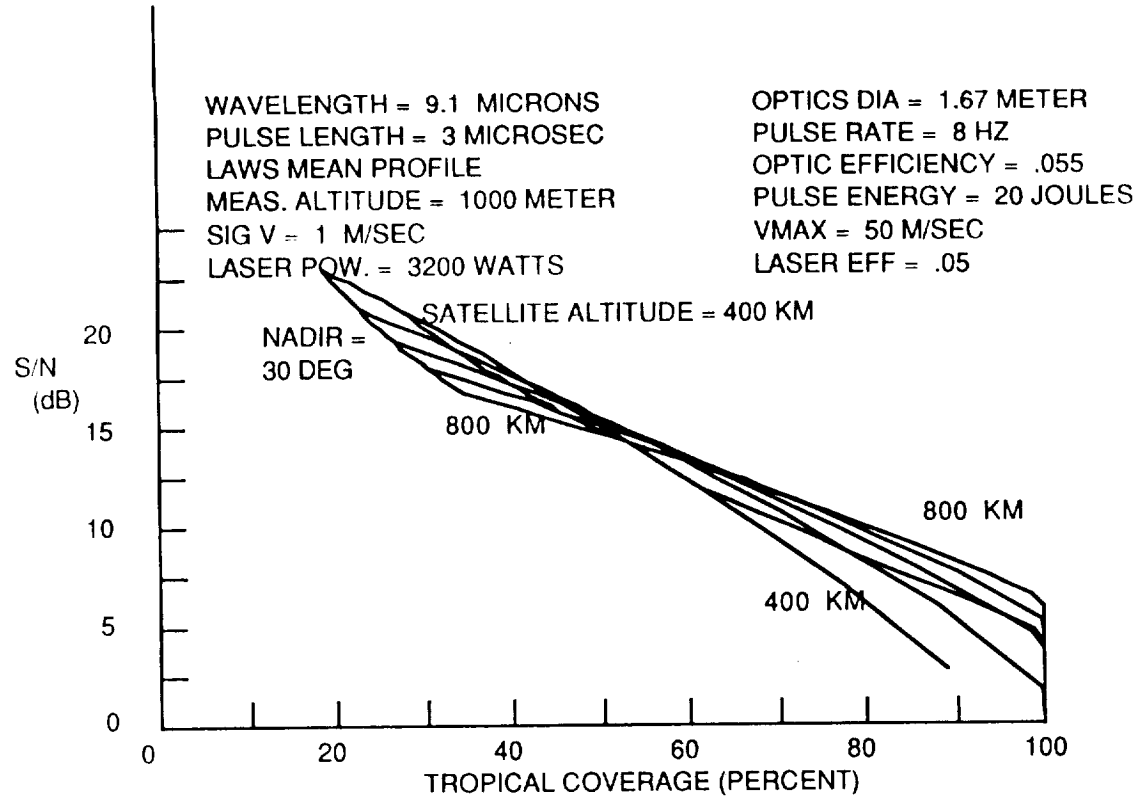

Figure 4-15. Trade of Tropical Coverage versus Data Quality as Expressed by SNR for High Backscatter (Low Altitude)

curve is an issue which must be addressed by the LAWS Science Panel. Figure 4-15 shows that for a given value of tropical coverage, S/N is not a strong function of satellite altitude. That is, a given value of tropical coverage can be achieved by an infinite number of combinations of satellite altitude and nadir angle, and S/N is not sensitive to the particular combination of altitude and nadir angle which is used to achieve a value of tropical coverage.

Figure 4-16 shows the same data as Figure 4-15 but with the backscatter degraded by selecting a measurement altitude of 10 km from the LAWS mean backscatter profile. For the poorer backscatter, S/N is somewhat more sensitive to the particular combination of satellite altitude and nadir angle used to achieve a particular percentage of tropical coverage. Figure 4-17 shows the same data but with global coverage presented instead of tropical coverage. For a polar orbit, global coverage is always greater than tropical coverage.

Figures 4-18 and 4-19 show the same data as Figures 4-15 and 4-16 but with the data represented as the standard deviation of the error of velocity measurement instead of S/N.

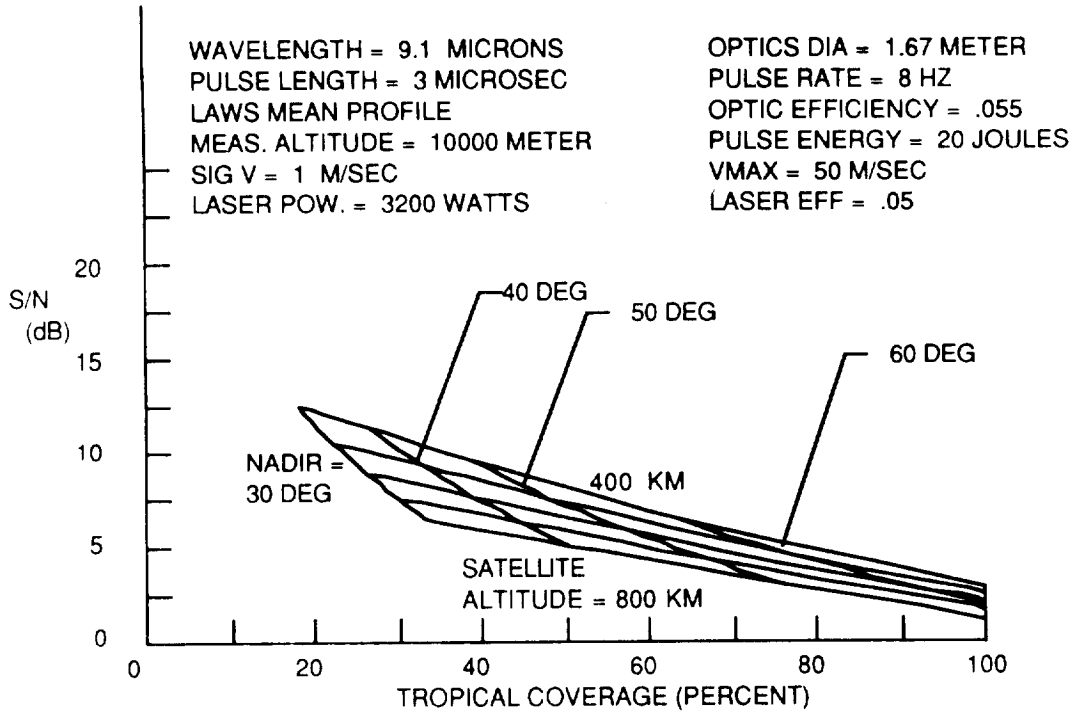

Figure 4-16. Trade of Tropical Coverage versus Data Quality as Expressed by SNR for Low Backscatter (High Altitude)

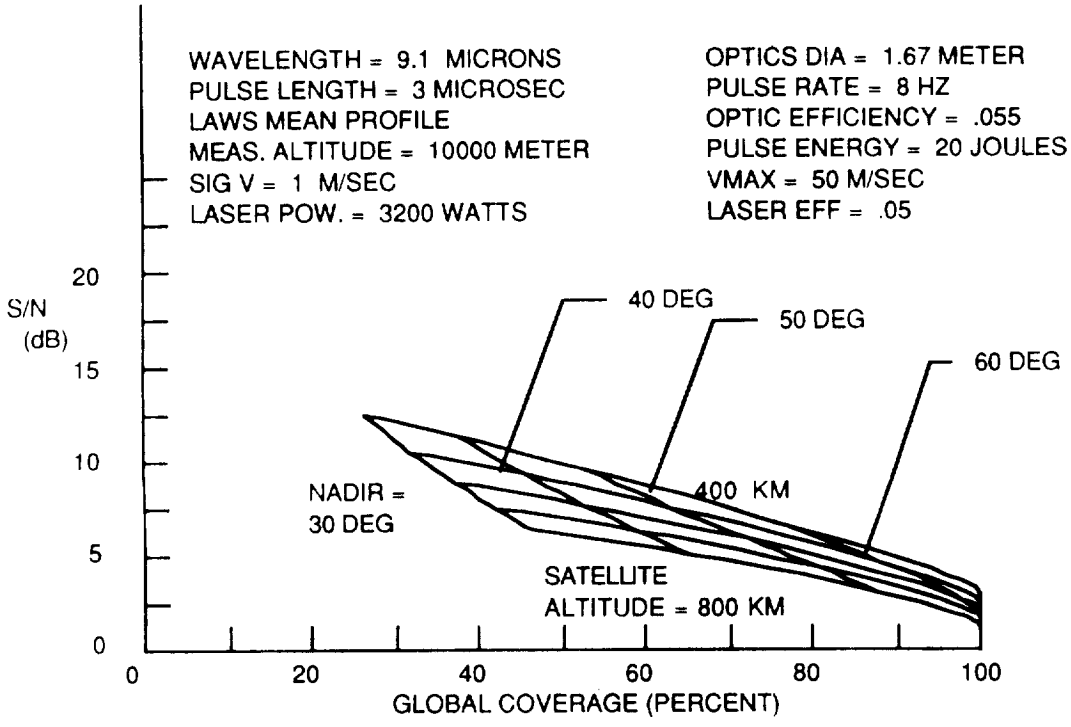

Figure 4-17. Trade of Global Coverage versus Data Quality as Expressed by SNR for Low Backscatter (High Altitude)

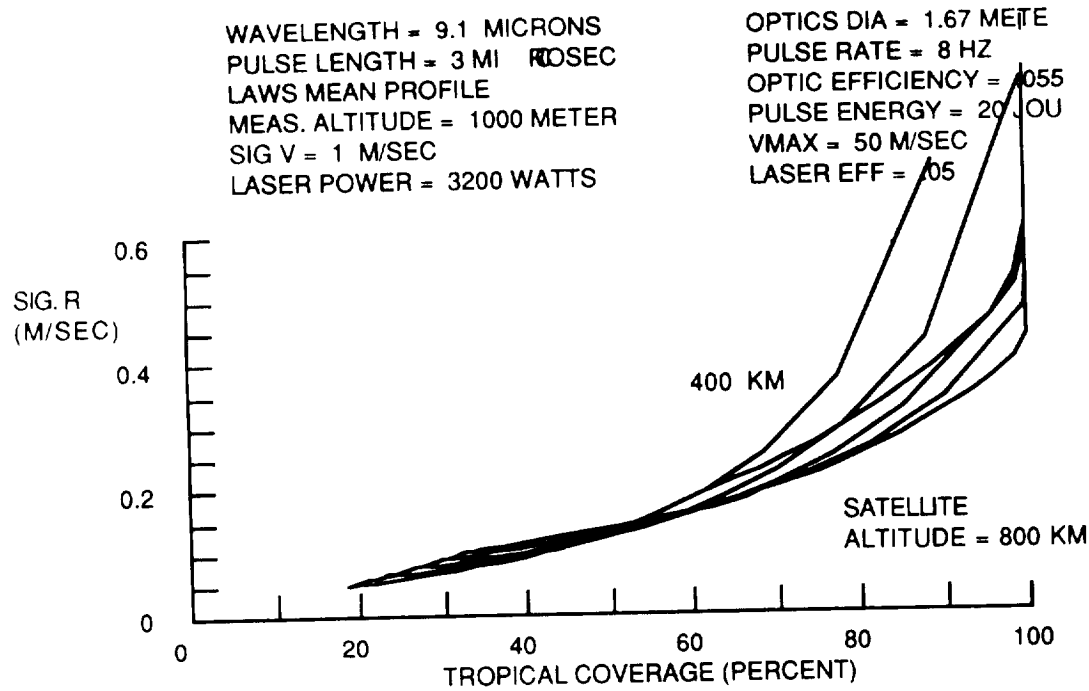

Figure 4-18. Trade of Tropical Coverage versus Data Quality as Expressed by Cramer-Rao Estimation of Velocity Error for High Backscatter (Low Altitude)

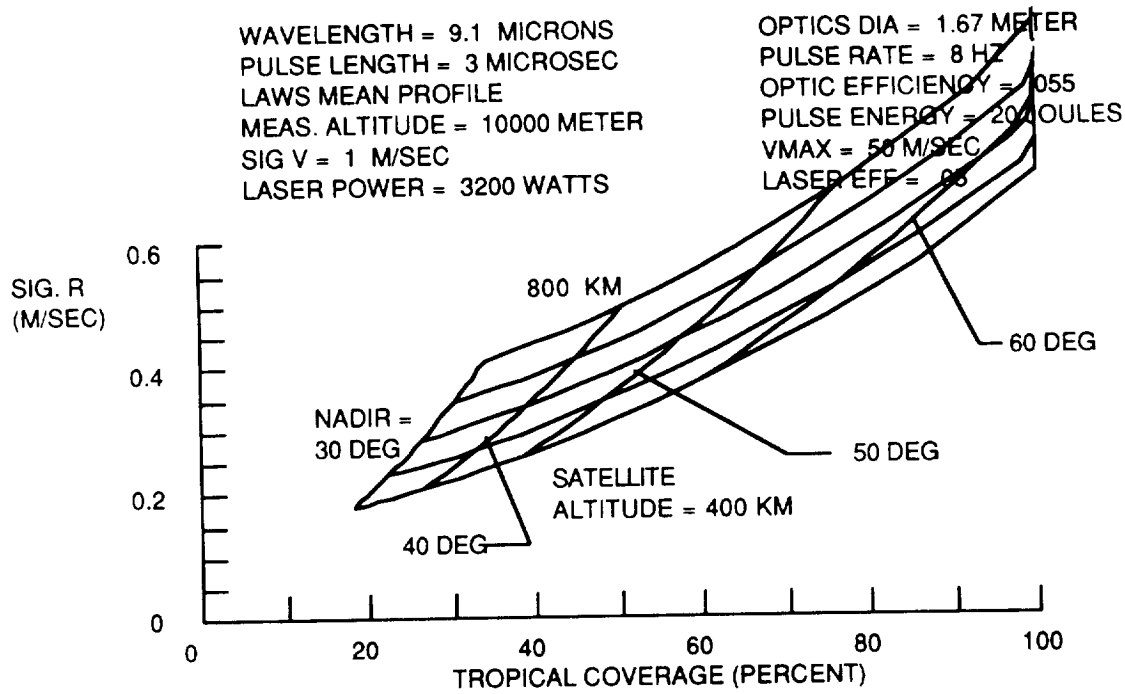

Figure 4-19. Trade of Tropical Coverage versus Data Quality as Expressed by Cramer-Rao Estimation of Velocity Error for Low Backscatter (High Altitude)

These curves show the reason that Lockheed has chosen a selectable nadir angle, particularly with backscatter data which may not be well-defined, especially over ocean areas. A selectable nadir angle will permit experimental determination of the relationships shown in Figures 4-15 through 4-19.

4.4.5 Performance as Function of Orbit Altitude and Scan Angle

This section presents a summary of the expert LAWS performance as expressed by S/N and σ_r. Figure 4-20 shows S/N as a function of measurement altitude for five satellite altitudes ranging from 400 to 800 km. The coverage numbers given in the lower right portion of the figure give the coverage limits corresponding to the satellite altitude limits shown on the figure. These plots were generated from a general computer program for LAWS performance. Therefore, parameter values which are not germane to this particular plot have been deleted from the labels on the right side of the plot.

Figure 4-21 shows S/N performance for several values of nadir angle at a satellite altitude of 800 km. Performance degraded near the surface for high values of nadir angle because of attenuation.

Figure 4-22 shows velocity accuracy as predicted by Cramer-Rao and by pulse-pair for several selected values of V_{mar}. Figure 4-23 shows the same information with satellite altitude reduced to 500 km. The value of lowered satellite altitude is clearly seen. Figure 4-24 depicts these data for a 705 km orbit, which is a potential JPOP orbit.

4.4.6 Shot Management

There are two aspects of shot management addressed in the baseline design. The first is the control of shots over each scan, and the second is the control of shots as a function of latitude over the polar orbit.

It is desirable for the scan pattern to be repeated over a 100 km by 100 km grid squared as the satellite proceeds around its orbit. Therefore, three scan rates were considered: 4.47, 6.71, and 8.94 scans per minute. These correspond to 1, 1.5, and 2 scans per 100 km under the satellite path, creating a repetitive pattern over each 100 km as the satellite moves around its orbit. The 6.71 scans per minute rate was selected as the baseline approach because, as shown in the following paragraphs, it most nearly matches the number of available intersection points of the scan with the desirable pulse repetition rate of the laser.

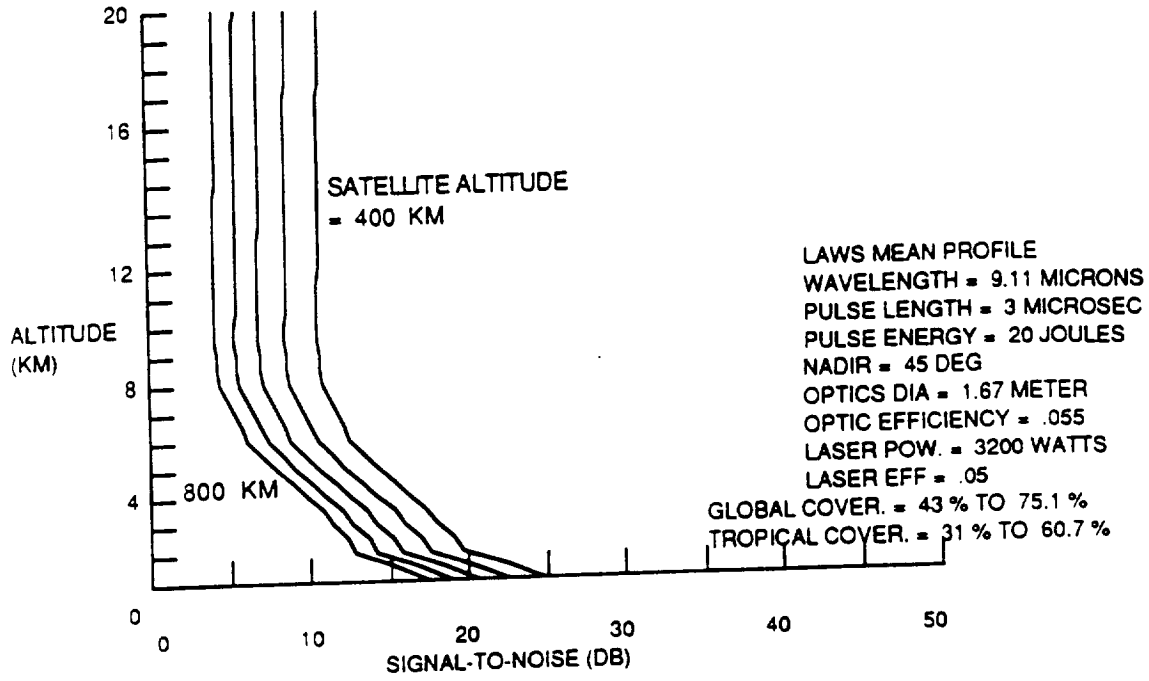

Figure 4-20. LAWS S/N Performance over a Range of Satellite Altitudes

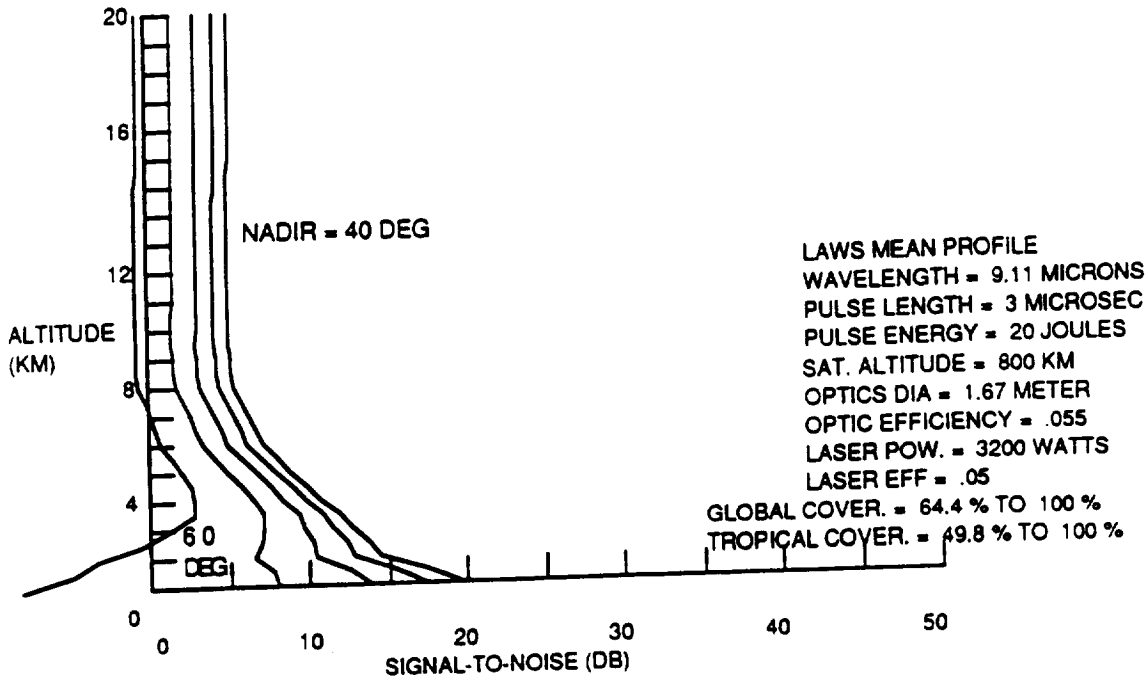

Figure 4-21. LAWS S/N Performance over a Range of Nadir Angles

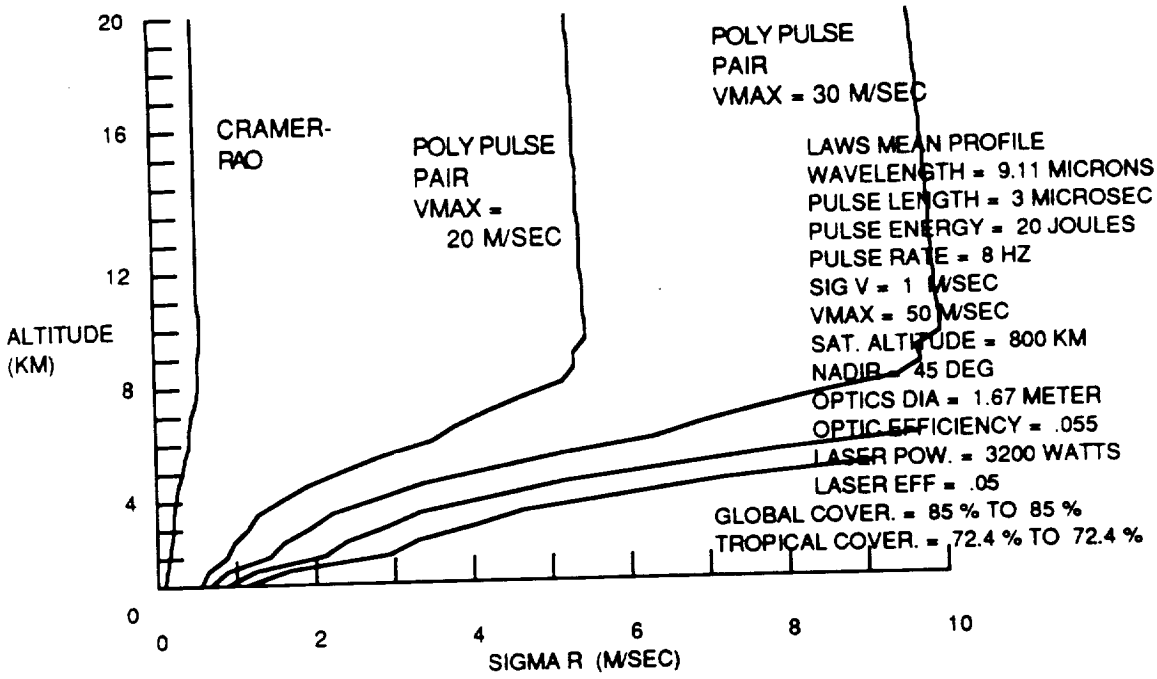

Figure 4-22. Estimate of Velocity Accuracy by Selected Velocity Resolution Estimators for 800 km Orbit

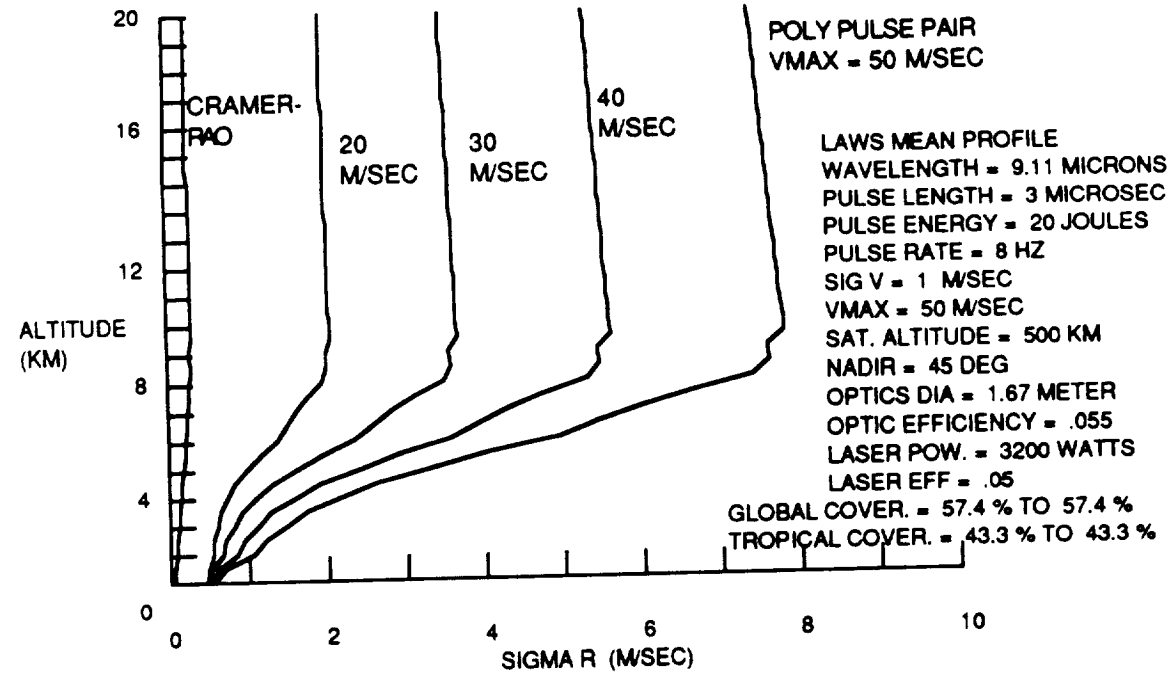

Figure 4-23. Estimate of Velocity Accuracy by Selected Velocity Resolution Estimators with Satellite Altitude Reduced to 500 km

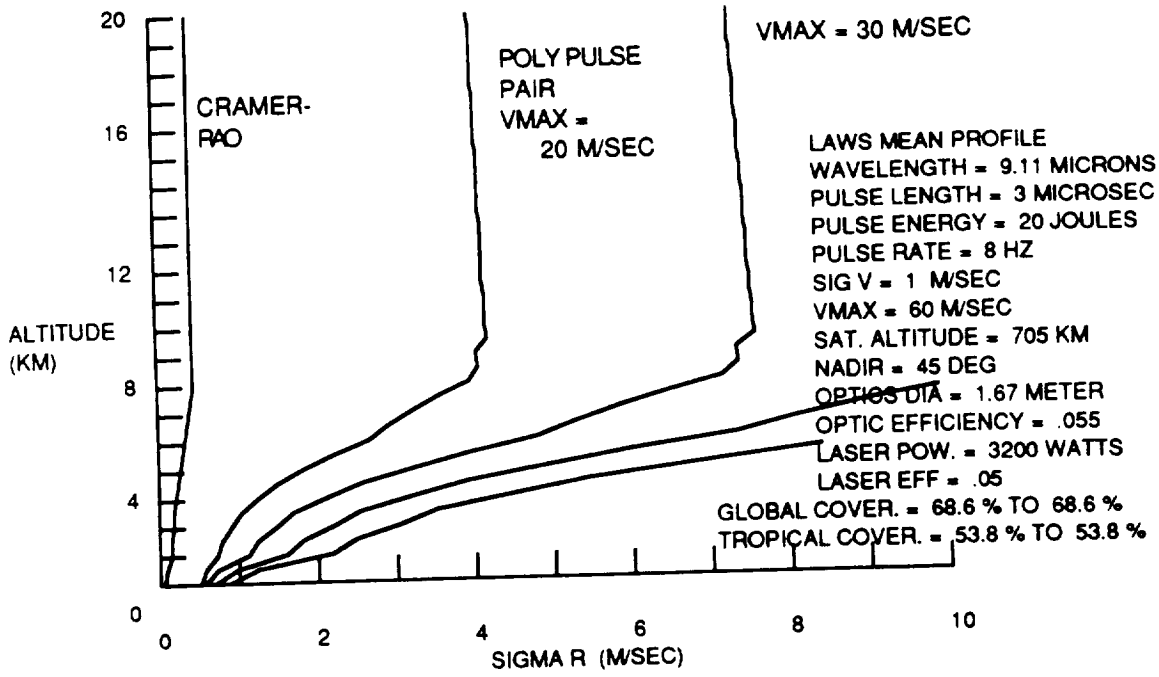

Figure 4-24. Estimate of Velocity Accuracy by Selected Velocity Resolution Estimators with Satellite Altitude Reduced to 705 km

4.4.6.1 Azimuth Angle Shot Management

There are two reasons for designing the pulse rate as a function of azimuth angle around the scan. The first reason is that for a uniform pulsing rate, the surface area of the globe represented by one pulse is proportional to the cosine of the scan angle. Thus, 50 percent of the shots would be spent on the outer 14 percent of the swath, and the accuracy of resolution into u, v components is poorest in that part of the swath. Clearly, in a shot limited system, this is not an efficient use of available shots.

The second and less significant reason for shot management around the scan is an attempt to match shots from the forward-looking and aft-looking scan. Shot matching is particularly valuable where u, v components are the desired end products. Because of the time lapse between the forward-looking shot and the aft-looking shot, and because of the impossibility of matching shots at more than one measurement altitude, there is clearly a limitation on the value of shot matching. However, shot matching is desirable if it does not place excessive constraints on other system characteristics.

Given both of these considerations, the recommended scan patterns are shown in Figure 4-25. The time for completion of the scan is 8.94 sec (i.e., 6.7 scans/min). The

squares in Figure 4-25 represent a burst mode (3200 W average laser input power with a 20 percent margin) scan pattern, and the circles represent a nominal (2000 W average laser input power) scan pattern. The left side of the figure shows how the resulting intersection points fill out the 100 km by 100 km grid squares. For the first two 100 km by 100 km grids normal to the satellite trajectory, measurements are line-of-sight only (i.e., no dual vector measurements). As shown in the next section, errors in reconstruction of u and v components would be very large. The burst mode scan pattern and nominal scan pattern are selectable by latitude or on command from the ground according to wind fields or cloud cover patterns that may exist in a particular area of interest.

It is noted that the selection of scan parameters presented in this section is a result of minimizing line-of-sight velocity error and the resultant 20 J per pulse. If the knowledge of velocity accuracy were formally stated as a system requirement and/or it were determined that 20 J per pulse could not be achieved. For example, if the pulse energy were to decrease to 10 J, the pulse rate would double, and a scan rate of 8.94 scans per

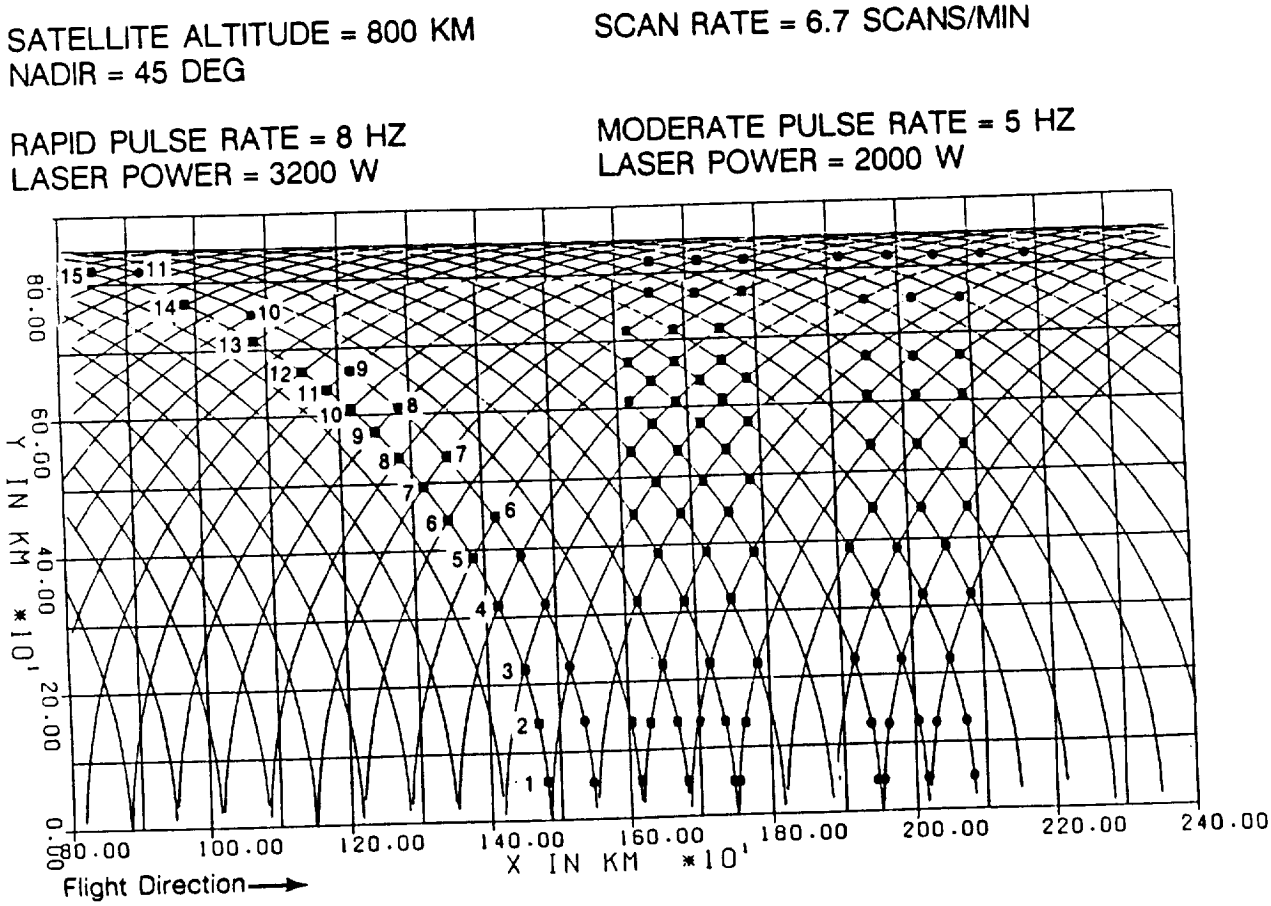

Figure 4-25. Azimuth Controlled Pulsing

of 8.94 scans per minute would be more appropriate. However, as shown earlier, the error in the data averaged over a 100 km by 100 km grid would increase.

4.4.6.2 Orbit Latitude Shot Management

Figure 4-26 shows two successive swaths on a polar orbit. The swaths begin to overlap north of 52 deg north latitude. Since polar wind data may be less valuable than tropic wind data, this condition creates the possibility of orbit latitude shot management. Shots which are near the center and edges of the swath are eliminated first because they are the points for which u, v resolution errors are largest. The yellow and green areas in Figure 4-26 show the areas covered by each swath. The areas shown as white under the yellow and green swaths are covered by adjacent swaths not shown explicitly in the figure.

The elimination of overlapping points near the poles permits more efficient allocation of laser power around the orbit. Figure 4-27 shows allocation of laser power around one quarter orbit. The laser is operated at 3200 W input power from the equator to 31 deg latitude, and at decreasing scan-averaged power to the poles. The average laser input power for the quarter orbit is 2000 W. This assumes a conservative 5 percent laser efficiency and provides a 10 percent laser input power contingency. If the laser efficiency is increased or the contingency is reduced, the overall instrument power requirement can be reduced.

4.4.7 Pointing Knowledge

Figure 4-28 represents a Monte Carlo simulation of the reconstruction of horizontal wind components from the two line-of-sight velocity component measurements. The line-of-sight measurements are given an error (3σ) of 1.5 m/sec. The numbers on the right of the figure give the standard deviation of the u and v components for each 100 km increments normal to satellite trajectory.

Figure 4-29 shows the same information as Figure 4-28 but with a 100 μrad (3σ) error introduced into beam pointing. The figure shows that overall errors are increased only slightly. Figure 4-30 shows the same information but with a 500 μrad (3σ) error introduced into beam pointing. Errors due to beam pointing are now significant. The conclusion of this analysis is that pointing knowledge should be less than 100 μrad (3σ). Based on current technology, this is not a severe constraint.

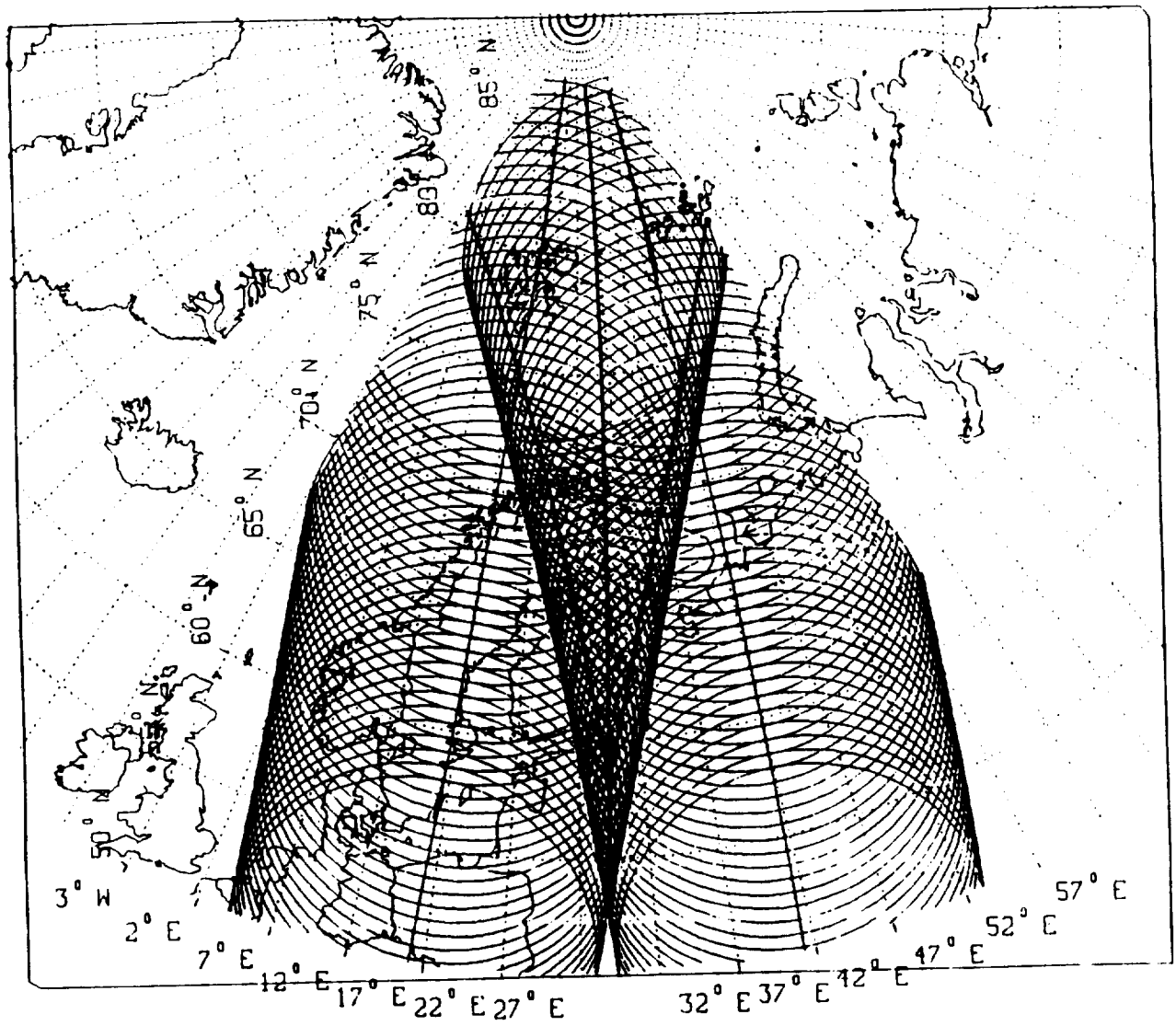

Figure 4-26. Scanning and Latitude Shot Management

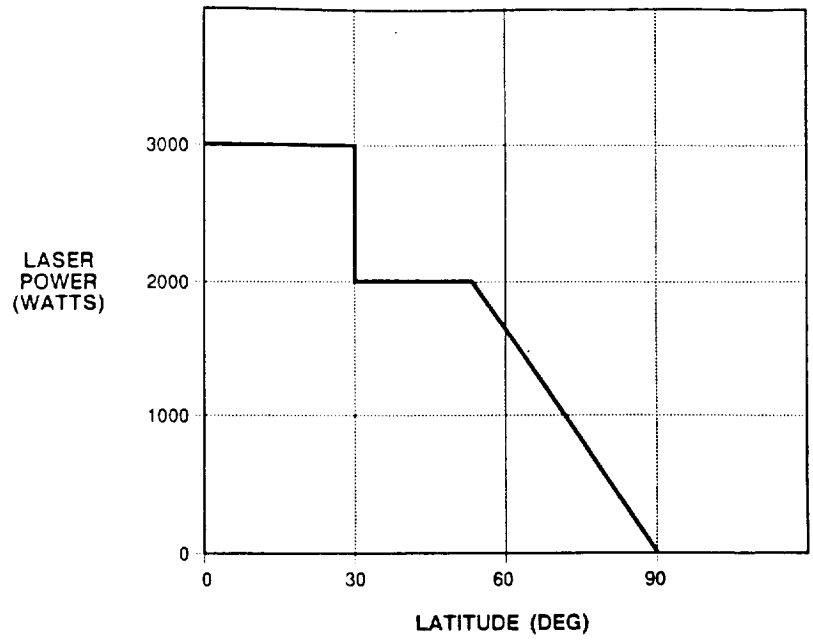

Figure 4-27. Allocation of Laser Power Around One Quarter Orbit

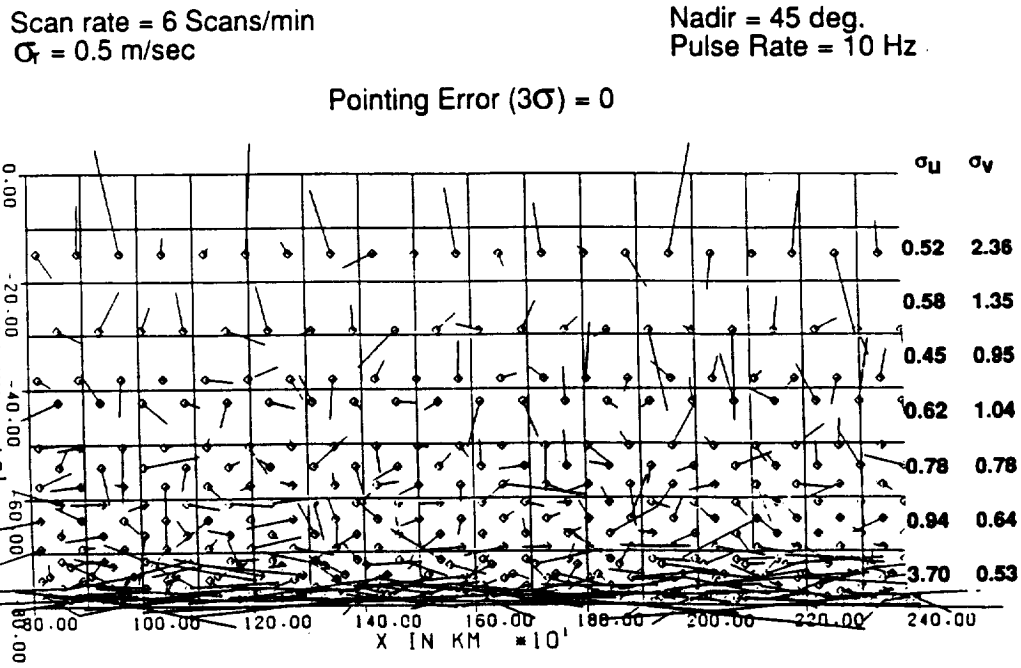

Figure 4-28. Velocity Errors from Monte Carlo Simulation

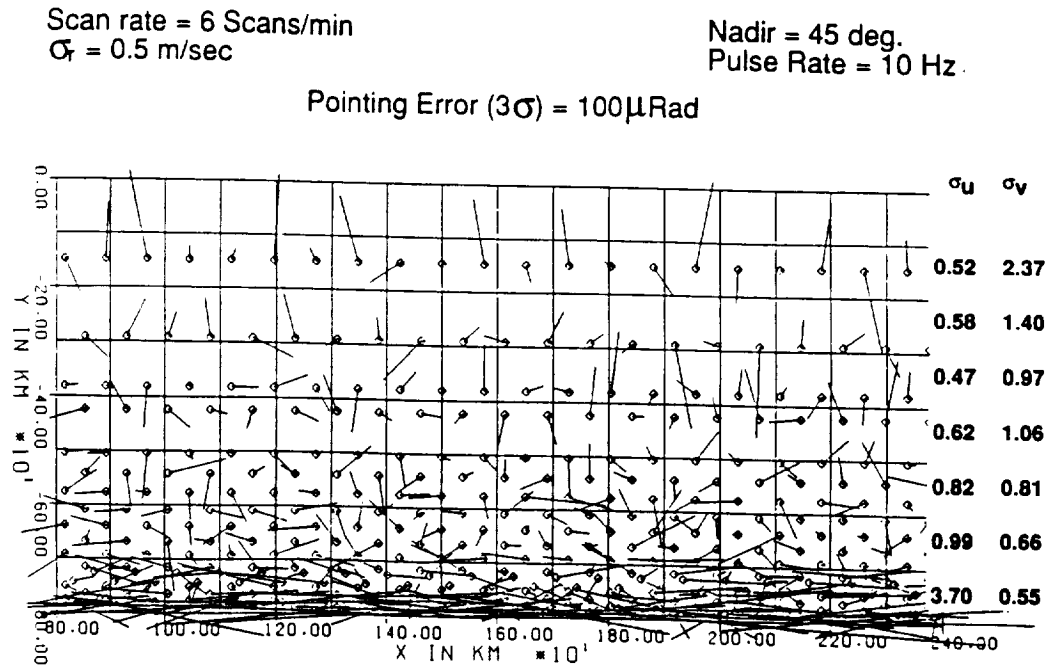

Figure 4-29. Effect of Pointing Errors on Velocity Error

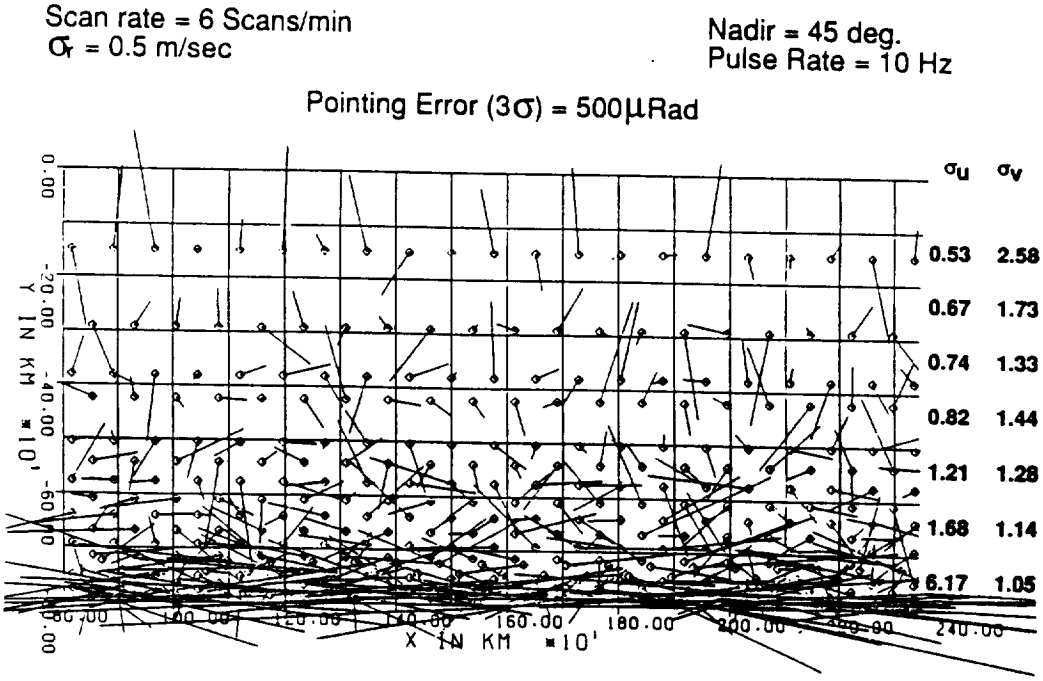

Figure 4-30. Effect of Pointing Errors on Velocity Error

4.4.8 Pulse Length/Sample Window Length Effects

A generic coherent lidar sensor simulation has been developed under a Lockheed Independent Development Effort. This simulation combines lidar hardware/software characteristics with atmospheric characteristics to determine expected sensor output as a function of the several variables. Hardware variables include laser pulse length and shape, analog-to-digital converter dynamic range and digitization rate, signal level and noise, satellite altitude, and off-nadir look angle. Software variables include processing window length and maximum processed data altitude. Atmospheric variables include wind profile (i.e., gradients), attenuation coefficient profile, aerosol distribution profile, and turbulence level.

Outputs of the simulation currently include the standard deviation of the calculated wind field at each altitude. In order to obtain this statistic, the simulation generates 25 pulses along each line of sight to provide a statistical basis for the output data. Multiple pulses along the identical line of sight are not possible in the real world. However, in this generic simulation, multiple pulses along each line of sight allow development of a statistical data base for comparing different system and processing parameters. Using this approach, the following simulation output parameters are plotted as a function of altitude above the ground:

1. Line-of-sight measured velocity with mean and ±1 sigma profiles compared to the operator entered winds
2. ±1 sigma line-of-sight velocity error profiles using an FFT estimator for the instrument measured winds
3. percent of measurements which fall within 1 m/sec at each altitude
4. turbulence of the last of the 25 pulses
5. SNRs.

Figure 4-31 is a tabulation of simulation runs performed with input parameters which are relevant to LAWS. Additional runs will be performed as the simulation is upgraded and as additional LAWS hardware/software questions arise.

Among some of the more relevant issues addressed by using the simulation to model LAWS data are those of pulse length and processing window length. (The simulation monitors detected amplitude/phase returns from particle groups created at intervals of half the distance light travels between the A/D samplings.) The chart presented in Figure 4-31 shows that pulse lengths of 1.6, 3.2 and 6.4 μsec were modeled with sampling windows varying from 32 to 256 A/D samples. (For the modeled 20 MHz A/D, a

Test No.	Window Size	Pulse Length	Noise Level	A/D Bits	Zig-Zag vs Const. Grad.	No Cloud vs Thin Cirrus
2	64	3.2	10	12	CG	NC
2	64	3.2	10	12	CG	NC
3	64	3.2	10	8	CG	NC
3a	64	3.2	10	6	CG	NC
4	64	3.2	3	6	CG	NC
4	64	3.2	3	12	CG	NC
5	64	3.2	1	12	CG	NC
5	64	3.2	1	12	CG	NC
6	256	3.2	10	12	CG	NC
7	128	3.2	10	12	CG	NC
8	32	1.6	10	12	CG	NC
9	128	6.4	10	12	CG	NC
12	64	3.2	10	12	ZZ	NC
12	64	3.2	10	12	ZZ	NC
16	256	3.2	10	12	ZZ	NC
17	128	3.2	10	12	ZZ	NC
18	32	1.6	10	12	ZZ	NC
19	128	6.4	10	12	ZZ	NC
28	64	1.6	10	12	CG	NC
29	64	6.4	10	12	CG	NC
38	64	1.6	10	12	ZZ	NC
39	64	6.4	10	12	ZZ	NC
40	64	3.2	1000	6	CG	NC
50	128	1.6	10	12	CG	NC
51	128	1.6	10	12	ZZ	NC
54	64	3.2	3	12	CG	TC
55	64	3.2	1000	12	CG	TC

Figure 4-31. Tabulation of Simulation Runs

sample window of 32 is matched to a 1.6 μsec pulse length. A/Ds with higher sample rates, e.g., 50 MHz, can be modeled with considerably increased computer run time.) These parameters were tested with both a constantly varying wind profile and with a profile which zig-zags with altitude (standard LAWS wind profiles from Simpson Weather).

Figure 4-32 provides a sample of several of the outputs from the simulation. Four types of plots are depicted, all with parameters as a function of distance above the earth

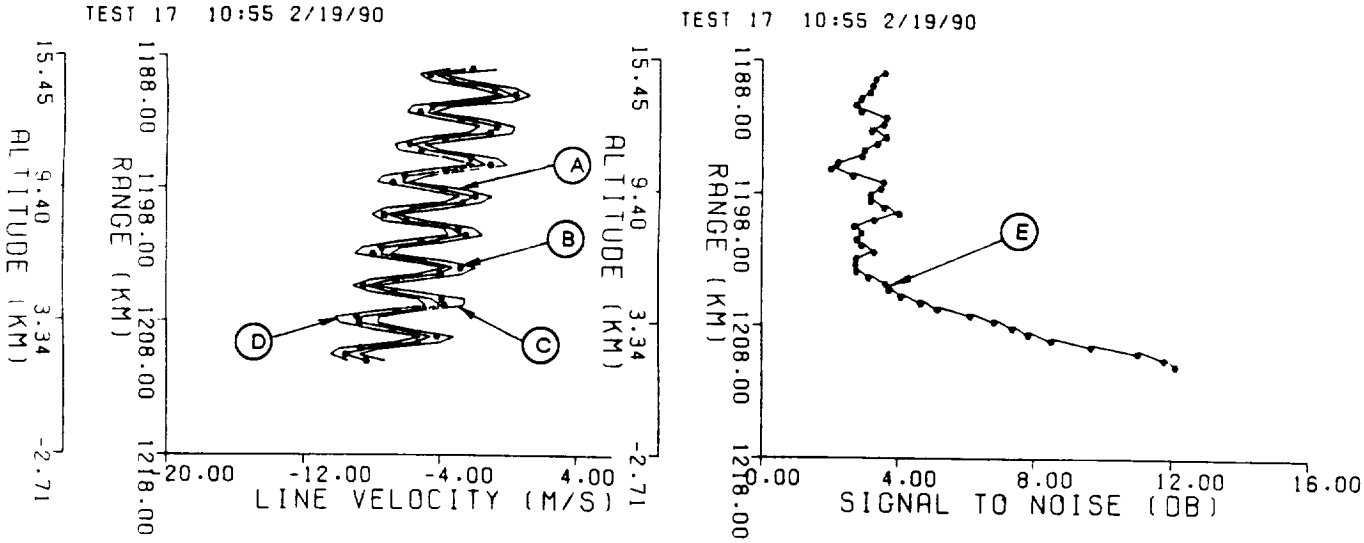

(A) The center line is the mean line of sight real wind.
(B) The "*" are the mean line of sight doppler wind.
(C) The maximum velocity line is the plus three sigma line of sight doppler wind from the "*".
(D) The minimum velocity line is the minus three sigma line of sight doppler wind from the "*".
(E) The data on this frame is plotted as signal to noise vs range from satellite. The data is shown for each sampling window.

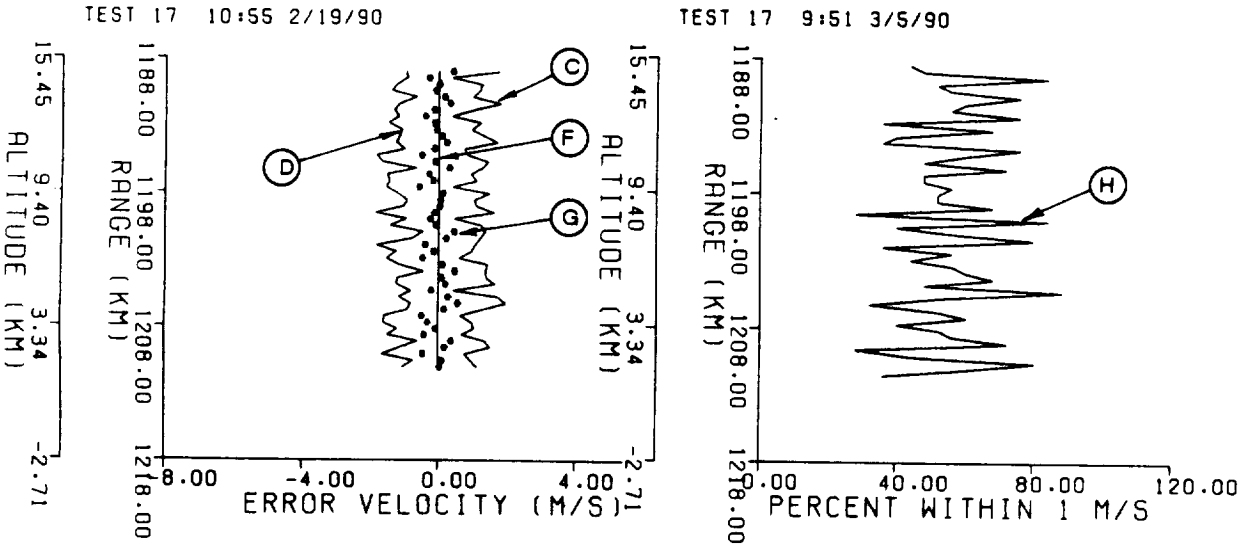

(F) The zero velocity line is the mean line of sight real wind relative to itself.
(G) The "*" are the mean line of sight doppler wind relative to the mean line of sight read wind.
(H) The data on this frame is plotted as percentages of measured line-of-sight velocities which are within on meter/sec of the simulated line-of-sight velocity at each altitude.

Figure 4-32. Data Plots of Simulated LAWS Parameters for 3.2 μsec Pulse and Double Length Sampling Window (Window size = 128)

(altitude) and distance from the satellite (range). The upper left hand plot is a line-of-sight velocity comparison of simulated doppler measured data versus simulated actual data. For this case, we use the zig-zag wind profile. The central line in the plot is the mean actual line-of-sight wind velocity, and the dots represent the measured mean velocities (from the simulated 25 shots) at each altitude. The jagged lines to the left and right of the dots are, respectively, the negative and positive 1 sigma measured Doppler velocity deviations.

The upper right hand plot is relative SNR versus range (or altitude) for the subject data. For the selected simulation cases, a constant noise level was picked. The noise level is selected as a function of the average field squared and an operator entered S/N value (chosen as 10 in the above cases). The constant noise level results in a varying S/N over range according to the backscatter and attenuation profiles.

The lower left hand figure is similar to the figure above it except the mean line-of-sight wind is normalized at zero, and the other parameters are plotted around this. Note that the (error) velocity scale is expanded.

The lower right hand plot is a plot of the percentage of data points (within the 25 imaginary shots) whose error values are within one m/sec. This value could have likewise been chosen as 2,3,5 etc. m/sec. One m/sec was chosen since it is the lower tropospheric LAWS accuracy requirement.

The window length for processing the data in Figure 4-32 is twice the pulse length; i.e., window length = 128 samples, and pulse length = 3.2 μsec. Cases were run with the pulse length varying from 1.6 to 6.4 μsec and window lengths varying from 32 samples (matched to the 1.6 μsec pulse) to 256 samples.

With the zig-zag wind velocity profile, the effect of varying the sampling window length can be seen in Figures 4-33 and 4-34. In Figure 4-33, the sample window size matches the pulse length, while in Figure 4-34 the window is four times (x4) the pulse length. The effects of these window sizes can be seen in the plots. Figure 4-32, which shows the pulse length and window matched, provides the largest percentage (mean value above 60 percent) of points with velocity errors of less than 1 m/sec. For the sample window of two times the pulse length less than 60 percent of the points have errors less than 1 m/sec (Figure 4-32). Figure 4-34 shows the largest sample window, and the results degrade further for this zig-zag wind profile. These plots also display turbulence levels.

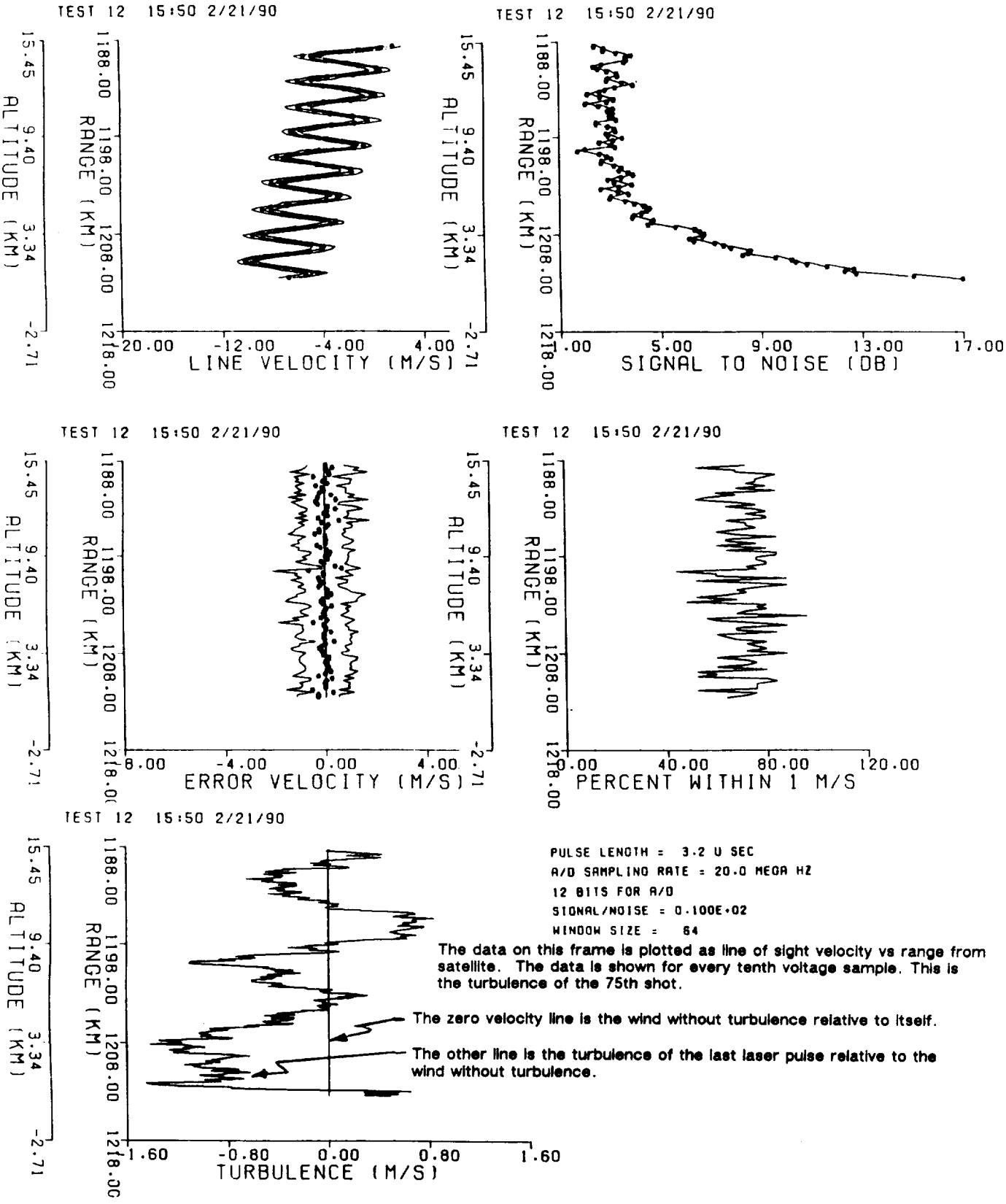

Figure 4-33. Data Plots for Zig-Zag Wind, 3.2 μsec Pulses and 3.2 μsec Sample Window (Window size = 64)

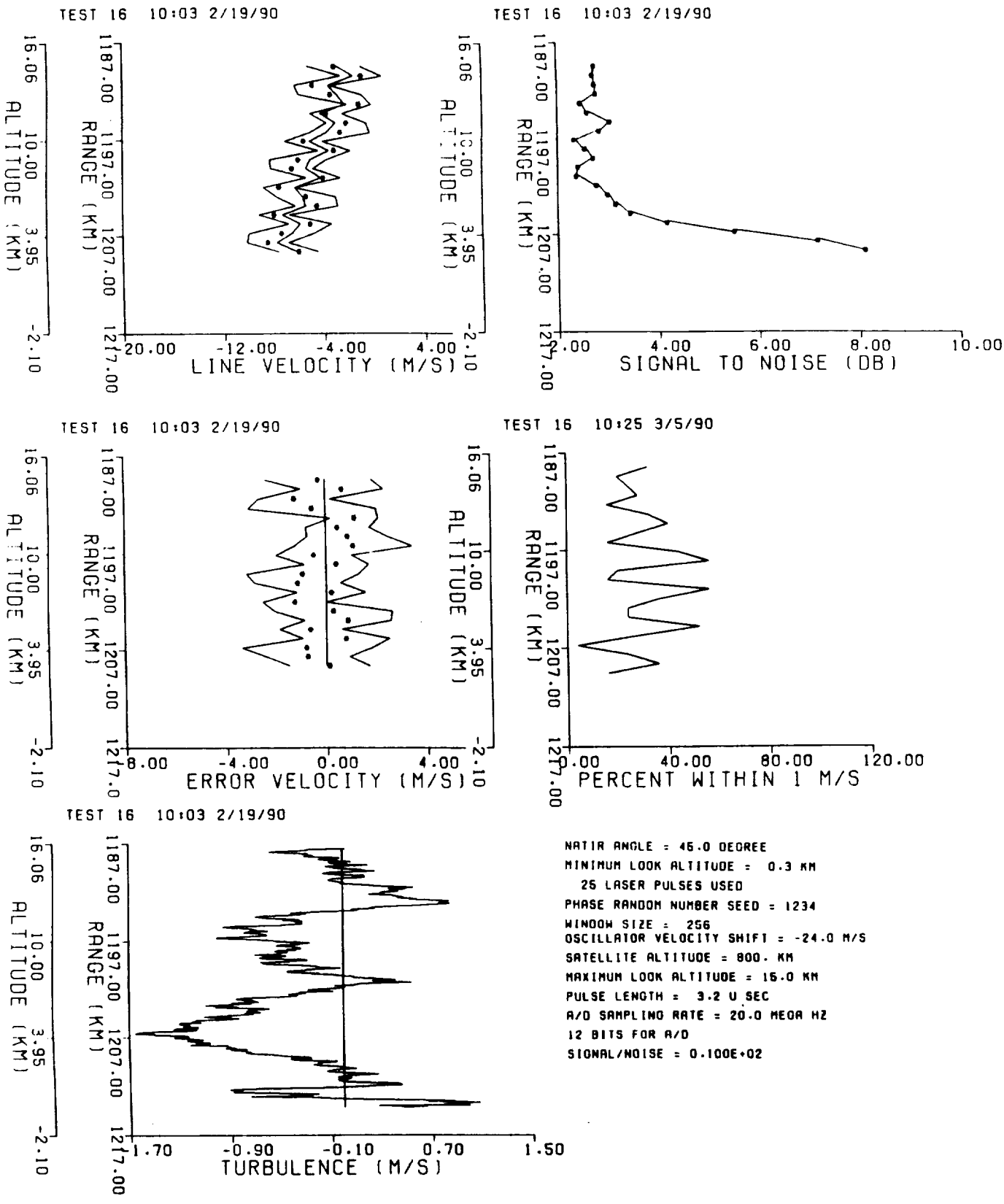

Figure 4-34. Data Plots for Zig-Zag Wind, 3.2 μsec Pulses and 12.8 μsec Sample Window (Window size = 256)

In Figures 4-33 and 4-34, a plot of turbulence versus altitude is added in the lower left-hand corner. An independent turbulence profile was used for each of the 25 laser shots. The turbulence profile displayed corresponds to the last of the 25 laser shots. The turbulence level relates to the decorrelation time for the laser pulse backscattering off the atmosphere aerosols.

The contrast between the zig-zag and continuous gradient velocity cases for the same pulse and processing parameters is apparent in Figures 4-35 through 4-37. Figure 4-35 corresponds to Figure 4-32; Figure 4-36 corresponds to Figure 4-33, and Figure 4-37 corresponds to Figure 4-34. For the continuous gradient case (i.e., non zig-zag), the longer the sampling window, the larger the percentage of the values within the 1 m/sec error band. Likewise, the standard deviation of the error decreases with the longer sample window. In the longest window case, almost 100 percent of the points have errors of less than 1 m/sec.

Two long pulse cases are presented for comparison, both with 6.2 μsec pulses and 128 sample window sizes (matched to pulse length). For the zig-zag velocity case (Figure 4-38) the mean of the percentage of points within 1 m/sec is approximately 55 percent; while with the continuous gradient winds (Figure 4-39), between 90 and 100 percent of the points lie within the 1 m/sec error bound. For the continuous gradient winds, this is slightly better than the 3.2 μsec pulse with a times two receiver sample length, but not quite as good for the 3.2 μsec pulse with the times four receiver sample length. For the zig-zag wind case, it is comparable with the 3.2 μsec window with a times 2 sample window but not as good as with a matched window.

Shorter pulse cases have also been examined. The shorter pulse cases allow more independent samples per pulse without overlapping the sample windows. Figure 4-40 depicts data from simulations of shorter pulses (1.6 μsec) with sample window lengths varying from 32 samples for the cases at the top of the figure (matched to the pulse length) to 64 samples at the middle of the figure and finally to 128 samples for the cases at the bottom of the figure. With the zig-zag profiles of Figure 4-40(1 of 2), the percentage of points within 1 m/sec improves between the top case (matched receiver window) to the middle case (x2 receiver window length) and then degrades again for the bottom case. For the bottom case with the x4 window (i.e., 6.4 μsec), the window length overlaps reversals of the wind gradient and thus degrades the accuracy of the results.

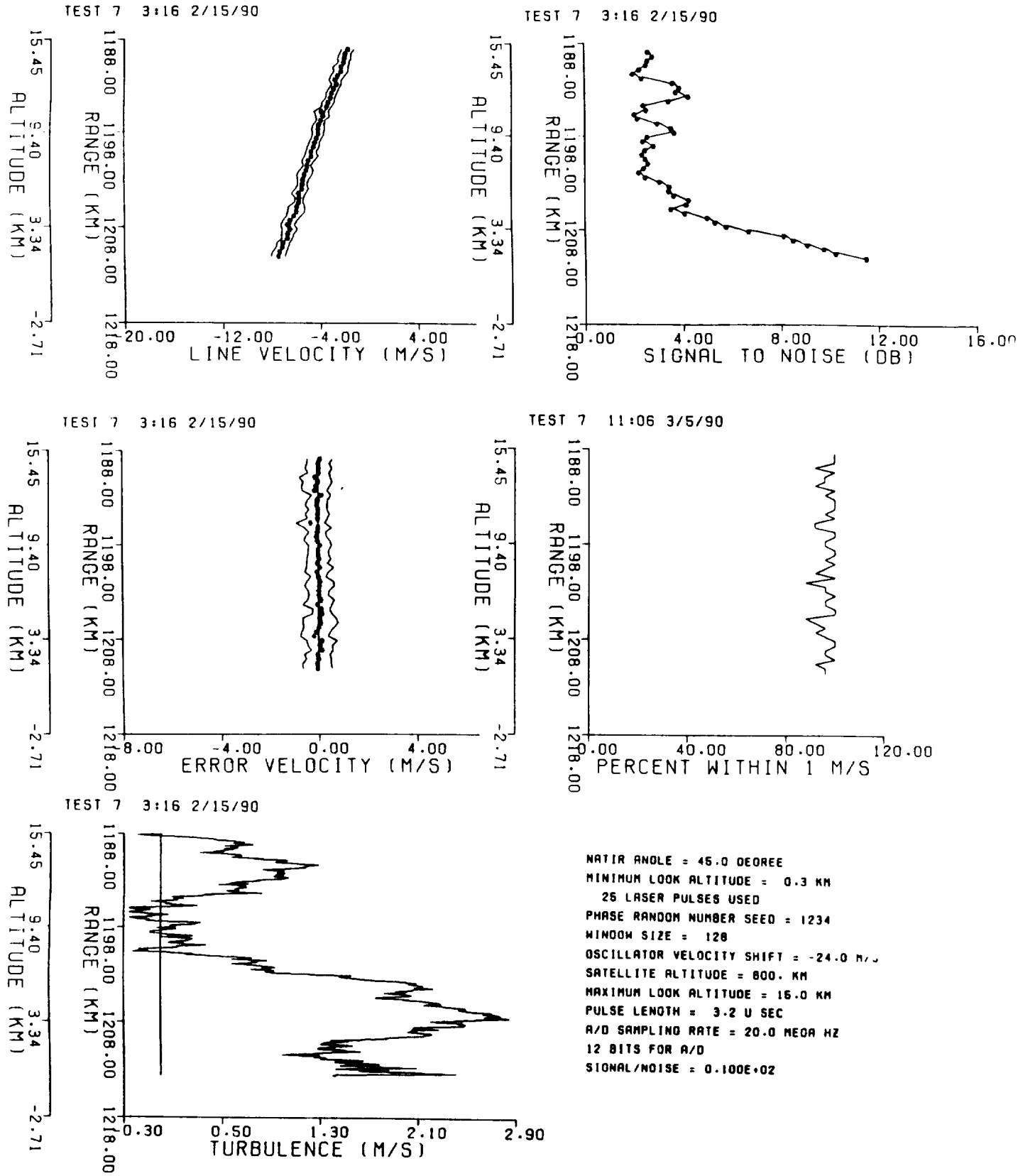

Figure 4-35. Data Plots for Constant Gradient Wind, 3.2 μsec Pulses and 6.4 μsec Sample Window (Window size = 128)

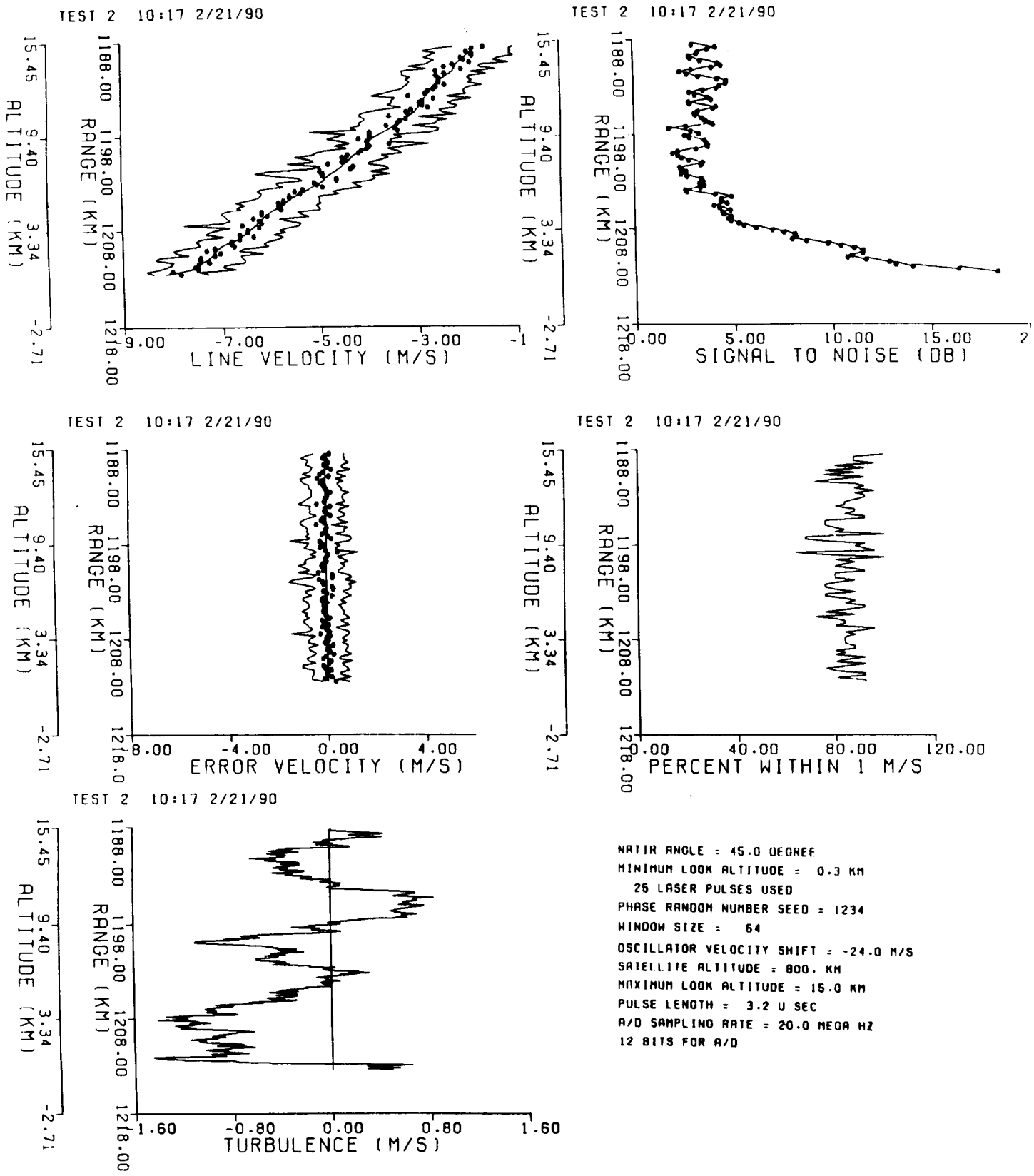

Figure 4-36. Data Plots for Constant Gradient Wind, 3.2 μsec Pulses and 3.2 μsec Sample Window (Window size = 64)

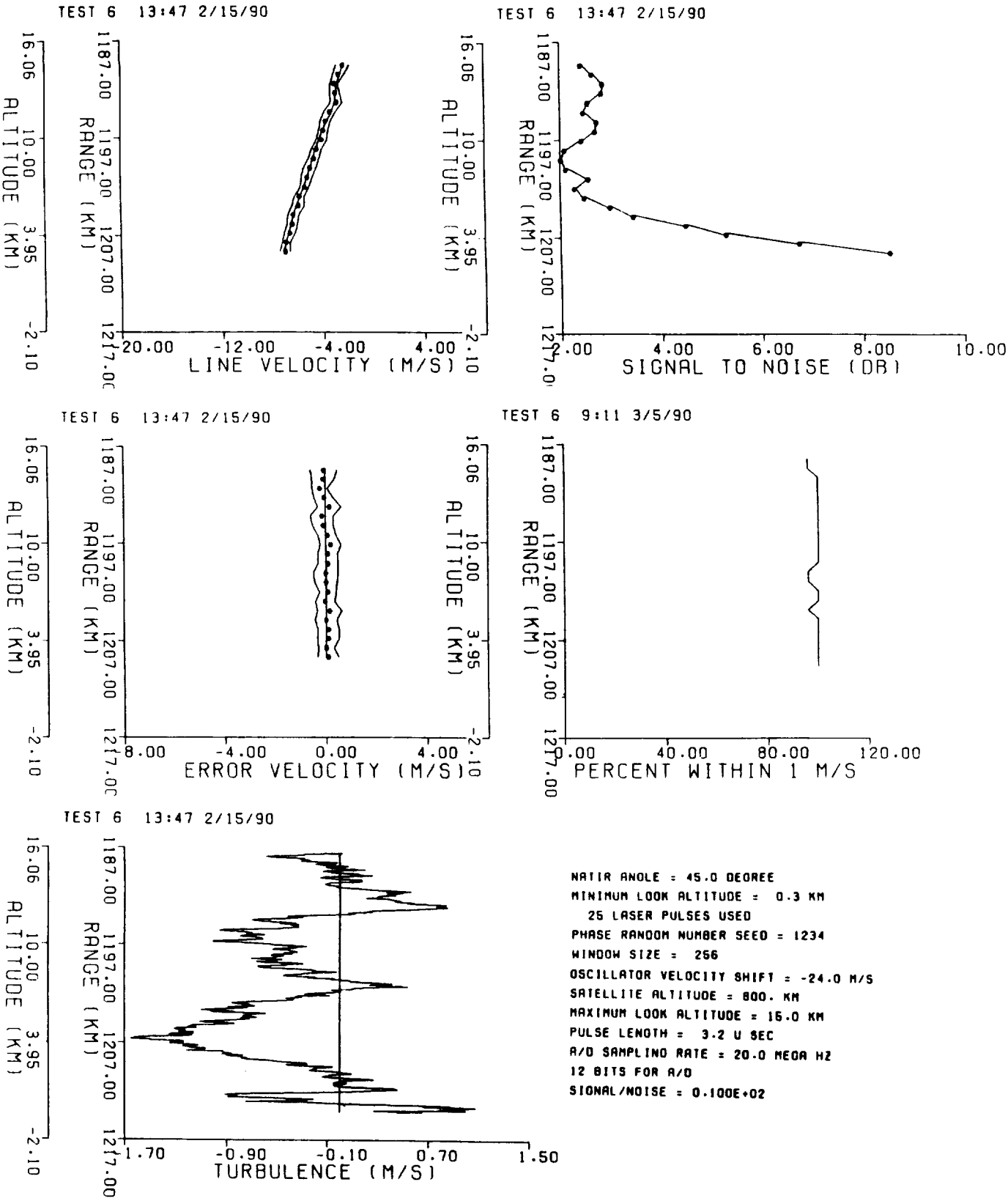

Figure 4-37. Data Plots for Constant Gradient Wind, 3.2 μsec Pulses and 12.8 μsec Sample Window

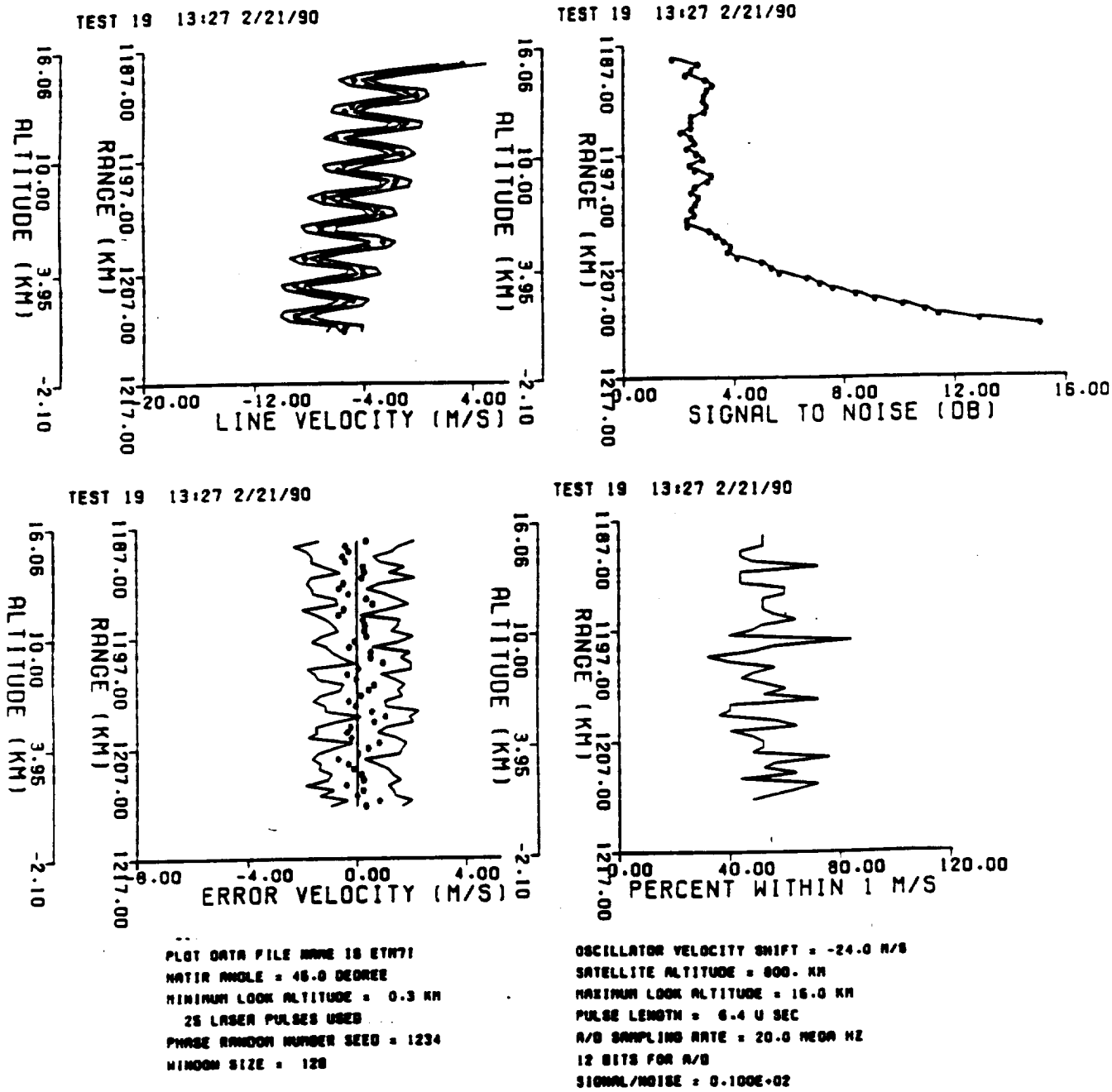

Figure 4-38. Long Pulse (6.4 μsec) with Zig-Zag Wind Profile and Matched Window

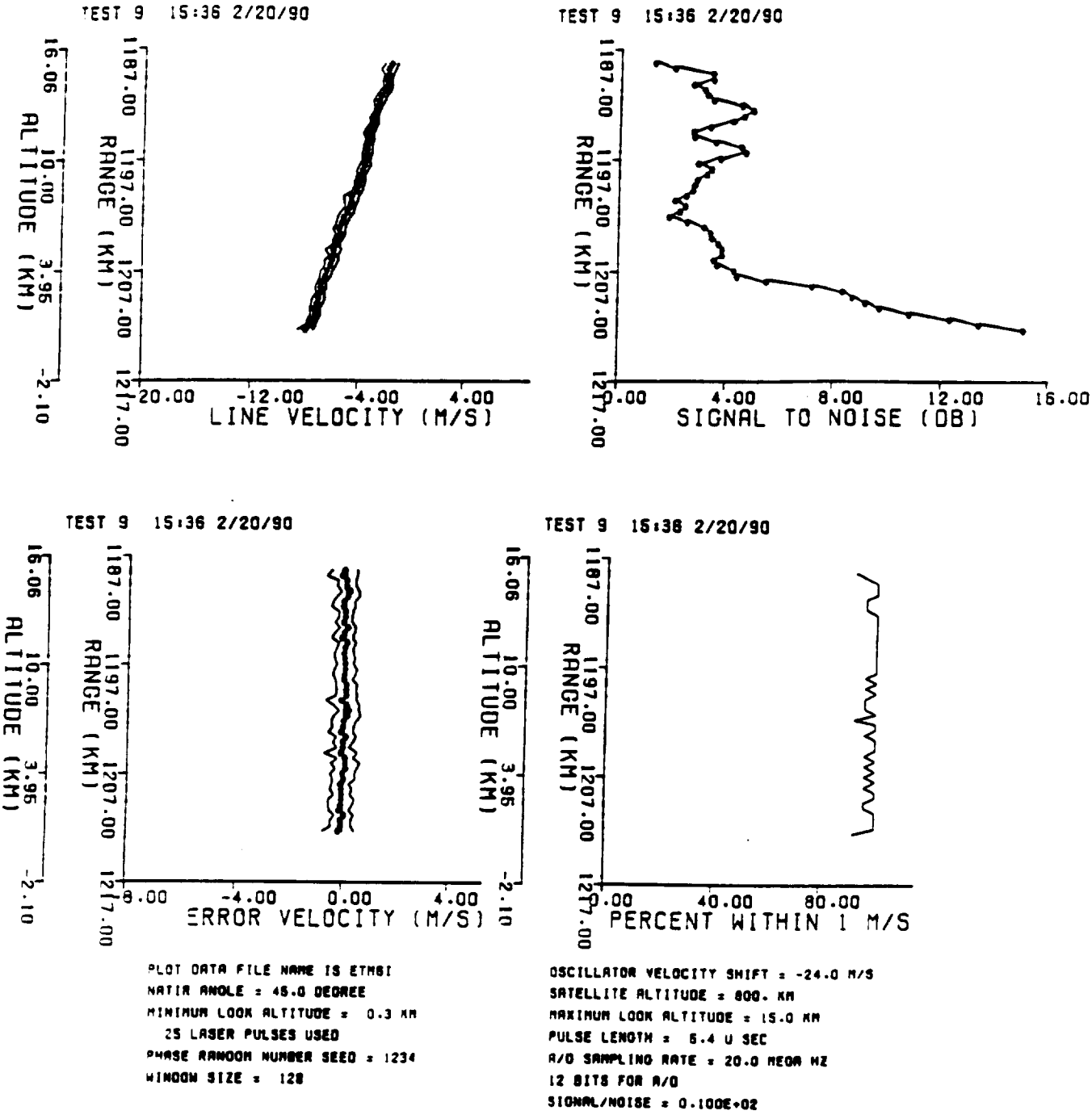

Figure 4-39. Long Pulse (6.4 μsec) Data with Continuous Gradient Wind Profile and Matched Window

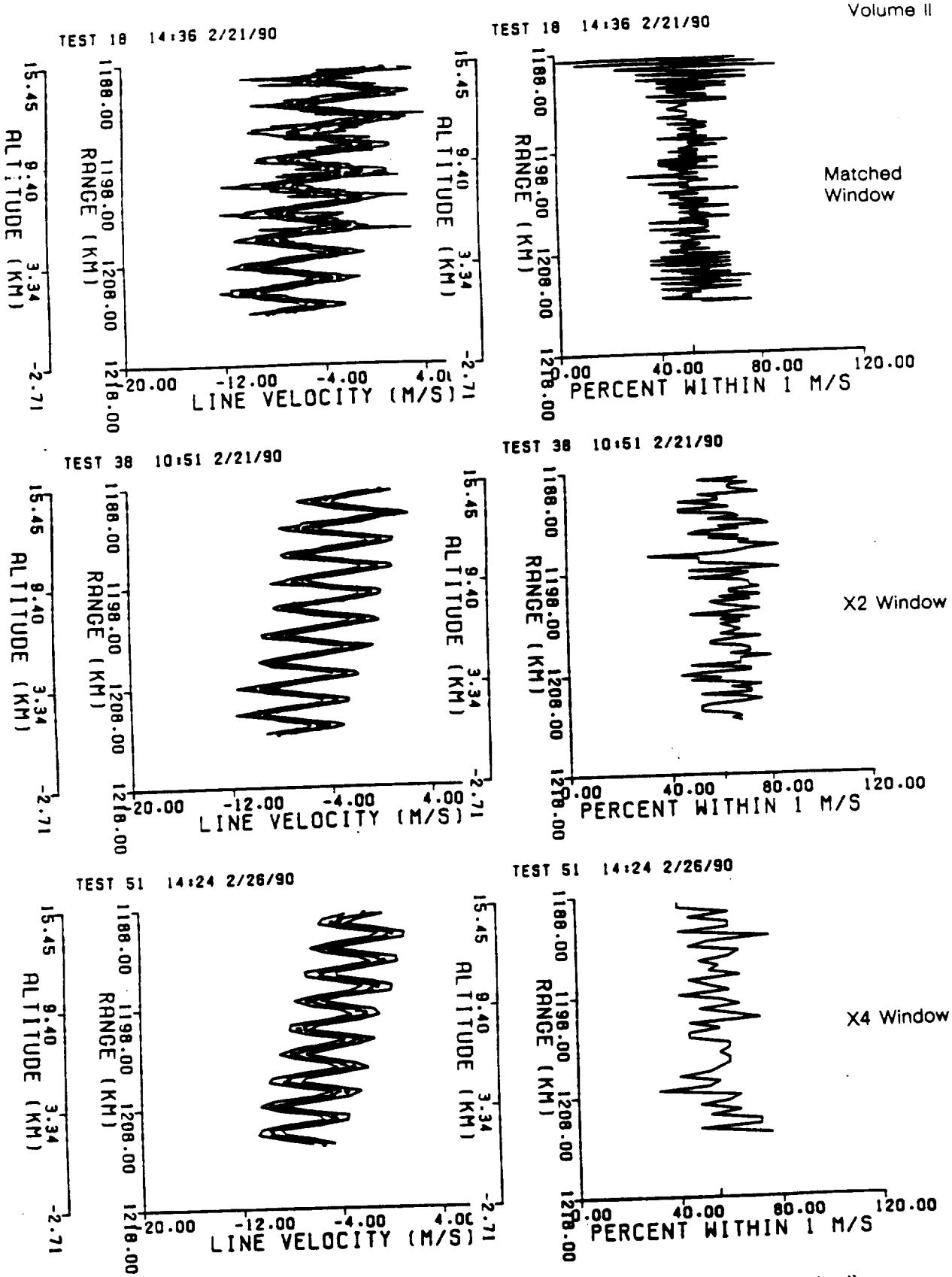

Figure 4-40. Short Pulse (1.6 μsec) and Window Lengths of 32 (matched), 64 (x2) and 128 (x4) Samples (1 of 2)

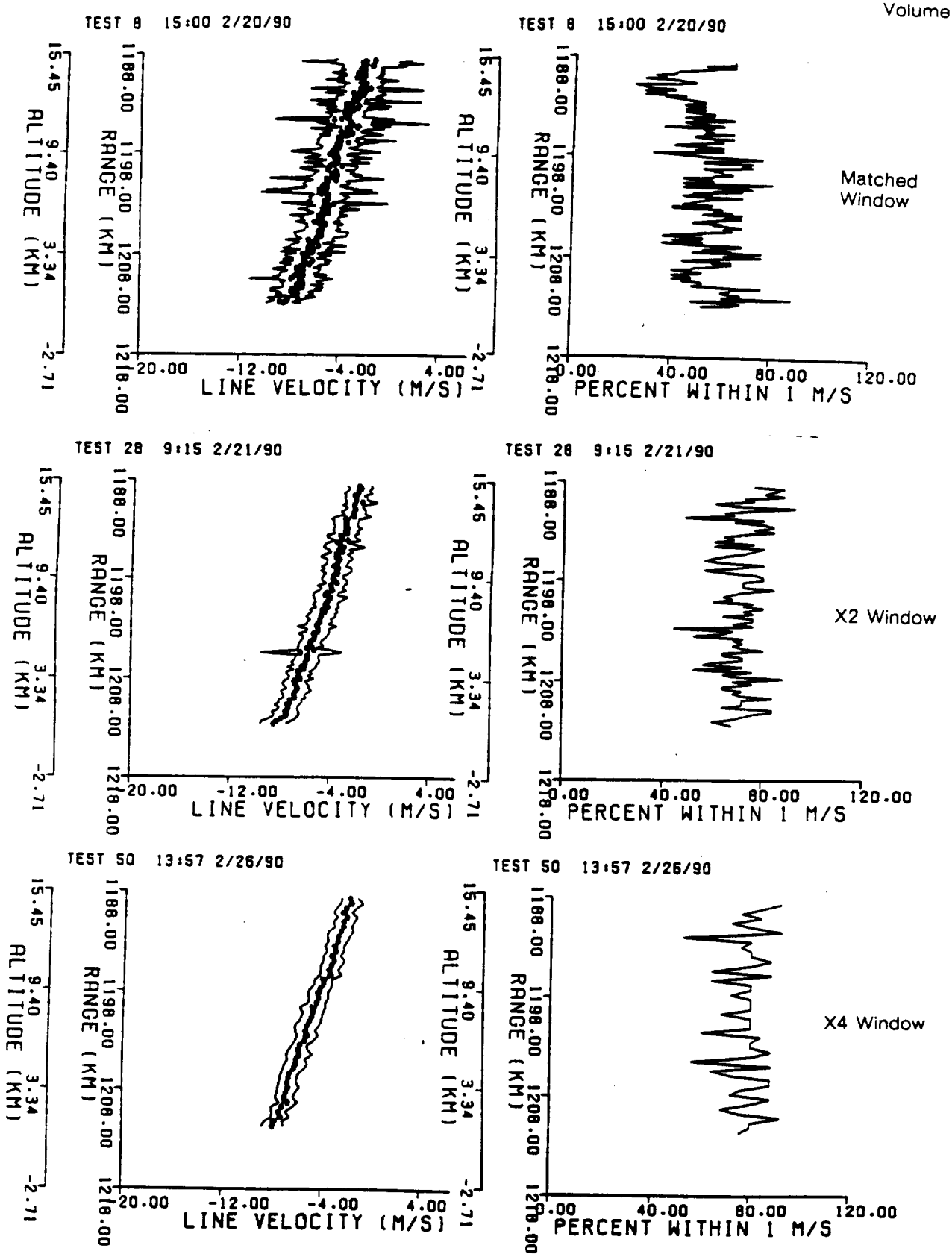

Figure 4-40. Short Pulse (1.6 μsec) and Window Lengths of 32 (matched), 64 (x2) and 128 (x4) Samples (2 of 2)

For the cases where the wind velocity continuously increases with altitude with no reversals (Figure 4-39), the longer the sample window, the larger the percentage of points with errors within the one m/sec bound. However, with the short 1.6 μsec pulse (Figure 4-40), the errors are larger than with the longer pulses of Figures 4-33 and 4-39 when no wind reversals (i.e., zig-zag winds) are present. The short pulses with matched windows appear better for zig-zag winds.

Several runs were also made with both higher and lower S/N levels with truncated A/D conversion dynamic ranges (6 and 8 bits instead of 12 bits). Additional cases are being run with non-ideal pulse shapes, i.e., gain switched spikes and tails, and with thin cirrus clouds in the upper troposphere. The depicted cases were run to 15 km altitude but can be run to any selected altitude.

The FFT signal estimator was used for these runs. According to Anderson (Ref. 10), this estimator is better for the "50 percent error less than 1 m/sec" criterion than the pulse-pair estimator by approximately 4.3 dB but not as good as the Capon estimator. This simulation can be modified to include additional estimators.

4.4.9 Conclusions

Initial trade studies on LAWS Instrument performance have produced several conclusions related to optimal LAWS configuration. These conclusions have been summarized in the LAWS concept summary given in Section 4.2 of this report and the principles of concept design given in Section 4. Numbers shown in these sections are current estimates of best values but are subject to change with further investigation.

Response from the LAWS Scientific Panel is both appropriate and required. In particular, their views on the most appropriate trade between data coverage and data quality are desired.

4.4.10 References

1. J. Bilbro, et al., "Accommodations Assessment: Spaceborne Doppler Lidar Wind Measuring System," NASA TM 82435, George C. Marshall Space Flight Center, MSFC, AL, August 1981.
2. D. Fitjarrald, Personal Communication.
3. R.T. Menzies et al., "Altitude and Seasonal Characteristics of Aerosol Backscatter at Thermal IR Wavelengths Using Lidar Observations from Coastal California," Jet Propulsion Laboratory, Pasadena, CA, November 1988.

4. R.M. Huffaker, "Feasibility Study of Satellite-Borne Lidar Global Wind Monitoring System," NOAA Tech Memo ERL-WPL-37, Wave Propagation Laboratory, Boulder, CO, 1978.

5. R.M. Huffaker, "Feasibility Study of Satellite-Borne Lidar Global Wind Monitoring System, Part II," NOAA Tech Memo ERL-WPL-63, Wave Propagation Laboratory, Boulder, CO, 1980.

6. R.T. Menzies et al., "Altitude and Seasonal Characteristics of Aerosol Backscatter at Thermal IR Wavelengths Using Lidar Observations from Costal California," Jet Propulsion Laboratory, Pasadena, CA, 1988.

7. J. Bilbro et al., "Shuttle Coherent Atmospheric Lidar Experiment," NASA TM 100307, NASA/MSFC, 1987.

8. S.S.R. Murty, "Atmospheric Windows and Infrared Transmission," Alabama A & M University, Huntsville, AL, 1982.

9. B. Grant, "Spaceborne CO_2 Doppler Lidar Atmospheric Transmission Calculations," JPL, Pasadena, CA, 1981.

10. J.R. Anderson, "An Initial Study of the Use of High Performance Signal Processing Algorithms for the LAWS Instrument" Final Report, University of Wisconsin, Madison, WI, December 1989.

SECTION 5. RECOMMENDED LAWS CONFIGURATION

Top level requirements for the LAWS Instrument, as specified in the NAS8-37590 SOW, are given in Section 2, Table 2-1. Lockheed has developed a system concept and a system configuration that satisfy the requirements specified by NASA for a viable LAWS Instrument. These requirements are being expanded and flowed down to lower levels to specify hardware, software, support equipment, and methods to verify the satisfactory performance of the complete system.

Analysis of the NASA SOW revealed a defined organization for the LAWS system functions. This organization is shown as a functional hierarchy in Figure 5-1. Analysis of these functions resulted in the functional flow diagram for the LAWS system shown in Figure 5-2.

The objective of the LAWS Instrument is to measure and report wind data. To reach this objective, the functional activities described in Figure 5-1 are performed by allocation of tasks to various hardware elements as shown in Figure 5-2. The performance of a single function may require multiple hardware elements; for example, the establishment of the spatial position involves both the attitude determination system and flight processor. On the other hand, a single hardware element may be involved in multiple functions; i.e., the flight processor is used to generate the telescope scan position and drive rate, process the returned signal data from the detector, determine instrument position, monitor health and status of subsystems, and perform other functional activities.

Once the LAWS Instrument functions have been derived and allocated to hardware elements to accomplish these activities, the LAWS system is defined.

The LAWS Instrument configuration recommended by Lockheed provides a system which measures wind vectors from an orbiting satellite platform. These wind vectors are accompanied by earth coordinate values of geodetic latitude, longitude, and altitude plus Universal Time. These position coordinates accurately locate each lidar pulse relative to each of the twenty 1.0 km thick layers of the troposphere. Measured wind vectors associated with each of the selected altitude levels can be sorted and continuously plotted on global-scale maps.

Pulses of energy, developed by a CO_2 laser, are directed by a large aperture telescope through the troposphere to measure wind vector components at selected altitude levels above the earth's surface. Aerosol particles, suspended in the air, scatter a portion

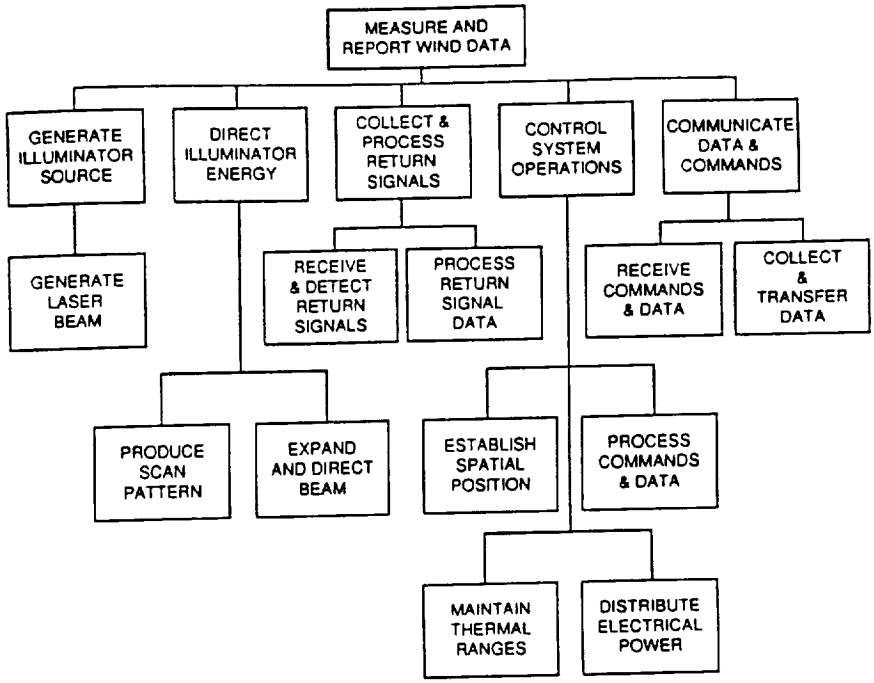

Figure 5-1. LAWS Functional Hierarchy

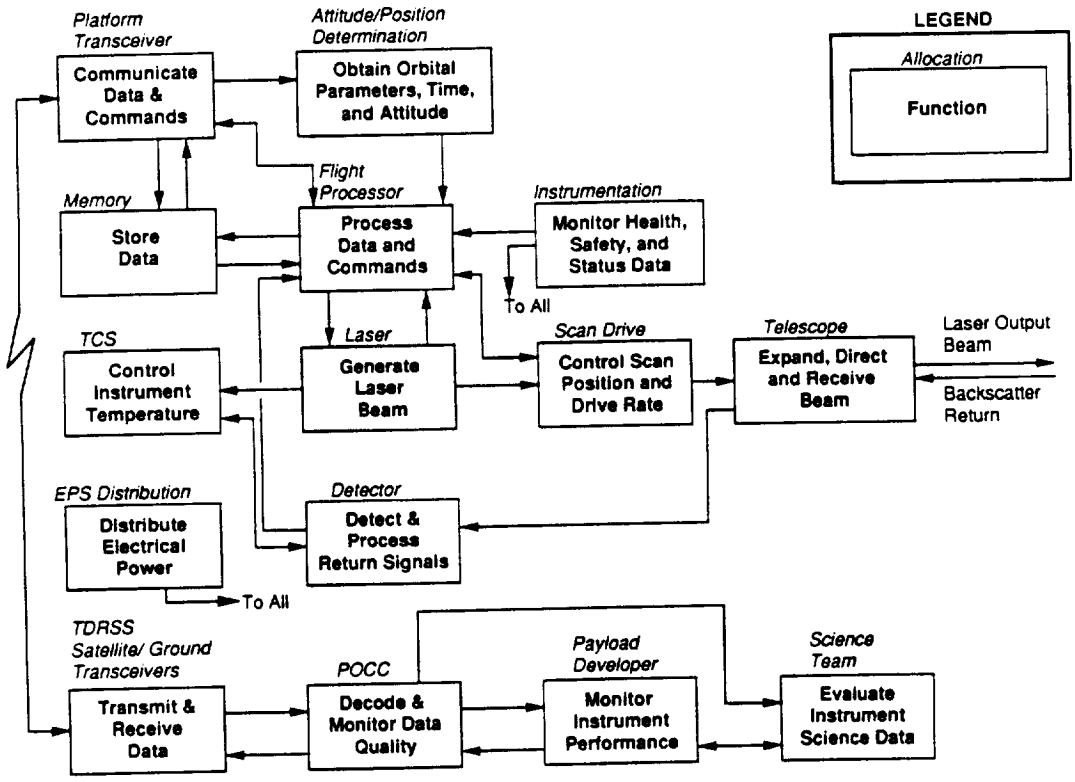

Figure 5-2. LAWS System Functional Flow Diagram

of the energy when illuminated by the laser beam. Some of this energy is backscattered and captured by the telescope. A sensitive heterodyne receiver detects the radial component of the Doppler frequency shift introduced by the relative motions of the suspended aerosol particles, the rotation of the earth under the platform, and the orbiting velocity of the LAWS platform.

When processed, the radial components of the frequency shifted signals are converted to velocity vector components. The effects of the velocity vector of the orbiting platform and the rotation of the earth with respect to the platform in its orbit are removed from the measured velocity vector components to leave only the radial components of the air mass wind vectors. Additional measurements of selected volumes of air are made from different spatial locations as the sensor platform continues along its orbit. By combining these radial velocity components in the geometry of the measurement locations, correct values of air mass movement are determined. Measurements of air mass movements quantify the values of wind velocities and directions. Earth coordinate locations and altitudes for each of the sampled air mass volumes are required, not only to permit additional samples of air mass volumes to be collected from other spatial locations, but also to plot the wind data on global charts.

5.1 LAWS SYSTEM CONFIGURATION

Lockheed has developed a system configuration to measure, collect, and update global-scale wind vector data as defined by the NAS8-37590 SOW. This configuration is comprised of six basic subsystems as shown in Figure 5-3. A description of each of these subsystems follows.

5.1.1 Laser Subsystem

The Laser Subsystem is comprised of a master oscillator and a laser transmitter. This subsystem produces pulses of laser energy that illuminate the earth's troposphere upon command and provide a reference frequency for the extraction of wind vector components from backscattered signals.

A coherent, CO_2 laser develops pulses of energy having a wavelength of 9.11 μm. Each of these 3.0 μsec wide pulses has an energy level of 20 J.

Shot management controls from the flight computer are employed to achieve optimum utilization of each laser pulse. Shot management also conserves the life of the laser and provides the capability to obtain measurements of wind vector components from selected volumes of atmosphere.

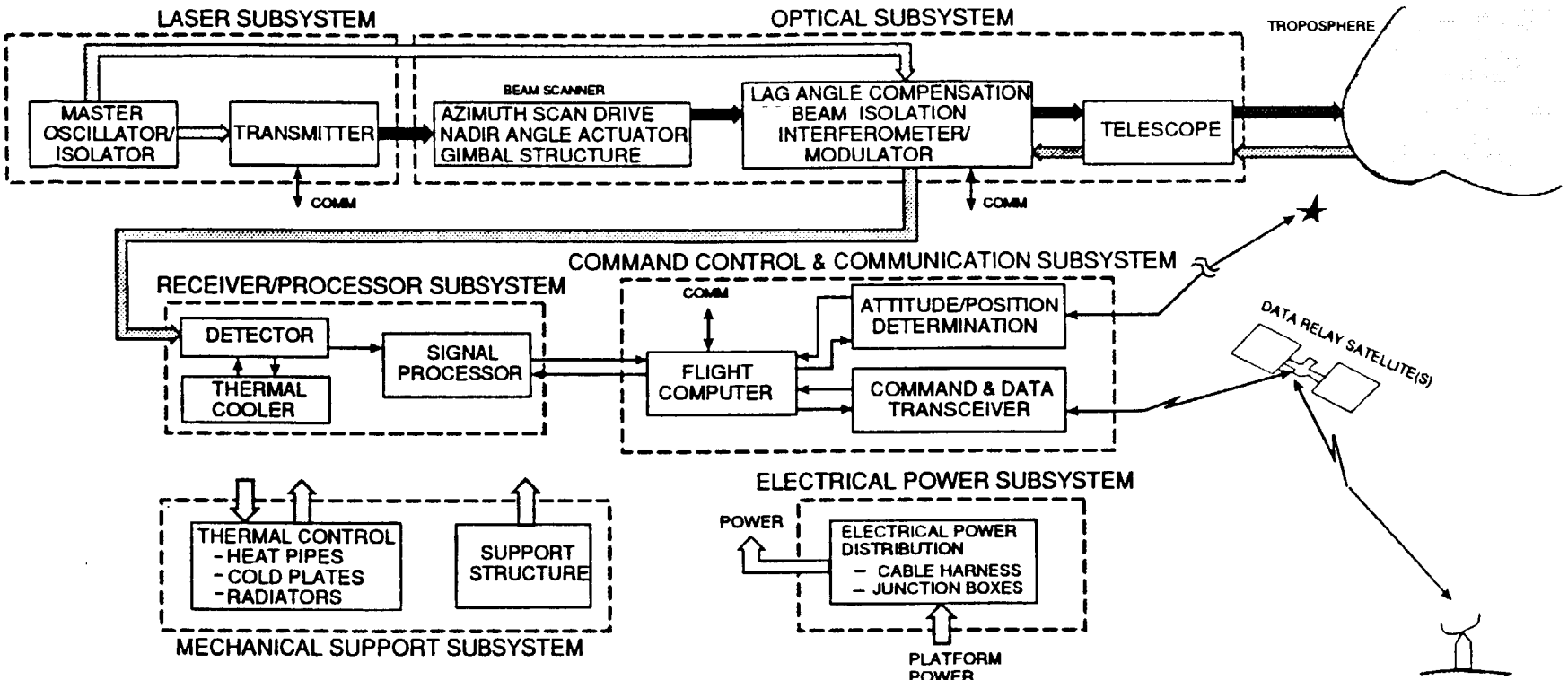

Figure 5-3. LAWS System Diagram

A highly stable, low power laser, serving as a master oscillator, is provided as an integral part of the Laser Subsystem. This isolated reference optical wavelength source permits the precise determination of the Doppler frequency shift imparted to the back-scattered laser energy by the motion of the aerosol particles in the atmosphere. The output of the Laser Subsystem is coupled to the input port of the Optical Subsystem.

5.1.2 Optical Subsystem

The Optical Subsystem is comprised of a beam scanner assembly, special purpose optical assemblies, and a large telescope. The beam scanner includes a gimbal structure that holds the telescope and provides an alignment reference, an azimuth drive motor, and an elevation angle actuator. Special purpose optical assemblies provide lag angle compensation for return signal enhancement, isolation for protection of the detectors, and an interferometer/modulator/detector to extract the Doppler shifted velocity information. The telescope directs the laser beam in a precise direction and collects returning backscattered signals.

The laser beam is expanded and directed in a pre-selected conical scan pattern by the Optical Subsystem. The elevation angle of the optical axis of the 1.67 m aperture telescope is remotely positioned by setting its gimbal to one of three selectable pointing angles. These angles are 35, 45, and 55 deg with respect to the nadir. The telescope assembly is then rotated in azimuth about the nadir at a constant angular rate to produce the conical scan pattern. Isolation is provided to prevent the high energy of the outgoing laser pulse from damaging the sensitive detector in the Receiver/Processor Subsystem.

When an elevation angle of 45 deg with respect to the nadir is selected, the outgoing laser pulse, traveling at the speed of light, reaches the upper level of the troposphere in approximately 4.07 msec from a platform altitude of 824 km. Energy from the laser transmitter reaches the earth's surface in approximately 4.18 msec. Backscattered energy from the top and bottom of the 20 km thick troposphere returns to the LAWS Instrument within the timespan of approximately 8.14 and 8.36 msec after a pulse is transmitted. If the telescope is rotating at 6 rpm, the telescope line-of-sight rotates through an arc of 5.11 mrad during the time the laser energy takes to reach the upper level of the troposphere and the backscatter signals take to return to the orbiting LAWS Instrument.

Since the diffraction limit of the telescope is only 13.1 μrad, little of the returning backscattered energy would be captured because of misalignment of the telescope

line-of-sight with the illuminated patch of the troposphere without widening the field-of-view. Lag angle compensation is therefore provided as an integral part of the Optical Subsystem to force the telescope to effectively "look back" after each transmission to capture the returning backscattered energy.

Portions of the optical system are used by both the high level laser pulses and the very low level backscattered signals. The transmitter laser produces very high energy level pulses which could destroy the sensitive detector array elements if they are not properly protected. Optical beam isolation elements are included in the optical train to prevent these high levels of energy from damaging the detector elements while not appreciably attenuating the low level backscattered return signals.

An optical interferometer mixes the received backscatter signals with a precisely controlled frequency local oscillator radiation to provide a detectable beat frequency at the receiver photodetector. One input to this interferometer is the modulated backscatter return signal. Another input is from the stable local oscillator laser in the Laser Subsystem used to beat the return signal into an acceptable BW to be detected by a 300 MHz BW detector. The output of the interferometer is directed onto the detector array in the Receiver/Processor.

A three position elevation angle actuator is employed to attach the telescope metering structure to a gimbal yoke structure. The three remotely selectable elevation angles included in the design for this actuator are 35, 45, and 55 deg with respect to the nadir. A minimum profile stow position is also provided for the launch configuration.

The gimbal yoke structure is attached to the rotating armature of an azimuth drive motor. The drive rates of this motor accommodate the planned orbital altitude requirements. The stator of the azimuth drive motor is attached to the mechanical base support structure.

5.1.3 Receiver Processor Subsystem

The Receiver Processor Subsystem consists of a photodetector, an active cooling subsystem, preamplifiers, and signal processing electronics.

A multi-element photodetector converts the output of the optical interferometer into electrical signals retaining the Doppler frequency-shifted modulation which contains the radial components of the measured wind vectors. Designs for achieving high levels of detection efficiency are being evaluated because improved efficiency is equivalent to a

higher level of laser output power and/or a larger effective telescope aperture. Active cooling of the photodetector elements to approximately 77 K is required to achieve a BW of 300 MHz and a quantum efficiency of 50 percent. The much wider BW received signal is downshafted to this range via the modulated local oscillator signal.

Low noise level preamplifiers, having sufficient bandwidth and dynamic range to accommodate the wide range of signal returns from dispersed aerosols found in different zones of the global troposphere, are used to amplify and isolate the 0 to 300 MHz outputs of each of the detector elements.

The 0 to 300 MHz output signal of the signal detector preamplifier is downshifted to 0 to 20 MHz signals. The azimuth scan angle (θ), nadir angle (α), time, and date associated with each laser shot are also used to scale and tag the geographical location of each of the input signals for the correct radial velocity vector component values. A 12 bit, 50 MHz analog-to-digital converter is employed to accommodate the wide dynamic range of the measured signal returns.

A FFT processor is included as an option to permit the transmission of limited amounts of wind velocity data for real time evaluation by members of the Science Team.

5.1.4 Command, Control, and Communication Subsystem

The Command, Control, and Communication Subsystem is comprised of a flight computer, attitude and position determination sensors, and command and data transceiver interface modules. The flight computer, applying associated software, provides autonomous direction to the LAWS Instrument, controlling when the laser is to be fired to achieve simultaneous measurements for selected wind component measurements. The flight computer also receives and executes commands from ground control, and exercises stored math models to compute the time associated with the telescope pointing angles for the laser pulses. Attitude and pointing reference sensors are provided by the platform. Outputs from these sensors to the LAWS Instrument are managed by the attitude and position determination elements of this subsystem. The command and data transceiver assembles and transfers data from the LAWS Instrument to the platform for transmission via data relay satellites.

All communications with the LAWS Instrument, to and from the orbiting platform, and with the NASA Control Centers are directed through the LAWS Command, Control, and Communication Subsystem. The few interfaces that are not controlled by this

subsystem are related to the LAWS JPOP electrical, thermal, and mechanical interfaces. These interfaces, however, are monitored and reported by the health and status instrumentation sensors.

The flight computer controls laser shot management firing commands, computes orbital platform position location, controls telescope nadir angle actuation commands, collects telescope line-of-sight azimuth angle values for each laser shot, provides short time storage of wind vector data for transmission to the platform data management system, and performs other command and data management functions.

LAWS wind vector position measurements are located in a topocentric-horizon coordinate reference system relative to a reference geoid. An oblate spheroid is not a perfect model of the slightly pear-shaped earth, but it provides a much truer representation than that of a spherical earth model. The surface of the reference geoid represents sea level on the earth's surface. The troposphere is represented by twenty 1 km thick layers that are concentric with the surface of the earth. The topocentric-horizon coordinate system allows each of the wind vector components to be located in familiar map coordinates. The platform orbit parameters are best defined in a nearly inertial geocentric-equatorial coordinate system. It is assumed that a Star Tracker sensor and an Earth Horizon sensor will be provided by the platform to provide an accurate frame of reference to which the telescope gimbal can be aligned. This alignment provides a reference line which is precisely related to the vernal equinox direction and to the nadir. The X and Z axes of the geocentric-equatorial coordinate reference frame are thus precisely determined and maintained in orbit with sufficient precision for LAWS requirements. Transformation matrices, incorporated in the LAWS software, transform line-of-sight measurements to geodetic latitude, longitude, and altitude coordinates. Although this measurement technique appears to be complex, once it is committed to software, its complexity becomes trivial. Without it, automatic sorting, processing, and plotting of the mass of data accumulated by the LAWS Instrument will be impractical.

A Command and Data Transceiver provides an interactive interface between the LAWS Instrument and the JPOP Data Link subsystem. Command messages from the ground, health and status information, and all scientific wind vector data are transferred from the LAWS Instrument in a coordinated two-way data stream.

5.1.5 Mechanical Support Subsystem

The Mechanical Support Subsystem consists of active and passive thermal control elements and structural support members. Thermal control system elements employed

to regulate the temperature of critical parts of the LAWS Instrument include heat pipes, heat exchanger reservoirs, cold plates, electric heaters, radiators, conductive heat sinks, and multilayer insulation (MLI) blankets. Structural assemblies provide a controlled mounting base which maintains the critical alignment of the electro-optical elements of the LAWS Instrument during assembly, and which performs integration and alignment with the booster and platform during the boost phase and during long term operation and exposure to the space environment.

The LAWS Instrument requires electrical energy to perform its wind measurement functions. The Optical, Receiver/Processor, Command Control & Communication, Mechanical Support, and Electrical Power Subsystems collectively consume approximately 400 W on a continuous operation basis. The remainder of the electrical power is consumed by the Laser Subsystem. Nearly all of the electrical power consumed by the LAWS Instrument is converted to heat and must be removed to maintain the equipment within normal operating temperature ranges of 0 to 20 °C. Except for the Laser Subsystem, the thermal energy generated is radiated directly to space or conducted into the base structure and then radiated to space. Some of the equipment items, such as the detector, require critical design consideration to insulate the operation of the active thermal cooler. MLI blankets are used to insulate the optical elements of the Optical Subsystem in order to maintain the alignment of the optical elements and to reduce thermal distortion. Heater elements are used for thermal stabilization only where satisfactory passive means cannot be employed.

The Laser Subsystem is the largest consumer of electrical power in the LAWS Instrument. Because of its inherently low operating efficiency level, it is also the largest source of thermal energy. With the laser operating at a pulse rate of 10 Hz, an output power level of 10 J/P, and a wall plug efficiency of 5 percent; 2 kW of electrical power are consumed by the laser. Ninety-five percent of this power is converted to heat that must be removed from the laser to maintain the required operating temperature range. Trade studies conducted by Lockheed revealed that a power level of 20 J/P is desirable. For the same operating conditions given above, this level would double the input electrical power and the heat to be removed. This requirement is above the reported capability of the JPOP electrical power subsystem and would double the capacity of the thermal control system. This reveals an additional justification for a Laser Shot Management capability for the LAWS Instrument.

The internal design of the Laser Subsystem provides circulating liquid coolant lines for the removal of excessive thermal energy from the circulating gas active media and other critical heat producing elements within the laser. These lines transfer the thermal energy to an external thermal reservoir which is mounted on a cold plate provided as an integral part of the LAWS Instrument base plate. Heat pipes within the cold plate transfer the heat to a radiator which points toward deep space.

The LAWS hardware is designed to be mounted on a common, precision alignment baseplate which is integrated for installation, launch, and operation with the JPOP. Accommodations for Space Shuttle launch and subsequent installation and operation on the SSF are also provided.

5.1.6 Electrical Power Subsystem

The Electrical Power Subsystem for the LAWS Instrument is comprised of power conditioning and distribution elements. Parts such as wire, connectors, circuit breakers, junction boxes, and power conditioner circuits that have been used successfully in space are used in the design of this subsystem.

The LAWS Instrument receives electrical power from the JPOP or SSF. Redundant, remotely resettable circuit breakers are installed in the power source circuits to protect the LAWS Instrument from power surges that might be introduced by faults from other payloads on the platform.

Junction boxes are installed at selected locations to accommodate interconnect branching for the distribution of power to all elements of the Instrument. These boxes enclose special power conditioning circuits.

Space qualified wire is specified for the LAWS power distribution harness. Shielding and low noise, single point grounding techniques are employed. Low-level sensitive signal circuits are routed separately from power distribution circuits, and filters are employed to prevent the introduction of unwanted interference.

5.2 LAWS SUBSYSTEMS

The LAWS subsystems will be integrated as described above to configure the LAWS Instrument. The following paragraphs describe the individual subsystem in more detail.

The LAWS Instrument Baseline will be designed for electromagnetic compatibility (EMC) with the platform and orbital environment and will conform to the appropriate

design and test standards. The primary source of interference is the pulse laser. Typically, pulse amplitudes are tens of kilovolts, pulse widths are several microseconds, and the repetition rate is up to 20 Hz. Background environments from appropriate polar and equatorial orbits will also be considered. The design will incorporate magnetic and electric field shielding for all subassemblies and cabling (based on near- and far-field levels) to accommodate out of limit emissions. Shielding to prevent upset or failure will be based on specification logic family used for control and processing with the susceptibility versus frequency function of these families, overlayed with the appropriate acceptance test limits to reveal critical out of limit frequencies. Waveguide beyond cutoff, nickel loaded polymer gaskets, metalized films, wire mesh, honeycomb section, electric filters, 360 deg shield grounding, single point grounding, and magnetic and electric field metallic barriers are methods and materials anticipated for the EMC design.

The discussion of the electron beam (e-beam) laser (option) of Section 5.2.1 presents a design with adequate shielding to maintain EMR levels below those of the orbital background. Shielding for the preionized laser (option) is also addressed.

While active thermal control of LAWS is addressed in Section 5.2.6, passive thermal control is performed at each subsystem. Passive radiators are designed into components to reject excessive heat, and MLI blankets are integrated into the design where required. The LAWS Instrument platform will be covered with MLI to provide thermal stabilization and maintain structural warping within specified tolerances for minimal impact upon the optics train. Advantage will be taken of radiative cooling on those electric components which effectively operate at elevated temperatures. A thermal model of the instrument will be developed to determine heat rejection requirements and system structural integrity.

5.2.1 Laser Subsystem

The transmitter laser is considered the area of greatest risk for the LAWS program. In order to reduce this risk, Lockheed chose the approach of dual sourcing the laser concept/configuration studies. The two sources selected for these studies were Avco, a leading U.S. source of pulsed carbon dioxide laser technology for coherent measurement, and GEC, a leading European source of pulsed carbon dioxide laser hardware for military operations. Both subcontractors developed concepts to meet the required specifications. GEC selected the e-beam sustained transverse excitation (TE) laser approach, while AVCO selected the corona pre-ionized, self-sustained TE laser approach

for their primary configuration design efforts. Subsection 5.2.2.1 presents a summary of Avco's approach, and 5.2.2.2 provides GEC's approach.

5.2.1.1 AVCO Laser Configuration Selection

The design goal was to develop a viable laser configuration that would satisfy the requirements listed in Table 5-1. Additionally, the issues of packaging, interfaces, and technology readiness had to be addressed.

Table 5-1. LAWS Laser Requirements

Energy per Pulse	≥ 20 J
Pulsewidth	1 to 3 μsec
PRF	8 Hz
Wavelength	9.1 μm
Weight	≤ 200 kg
Chirp	≤ 200 kHz
Wall Plug Efficiency	> 5%
Average Power Input	< 3200 W
Lifetime	10^9 Shots

In light of the very long lifetime requirement of the LAWS transmitter, AVCO Research Labs (ARL) has adopted a conservative approach in selecting the configuration so that risks can be minimized in technology areas that are already well understood. For other areas such as the pre-ionizer and the catalyst, in which some uncertainties remain, risk reduction experiments must be performed to ascertain their limitations.

5.2.1.1.1 Requirements Trades

The specific tasks that were performed to arrive at an optimum configuration are summarized below:

- Kinetics study to optimize gas mixture composition so that extraction efficiency is high
- Longitudinal mode control
- Resonator trades to optimize far-field energy delivery and transverse mode discrimination
- Frequency fidelity study for estimation of intra- and inter-pulse chirp.

The outcome of the above trade studies was a laser configuration which defined the aperture, cavity and gain lengths, mirror radii of curvature and mirror sizes, scraper and grating locations, etc. The next step was to design a flow loop to satisfy the medium homogeneity requirement derived from the frequency fidelity trades and the flush factor required for interpulse discharge clearing.

All the above information was then used to determine a package that would be compact and lightweight. Finally, the power requirements of the overall system were calculated and checked for compliance with the specification.

5.2.1.1.1.1 Kinetics Study

The ARL Kinetics code can predict laser performance under various operating conditions and for any selected CO_2 laser line. The code is based on published work found in Refs. 2 and 3. Rates for pumping the low-lying levels of CO_2 and N_2 are derived from Ref. 2, and the energy relaxation and optical flux build-up equations are derived from Ref. 3.

The input parameters to the Kinetics code are specific energy loading in the gas, mixture composition, pressure, pulse length, and cavity feedback. On the basis of these inputs, the code calculates the specific optical energy output in joules/liter. The temporal profile of the pulse gives quantitative information about the amplitude and the width of the gain switch spike, which is then optimized by controlling the intensity of the seed beam.

The specific energy loading has a major impact on the size of the laser because the laser volume scales inversely with this parameter. The size of the flow and acoustic components, flow velocity, and overall weight and volume are driven by the selected discharge loading. On one hand, a high specific loading is desirable for a low weight and a compact device. On the other hand, it is detrimental to the stability of the discharge and, hence, is to be avoided. Nevertheless, higher specific loadings can be tolerated for short pulse lengths (< 3 μsec).

ARL has demonstrated streamer-free discharge operation at specific loadings as high as 300 J/L-atm. However, for the LAWS Kinetics trades, the values chosen were between 100 and 175 J/L-atm. Such conservative loadings will provide reliable operation and yet result in a device that will meet the weight specification.

5.2.1.1.1.2 Mixture Selection Study

ARL performed a preliminary study to select a mixture composition that could be used to estimate the laser parameters including the weight and the volume. This study searched through a parameter space that included the total gas pressure (CO_2, N_2, and He concentrations) and the lasing transitions. The goal was to attain 20 joules/pulse in the near-field using an injection locked power oscillator.

For the purposes of this study, mixtures rich in He were primarily investigated. Our experience with the design of similar devices shows that for pulse lengths greater than 1 μsec it is necessary to have hydrogen or He to depopulate the lower laser level and thus avoid "bottle necking." However, with the presence of H_2 in the laser mixture, there could be water and other contaminant formations from the decomposition of CO_2 into CO and atomic oxygen, which could be harmful for long term duration.

He-rich mixtures also have an important advantage. Presence of He allows for a lower glow discharge voltage. Consequently, the PFN voltage can be kept at a reasonable level, i.e., 40 kV or lower. This would make design of the pulse power system easier and the choice of available high-voltage, high-power components wider.

However, He-free mixtures have the advantage that for short pulses they produce little or no chirp. Furthermore, because they have high gain, the resonator magnification can be higher. Consequently, far-field energy delivery will be more efficient. A comparison of the performances of a He-based and a He-free mixture was made for this study; the results are shown in Table 5-2 from which advantages for each mixture are evident. This study was, however, preliminary, and the issue of He-based or He-free mixtures will be re-examined in Phase II to determine what penalties are to be paid for a chirp-free operation. At the present time LAWS liftime requirements appear to preclude use of H2 mixtures.

Study Parameters. The pumping condition was varied between the conservative limits of 100 and 150 J/L-atm with a fixed duration of 5 μsec. The pressure parameter was varied between 1/3 and 1/2 atm. Generally, increasing pressure from 1/3 to 1/2 of an atm increased intrinsic efficiency by about 20 percent. A pressure of about 1/2 atm was the highest considered because conservative limits of 30 kV p.f.n. voltage and 5 cm gap separation were set.

The mixture parameter space spanned over the practical limits of He, CO_2, and N_2 mixtures. The optimal mixtures fall in the range of 50 to 75 percent He and 10 to

Table 5-2. Comparison of He-Based and He-Free Designs

	Mixture CO_2:N_2;He 1:2:3	Mixture CO_2:N_2:H2 1:2:3
• Extraction Efficiency	11%	13%
• Edge Clearance (4 x 4) cm^2		
τ = 3 μsec	81%	90.4%
τ = 1 μsec	93.5%	96.8%
• Volume	2.4 liters τ = 3 μsec	1.9 liters τ = 3 μsec
• Chirp (γ - 1)	0.2 MHz	0.12 MHz
• Discharge Voltage	20 kV	35 kV
• Gas Chemistry	Stable	H_2O
• Lifetime Issues	Good lifetime data	Comprehensive lifetime data is not available

25 percent CO_2. The lasing line parameter space consisted of the $^{12}C^{16}O_2$ P(20) 9.4 μm and the $^{12}C^{16}O_2$ R(34) transition.

The results of the optimization study are given in Tables 5-3 and 5-4. Table 5-3 shows how the output energy for the P(20) line varies with pump energy, pressure, and partial pressures of N_2 and He. Table 5-4 shows the same for the R(34) line. The gain length and the pump time were held constant at 150 cm and 5 μsec respectively. Concentration of N_2 and He were varied independently.

The output energy scales approximately with pumping energy. It was found that the strawman device, operating at 1/2 atm with 150 J/L-atm pumping, can deliver 21 J to the near field on the P(20) line. On the R(34) line the same device would put about 19 J in the near field.

Gas Mixture Optimization. From the preliminary study for mixture selection, it was found that optimal mixtures fall in the range of 50 to 75 percent He and 10 to 25 percent CO_2 with the rest being N_2. We also found that for the required output, an operating

Table 5-3. Optimization of Extraction Efficiency for the IIP(20) Transition

GAIN LENGTH = 150 cm — PULSE LENGTH - 5 μs

1/3 atm, 100 J/L - atm

% He \ N_2	1/4	1/2	1	2
85	2.0	1.9	1.5	.75
75	2.2	2.1	2.1	1.5
50	1.6	2.1	2.3	1.8
25	.78	1.4	1.9	1.6

N_2 (CO_2 - 1 CONSTANT)

1/3 atm, 150 J/L - atm

% He \ N_2	1/4	1/2	1	2
85	2.6	2.3	1.9	1.0
75	3.1	3.0	2.9	2.1
50	2.6	3.3	3.5	2.9
25	1.5	2.4	3.1	2.7

N_2 (CO_2 - 1 CONSTANT)

1/2 atm, 100 J/L - atm

% He \ N_2	1/4	1/2	1	2	3
85	2.8	3.4	3.3	1.8	1.2
75	2.9	4.4	4.4	33	2.4
50	1.6	4.2	4.1	4.0	3.1
25	0	2.9	3.5	33	2.7

N_2 (CO_2 - 1 CONSTANT)

1/2 atm, 150 J/L - atm

% He \ N_2	1/4	1/2	1	2	3
85	5.6	5.3	4.3	2.5	1.7
75	6.4	6.4	6.3	4.7	3.5
50	5.2	6.6	7.1	6.1	4.9
25	3.2	4.8	6.0	5.5	4.6

N_2 (CO_2 - 1 CONSTANT)

NOTE: NUMBERS INSIDE THE BOXES REPRESENT ENERGY OUTPUT IN J/L

89-430

pressure near 0.5 atm and a gain length of 150 cm were required with the pumping limited to a maximum of 175 J/L-atm.

On this basis, further optimization of the mixture was performed to attain the highest efficiency. The results of this study are shown in Figure 5-4. It shows the effect of mixture composition on extraction efficiency. The study was conducted for three different pulse durations: 2, 3, and 5 μsec. For each pulse duration, efficiency was determined as a function of the concentration of N_2.

For the pulse durations of interest (e.g., 2 μsec and 3 μsec), it is apparent that the efficiency is fairly insensitive to X (the ratio of N_2 to CO_2) varying from 1 to 2. The maximum efficiency is obtained with a $1CO_2$:$1N_2$:2He mixture for the given parameters. Experience with similar devices has shown the 1:1:2 mixture to provide good laser

Table 5-4. Optimization of Extraction Efficiency for the IIP(34) Transition

GAIN LENGTH = 150 cm

1/2 atm
150 J/l - atm

He %	N_2 1/4	N_2 1/2	N_2 1	N_2 2
85	5.3	3.9	3.4	2.1
75	6.0	5.9	5.8	4.2
50	4.8	6.1	6.6	5.5
25	2.7	4.3	5.4	4.8

N_2 (CO_2 - 1 CONSTANT)

PULSE LENGTH = 5 μs

1/2 - atm
100 J/l - atm

He %	N_2 1/4	N_2 1/2	N_2 1	N_2 2
85	3.9	3.7	2.8	1.4
75	4.1	3.9	3.9	2.7
50	2.8	3.7	4.0	3.2
25	1.4	2.4	3.1	2.6

N_2 (CO_2 - 1 CONSTANT)

NOTE: NUMBERS INSIDE THE BOXES REPRESENT ENERGY OUTPUT IN J/l

performance. It may be noted that the maximum extraction efficiency (near field) is between 10 and 11 percent.

Therefore, for the LAWS laser configuration, the 1:1:2 mixture was selected as the baseline.

5.2.1.1.1.3 Longitudinal Mode Control

Figure 5-5 depicts three possible architectures and lists the three different options available for attaining single frequency operation in a power oscillator. They are hybrid cell, Fabry-Perot etalon, and injection locking, also known more precisely as injection seeding.

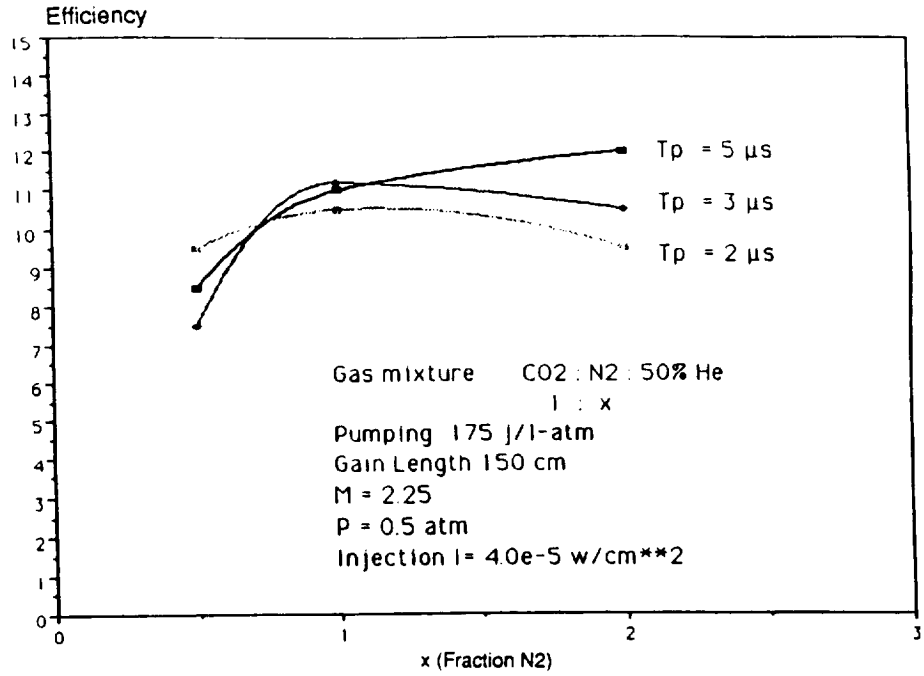

Figure 5-4. Gas Mixture Optimization

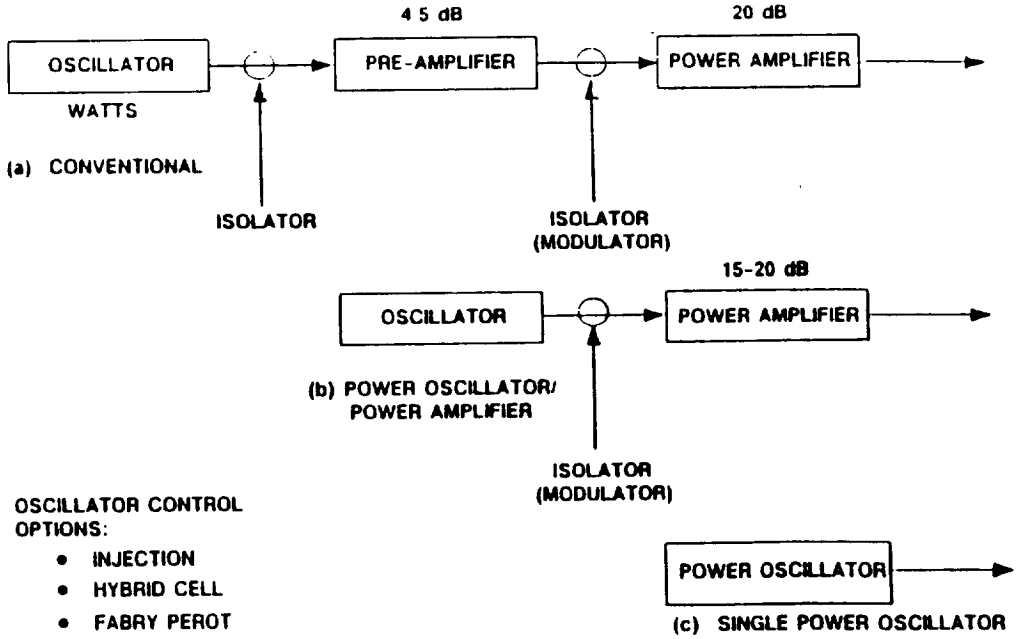

Figure 5-5. Transmitter Architecture Options

The hybrid power oscillator, in which a low pressure discharge is in series with the laser discharge, is an elegant solution. Since only one laser is required, there is no need for isolation. However, it requires two separate discharges that need synchronization. The two discharges are likely to operate at different pressures making flow loops more complex.

The second option is a Fabry-Perot etalon, which may be used to control the longitudinal mode. Several etalons with different thicknesses may be used in cascade in order to combine the narrow line width of a thicker etalon with the wider free spectral range of a thinner one. However, alignment of these multiple, passive elements and the accompanying insertion loss may pose problems with this option.

By the use of injection locking, a weak but well-stabilized CW laser can control the longitudinal modes of a much higher power laser, which is inherently more noisy and unstable (Ref. 1). An injection-locked oscillator is the optimum choice, particularly if a single laser can serve both as the local oscillator and as the injection source. This will eliminate the power consumption, weight, and volume required by a second laser.

However, it will require isolation of the reference laser from the high power transmitter oscillator. The isolation, and possibly attenuation, can be accomplished by using a small injection hole in the primary mirror. Alternately, the seed beam can be injected through a dielectric turning mirror which is 98 to 99 percent reflecting, or through the zero-order path of the grating which will be required for line selection.

Injection-Locked Power Oscillator. Figure 5-6 shows the basic injection locking scheme. With this technique, the laser resonator is length-tuned until the Fabry-Perot resonance matches that of the injection source. When the transmitter laser is pumped, the selected mode builds from the injection seed rather than random noise. A CW laser, such as a waveguide laser, can be used as the injection source. Cavity matching will be performed by locating the resonances of the cold cavity. A PZT drive on a light-weight resonator mirror in conjunction with a closed-loop servo system and the injection laser can be used to find the resonance position.

Injection seeding also provides an easy way of controlling the amplitude of the gain switched spike in the laser pulse. The spike can be reduced by increasing the intensity of the seed signal. This is important for the LAWS transmitter, which requires that most of the pulse energy be available for Doppler measurement of the wind velocity.

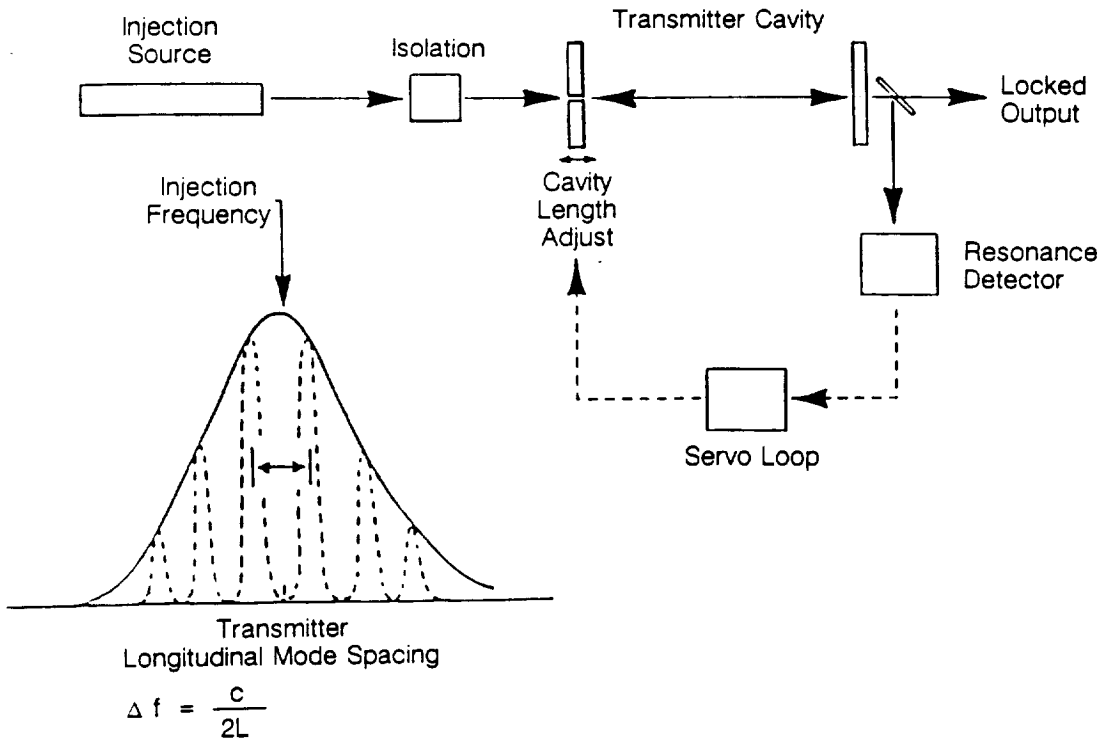

Figure 5-6. Schematic of the Injection-Locking Method

5.2.1.1.1.4 Resonator Trades

Two fundamental issues need to be addressed in the performance of trade studies for the optical resonator. They are the energy delivered into the far field and the control of transverse mode.

Far-Field Energy Delivery. In the preceding section, optimization of the near-field extraction efficiency of the laser was described. That was primarily needed to obtain an appropriate mixture. However, what is ultimately important is the energy that is delivered into the far field. Consequently, the resonator parameters such as magnification, which is essentially the feedback in an unstable resonator, has to be carefully chosen to maximize the energy delivered to the far field. Figure 5-7 shows the percentage of energy delivered into the far field as a function of cavity magnification, M. It is obvious that a high magnification is desirable for maximum far-field energy. But higher magnification can only be obtained at a sacrifice of the extraction efficiency. It is these two parameters in conjunction that determine the net far-field energy. This tradeoff is

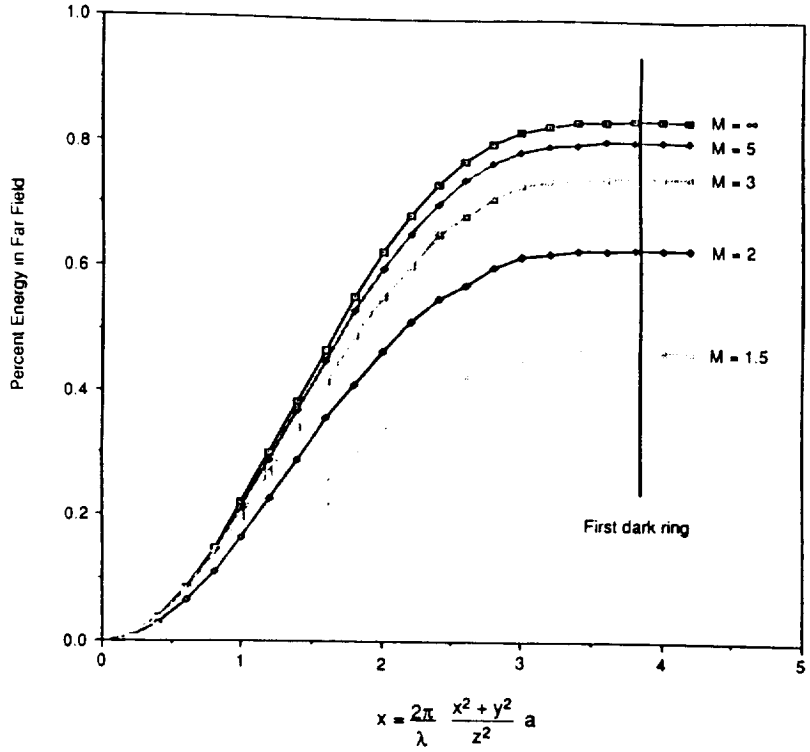

Figure 5-7. Far-Field Energy as a Function of Magnification

clearly shown in Figure 5-8, in which both near-field and far-field efficiencies are shown as a function of 1/M.

The present design point is at 1/M = 0.444, which translates to M=2.25. This is where the far-field energy efficiency is at its maximum.

Transverse Mode Control. The issue of how to obtain single transverse mode in the laser output is the most important for a coherent pulsed lidar. This is achieved by a judicious choice of the equivalent Fresnel number, (N_{eq}) of the resonator (Ref. 4), which is defined as follows:

$$N_{eq} = \frac{M-1}{2M^2} \quad \frac{a^2}{\lambda L}$$

where

M = magnification
L = cavity length
λ = wave length
2a = length of a side for the square beam.

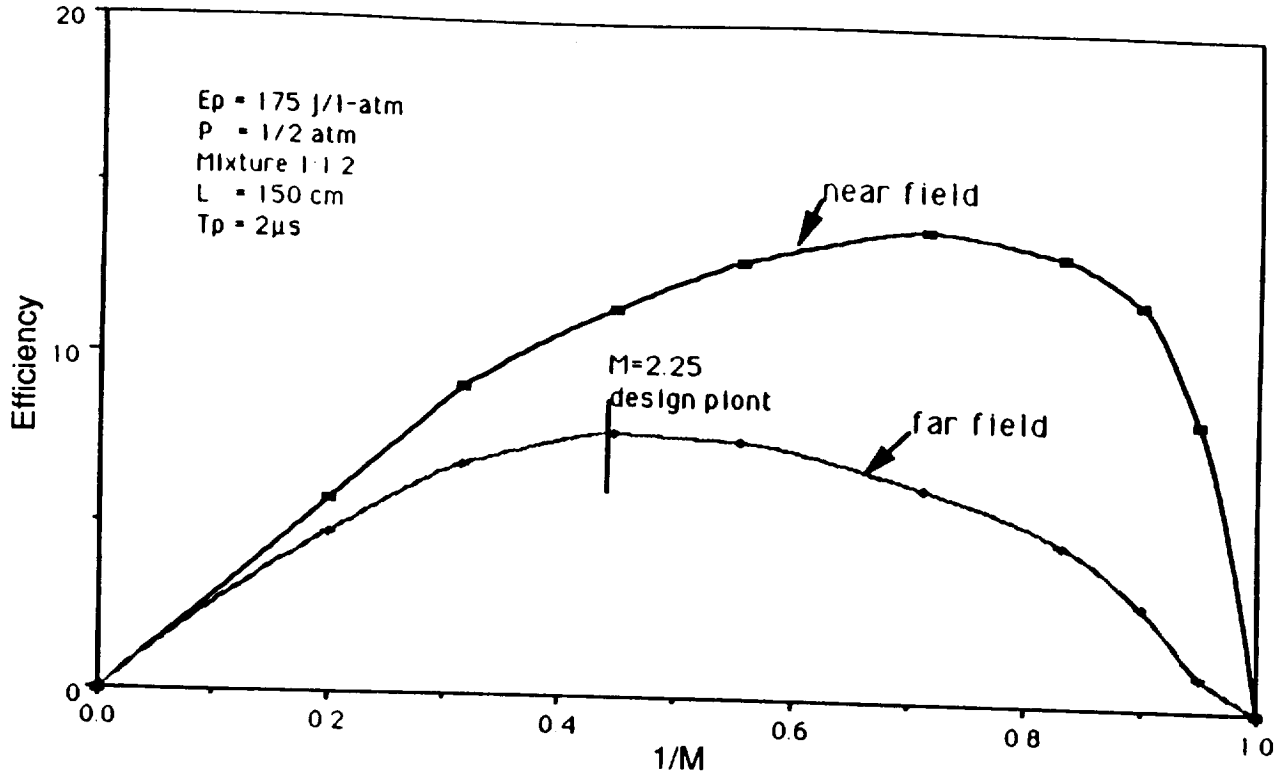

Figure 5-8. Extraction Efficiency versus Far-Field Energy Delivery

It is seen from the formula for Neq that it depends on several factors such as the cavity length (different from the gain length), the magnification, and the radius of the beam. Normally, the aperture is primarily determined by energy considerations, and obviously the wave length is given. Therefore, the two variables are M and L, which can be changed to arrive at the desired Fresnel number.

Earlier studies (Refs. 5 through 7) concluded that there is a quasi-periodicity in the mode losses as a function of Neq, such that the mode crossings (known to have mode degeneracy) occur very near to values of Neq = n, where n is an integer. The studies also concluded that the maximum mode separation points occurred at values of Neq = n + 0.5 for circular mirrors and at Neq = n + 0.4 for square mirrors. However, there is some weakness in these conclusions since they are based on studies which assumed perfectly aligned mirrors.

Recent studies conducted by ARL found that mirror alignment had a noticeable effect on the cavity losses for the different modes. This is easily seen from Figures 5-9 and 5-10. The case for perfectly aligned mirrors, i.e., the mirror tilt angle $\theta = 0$, is shown in Figure 5-9. It shows the behavior of the "loss coefficient" for the fundamental mode and the next higher order mode, as a function of Neq. It is apparent that the

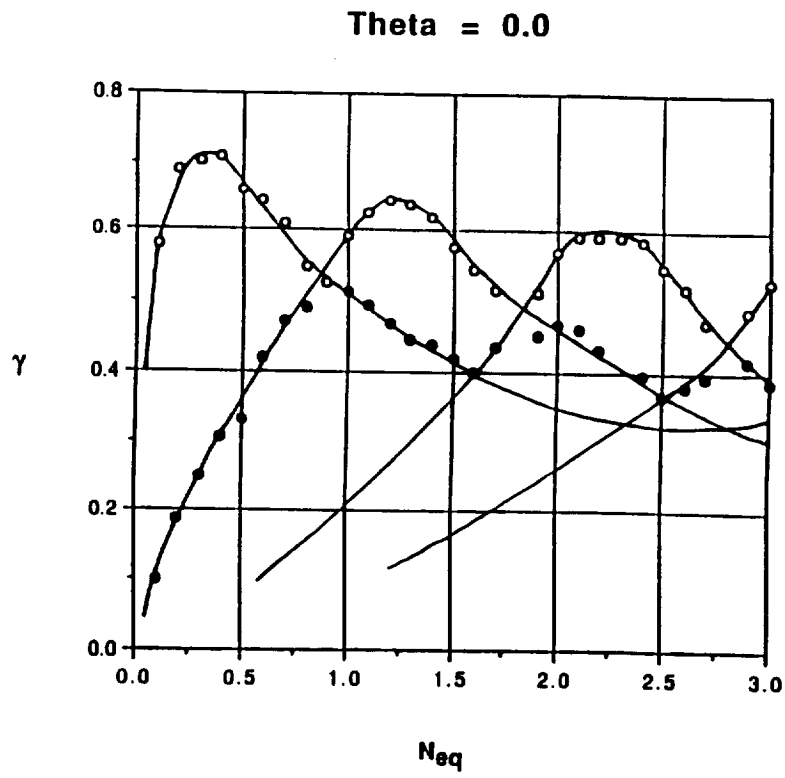

Figure 5-9. "Loss Coefficient" as a Function of Equivalent Fresnel Number (N_{eq}) for Perfectly Aligned Mirrors ($\theta = 0$)

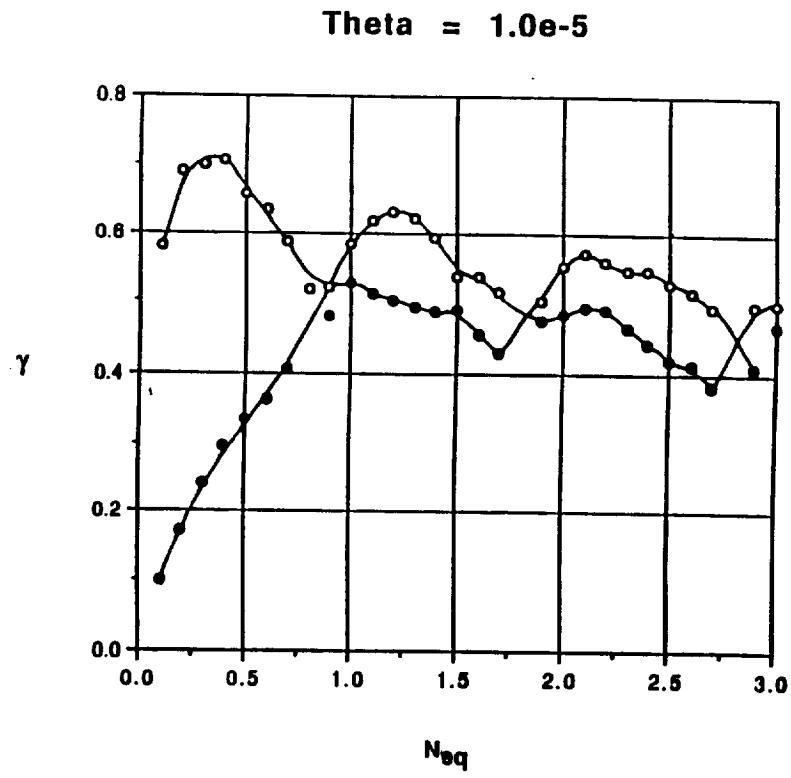

Figure 5-10. "Loss Coefficient" as a Function of N_{eq} for Misaligned Mirrors (θ = 10 rad)

highest mode separations occur at values of Neq near 1.4, 2.4, etc., which confirms the earlier conclusions. If a mirror is tilted even by a small angle, such as 10 μrad, the mode loss patterns change significantly as is evident from Figure 5-10, which is a plot for θ = 10 μrad.

Consequently, the effect of mirror misalignment must be addressed carefully during the detail design phase when materials and sizes of mirrors and their mounts are baselined.

5.2.1.1.1.5 Frequency Fidelity and Chirp Control

There are a number of processes that can cause the frequency of the output of a pulsed CO_2 laser to vary in time, i.e, chirp (Ref. 8). In general, they produce time dependent perturbations of the index of refraction of the lasing medium.

It has been generally assumed in previously reported work that the vibration-translation (V-T) transfer from the lower laser level to the ground state is instantaneous (Refs. 9 and 10). This implies that at laser onset, all V-T energy is deposited into the gas. This assumption has been incorporated into previous theory and used to explain chirp due to laser induced medium perturbation (LIMP) processes (Ref. 10).

In recent years, ARL has made detailed studies of the various physical phenomena that give rise to chirp in discharge-pumped pulsed CO_2 lasers. A new theory, which extends the presently accepted theory, has been developed and experimentally verified.

It has been found that the principal mechanism governing chirp is the heat deposition in the medium due to V-T transfer which results in a change in the index of refraction of the medium.

ARL has demonstrated that by changing the pressure and composition of the gas mixture, the lower level relaxation rate can be significantly altered and thus control the chirp. Further, ARL experimentally determined that discharge induced chirp in our lasers is negligible.

It may be noted that the presence of either He or H accentuates the V-T transfer rate and thus enhances chirp. For reasons explained earlier, a He-rich mixture has necessarily been baselined for LAWS at this time.

Initial estimates of chirp were based on a simplified Rigrod calculation, in which the intensity profile of the laser output was assumed to be Gaussian. This approach normally provides a pessimistic estimate for the chirp, because the extraction-induced heating is higher in the resonator core region where the chirp is generated.

However, more precise wave calculations performed recently show that, for the proposed LAWS laser resonator, the maximum intensity occurs at the wings instead of the core region of the gain medium. This will result in a lower chirp than previously estimated.

ARL's present estimate is that the 200 kHz chirp limit can be satisfied with a 4 x 4 cm^2 aperture and a maximum 3.0 μsec pulse duration.

5.2.1.1.1.6 Resonator Design and Performance

Design Description. Table 5-5 lists the specifications for the LAWS laser resonator as it is presently envisioned. Figure 5-11 shows a schematic of the resonator configuration.

The salient features of the proposed resonator are as follows. The cavity consists of a primary mirror and a light-weighted feed back mirror, which has a PZT driven mount for cavity matching. The gain medium is split in two in a proprietary ARL scheme to obtain a very compact package.

An intracavity plane blazed grating is needed for line selection. The design shown in Figure 5-11 permits wavelength tuning while maintaining collimated output. The intracavity laser intensity, as shown in Figure 5-12, poses no risk of damaging the grating. One of the turning mirrors is coated with 98 to 99 percent reflectivity. It allows the use of a CW laser to injection-lock the power oscillator, and it also makes mode-matching less complicated. Because the feed back from the power oscillator might pull the frequency of the injection source, optical isolation between the power oscillator and the injection source will be necessary if the injection source is also used as local oscillator for detection.

The PZT drive on the feed back mirror, in conjunction with a closed-loop servo system, and the injection laser will be used to find the cavity resonance. Since the discharge electrons will shift the cavity frequency by some amount, the mirror will be driven to the correct position to compensate for the electron induced frequency offset. A preprogrammed mirror acceleration/deceleration within the PZT tuning range will be used to minimize the mirror relocation and settling time, although for a 10 Hz operating repetition rate there will be more than adequate time for the servo system to stabilize.

With the possible exception of the primary mirror, all mirrors are liquid-cooled and Cu-plated. Such mirrors have demonstrated high damage thresholds well in excess of the present requirements. Since the primary mirror sees the lowest power level, it may

Table 5-5. Proposed Resonator for LAWS Transmitter

Type: Confocal Unstable Resonator with Square Mirrors	
Equivalent Fresnel Number	2.4
Magnification	2.25
Cavity Length	2.2 m
Gain Length	1.50 m
Beam Size	4 cm x 4 cm
Radius of Curvature	
Primary Mirror*	17.5 m
Feedback Mirror	7.7 lm

* *Combination of mirror and grating.*

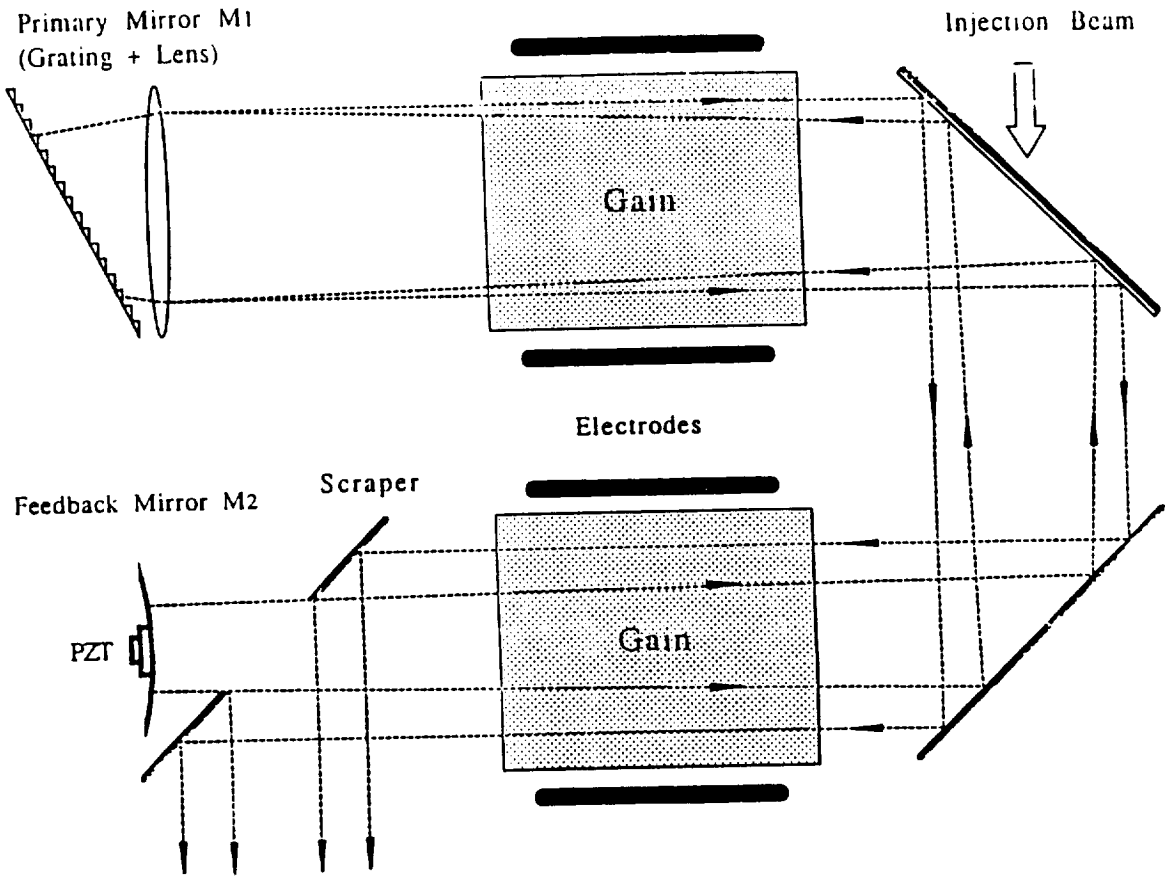

Figure 5-11. LAWS Laser Resonator Configuration

be configured as an uncooled low mass mirror to facilitate cavity alignment. It has a high reflectivity coating on a thin Si substrate.

The windows preferred for a space-bound system are anti-reflection-coated NaCl. These yield the lowest thermal distortion and highest damage thresholds. Zinc Selenide has poorer damage and thermal performance, but does offer improved resistance to water vapor absorption, and can be used in ground-based tests.

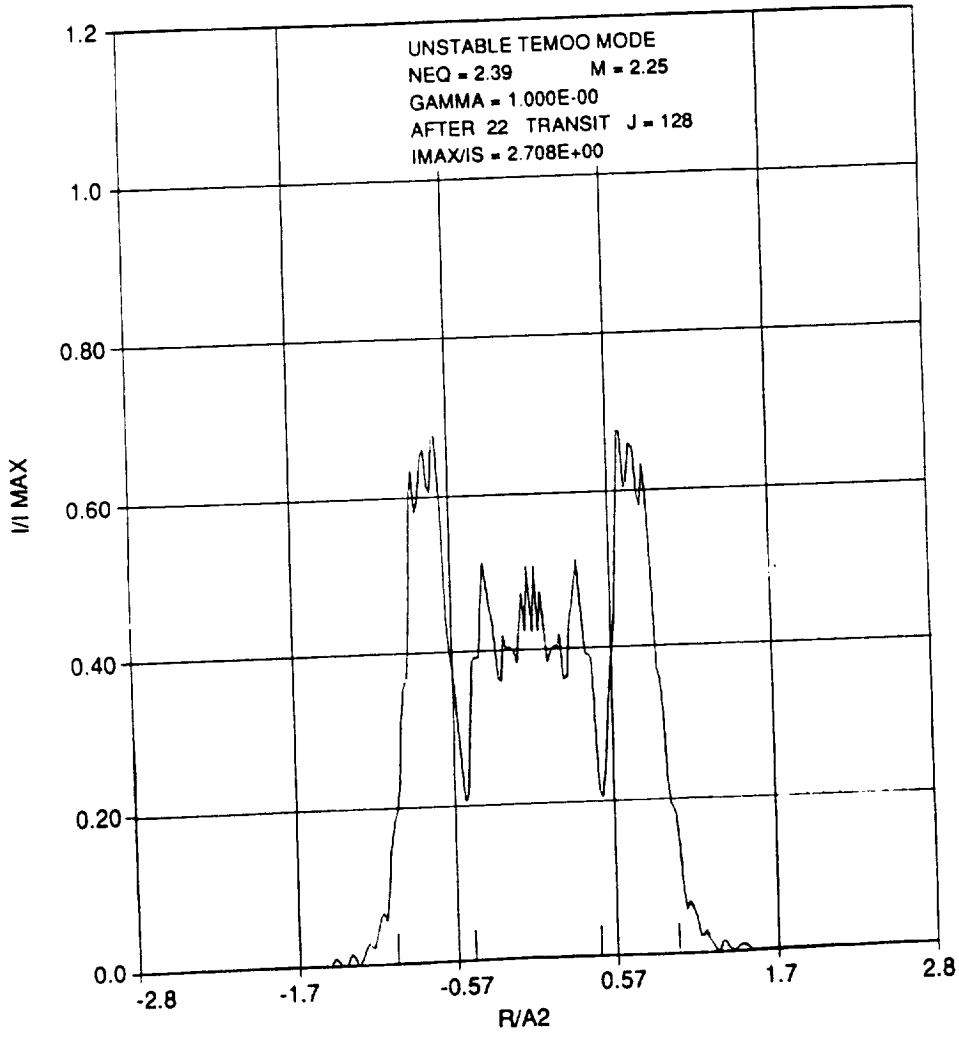

Figure 5-12. Intracavity Intensity Profile (2-D)

Resonator Performance. An evaluation of the electromagnetic-field distribution in the proposed resonator loaded with a saturated gain medium requires a numerical solution of the nonlinear paraxial-wave equation. The ARL computer code which solves the Fresnel-Kirchhoff diffraction integral equation using a fast-Fourier-transform (FFT) algorithm was used for the purpose. The continuous gain medium was approximated by a series of thin gain sheets with free propagation between them. Convergent solutions of the lowest-loss modes were obtained successfully.

Figure 5-12 shows the intensity profile of the lowest-loss mode, normalized by the maximum value, incident upon a center-line of the feedback mirror. The tick marks on the abscissa indicate the feedback mirror size, and A2 is the beam size. A three-dimensional plot of the same normalized intensity is shown in Figure 5-13. Figures 5-14 and 5-15 respectively show the 2-D and 3-D profiles of the relative phase of the lowest-loss mode at the same location. These figures suggest that the output beam is well collimated as desired.

5.2.1.1.2 Transmitter Design

5.2.1.1.2.1 Discharge Techniques

There are principally two types of schemes employed for the discharge-pumping of TEA CO_2 lasers: the e-beam sustained and the self-sustained discharges.

In an e-beam sustained discharge, an external e-beam pumps the medium throughout the duration of the laser operation. Hence, it allows for precise control of the pumping process by controlling the parameters of the e-beam. Further, a copious supply of electrons facilitates uniform pumping of the gain medium.

A self-sustained discharge typically requires an initial injection of a large number of electrons into the gas which initiates the discharge process by one or more mechanisms. Once the conditions for a glow discharge are achieved, the discharge sustains itself as long as the applied e-field is maintained. Pre-ionization is the necessary means for providing the initiating electrons in the main electrode gap.

A careful study of the advantages and the disadvantages associated with the various options has been made. In conjunction with this study and a review of the laser requirements, we have concluded that a corona UV pre-ionized self-sustained discharge is the excitation option that is best suited for the LAWS laser.

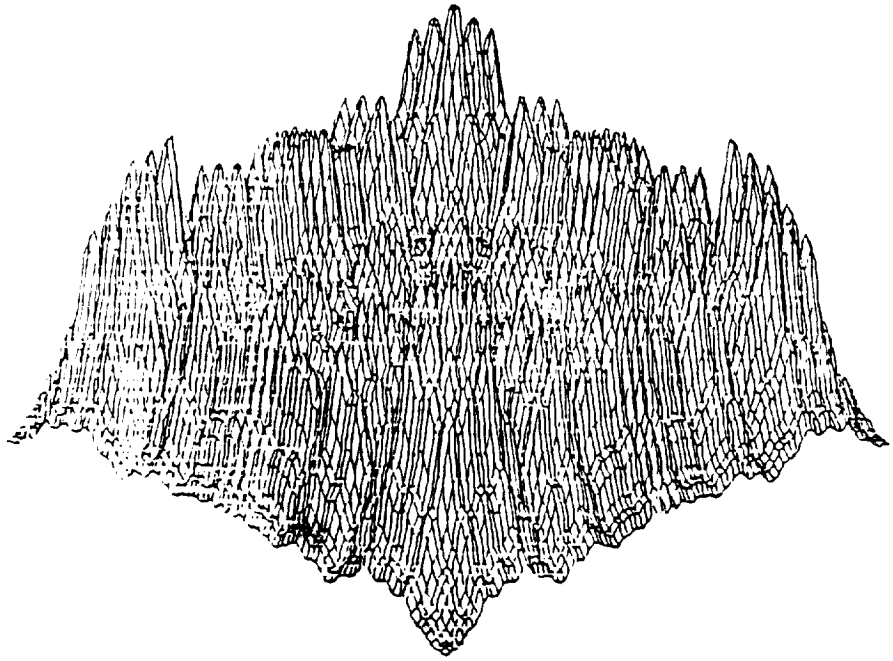

Figure 5-13. Intracavity Intensity Profile (3-D)

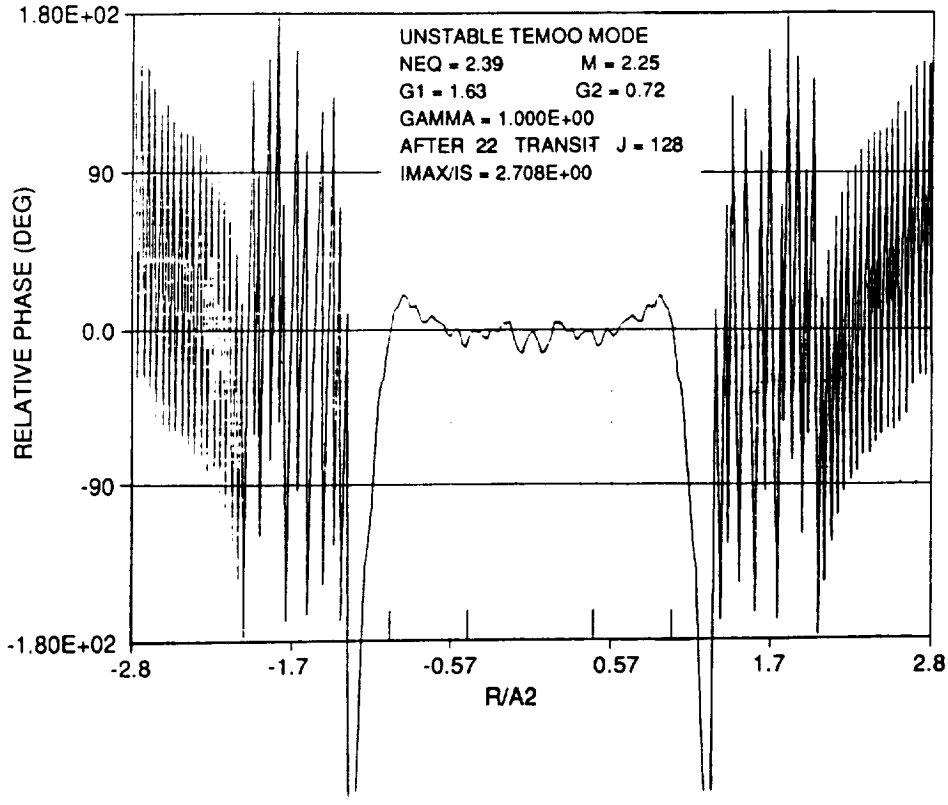

Figure 5-14. Phase Distribution (2-D)

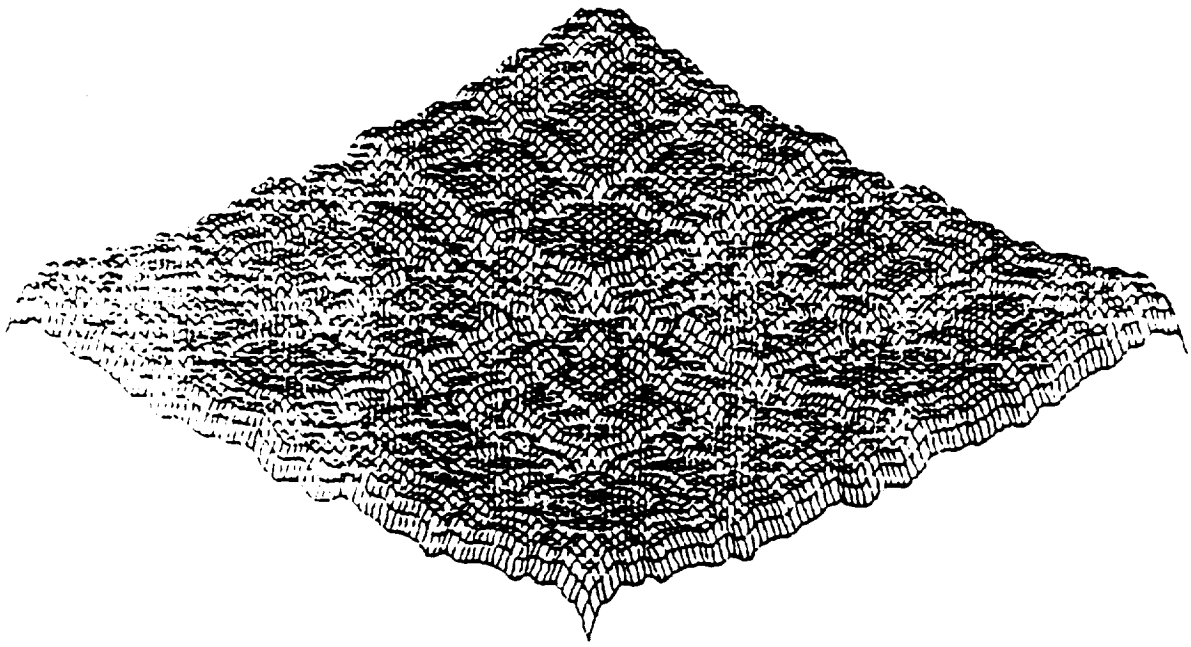

Figure 5-15. Phase Distribution (3-D)

U.V. Pre-ionization. Pre-ionizing ultra-violet radiation can be generated by a number of techniques. Some of these include spark discharges, semi-conductor discharges, UV lamps, and most importantly for long-life lasers, corona discharge.

Semiconductor surface discharge pre-ionizers are too weak for apertures greater than a few millimeters and hence are of no interest to us. UV lamps are also not a serious candidate since their wave lengths are typically too long for penetration in high pressure CO_2 mixtures. That narrows the choice to spark discharge and/or corona discharge sources.

Spark discharge sources have currently been ruled out for the baseline design primarily because of anticipated difficulties in achieving 109 pulses lifetime. However, spark discharge sources, especially a surface spark discharge source, have spectral content and intensity that are ideal for pre-ionization of large electrode gaps (Refs. 11 and 12). ARL has recently developed a surface spark source with a lifetime of 107 shots. Further development in the materials area can extend it to 109 shots. However, there may still be potential problems with contamination of the medium for long sealed-off operation. Spark discharge source will, however, continue to be the backup option.

Surface Corona Pre-Ionizer. Surface corona pre-ionization has been cited as superior to other types in a large number of applications. This is because of its uniform pre-ioni-

zation, its potential for pre-ionizing a relatively large electrode gap, and the simplicity of a single discharge (Ref. 13).

ARL has developed a proprietary discharge scheme using a corona pre-ionizer developed by V. Hasson and co-workers (Refs. 14 and 15). The scheme provides good control over local and volumetric instability phenomena. As a result low-chirp, self-sustained discharges can be produced at specific energy loadings exceeding 200 J/L and pulse lengths between 1 and 10 μsec.

In the ARL design, the pre-ionizer is integrated with a perforated plate anode to form a hard flow wall, which is essential to obtain an optimum flow geometry.

5.2.1.1.2.2 Flow Loop

General Considerations. Frequency fidelity requirements of a coherent lidar transmitter dictate that the medium homogeneity of the laser cavity prior to laser initiation, i.e., base flow medium homogeneity, be within a certain specified level and also that it be restored for succeeding pulses. Self-sustained discharge operation also places further constraints on the laser medium in that heated gases can provide a short circuit path for discharge to arc. Thus thermal clearing of the cavity between pulses is also required.

Base flow homogeneity is achieved through proper utilization of flow velocity and temperature control devices such as heat exchangers, passive thermal equalizers, turbulence control screens and honeycomb, and flow control fans and screens. Acoustic quieting between pulses is accomplished by use of mufflers and drag elements. Transient effects caused by initial device turn-on are controlled by active heat exchanger throttling.

A major consideration is the velocity of the gas in the flow loop. The required gas velocity in the cavity is set by the pulse repetition rate and the required flush factor (i.e., how many cavity dimensions downstream the ionized gas must be moved in the interpulse period to avoid interference with the next discharge). Typical flush factors range from 2 to 3 for UV pre-ionized self-sustained discharges.

The gas velocity in the flow loop is frequently reduced from that required within the cavity to reduce gasblower power requirements. This is done by increasing the area of the flow loop. A typical value for flow loop velocity is Mach 0.05 (approximately 15 m/sec).

Typical flow loop configurations are shown in Figure 5-16. The volume of the flow loop is driven by the distance required to reduce the medium disturbances, to the degree

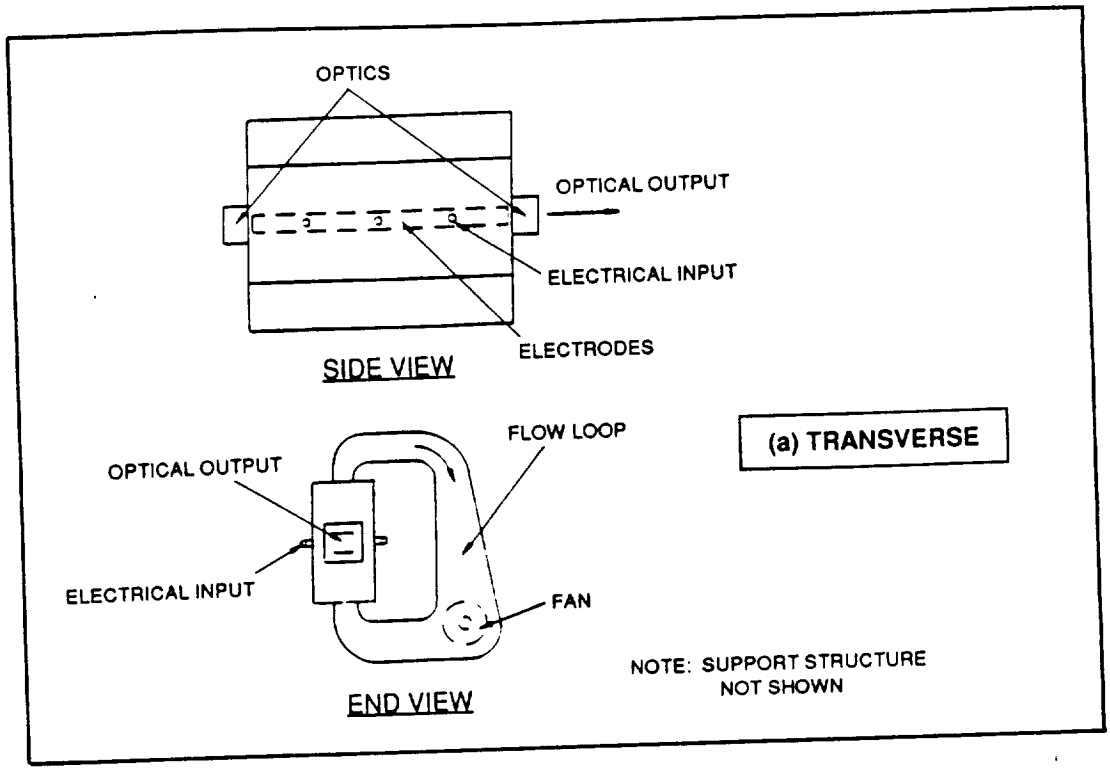

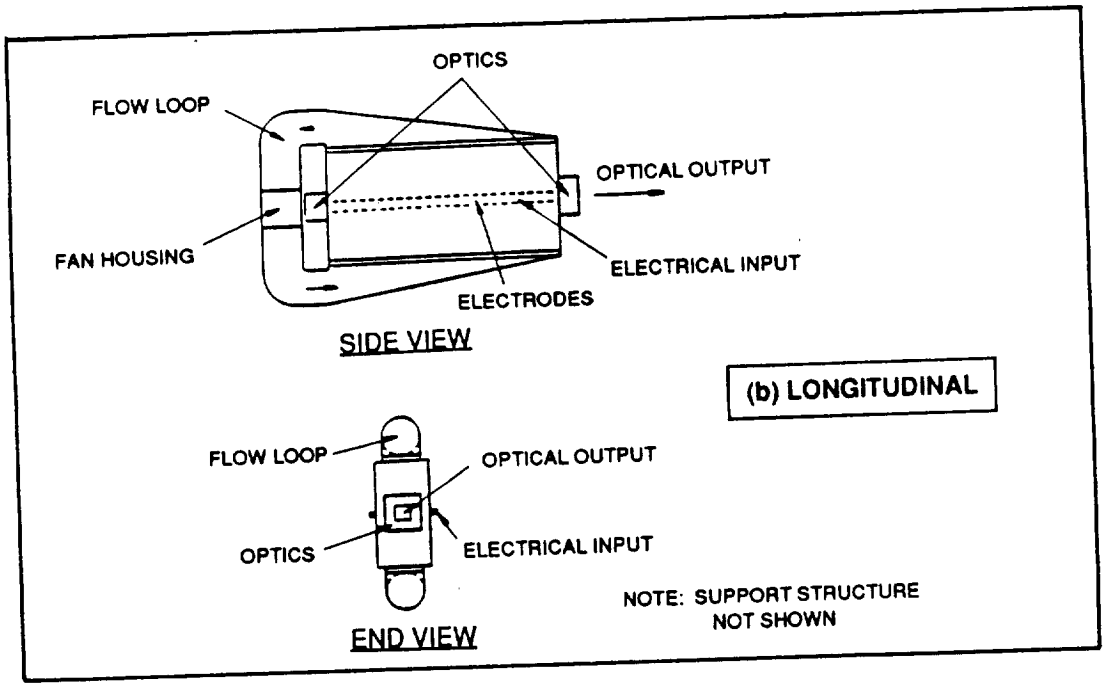

Figure 5-16. Flow Loop Configurations

of homogeneity required for the specified application, and the flow loop area increase required to keep fan power within a reasonable limit. For the configurations shown, typical total flow loop volumes for conventional designs are in the range of 100 to 200 cavity volumes, depending on pulse repetition rate and flush factor requirements.

The longitudinal flow loop configuration as shown in Figure 5-16(b) has the advantage of compatibility with a larger number of fans; however, it does require a good distribution system to ensure homogeneity over the length of the cavity. The transverse flow loop shown in Figure 5-16(a) uses a long fan or a series of fans arranged along the length of the laser. The differences in geometry are obvious from the figure. However, the total volume required is generally less with the transverse configuration.

Several recent design studies at ARL have been focused on compacting laser transmitter designs. Alternate means of closing the flow system were investigated as were alternate means of driving the flow. The most significant compacting of the flow system is achieved by utilizing a dual folded cavity concept. With this concept, wasted space in the flow return is virtually eliminated. The compacting techniques have all been studied in the laboratory at Avco Research over a wide range of parameters.

Flow Loop Configuration. The compaction concepts discussed above have been incorporated in the conceptual LAWS laser system as shown in Figure 5-17. Table 5-6 shows the flow system design specification that was developed to satisfy the requirements of the LAWS transmitter. The flow loop is configured with dual discharge cavities, formed by the opposite legs of a rectangular flow section.

The residual thermal energy in the laser gas associated with the pulsed laser operation is removed by the two highly-efficient heat exchangers, while the gas thermal fluctuations/variations are controlled by the two thermal equalizers. An on-line catalytic converter will be incorporated in the flow loop to regenerate the CO_2.

Conceptual Design. To be conservative a cavity flush factor of 3 was selected. This allows us to relax any requirement for velocity control in the cavity and allows complete clearing of any entropy wave generated from the interaction of the upstream propagating pulse with the upstream heat exchanger.

The pulsing of the laser discharge causes hot slugs of gas to be formed which must be removed before passage to the following cavity. At the proposed flush factor they are widely spaced. The skewed heat exchanger inlet causes them to enter the heat exchanger over a substantial portion of that spacing, and this greatly smears that nonuniformity.

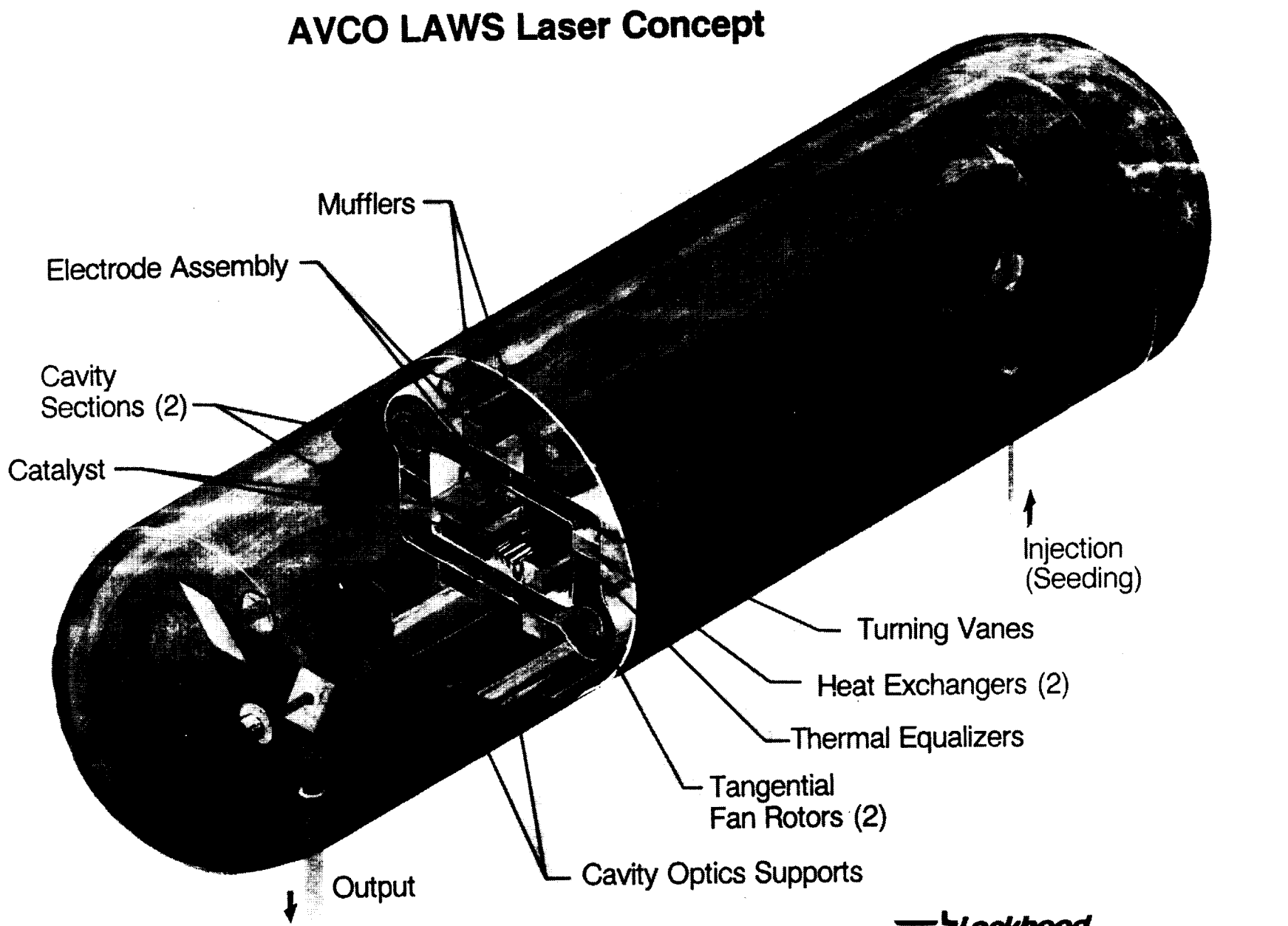

Figure 5-17. Laser Flow Loop and Packaging

Table 5-6. LAWS Conceptual Flow System Design Parameters

Input Energy per Pulse	95 J/L
Energy Out per Pulse	20 J
Cavity Size	4 x 45 x 75 cm^3 (two cavities)
Repetition Rate	10 Hz
Gas Pressure	1/2 atm
Gas Temperature	300 K
Gas Composition CO_2:N_2:He	1:1:2
Cavity Flush Factor	> 2.5
Desired Parameters	
Near Field Efficiency	8.8%
Cavity Input Power	2.3 kW
Input Power	1 W/cm^3
Cavity Acoustic Transits Between Pulses	> 50
Cavity Velocity	$\geq$ 1 msec

The fan choice is a tangential fan configured in a housing as derived from ARL IRAD analysis and laboratory data. The fan would be mounted with shafts leaving the laser gas region through seals with external bearings and motors sealed in separate enclosures.

The flow contracting tangential fan is followed by a ceramic thermal equalizer which provides thermal equilibration, reduces any turbulence scale size, removes any swirl from the fan, and provides a pressure drop; thus smoothing velocity nonuniformity. The ceramic can also serve as the support structure for the catalyst.

The laser cavity regions are configured with the inner flow wall made of perforated plate. Because of the compactness of the design, the wave from the cavity traverses mufflers more than fifty times between pulses making acoustic quieting a non-issue.

The outer flow walls in the laser cavity legs of the flow system are insulating and house the cathodes for the discharge. These walls are to be designed to prevent any surface tracking arcs. They could also serve as catalyst support.

5.2.1.1.2.3 Catalyst

$C0_2$ Regeneration. The major lifetime limiting process common to all CO_2 lasers is electron impact dissociation of CO_2:

$$CO_2 + e \rightarrow CO + 0.5O2 + e.$$

This process not only consumes CO_2, but has a major impact on laser power degradation due to production of O_2. It is known that buildup of even small concentrations of O_2 (0.1 to 1 percent) can cause rapid power loss and eventually lead to a complete laser failure.

ARL studies have shown that the corona pre-ionized discharge can operate reliably with an O_2 concentration of up to 0.5 percent. To keep the O_2 concentration below this level in a closed cycle system, a gas regeneration system with a solid catalyst is required for the CO-O_2 recombination process given below:

$$CO + 0.502 + \text{Catalyst} = CO_2.$$

Catalyst Design Considerations. An effective catalyst that will satisfy the LAWS mission requirement has to meet several criteria: (1) high activity at the ambient gas temperature, (2) minimal degradation of catalytic activity over 3 or more years of laser operation, (3) minimal atomic oxygen exchange between the catalyst substrate and the lasing medium, and (4) absence of dust or other deleterious by-products of catalyst operation.

Two issues are most important among the desired characteristics of a catalyst listed in the previous paragraph. These are efficiency of a catalyst and its degradation with operating time, and isotope exchange between $C18O_2$ gas and the 16O in the catalyst support.

Important design considerations for gas regeneration include the identification of the catalyst material itself, and the weight of the catalyst required to obtain a very high CO_2 regeneration efficiency and cleanup. CO_2 regeneration is achieved by heterogeneous catalysis of the CO-O_2 reaction with a selected set of noble metals on a reducible metal oxide. This class of supported noble metal catalysts is used in sealed-off CO_2 lasers because they perform the two major functions required of a CO oxidation catalyst: dissociative adsorbtion of O_2 and adsorbtion of CO next to reactive oxygen atoms. A Pt/SnO_2 or Pd/SnO_2 catalyst is expected to provide high conversion efficiencies, even at or below room temperature (Refs. 16 through18). This high efficiency is due to three

factors: the low adsorption enthalpy of Pt and Pd which decreases the extent to which CO inhibits the CO-O_2 recombination reaction at a given temperature (i.e., high rate of CO oxidation under stoichiometric conditions); the slow deactivation of Pt and Pd during continuous operation; and the synergistic metal-support effect associated with SnO_2 which acts to lower the strength of the bonds that hold oxygen atoms on the surface of the oxide. These factors contribute to the high turn-over frequency (TOF) ranking of these catalysts. The TOF is essentially a catalyst reaction rate normalized to a number which is a measure of the catalyst surface area (see Table 5-7).

Table 5-7. CO Oxidation Reaction Rates on Supported Noble Metal Catalyst at 373 K

Catalyst	CO/O_2	Turn-Over Frequency Molec/Site x 103	Ea kJ/Mole
Pt/SiO_2	2.0	1.53	54
Rh/SiO_2	2.0	0.674	110
Pd/SiO_2	2.0	0.474	90
Pt/SnO_2	2.0	17.0	55
$PrPdCn/SnO_2$	2.0	540.0	--

The high TOF catalytic activity of Pt/SnO_2 and Pd/SnO_2 have been investigated under both simulated laser conditions and in a sealed CO_2 laser by several research groups (Refs. 16 through 19), primarily to determine reaction rate constants for the catalytic oxidation of CO, and the temperature dependence of the rates if possible. The catalyst activity studies performed at ARL indicate that the CO oxidation efficiency is strongly dependent on the gas flow rate, reaction temperature, catalyst surface area, and the gas composition. In some of these tests, relatively high conversion efficiencies were obtained, even at low temperatures, with a moderate drop in pressure over the catalyst. These data were used to determine the range of useful operating conditions for the LAWS laser.

Preliminary Catalyst Configuration. There are several ways of incorporating the catalyst structure in the flow loop design. These include a by-pass loop with a fixed bed, i.e., a fixed bed of particulates, and a by-pass loop with a monolith structure. The other configurations are either an on-line/fixed bed or an on-line/monolith structure. These latter schemes will provide a more compact and low weight structure.

For the LAWS conceptual design, the on-line/monolith design with a $Pt/Pd/SnO_2$ catalyst, which has proven highly efficient in tests performed at ARL and elsewhere, was chosen. The on-line configuration also provides a lower pressure drop for the flow.

Catalyst Weight Estimation. In order to estimate the catalyst weight, the first step was to determine the O_2 production rate under the expected discharge conditions. It was estimated on the basis of experimental data under similar conditons that the worst case is 0.1 percent CO_2/shot. At the proposed repetition rate, this corresponds to a production rate of 4.5 cm^3/sec of O_2.

Experimental results suggest that a conversion rate of 6.5×10^{-2} cc/gm/sec is reasonable. With these assumptions, the weight of the catalyst required for nearly 100 percent recombination of CO and O_2 is about 70 g. With a safety factor of 2.0, the estimated weight is 140 g. It was also found that the catalyst overcoat weight is typically about 30 percent of the weight of the supporting monolith. Therefore, the combined weight of the catalyst/monolith structure will be about 470 g.

5.2.1.1.2.4 Pulse Power

Pulse Power Requirements. A pulse power system will be required to supply the necessary pumping of the laser gas in the self-sustained discharge mode discussed earlier.

Typical voltage and current waveforms observed in a self-sustained discharge are shown in Figure 5-18. It may be seen that the discharge striking voltage is much higher than the self-sustained glow voltage.

As discussed earlier, the presently envisioned configuration for the LAWS laser has an aperture of 4 cm x 4 cm with total gain length of 150 cm. This configuration will be able to generate a pulse up to 2.5 μsec duration and also stay within the specified chirp limit of 200 kHz. Precise numbers will be obtained at the design phase. The discharge parameters required to pump the lasers are summarized in Table 5-8.

The corresponding pulse power system requirements are listed in Table 5-9.

Pulse Power Configuration Options. To satisfy the requirements given in Table 5-9 as well as to produce the discharge waveforms discussed earlier, obviously requires a pulse forming network (PFN). There are several options in this regard which are listed in Table 5-10 along with the advantages and the disadvantages of each choice.

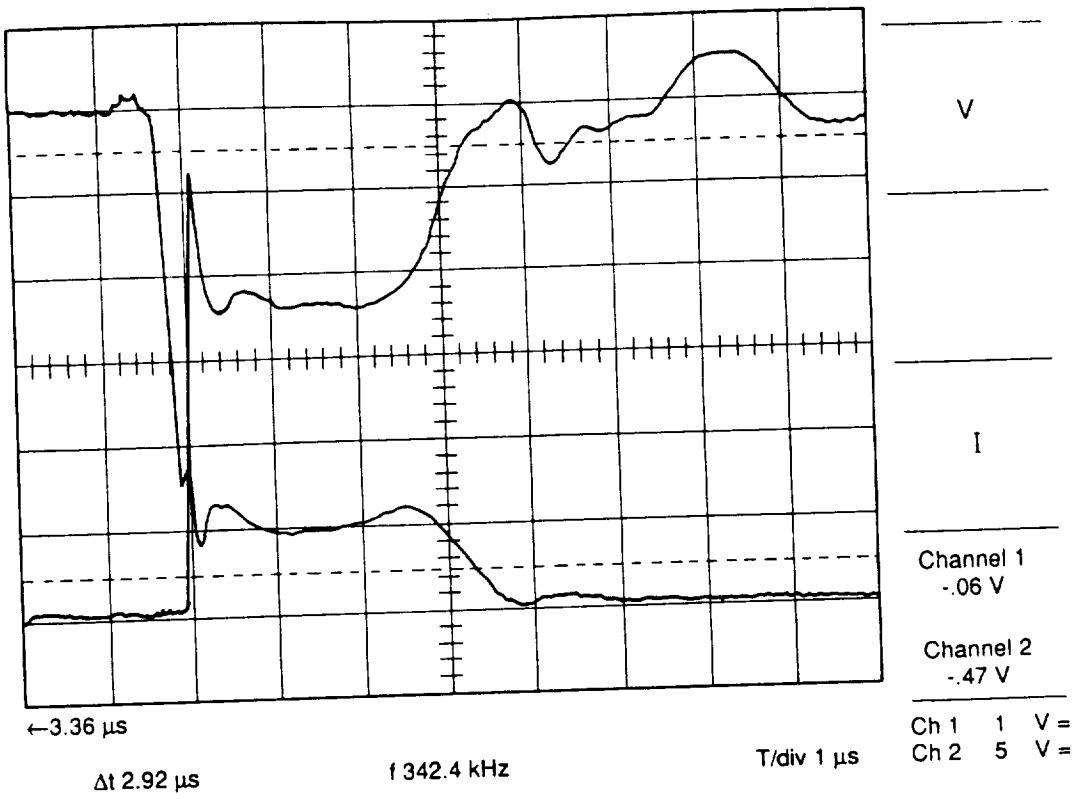

Figure 5-18. Typical Discharge Voltage and Current Waveforms

A full voltage Guillemin-type PFN has been tentatively selected because the required voltage of 40 kV is moderate enough to warrant such a choice. It also allows a wider choice of the components.

Unlike a Blumlein circuit, a full-voltage PFN has little voltage reversal on the capacitors. This is important from lifetime considerations. Furthermore, the relatively low LAWS discharge impedance of about 8 ohms makes a Blumleim less attractive. (The pulse transformer option although ruled out at present will be revisited in the design phase.)

Proposed Pulse Power Configuration. A block diagram of the LAWS pulse power system is shown in Figure 5-19. The system derives its prime power from the spacecraft's 28 Vdc power bus. A closed loop regulator circuit will be required to compensate for any variation of the prime bus voltage.

The 28 Vdc will be conditioned and stepped up to the required PFN charge voltage of 40 kV through an appropriate dc/dc converter, which typically consists of a series resonant inverter, a step-up transformer, and an output rectifier section. This unit will either be commercially procured or developed at ARL.

Table 5-8. Laser Discharge Parameters

Cross-Section	4 cm x 4 cm
Length	150 cm
Discharge Volume	2.4 L
Loading	175 J/L-atm
Mixture	1 CO_2:1N_2:2He
Pressure	0.5 atm
Discharge Pulse Duration	5 μsec

Table 5-9. Pulse Power Requirements

Enery Stored	262 Joules
Glow Voltage	20 kV
PFN Voltage	40 kV
Current	2.6 kA
Pulse Duration	5.0 μsec
PRF	
Nominal Impedance	7.6 ohms
Voltage Risetime	400 nsec
dI/dt	6 x 109 A/S

The PFN will be charged from this power supply unit at a constant current upon command. The PFN basically consists of passive elements such as capacitors and inductors and stores the energy for the discharge. At this time, a definite PFN-type has not been selected. It will probably be a type-E or type-A.

Several PFN discharge switch candidates were considered. As shown in Table 5-11, a thyratron has been selection for its apparent advantages.

5.2.1.1.3 Transmitter Packaging

5.2.1.1.3.1 Physical Description

The laser transmitter source uses a compact flow loop with dual cavities as indicated in Figure 5-17. Design studies show that such a compact flow loop would satisfy all flow and acoustics requirements, and has significant advantages in overall size and weight. The laser has been configured with a dual-cavity scheme which takes advantage

Table 5-10. Available Pulse Power Configurations

	ADVANTAGE	DISADVANTAGE
• BLUMLEIN	FACTOR OF 2 IN VOLTAGE	HIGHER CAPACITOR DUTY FACTOR
	PROMISING FOR 1μS OUTPUT	LOW BANDWIDTH ADVERSELY AFFECTS RISE-TIME
	SWITCH REQUIREMENT EASED	FACTOR OF 2 LOWER IN IMPEDANCE
• GUILLEMIN TYPE PFN'S	SIMPLE GOOD WAVEFORM	FACTOR OF 2 HIGHER IN VOLTAGE
(TYPE A,C OR E)		HIGH VOLTAGE SWITCH REQUIRED
• PULSE TRANSFORMER AND LOW VOLTAGE PFN	LOW VOLTAGE PFN LOW VOLTAGE SWITCH EASIER PACKAGING	POSSIBLE WEIGHT PENALTY TRANSFORMER INDUCTANCE AN ISSUE

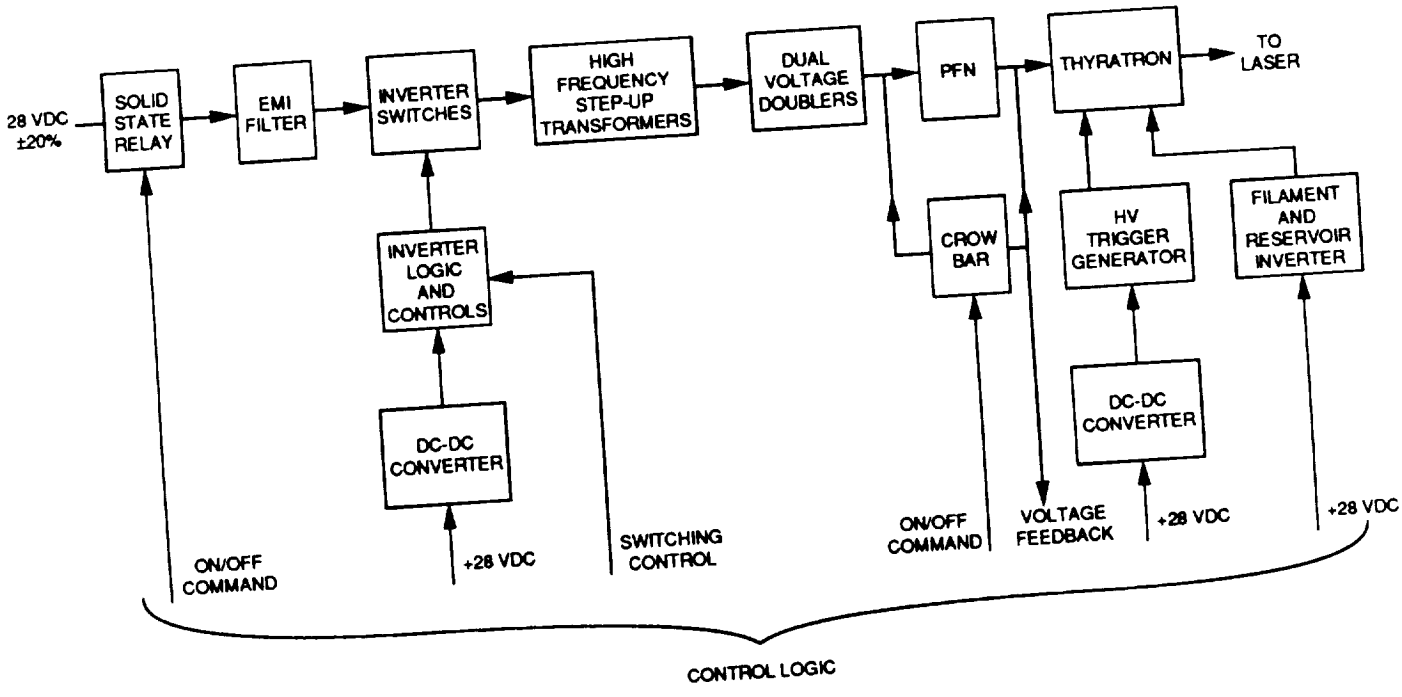

Figure 5-19. Block Diagram of LAWS Laser Pulsed Power System

Table 5-11. PFN Discharge Switch Candidates

- THYRATRON SWITCH SPACE QUALIFIABLE
  - HAS BEEN QUALIFIED FOR MISSILE APPLICATION IN THE U.K.
  - 8.5 X 10^9 SHOTS DEMONSTRATED AT LANL
  - RADIATION INSENSITIVITY AN ADVANTAGE IN SPACE APPLICATIONS
  - TECHNOLOGY IS HIGHLY MATURED
  - EXTREMELY LOW JITTER
  - VERY HIGH DI/DT CAPABILITY
- SOLID-STATE DRIVER NEEDS PULSE COMPRESSION
  - INCREASED WEIGHT AND VOLUME FOR 1 S OR LONGER PULSE DURATION
  - TECHNOLOGY NOT QUITE MATURE
  - DI/DT LIMITATIONS A MAJOR PROBLEM
  - POSSIBLE RADIATION SUSCEPTIBILITY
- CROSSATRON
  - TECHNOLOGY NOT MATURE
  - DISSIPATION DUE TO HIGH FORWARD DROP NEGATES
  - ABSENCE OF CATHODE HEATER POWER
- SPARK GAP
  - RULED OUT FOR LACK OF EXPECTED LIFE

of the inherent symmetry in the compact loop and reduces the required length. The active laser medium is folded with one section in each of the opposite legs of a rectangular flow section. Two heat exchangers are located in the remaining two legs.

The laser module (not including the PFN) has a diameter of 66 cm, a length of 121 cm, and a volume of 405 L. Material in the laser module is either metal or ceramic with limited amounts of glass. There is a small differential pressure between the inside and outside of the flow channels. Slow flow is introduced in all sections of the optical beam path external to the cavities to prevent stagnant gas buildup and beam degradation.

The transmitter and pulse power assemblies are integrated to form the total transmitter subsystem package and will be configured to fit within the designated space of the complete LAWS assembly. The laser assembly is designed for nominal operation at 1/2 atm pressure with vacuum on the outside. The PFN is designed to contain freon at several atmospheres. The total transmitter subsystem, shown in Figure 5-20, is supported by a platform frame (not shown) with vibration dampers. The optical bench is mounted independent of the flow loop within the laser assembly. The optical bench rods penetrate the laser module shell structure using metal bellows as seals and are shock-mounted on the outside to the laser module housing. A reference laser diode, mounted

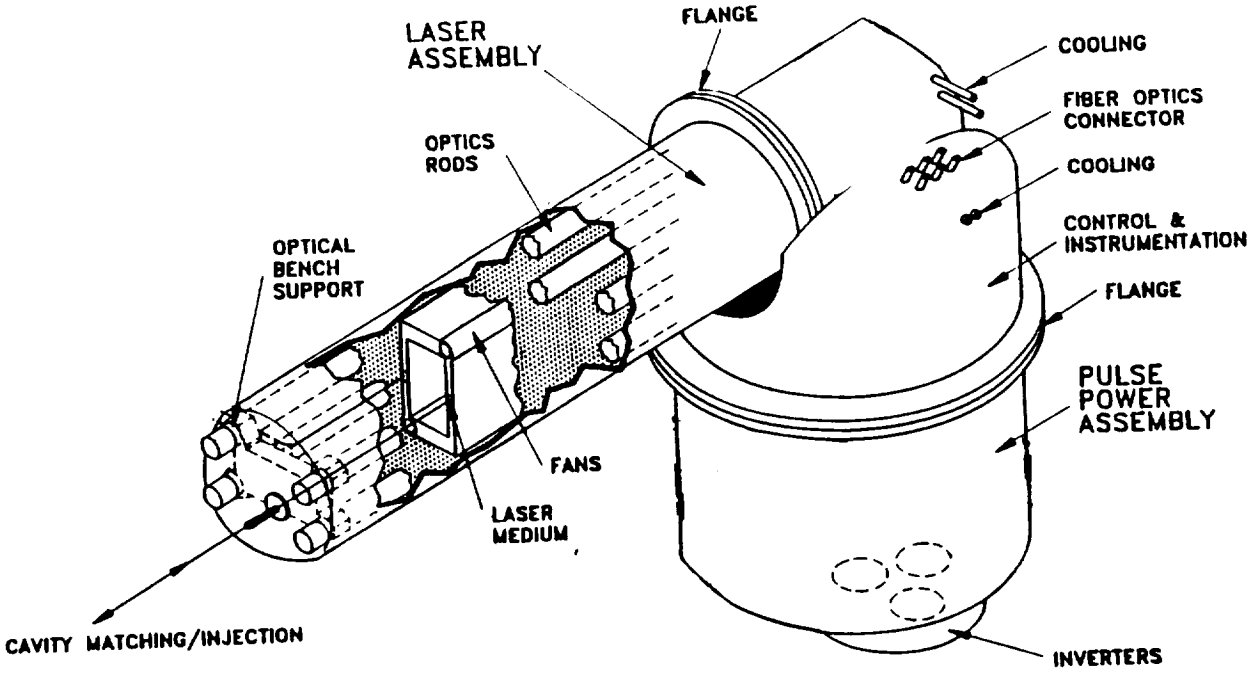

Figure 5-20. LAWS Transmitter Assembly

on the optical bench of the laser, provides an accurate reference beam to allow the high speed steering mirror to compensate for the angular displacement of the optical laser resonator in relationship to the system optical bench.

Both the laser assembly and pulse power assembly are configured to allow ease of assembly and inspection, with the removable shells allowing access to important components. All control, cooling, and electrical connections penetrate the nonremovable parts of the shell structure. Metal gaskets will be used to seal the laser assembly to ensure that lifetime requirements are met. In addition, RF gaskets will be used for both assemblies.

The two assemblies are connected by a small circular section for pulse power, electrical, control function feedthroughs, and mechanical integrity. The actual shape of the pulse power assembly will be strongly influenced by the available space. With the PFN shell flange removed, the complete pulse power assembly becomes accessible. The majority of the space in the pulse power assembly is occupied by the high voltage PFN components, with additional space required for high voltage hold-off. The front end of the inverter section and instrumentation and control electronics are contained in separate EMI shielded enclosures within this assembly.

5.2.1.1.3.2 Weight and Volume

Weight and volume trades were performed as a function of the energy output. Energy scaling was carried out by varying the gain length. Table 5-12 shows the breakdown of weight and volume by major subsystems of the transmitter.

The baseline configuration is represented by the column for 150 cm gain length which has an output energy of 20 J as required. It should be pointed out that weight estimates include an approximately 10 percent contingency. The cylindrical construction of both assemblies minimizes the structural and pressure vessel weight, the assembly complexity, and the pressure seal surfaces. The folding of the laser cavity allows the reduction of the laser length and minimizes the overall system dimensions. The "L" shape laser/pulse power packaging has been adopted to minimize the overall length. However, the design is modular and flexible so that other configurations may be easily accommodated.

Table 5-12. Summary of Estimated Weights and Volumes (Two-Cavity Design)

GAIN LENGTH (CM)	130	150	180
NEAR FIELD ENERGY (J)	16	20	25
ASSEMBLY NAME	ASSEMBLY WGT (KG)	ASSEMBLY WGT (KG)	ASSEMBLT WGT (KG)
FLOW LOOP	33.82	38.42	45.03
POWER SUPPLY/PFN	38.66	43.80	51.76
OPTICAL	35.17	37.16	40.17
CONTROL & INSTRUMENTATION	4.50	4.50	4.50
SUPPORT STRUCTURE	34.67	40.00	48.00
MISC. ITEMS	6.50	7.50	9.00
TOTAL WEIGHT: (KG)	153.32	171.37	198.46
FLOW LOOP VOLUME (Liters)	353.1	405.3	483.5
PFN VOLUME (Liters)	139.9	174.9	218.6
TOTAL VOLUME (Liters)	493.0	580.2	702.1

The weight of the pulse power module is dominated by the capacitors. The capacitors were conservatively selected with an energy storage density of 8 J/lb to increase the reliability by minimizing the risk of capacitor failures. The subsystem weight can be reduced with a higher energy-density capacitor, if it can be demonstrated to have the required lifetime.

The total weight is shown for an aluminum shell structure with flanges. This construction is compatible for both ground and space-based devices. Further weight reductions could be incorporated into a space-qualified system through the use of other materials and the possible elimination of the flanged packages.

5.2.1.1.3.3 Transmitter Power Requirements

The power requirements for the baseline transmitter are given in Table 5-13. It can be seen from the table that the baseline configuration meets the limit of 3200 W set by the LAWS platform. Table 5-14 lists the power requirements for a 1 μsec, 10 Hz option.

5.2.1.1.4 Transmitter Interfaces

The transmitter will have both physical interfaces (power, structure, and thermal control) and data interfaces (input/output) to the LAWS platform. The implementation of these interfaces for a brassboard will be different than for the device on the spacecraft.

The transmitter laser assembly will be designed as a self-contained and modular building block. All interface points will be selected to allow the laser to be fully tested to specification prior to system integration. All container metal construction will use appropiate RF shielding (gaskets, a shielded inverter transformer, and microwave cutoff structure), and all fiber optics control and instrumentation interfaces will be designed to minimize EMI radiation in accordance with the applicable MIL standards.

The physical interfaces, which include power, thermal transfer, and structures, are described as follows.

5.2.1.1.4.1 Mechanical

The self-contained laser assembly will be mechanically supported by an integrating structure through vibration isolators. To compensate for the relative motion of the transmitter module structure with respect to the main optical bench, and the motion of the

Table 5-13. Baseline Transmitter Power Requirement 20 J/Pulse, 8 Hz, 3μsec (tp)

	COMPONENT	NUMBER	UNIT	TOTAL
1.	LASER			
	Required Output	20	Joule	
	Intrinsic Efficiency	11.5%	-	
	Edge Effects	81%	-	
	Non-Uniform Pump	90%	-	
	Overall Efficiency	8.38%	-	
	Rep. Rate	8	Hz	
	Input to Laser	1908	Watt	
2.	PULSE POWER SYSTEMS			
	Required Output	1908	Watt	
	Pulse Modulator Efficiency	81%	-	
	DC Power Supply	90%	-	
	Overall Pulse Power	72.9%	-	
	Prime Power Input	2618	Watt	2618
3.	FLOW LOOP			
	Required Flow Power	4	Watt	
	Fan Efficiency	12%	-	
	Bearing Losses	2	Watt	
	Shaft Power	35	Watt	
	Motor Efficiency	80%	-	
	Total Flow Power	44	Watt	44
4.	INJECTION LASER	50	Watt	50
5.	INSTRUMENTATION & CONTROL	100	Watt	100
	Total Transmitter Power Requirement (Max PRF)			2812 Watts
	Total Transmitter System Efficiency			5.68%

Table 5-14. Transmitter Power Requirement for the 1 μsec Option 20 J/Pulse, 10 Hz, 1 μsec (tp)

COMPONENT	NUMBER	UNIT	TOTAL
1. LASER			
Required Output	20	Joule	
Intrinsic Efficiency	11.0%	-	
Edge Effects	93.0	-	
Non-Uniform Pump	90%	-	
Overall Efficiency	9.2%	-	
Rep. Rate	10	Hz	
Input to Laser	2172	Watt	
2. PULSE POWER SYSTEMS			
Required Output	2172	Watt	
Pulse Modulator Efficiency	81%	-	
DC Power Supply	90%	-	
Overall Pulse Power	72.9%	-	
Prime Power Input	2980	Watt	2980
3. FLOW LOOP			
Required Flow Power	4	Watt	
Fan Efficiency	12%	-	
Bearing Losses	2	Watt	
Shaft Power	35	Watt	
Motor Efficiency	80%	-	
Total Flow Power	44	Watt	44
4. INJECTION LASER	50	Watt	50
5. INSTRUMENTATION & CONTROL	100	Watt	100
Total Transmitter Power Requirement (Max PRF)			3174 Watts
Total Transmitter System Efficiency			6.3%

transmitter optical bench within the transmitter laser, a high speed steering mirror may be employed in the beam path on the sensor module optical bench. The other mechanical interfaces are the three cooling loops for the laser heat exchanger, power inverter and electronics heat removal, and the mirror temperature stabilization.

The thermal transfer interface provides for the transfer of waste heat from the laser transmitter to the host platform. A heat exchanger is used to transfer the energy (waste heat) from the laser to a host platform cold plate, which is expected to be at 270 K. A trade study will be performed on all subsystems to determine cooling requirements and optimal applications (radiative, convective, conductive). The major laser components contributing to the thermal load are the laser discharge, the electrical power conditioner, the electronics, and the optical components.

5.2.1.1.4.2 Optical

To provide an alignment reference for the laser output, a CW alignment laser will be mounted on the optical bench. The beam reflects off the two folding mirrors, the scraper mirror, and off several relay and folding mirrors located on the platform optical bench. The directional alignment error may be detected and used in a closed loop system to null the error by means of the steering mirror. The alignment laser beam is located outside the laser footprint but within the circular area inscribing the square laser beam. It passes through the laser gas upstream of the laser medium.

The injection laser is located on the platform optical bench outside the transmitter assembly. To eliminate the alignment sensitivity as a result of the soft transmitter module mounting, an unattenuated injection beam will be used for injection through a dielectric turning mirror.

5.2.1.1.4.3 Electrical Power and Instrumentation

The electrical power and instrumentation interface will be designed to support a 28 Vdc, 3200 W prime power bus from the spacecraft. ARL anticipates a dual power bus configuration to separate the laser pulse power lines from those that belong to the subsystem support power system, such as instrumentation and control.

The interface will be designed to minimize EMI generated in the transmitter assembly from being fed back into the power supply line. Fiber optic links will be used for instrumentation and data transfer interfaces.

5.2.1.1.5 References

1. A.E. Siegman, Lasers, University Science Books, p. 1163, 1986.
2. P. Das, "A Boltzmann Equation Solver," unpublished.
3. K.J. Andrews et al., "A Rate Equation Model for Design of TEA CO_2 Oscillators," J. Phys. E: Sci. Inst. 8, 493, 1975.
4. A.E. Siegman, Lasers, University Science Books, p. 877, 1986.
5. K.E. Oughstun, "Unstable Resonator Models," Progress in Optics, edited by E. Wolf, North Holland, NY, pp. 165-387, 1987.
6. M. Lax, G.P. Agrawal, M. Belic, B.J. Caffey, and W.H. Louisell, "Electromagnetic-Field Distribution in Loaded Unstable Resonators," J. Opt. Soc. Am. A, Vol. 2, p. 731, 1985.
7. P. Horwitz, "Asymptotic Theory of Unstable Resonator Modes, J. Opt. Soc. Am. 63, p. 1528, 1973.
8. S. Lovold, Frequency Chirp in a 10 atm RF-Excited CO_2 Waveguide Laser, IEEE J. Quant. Electron, Vol. 24, No. 12, p. 2514, 1988.
9. D.V. Willetts and M.R. Harris, Attainment of Frequency Stable High-Energy Operation of a CO_2 Laser by Use of a Telescopic Resonator, IEEE J. Quant. Electron, QE-21, No. 3, p. 188, 1985.
10. D.V. Willetts and M.R. Harris, Laser-Induced Frequency Sweeping in an Electron-Beam Sustained Carbon Dioxide Laser, Opt. Commun., Vol. 49, No. 2, p. 151, 1984.
11. D.Y. Zaroslov et.al., Spectral Characteristics of Vacuum Ultraviolet Pre-ionization Sources for CO_2 Lasers, Sov. J. Quantum Electron. 8 (6), June, 1978.
12. M.C. Richardson, et al., Large Aperture CO_2 Laser Discharges, IEEE J. of Quantum Electron., Vol. QE-9, No. 9, September, 1973.
13. W.J. Witteman, The CO_2 Laser, Springer Verlag, Berlin, 1987.
14. D.J. Brink and V. Hasson, J. Appl. Phys. 49, 2250, 1978.
15. V. Hasson and H.M. Von Bergmann, Rev. Sci. Instrum. 50, 1979.
16. D.S. Stark and M.R. Harris, "Catalysed Recombination of CO and O_2 in Sealed CO_2 TEA Laser Gases at Temperatures Down to -27 C," J. Phys., E. 16, p. 492, 1983.
17. D.S. Stark, A. Crocker, and G.J. Steward, "A Sealed 100-Hz CO_2 TEA Laser Using High CO_2 Concentrations and Ambient-Temperature Catalysts," J. Phys. E. 16, p. 158, 1983.

18. B.T. Upchurch, D.R. Brown, I.M. Miller, and D.R. Schryer, "LARC-Developed Catalysts for CO_2 Lasers," NASA CP-10037, p. 47, 1989.

19. M.R. Harris and D.V. Willets, "Dissociation Phenomena in Electron-Beam-Sustained Carbon Dioxide Lasers," NASA CP-10037, pp. 97-115, 1989.

5.2.1.2 GEC Laser Configuration Selection

5.2.1.2.1 Requirements Trades

This section consists of studies of relevant areas of laser technology, and describes the laser configuration selected by GEC Avionics, and the reasons for that selection.

5.2.1.2.1.1 Comparison of Requirements for CO_2 Gas Laser and Solid State Laser for LAWS

The factors affecting the suitability of the different laser types for use in the LAWS project can be divided into three main areas: laser transmitter technology, laser radiation interaction with the atmosphere, and optical system. Two laser types were considered for the LAWS project; a rare earth doped solid state laser, and a carbon dioxide gas laser. The necessity for the system to be "eye-safe" precludes the well established Nd:YAG laser and necessitates either Raman shifting, or the new Erbium and Holmium doped YAG lasers, operating around 2.1 μm. The choice of carbon dioxide isotope and line selection within the 9 to 10 μm wavelength region will be discussed in the next section.

5.2.1.2.1.1.1. Atmospheric Interaction

The wind velocity measurements will be made from backscatter of the laser radiation from aerosols. The backscatter coefficient has a wavelength dependence of $\lambda^{-1.2}$, which would tend to favor shorter wavelengths. However, Menzies (Ref. 1) has investigated the effect of the atmospheric interaction on the laser requirements for a given velocity uncertainty, for 1 μm and 9 μm wavelengths. At the LAWS system requirement of a one m/sec velocity uncertainty, the estimated required pulse energies are 7 J and 9 J for 1 μm and 9 μm wavelengths respectively. There will probably be less difference between 9 μm and the 2 μm wavelength required by eye safety consideration.

Other considerations, such as atmospheric turbulence and penetration will slightly favor the longer wavelengths. Therefore, because of atmospheric reasons alone, it is difficult to favor one wavelength or the other.

5.2.1.2.1.1.2. Optical System

For a given mirror diameter (1.5 m for LAWS) the 9 μm beam will have a larger divergence than that at 2 μm. This implies that the rotating telescope and lag-angle compensation will not need such stringent design considerations for the 9 μm case. Another factor is that the local oscillator and return beam must be aligned on the heterodyne detector to within a criterion which is linearly related to wavelength. Thus, these factors favor the longer wavelength.

With regard to the detector, necessary performance for 9.1 μm operation using a cadmium mercury telluride (CMT) detector has been demonstrated. For 2.1 μm operation, InGaAs is a possible material for detectors, but is not as yet proven in heterodyne detectors of the required parameters. It should be noted that the bandwidth required for the 2 μm detector is a factor of 4.5 greater than for the 9 μm case. This is governed by the variation of the line-of-sight component of the satellite's velocity throughout a scan period. For a 800 km orbit and 55° from nadir observation angle the bandwidths are 1.3 GHz for 9.1 μm and 6.1 GHz for 2.1 μm. However, as it is in general easier to make an efficient wide-band detector at shorter wavelengths, this might help to compensate, in technology terms, for the wider bandwidth.

In general, technology considerations for the optical subsystems would seem to favor the longer wavelength operation.

5.2.1.2.1.1.3. Laser System

The LAWS requirement is for a maximum horizontal wind vector accuracy of one m/sec and a vertical resolution of 1 km. For a 45 deg nadir scan angle this implies a line-of-sight velocity resolution of 0.7 m/sec for a simplified geometrical analysis; although the individual pulse velocity resolution will probably be able to be relaxed due to poly-pulse averaging techniques employed.

For purposes of this simple comparison, a one m/sec required velocity resolution will be used.

The Doppler shift $\Delta\lambda$ for light of wavelength λ reflected off an aerosol with line-of-sight velocity, u (assuming $u << c$) is given by $\Delta\lambda = -2\ u/\lambda$. It is seen that the necessary frequency resolutions are 219 kHz for 9.11 μm radiation and 0.95 MHz at 2 μm wavelength. The Fourier transform of these pulse frequency stabilities implies a 4.5 μs pulse length at 9.1 μm and 1.05 μs at 2.1 μm. Both pulse lengths would lie within a 1 km

vertical range bracket. Thus, both systems can simultaneously meet the horizontal velocity and vertical resolution requirements. As described previously, both system types will also require a pulse energy of approximately 10 J. Requirements on system lifetime and data coverage give laser pulse repetition frequency of 10 Hz for 109 pulses.

For the normal CO_2 laser isotope operating at 10.6 μm, all the system requirements have been obtained, with the exception of the 109 pulse lifetime in a sealed-off laser. Comparison with lasers operating on the oxygen-18 isotope necessary for 9.11 μm operation is reviewed in Section 5.2.1.2.1.2. The CO_2 laser has a long history of research and development, over twenty years, and is at a more advanced stage of technology than the much newer lasers operating around 2 μm.

Potential candidates for a 2 μm laser are Erbium:YAG and Holmium:YAG based systems, with the latter laser often being co-doped with Thulium. The Er^{3+}:YAG laser operates at 2.6 μm and the Tm^{3+}:Ho^{3+}:YAG at 2.09 μm. Of these two, only the Ho:YAG systems need to be considered for the LAWS application, due to high atmospheric attenuation at 2.6 μm.

The Thulium:Holmium:YAG laser technology is at an early stage of development, especially with the diode pumping. The Ho:YAG laser has been demonstrated with a 109 pulse lifetime, but has not met the pulse energy requirement of 10 J. Indeed, the maximum reported pulse energy is only 250 mJ.

To achieve higher powers, it will be necessary to cool the laser, thus adding to the complexity of the system. Optical slope efficiencies of 25 percent for room temperature operation have been demonstrated. This implies that for a 10 J pulse output, 40 J of laser diode pump power will be required. Such large laser diode arrays have not been reported, and it is expected that they could have a very large cost of tens of millions of dollars. The laser is expected to meet the pulse width and frequency stability requirement, especially under the cryogenically cooled conditions necessary for high energy operation.

It is possible to produce high power, eye-safe, laser radiation at 1.54 μm by Raman shifting the 1.06 μm radiation from a Nd:YAG laser. A multi-atmosphere methane cell is used, probably incorporating gas circulation and a heat exchanger for a high pulse repetition frequency, high energy operation. Efficiencies of a few tens of percent have been achieved for these systems, but this will still bring the overall laser system efficiency below that required for LAWS. Because the Raman effect is a non-linear process, the efficiency will increase with laser peak power, which will tend to favor short

pulse, high peak power pulses, which are not compatible with the LAWS system. The Raman shifting process will also have a pulse shortening effect, further moving the transmitted pulse from that which is required.

These factors, and especially the lack of maturity of the technology of these short wavelength laser systems, indicate that the CO_2 laser should be the primary choice for the LAWS project.

5.2.1.2.1.2 Comparison of Isotopic CO_2 Wavelengths

There are three candidate transitions for the LAWS laser. These are the high gain 10P(20) transition at 10.59 μm, the 9R(24) transition at 9.25 μm and the 9R(20) transition of the $C^{18}O_2$ isotope at 9.11 μm.

The 10.59 μm transition has the highest gain transition of the normal $C^{16}O_2$ isotope. This transition oscillates in the absence of intracavity wavelength selective optics, and its characteristics are well understood. This transition is expected to have the greatest energy and efficiency, both advantageous for LAWS.

The 9.25 μm transition is chosen due to the enhanced aerosol backscatter coefficient observed for this wavelength (Ref. 2) especially over oceans. There is an enhancement factor of three to four times in the troposphere over the backscatter at 10.6 μm. This enhancement is thought to be due to ammonium sulphate aerosols because its spectral dependence cannot be accounted for by Rayleigh scattering. The atmospheric attenuation is also less, around 9.2 μm, than at 10.6 μm. There has also been some interest in the 9R(34) transition at 9.20 μm which has a higher atmospheric transmission, but is further away from the peak of the R branch gain curve at 9.27 μm (R20). The 9.25 μm line is favored for the R branch as the best combination of laser energy and efficiency, aerosol backscatter, and atmospheric transmission.

By using a rare isotope CO_2 laser, there will be a much reduced atmospheric concentration of the CO_2 to absorb the laser radiation, leading to a greater transmission. A good candidate for such a transition is the R20 transition of the $C^{18}O_2$ molecule at 9.11 μm. This wavelength undergoes enhanced aerosol backscatter as for 9.25 μm, has a high atmospheric transmission (leading to two orders of magnitude greater signal at 100 km compared to 10.6 μm for the same laser output), and is at the peak gain of the 9 μm R branch.

For similar conditions, the 9.11 μm line of $C^{18}O_2$ is found to have a 20 percent greater gain than the 10.59 μm $C^{16}O_2$ line, but a 20 percent faster decay of the gain with time.

Thus, it is expected that for medium length pulses (3 to 5 μsec) the 9.11 μm laser will have a similar performance in terms of output energy and efficiency to the 10.59 μm CO_2 laser. Two disadvantages of using the oxygen-18 isotope are isotopic exchange with the catalyst and laser body, and the increased cost of rare isotope CO_2. The first problem can be overcome by pre-conditioning the laser body, to remove oxygen, and pre-treatment of the surface of the catalyst to ensure replacement of all oxygen atoms with the required isotope (operation of catalyst below 100 °C then inhibits migration of oxygen-16 from the bulk of catalyst). The relatively high cost of $C^{18}O_2$ of about $600 per liter atmosphere implying approximately $10,000 for a LAWS laser fill, is not prohibitive considering the total budget for this project.

In conclusion, the optimum choice for the laser transition for LAWS should be the 9.11 μm wavelength from $C^{18}O_2$ 9R20 transition as it combines high energy and efficiency with good atmospheric transmission and large aerosol backscatter.

5.2.1.2.1.3 Laser Efficiency

To determine the expected laser efficiency it has been necessary to use experience gained with lasers which have not been operated under the same frequency stability and resonator design conditions as will be applicable to the LAWS laser. The method employed has been to ascertain the multimode efficiency of the lasers operating with the discharge technologies of interest for this work. An efficiency factor, equal to the expected reduction in overall efficiency for a single mode, single line output of low frequency chirp was then applied to each laser type. This then gives an overall laser efficiency relating energy deposited into the discharge to the useful laser energy extracted with the required beam properties. The overall efficiency factor has terms depending on active volume filling factor and single longitudinal mode operation, single transverse mode operation, and single line operation.

5.2.1.2.1.3.1 Multimode Efficiencies

Self-Sustained Discharge. An X-ray pre-ionized TEA self-sustained discharge has been operated at GEC Avionics with output pulse energies up to the 12.5 J level. A multimode efficiency of 7 percent was measured for this device for an input energy density of 180 J/L. Increasing the energy loading to 260 J/L caused a slight reduction in

efficiency, but gave an increased output pulse energy. These efficiencies do not include the energy supplied to the pre-ionization source.

Pulser Sustained Discharge. An extensive study of a laser operating with a Photo Initiated Impulse Enhanced (PIE) pulser sustainer discharge technology has been made at GEC Avionics. The multimode efficiency of the system was calculated from the output energy density, and the total input energy density of both pulser and sustainer discharge circuits. The optimum efficiency obtained was 11.7 percent for an output energy density of 4.3 J/L. However, for different discharge conditions and at a slightly reduced efficiency of 11.5 percent, the output energy density was 5.2 J/L.

e-beam Sustained Laser. A number of e-beam sustained lasers have been operated at Royal Signals and Radar Establishment (RSRE) at Malvern, England. The operational characteristics of one laser developed and built in conjunction with GEC-Marconi companies have been published (Ref. 3). This laser has been operated at high pulse repetition frequencies (66 Hz) and pulse energies of 600 J. The quoted laser efficiency was 15 percent.

Summary of Multimode Efficiencies. The multimode efficiencies summarized in Table 5-15 will be used as the starting point for the calculation of the overall laser efficiency for each discharge technology type:

Table 5-15. Multimode Efficiencies

Self-sustained discharge	6.8%
Pulser sustainer discharge	11.5%
e-beam sustained discharge	15.0%

5.2.1.2.1.3.2 Active Volume Filling Factor

The multimode laser output is assumed, for this exercise, to extract energy uniformly from the discharge region; that is, it has a filling factor of unity. This is not totally accurate, due to the roll-off in intensity toward the edge of the laser beam. However, in comparing the filling factors derived in this section to a multimode filling factor of one, a conservative estimate of the filling factor will be made.

The active volume filling factor is the ratio of the laser mode volume to the discharge volume, and is a measure of how effectively energy can be extracted from the active volume. This factor itself has a number of components, as described below.

Circular Aperture Effect. Aperturing a square discharge volume with a circular aperture, whether deliberately inserted or as mirror edges, will produce a geometric factor of $\pi/4$ from the ratio of the area of a square to its inscribed circle for the discharge volume available to the laser mode. It is assumed that the LAWS system telescope will be of circular cross-section; and thus it will be necessary for the laser beam to be circular in order to match the telescope.

Cathode Shock Wave Factor. As the discharge occurs, there is enhanced heating close to the cathode due to greater energy deposited in the cathode fall region. This leads to a shock wave propagating into the discharge region from the cathode. There are similar, but very much weaker effects from the anode and the rarefactions propagating into the discharge region from its boundary with the unheated gas along its sides. These smaller effects can be ignored. The effect of the cathode shock wave on the CO_2 laser medium homogeneity is readily evident from work published (Ref. 4).

The shock wave will propagate at the speed of sound, and if it reaches the mode volume, it will degrade the laser beam quality and frequency stability. Thus the intracavity aperture must be sited a distance above the cathode governed by pulse length and the speed of sound in the laser medium. The speed of sound will depend on the ratio of the components of the gas mixture, and the gas temperature which will be increasing throughout the laser pulse.

The speed of sound will be greatest in a He-rich mixture, so a worst case will be investigated of a 3:1:1 $He:CO_2:N_2$ gas mixture. Under room temperature and pressure conditions, the speed of sound is found to be 461 m/sec. Thus, for a 3 μsec pulse, the shock wave will propagate 1.4 mm. For a 200 J/L input energy, the laser gas medium temperature is expected to rise by 130 °C during the pulse. Integration of the distance travelled in each elemented time during the pulse for the changing velocity gives a total shock wave propagation distance of 1.53 mm.

Thus, the aperture edge must be sited 1.53 mm from the cathode, and the cathode shock wave effect factor is $(1-\frac{0.153}{d})$, where d is the discharge gap in centimeters. Taking a typical discharge gap for the LAWS laser of 6.7 cm gives a cathode shock wave factor of 0.98.

Spatial Mode Profile Factor. For a uniform mode radius along the gain length as for a Cassegrain unstable resonator, or a stable resonator with large radius of curvature mirrors, the laser mode volume is directly proportional to mode area, that is the area under an intensity against radial distance plot for the mode distribution.

For a uniform intensity I_0 filling the intracavity aperture of radius a, the power extracted is proportional to $\pi a2I_0$.

For a Gaussian mode profile, $I(r) = I_0 e^{-2r^2/w^2}$, where w is the beam radius at the 1/e2 of peak intensity points, and setting 2a = 3w as the normal criterion for transverse mode selection in stable cavities, the power extracted will be proportional to

$$P = I_O \int_O^a e^{-2r^2/w^2} 2\pi r dr$$

which yields on integration $P = 0.22\pi\ I_0a2$. So for a Gaussian beam with 2a = 3w the Spatial Mode Profile Factor would be 0.22.

Parent, McCarthy, and Lavigne (Ref. 5) have performed similar calculations for the mode profiles of unstable resonators employing Gaussian reflectivity mirrors. For good quality mode profiles and transverse mode discrimination, the aperture radius, a, needs to be such that w/a = 0.56. Under these conditions, the Spatial Mode Profile Factor is found to be 0.30 for a cavity magnification factor M, of two.

Tratt and Menzies (Ref. 6) state that for an unstable resonator with uniform reflectivity mirrors, a comprehensive parametric study has shown that the optimum energy extraction is greatest for cavity magnification factor, M, less than 2. However, other factors, described in more detail in Section 5.2.1.2.1.8, indicate a larger value for M is preferred. Thus a value of M around 2 is taken as optimum. Under this condition, Tratt and Menzies have taken the cavity filling factor for an unstable resonator as unity. This figure seems an optimistic approximation. A clear understanding of the radial profile for an arbitary unstable resonator is not easily achievable. However, a better value will be to use 0.9 for the Spatial Mode Profile Factor for an unstable resonator. This value will be used for the efficiency calculation because a hard mirror unstable resonator is the most likely choice for the LAWS laser.

5.2.1.2.1.3.3 Single Longitudinal Mode Operation

For a homogeneously broadened laser, a superficial investigation of the gain mechanism predicts that only one laser cavity mode should oscillate. However, in a practical

cavity, it is possible for more than one mode to oscillate as their standing patterns will "feed off" spatially separated areas of the gain medium. Mode competition will then share the available laser energy between these modes. Forcing the cavity to oscillate on only a single longitudinal mode should not reduce the overall laser energy by a large factor.

A comparative study was undertaken at GEC Avionics using a TEA CO_2 laser of multi-longitudinal mode and single longitudinal mode (SLM) pulse energy. The SLM operation was achieved using an intracavity low pressure discharge. Pulse energies with the low pressure discharge on and off were compared. The low pressure discharge cell was at a pressure of 20 mbar and a discharge voltage of 20 kV was used.

The single longitudinal mode operation resulted in a reduced laser pulse energy by a factor of 0.83.

5.2.1.2.1.3.4 Single Transverse Mode Operation

This effect has been discussed above in that the Spatial Mode Profile Factors all apply to single transverse mode operation, whether for the Gaussian mode of a stable cavity, or the nearly uniform transverse intensity distribution of the hard mirror unstable resonator, which has inherently good transverse mode discrimination for correct choice of the cavity parameters. Thus for the efficiency calculations, this effect will be considered to be included in the Spatial Mode Profile Factor.

5.2.1.2.1.3.5 Single Line Operation

The multimode efficiencies would all correspond to single line operation of the CO_2 laser. This would be the high gain 10P(20) line at 10.59 μm. For the LAWS laser, it is desired to operate on the 9R(20) line of the $^{12}C^{18}O_2$ isotope at 9.11 μm. Hamilton et al. (Ref. 7) have measured a 20 percent higher gain at 9.11 μm than at 10.59 μm, but also noted that the small signal gain decay was 20 percent faster than for the normal isotope. It was expected that these factors would combine to give a comparable performance for a laser operating on 9R(20) $C^{18}O_2$ as for 10P(20) $C^{16}O_2$.

Work undertaken at GEC Avionics has shown that it is possible to introduce tuning optics to a laser cavity with only a small degradation of laser output. Comparing the untuned output from a 3 J laser to the output on 10P(20) from the line tuned cavity, a reduction factor to 0.85 was obtained. If an injection seeded arrangement is chosen, then this factor will not be needed as the power oscillator will have a non-dispersive cavity.

5.2.1.2.1.3.6 Overall LAWS Laser Efficiency Factor

The overall laser efficiency for the LAWS laser will be determined by the multi-mode efficiencies summarized in Table 5-16 for each laser type and an efficiency factor as summarized below.

Table 5-16. Expected Laser Efficiencies

	Dispersive Cavity	Injection Seeded
Self-sustained discharge	3.3%	4.0%
Pulser sustainer discharge	5.6%	6.8%
e-beam sustained discharge	7.3%	8.8%

- Active volume filling factor of 0.69 comprising:
  - circular aperture effect factor of 0.79
  - cathode shock wave factor of 0.98
  - spatial mode profile factor of 0.9
- Single longitudinal mode operation factor of 0.83
- Single line tuned operation factor 0.85.

Therefore, the overall efficiency factor is 0.49 for a dispersive cavity or 0.59 for an injection seeded option.

Thus, the expected laser efficiencies for each discharge technology in the LAWS configuration are as given in Table 5-16.

It should be noted that these efficiencies are defined as:

$$\text{Laser efficiency} = \frac{\text{energy out of laser}}{\text{energy into laser and pre-ionizer}}$$

They do not include the effects of power supply efficiencies, or other system power requirements. The wall-plug efficiencies, as discussed in Sections 5.2.1.2.1.4 and 5.2.1.2.2.6, are considerably less than the above.

5.2.1.2.1.4 Discharge Technology

In this section, the discharge technologies considered are discussed, and a preliminary selection is made.

5.2.1.2.1.4.1 Conventional Self-Sustained Laser

As described in Section 5.2.1.2.1.3, the estimated laser efficiency for a conventional self-sustained laser is 4.0 percent. This is already below the 5 percent wall plug efficiency requirement, even before power supply efficiencies are taken into account. This discharge technology is therefore unsuitable for LAWS applications.

5.2.1.2.1.4.2 Pulser-Sustainer Laser

The pulser-sustainer concept produces pressure and volume scalable plasmas by essentially applying two successive discharges to the gas. The first high voltage pulse creates the electron density uniformly between the electrodes, using only a small amount of energy. A second discharge applies the proper voltage to this plasma to tune the electrons to a temperature sufficiently high for efficient laser pumping but not high enough to create any further increase in electron density. Thus the dominant amount of energy is put into the gas (by the sustainer) exactly where it is desired, i.e. in vibrational excitation of N_2 and CO_2. The system is then one with two discharge circuits, one controlling electron density, the other electron temperature. The maximum working pressure is around 100 torr; this has been extended at GEC Avionics by pre-ionizing the discharge volume with UV radiation. By this means the working pressure has been extended to 250 torr.

As described in Section 5.2.1.2.1.3, the laser efficiency is less than that of an e-beam sustained laser, but 5 percent wall plug efficiencies should be obtainable. However, the maximum input energy loading was found at GEC Avionics to be 42 J/L. This compares with a value of 180 J/L for an e-beam sustained laser, resulting in a considerably larger and heavier laser head.

The pulser-sustainer laser, therefore, is considered a useful possible discharge technology but is slightly less efficient, and considerably heavier than an e-beam sustained laser, particularly for high output energy levels. However, it does not have the disadvantage of the e-beam sustained laser of foil lifetime issues.

5.2.1.2.1.4.3 Long Pulse Self-Sustained Laser

In general, two main approaches have been used to obtain stable discharges from long pulse self-sustained lasers. In the seventies, the main approach was the use of a very high level of pre-ionization to obtain electron densities of the order $10^{12}cm^{-3}$ (Ref. 8). Obtaining these high electron densities required the addition of organic com-

pounds, with low ionization potentials, to the gas mix. Having obtained these high electron densities, long pulse sustaining currents were applied to the electrode gap to pump the gain medium. Using this technique, pulse lengths of 5 μsec have been obtained with stable discharges at one atmosphere pressure in $1CO_2$:$2N_2$:3He gas mixes. This approach has the advantage of being able to operate at atmospheric pressure thereby giving good output energy densities, typically up to 15 J/L. There are several major disadvantages of this stabilization technique which are particularly relevant to long-life, sealed-off operation. The organic additives are dissociated by the discharge and must be replenished, and the by-products must be removed to avoid coating of the optical elements. The efficiency of this approach is also impaired by the large energy required to pre-ionize the discharge. For these reasons, this approach is not appropriate for LAWS applications.

In standard TEA lasers, pre-ionization levels with electron number densities of $10^7 cm^{-3}$ are sufficient to obtain a stable glow discharge. Electron multiplication to the required level being achieved by substantially overvolting the electrode gap. Recently, work at AVCO (Ref. 9) and by Chakrabarti and Reid (Ref. 10) has demonstrated that self-sustained lasers can be operated with long pulse length, up to 20 to 30 μsec, in a similar manner to TEA lasers without the use of low ionization potential additives. Their work has demonstrated that stable discharges can be obtained by a three-step approach. The first step is to create a uniform volume pre-ionization with electron densities similar to that of the standard TEA laser. This is followed by careful avalanching to obtain the electron density required. Thirdly, the electric field strength has to be carefully regulated to control the ionization and recombination rates. This is because a stable glow discharge, for a long pulse self-sustained laser, can only be obtained when the ionization and recombination rates are equal. Work by AVCO (Ref. 9) has shown that this condition is only fulfilled for a sustaining voltage around 30 to 40 percent lower than the static breakdown voltage.

In practice, this result implies a reduction in the operating pressure to 200 to 600 torr followed by an increase in the He content of the gas mix to around 75 percent. The combination of these changes coupled with uniform pre-ionization and a pulse forming network to extend the sustaining current to the appropriate pulse length has allowed them to obtain output energy densities of 5 J/L at efficiencies of up to 8 percent from TEA lasers with pulse lengths of up to 30 μsec.

Although this technology appears promising, it suffers from the efficiency being lower than for an e-beam sustained laser, as higher excitation voltages are used for the laser discharge, and lower volumetric efficiency, leading to a larger and heavier laser subsystem. More important, though, is the fact that the conditions for maintaining a stable discharge are critical, and any change in operating parameters (for example, an increasing oxygen level) could upset the discharge control and cause arcing. This is of particular concern for LAWS, where a 10^9 pulse lifetime is required, and long-term reliability is essential.

GEC Avionics' perception of the principal benefits and risks of the pulser sustainer/long pulse self-sustained technology are summarized in Table 5-17.

Table 5-17. Pulser Sustainer/Long Pulse Self-Sustained Discharge Laser Trades

ADVANTAGES

- No foils or very high voltages
- 5 percent wall-plug efficiency should be achievable

MAIN RISK AREAS

- Lifetime of low ionization potential compounds (if used)
- Achievement of required pre-ionization intensity
- Pre-ionizer lifetime (e.g., dielectric failure of corona board)
- Pulse shape; cut-off after 3 μsec may not prove straightforward
- Long-term discharge stability and reliability
- Attainment of high input energy densities and pressure

While the long pulse self-sustained technique appears promising, GEC Avionics' assessment is that, at the high levels of pressure and input energy densities required for a compact light-weight system, it is on the very edge of technology. The conditions for stable operation appear to be critical and may be difficult to maintain over a long period. The technique is apparently as yet unproven for long term, reliable systems.

5.2.1.2.1.4.4 e-beam Sustained Laser

GEC's perception of the principal benefits and risks of the e-beam sustained laser are summarized in Table 5-18.

Table 5-18. e-beam Sustained Laser Trades

ADVANTAGES

- The reduced electric field strength value for the laser discharge can be independently optimized to give maximum efficiency; hence the e-beam sustained laser is inherently more efficient than other technologies
- Low CO_2 dissociation rates lead to reduced catalyst requirements
- Less isotopic scrambling due to low dissociation rates
- Good pulse temporal shape: a 3 μsec top-hat pulse can be generated, resulting in cut-off after the pulse, which prevents confusion over returns from clouds
- Better frequency control, as the current is essentially constant during the optical pulse, and any ripple can be controlled
- No arcing if properly set up, as arcing due to electron attachment is not an issue
- Demonstrated at the required energy levels, so low risk
- Demonstrated sealed-off operation
- Only the electron gun PFN is switched, which eases high voltage switch requirements

MAIN RISK AREAS

- Foil lifetime
- Radiation issues
- High voltages (160 kV for electron gun)

Of these, the issue of high voltages is not especially onerous. The switch and pulse forming networks all operate at lower voltages, so the only very high voltages are in the electron gun and transformer. The electron gun design includes an earthed metal screen which contains the high voltage areas. The transformer will be insulated and screened. The principal disadvantages of the e-beam sustained laser are therefore foil lifetime, and radiation, discussed fully in Sections 5.2.1.2.1.9 and 5.2.1.2.1.10.

5.2.1.2.1.4.5 Discharge Technology Selection

It is the opinion of GEC Avionics that, on balance, the risks of the pulser-sustainer/ long pulse self-sustained technology are greater than for an e-beam system where the

principal risk is that of foil lifetime, an engineering issue for which initial analysis indicates that it is a problem which can be overcome.

GEC Avionics therefore selects an e-beam sustained laser as the primary choice for the LAWS system. A laser based on the pulser-sustainer technology, probably X-ray pre-ionized, would be a secondary choice, with a lower efficiency, greater weight, and higher risk.

5.2.1.2.1.5 Pulse Shape

A photograph of an e-beam sustained laser output pulse, similar to that which would be expected from the LAWS laser configuration proposed by GEC Avionics, is shown in Figure 5-21. This was obtained with an e-beam sustained laser hybridized with an intracavity continuous wave discharge. Because laser radiation is present throughout the build-up of the pulse, this is a similar situation to pulsed injection. The LAWS laser configuration proposed by GEC Avionics would therefore be expected to produce an output pulse of similar shape.

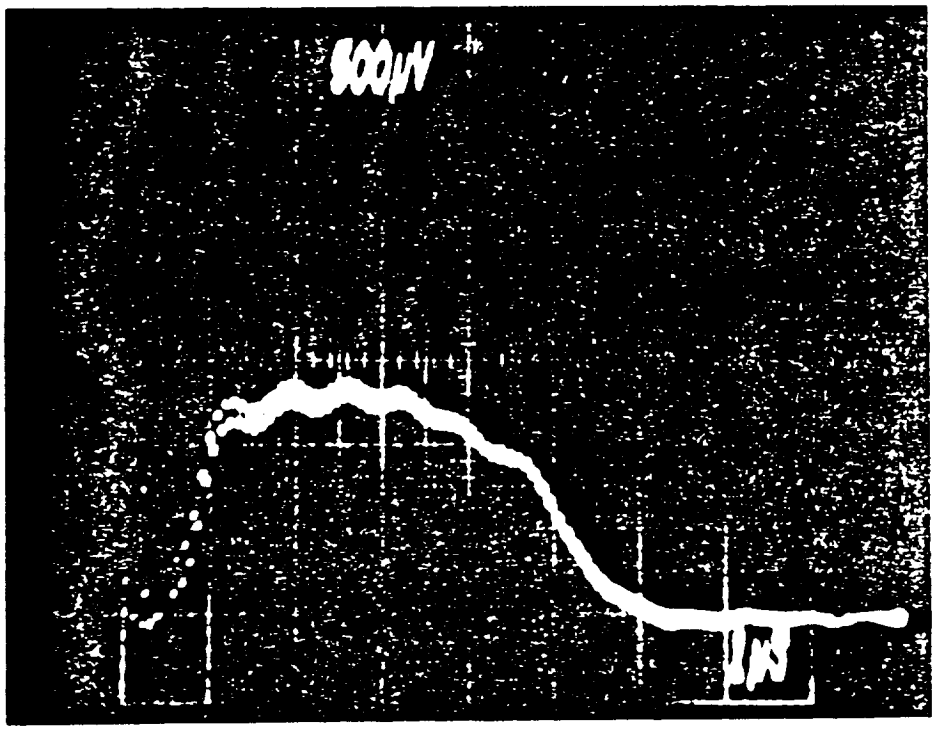

Figure 5-21. Temporal Output of Hybrid e-beam Laser

As can be seen, the pulse shape is almost ideal for LAWS applications, with no gain-switched spike, a full width half maximum of 4 μsec, and complete cut-off of the

tail of the pulse by 6 μsec. These figures could be easily adjusted, if required, by appropriate circuit design. The required LAWS horizontal wind vector accuracy of ±1 m/sec in the lower troposphere will be significantly easier to obtain with this type of laser output pulse shape than a 1 μsec pulse. In addition, the absence of a tail for the e-beam sustained laser prevents any confusion over returns from clouds.

5.2.1.2.1.6 Gas/Catalyst Effects

During operation of the laser, carbon dioxide dissociates into carbon monoxide and oxygen, which are then recombined using a room temperature catalyst. The degree of dissociation, and hence the quantity of catalyst required, varies according to the discharge technology used.

Work at GEC Avionics (Ref. 11) has demonstrated sealed-off laser lifetimes of 2×10^7 pulses and component lifetimes of 10^8 pulses. Catalysts have also been successfully used with e-beam sustained lasers (Ref. 12) and at low temperatures (Ref. 13).

5.2.1.2.1.6.1 Self-Sustained Laser

Measurements at GEC Avionics using mini TEA lasers of output energy 70 mJ, show an oxygen generation rate of 0.196 μmoles per pulse, from a discharge volume of 0.011 L, equivalent to 17.8 μmoles per pulse per liter.

Mr. W. Upchurch's group at NASA, Langley has measured the oxygen generation rate for a Lumonics-820 CO_2 laser. He measured a rate of 6×10^{17} molecules of CO_2 dissociated per pulse, for a discharge volume of 0.30 L. The gas mix used was $9He:2CO_2:1N_2$, and the output energy 700 mJ. This is equivalent to an oxygen generation rate of 0.5 μmole per pulse, or 1.66 μmoles per pulse per liter. The fact that the volumetric figure is lower than that obtained at GEC Avionics may be due to the fact that the process does not scale linearly with volume, or could be caused by the lower E/N values used for the He-rich mix in the Lumonics Laser, of approximately 5 kV/cm.

Assuming a 2 L discharge volume for LAWS and volume scaleability, the following figures for oxygen generation rate are obtained:

High E/N: 35.6 μmole per pulse
Low E/N: 3.3 μmole per pulse.

5.2.1.2.1.6.2 E-Beam Sustained Laser

D.V. Willetts and M. Harris have measured the oxygen generation rate for an e-beam sustained laser as 30 μmoles per coulomb of charge passed (Refs. 14 through

17). For a typical LAWS configuration, this is equivalent to an oxygen generation rate of 0.325 μmoles per pulse.

5.2.1.2.1.6.3 GEC Avionics E-Beam Test Bed

As reported in the 1989 NASA CO-Oxidation Catalyst Conference, GEC Avionics has undertaken recent tests using an e-beam sustained CO_2 laser amplifier with discharge dimensions similar to LAWS; if configured as an oscillator, outputs over 20 J would be expected. It is a totally sealed system with vacuum compatible materials.

A lifetest of two million pulses was carried out at a repetition rate of 8 Hz using a catalyst monolith. The oxygen level was maintained below 0.001 percent throughout the test, and operating parameters remained constant throughout. This is a particularly significant result as an excellent level of gas control has been demonstrated with a device of LAWS discharge dimensions.

Based on the above discussion, an e-beam sustained LAWS laser will have a significantly lower dissociation rate than a self-sustained laser, by a factor of 10 to 100 depending on the operating E/N. This will result in a reduced catalyst requirement, less oxidation of surfaces, less isotopic scrambling, and a constant output energy for long-term operation. It may also mean that no gas refilling system will be necessary.

5.2.1.2.1.7 Frequency Stability

Having achieved oscillation on the correct line and single longitudinal mode and single transverse mode operation, as discussed in Section 5.2.1.2.1.8, it is necessary for that oscillating cavity mode to remain constant to the required level (200 kHz) throughout the pulse. The cavity resonance condition is $m\lambda = 2\ nL$ where m is an integer, and L is the cavity length. There is thus a requirement on the stability of both the cavity refractive index, m, and length, L, for the duration of the optical pulse. The refractive index can be altered due to contributions from the LIMP effect and the plasma electron density.

The LIMP effect has been analyzed extensively by GEC; summary results are discussed in Section 5.2.1.2.1.7.3 where it is shown that correct choice of cavity aperture will hold the LAWS laser frequency to the required stability level. The plasma effect is similarly discussed in Section 5.2.1.2.1.7.1, where it is seen that there is a requirement that the discharge current be held constant to within 3 percent throughout the optical pulse. The stability requirement on the cavity length is discussed in Section

5.2.1.2.1.7.2. By correctly choosing the materials and design of the resonator support structure, the criterion for control of the resonator length will be met.

5.2.1.2.1.7.1 Plasma Effects

Within a gas discharge, there is a contribution to the refractive index of the discharge medium due to the electron density. Therefore in a gas discharge laser if the discharge current varies, the electron density and thus refractive index of the gain medium will vary. This, in turn, will cause the cavity resonance condition to be fulfilled for a different oscillating frequency.

Thus for the LAWS laser, the discharge current must be held within controlled values for the duration of the optical pulse.

The contribution of the plasma to the refractive index, n, is given by

$$n = \left[1 - (wp/w_o)^2\right]^{1/2}$$

where wp is the plama frequency given by

$$wp = \left[\frac{Ne^2}{m\varepsilon_o}\right]^{1/2}$$

and N is the electron density.

The electron density is related to the discharge current density, J, by

$$J = NeV$$

where V is the electron drift velocity, and the discharge current density, J, is related to the current, I, by

$$J = I/ld$$

where l is the discharge length and d is the discharge width.

The cavity resonance condition is

$$m\lambda = 2\ nL$$

where m = integer
L = cavity length
λ = wavelength of cavity radiation.

Therefore the cavity oscillation frequency, ν, is given by

$$\nu = \frac{mc}{2nL}.$$

Differentiation gives

$$\frac{d\nu}{dn} = \frac{-\nu}{n} \qquad \text{so} \qquad \Delta\nu = \frac{-\nu}{n}\Delta n.$$

For w >> wp

$$n = 1 - wp2/2w2 \qquad \text{and} \qquad \Delta n = \frac{-wp^2}{2w^2}$$

$$\text{so} \qquad \Delta\nu = \frac{\nu}{n}\frac{wp^2}{2w^2}\frac{1}{L}$$

where the cavity filling factor l/L has been included to allow for the gain medium not totally filling the cavity.

Insertion of the equations for wp and N gives

$$\Delta\nu = \frac{e}{8\pi^2 m\varepsilon_o} \cdot \frac{I}{nvVLd} = 2.51 \times 10^{20}\frac{I}{nvVLd}$$

For the LAWS laser, assuming the most likely configuration of an e-beam sustained laser, then the quantities have the following values:

n = 1.0002
ν = 3.28 x 1013 Hz
V = 5 x 104 m/sec
L = 0.6 m
d = 0.067 m
I = 2000 A.

Thus, ν = 3.8 x 103 I.

Now it is necessary to keep the frequency of the laser constant to within 200 kHz throughout the laser pulse, that is $\Delta\nu$ must not vary by more than 200 kHz. From the previous equation it can be seen that

$$\delta(\Delta\nu) = 3.8 \times 103\ \delta\ I$$

and thus the current must not vary by more than 52.5 A throughout the duration of the optical pulse to maintain the required frequency stability.

Therefore the peak to peak ripple on the discharge current from the discharge PFN must be less than 50 A, or alternatively the current must be constant to ±1.3 percent.

5.2.1.2.1.7.2 Cavity Length Effects

The requirement on the cavity length stability can be found by differentiating the cavity resonance condition to give

$$\frac{\Delta L}{L} = \frac{\Delta \nu}{\nu}$$

Inserting a cavity frequency of 3.28 x 10¹³ Hz (9.11 μm) and a length of 0.6 m (typical of expected LAWS laser design) then the 200 kHz stability implies that ΔL must be less than 3.7 nm for the 3 μs optical pulse length. Variations to the cavity length could be caused by thermal drift, shock waves, or mechanical vibration of the cavity mirrors.

Thermal Drift. The optical resonator will be mounted on three multi-ply carbon fiber tubes. These have a temperature coefficient in the longitudinal direction of less than 0.02 x $10^{-6}K^{-1}$. Thus, for the conditions stated above, the temperature of the laser structure must be held constant to 0.3 °C for the duration of the optical pulse. This implies a temperature drift of less than 100,000 °C per second and so will present no problem in its achievement.

Shock Waves. The current design of the laser head has a 120 mm distance between the discharge and the cavity mirrors. The pressure shockwave from the discharge will travel at less than 1 mm/μsec and will not affect the mirror position in the duration of the optical pulse. However, the mirror mounts must be designed to damp out in the interpulse period any oscillation caused by this shockwave.

Mechanical Vibration. Any vibration of the laser envelope structure could couple to the mirror mounts and cause an oscillation of the mirrors and thus the cavity length. The cavity mount should thus be designed to be decoupled from external vibrations as much as possible and to be stiff enough to resist oscillating driving forces. Of the possible internal vibrations, the main contender would appear to be the fan circulating the gases around the laser envelope. This could be revolving at 6000 rpm and might be expected to drive 100 Hz vibrations of the laser envelope and gas.

Assume that these acoustic vibrations cause the mirror to oscillate around its mean position with deviation x described by

$$x = x_0 \text{ Sin } wt$$

then the instantaneous velocity will be

$$\frac{dx}{dt} = x_o w \cos wt$$

and the maximum velocity will be $v_{max} = x_o w$. Setting this to the average rate of change of position of mirror allowed from frequency stability requirements gives

$$x_o w = \frac{3.66 \times 10^{-9}}{3 \times 10^{-6}} = 1.22 \times 10^{-3} \text{ m/sec}$$

and

$$x_0 = 2 \ \mu m \text{ for } w = 628 \text{ rad/sec.}$$

This is a fairly large amplitude oscillation to be set up in a well designed and constructed stiff mirror mount due to coupling of acoustic vibrations from the laser gas. It is therefore unlikely that acoustic vibrations from the fan will adversely affect the frequency stability requirement.

5.2.1.2.1.7.3 Intrapulse Chirp in CO_2 Lasers due to LIMP

The laser induced medium perturbation (LIMP) in a CO_2 laser occurs due to the faster relaxation of the lower laser level over the upper laser level. This leads to a gas heating rate related to the intracavity intensity. This gas heating causes an adiabatic expansion and consequent density reduction thus altering the refractive index of the gas. As the intracavity refractive index changes, so does the resonant frequency of the cavity. Throughout the laser pulse, the refractive index reduces. This leads to an increasing laser frequency, or chirp. To find the magnitude of this chirp a reduced form of the gas transport equations from hydrodynamic theory is used in detailed analysis (Refs. 14 through 17).

A laser pulse will have a minimum bandwidth associated with it of the Fourier transform limit. There will be no gain in reducing the chirp below this value. In designing the laser system, the chirp limit will thus be given by

$$\Delta\nu = 103/\tau \qquad (5.1)$$

(τ in μsec, $\Delta\nu$ in kHz)

Willetts and Harris have looked at the chirp rate for a number of CO_2 laser systems, including injection locked, self-sustained CO_2 laser (Ref. 14), hybrid TEA laser (Ref. 15), e-beam sustained oscillator (Ref. 16), and an e-beam laser with telescopic resonator (Ref. 17) with good agreement between theory and experiment, leading to the design criterion of

$$\Delta\nu = 11\ E\tau^2/\sigma^4 L \quad , \quad L \text{ in meters} \tag{5.2}$$

$$\text{i.e.,} \quad \sigma^4 L = 11 \times 10^{-3}\ E\tau^3 \quad \text{(at transform limit)} \tag{5.3}$$

where E (joules) is the total enery input to the gas in volume V, and σ (cm) is the radius at which the laser mode intensity has fallen to $1/e^2$ of its on-axis intensity.

Figure 5-22 shows the laser spot diameter at the $1/e^2$ of peak height points ($2W = 2\sqrt{2}\sigma$) as a function of pulse length for three different pulse energies, assuming a 1 m long cavity. This figure gives the minimum spot diameter required to produce a laser pulse with a frequency chirp no more than the transform limit bandwidth of the pulse.

For plane-plane cavities it has been found (Ref. 16) that the spot radius, W, is related to the intracavity aperture radius, a, by

$$W = 0.76a \tag{5.4}$$

The dimensions, d, of the laser discharge for both gap and width would then need to be

$$d = 2a \tag{5.5}$$

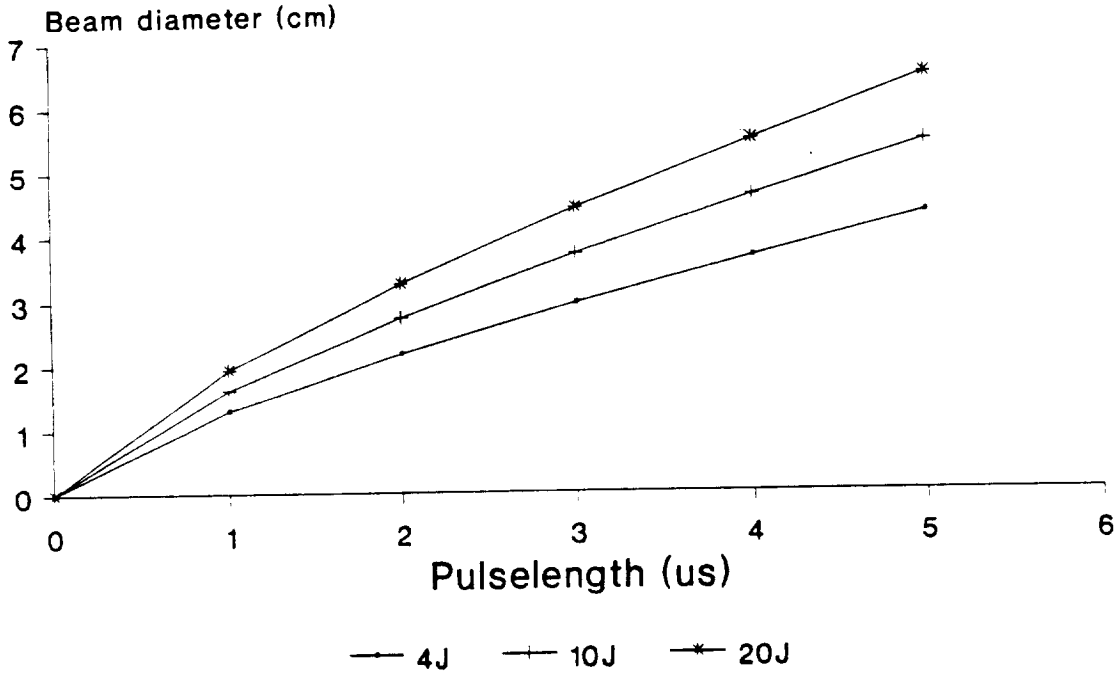

Figure 5-22. Required Beam Diameter for Frequency Stable Operation

Thus, combining the previous three equations (5.3) (5.4) and (5.5), the following design formula is obtained

$$d^4L = 2.11\ E\tau^3 . \tag{5.6}$$

For a laser with specified discharge volume, in liters, of V = 0.1 d^2l and cavity filling factor, f = l/L where l is the discharge length in meters, then

$$d^2 = 0.211 f \frac{E\tau^3}{V} . \tag{5.7}$$

This equation has been used to calculate the discharge dimensions for various configurations for the LAWS project. For configurations other than a plane-plane resonator a different constant of proportionality will exist between W and a in equation (5.4). Although the experimentally derived constant value of 11 in equation (5.2) gives the best fit to all the cases where chirp is observed throughout the laser pulse, it does not give good agreement to the one case where the laser resonator design did not give the pulse frequency bandwidth greater than the transform limit (Ref. 15). In that case, the observed frequency deviations would be better fitted by using a value of 6 kHz cm^4 $\mu sec^{-2} J^{-1} m$. If this constant value is to be used for cases of low frequency deviation, then equation (5.7) will give discharge dimensions a factor of 1.35 too large. Thus the results of equation (5.7) should be interpreted as the maximum discharge dimensions that will be required.

5.2.1.2.1.8 Mode Control and Wavelength Selection

The requirements for the LAWS laser are that its intrapulse frequency bandwidth be less than 200 kHz and that the oscillation be confined to the 9R(20) line of the $C^{18}O_2$ isotope at 9.11 μm. The control mechanisms for these factors are all related and so will be considered together in this section.

The single wavelength oscillation requires that the optics of the laser system have elements which will favor oscillation on the 9R(20) line and suppress the other lines, particularly the high gain line which would oscillate in the absence of any wavelength selective optics. The low frequency bandwidth further requires that the laser oscillate on a SLM and a single transverse mode (STM) and that the cavity resonance condition for this single mode remain constant throughout the pulse to within 200 kHz. This necessitates constraining the cavity length and refractive index within limits for the duration of the pulse.

On a longer timescale, the cavity frequency will need to remain within a certain frequency of the system local oscillator to enable heterodyne detection with the system

detector of a certain bandwidth. This will place a long term stability requirement on the cavity length, achievable by active or passive techniques.

5.2.1.2.1.8.1 Wavelength Selection

Wavelength selection could be achieved either by an intracavity dispersive element or by cavity optics coated to have a high reflectivity only for the required wavelength. This latter technique is likely to be impractical for the following reasons.

- It is not clear that coatings with such narrow band reflectivities can be fabricated.
- A coating of this type would have to consist of many layers and might thus be susceptible to damage.
- The maximum achievable reflectivity would possibly not be the optimum required for the LAWS laser. A variant on this theme which could be practical and beneficial would be to incorporate optics coated for high reflectivity over the R-branch transition wavelengths, in a cavity containing other dispersive elements, to assist in suppression of parasitic oscillation on the higher gain P-branch transitions. Thus an intracavity grating will be needed within the LAWS system to provide wavelength selectivity.

5.2.1.2.1.8.2 Single Longitudinal Mode Operation

The essence of SLM operation is to have only one cavity mode frequency within the laser medium bandwidth with a round trip gain greater than the cavity losses. This situation can be achieved by using a cavity with wide mode spacing (implying short cavity length) and a laser medium with a narrow gain bandwidth (obtained by operating laser at a reduced pressure). Other techniques can be applied to select only certain cavity modes by reducing the cavity losses on these modes only. These methods include the use of intracavity etalons, low pressure discharges, and three-mirror cavities. The use of etalons will not be appropriate for LAWS due to their low damage thresholds. A CW CO_2 low pressure discharge will be stable in a narrow bore discharge tube. This will be incompatible with the other system requirements, such as efficient extraction of energy from a wide aperture main discharge. However, a pulsed intracavity low pressure discharge in a He, N, CO_2 mixture could be incorporated into a wide aperture cavity. This would selectively enhance the gain on one cavity mode and cause laser oscillation on that mode only. This technique has been employed by GEC Avionics to produce SLM oscillation on high energy TEA CO_2 lasers.

Another possibility is to use a three-mirror cavity, which, being a normal cavity with either a partial reflector inserted or an intracavity beam splitter reflecting onto a total reflector, has in effect two different resonator lengths within the cavity. These are arranged so that only one mode from each resonator overlaps within the laser gain bandwidth. The two cavity lengths need to be stabilized to maintain the resonance condition.

5.2.1.2.1.8.3 Single Transverse Mode Operation

For a stable cavity, the normal method of producing STM oscillation is to use an intracavity aperture of a certain diameter. This increases the losses of higher order modes, while keeping the losses low for the TEM_{00} mode which has a Gaussian profile and thus the majority of its energy concentrated along the cavity axis. For the LAWS laser, it will not be possible to use a small intracavity aperture as this conflicts with other system requirements such as the need for low frequency chirp due to LIMP.

An unstable resonator has an inherent selectivity for oscillation on a STM for correct choice of cavity parameters. Because an unstable resonator also allows efficient extraction of energy from a large gain volume, it would seem to be a good method to use for STM oscillation.

5.2.1.2.1.8.4 Resonator Configuration Options

The two major classes of options available for the design of the LAWS laser are either to include the wavelength and mode selection elements in a high energy oscillator, or to decouple the frequency selection and energy production parts of the laser into a master oscillator and power oscillator respectively. The master oscillator is then used to injection seed the power oscillator. A master oscillator power amplifier configuration option has been considered, but has been rejected due to its low overall efficiency because of poor energy extraction from the amplifier stage.

As discussed in Section 5.2.1.2.1.8.3, the LAWS laser will need to use an unstable resonator. This will affect the configurations available within the two main classes discussed below.

Single Oscillator. For this option, both mode and wavelength selective optics are included in a high energy unstable cavity. The standard configuration would be to replace one cavity mirror with a curved grating used in the Littrow orientation. However, this leads to astigmatism in the cavity mode and output beam. The astigmatism, which

means that the beam wavefront has unequal radii of curvature in two orthogonal directions, can be lessened by reducing the angle of incidence on the curved grating. Maintaining the Littrow arrangement at near normal incidence requires a large spacing grating. Therefore astigmatism is reduced at the expense of low dispersion from the grating. Calculations show that it is not possible to meet the Littrow condition for a grating at small angles of incidence, and still obtain the necessary dispersion around 9.11 μm to ensure single line oscillation.

The problem with astigmatism can be overcome by producing plane wavefronts to enable a plane Littrow mount grating to be used. This is achieved by placing a lens in front of the grating as shown in Figure 5-23. If the surfaces of the lens are made partially reflecting, then several advantages of this system are realized. One advantage is that energy density on the grating is reduced, thus protecting it from damage. This technique has been used in line tuned CO_2 lasers employing plane-plane cavities to produce high energy pulses over a wide range of lines. Another advantage is that a short length resonator is formed between the grating and the lens. This has a wide resonator mode spacing. The total laser cavity would only oscillate at those frequencies within the active medium gain BW where the cavity resonance condition was fulfilled for both resonators simultaneously. Thus, this three element cavity would produce both line and longitudinal mode selection. In this configuration, the short resonator length would have to be controlled to keep its frequency matched to the long resonator mode closest to the laser line center. At the same time, the long resonator length would need to be controlled to keep the resonator frequency within a predetermined maximum offset from the system local oscillator frequency.

Another possible option is the use of a thin intracavity metal film. This has been demonstrated for line selection of continuous wave CO_2 lasers (Ref. 18) and also mode selection of other continuous wave gas lasers. This would prove an attractive and compact solution if its use with high energy unstable resonators can be demonstrated. However, at present it would seem to be too high risk an option to be considered.

Injection Seeding. In the injection seeded configuration, the longitudinal mode and line selection functions of the system are performed in a master oscillator which is used to seed the power oscillator to produce high energy oscillation on the required line and of single longitudinal mode. Although the power oscillator has the same wavelength as the master oscillator, it will not have exactly the same frequency. The master oscillator will not have enough power to lock the power oscillator modes to its frequency, but will

preferentially seed the power oscillator mode closest to its frequency, and this mode will dominate the power oscillator output. There are two consequences of this approach. First, the master oscillator must not be allowed to oscillate midway between two power oscillator modes as this could cause dual power oscillator mode output. Second, the chirp requirement on the master oscillator is relaxed in that as long as its frequency does not vary by more than one half the power oscillator mode spacing, single longitudinal mode output from the power oscillator should be possible. For a 60 cm power

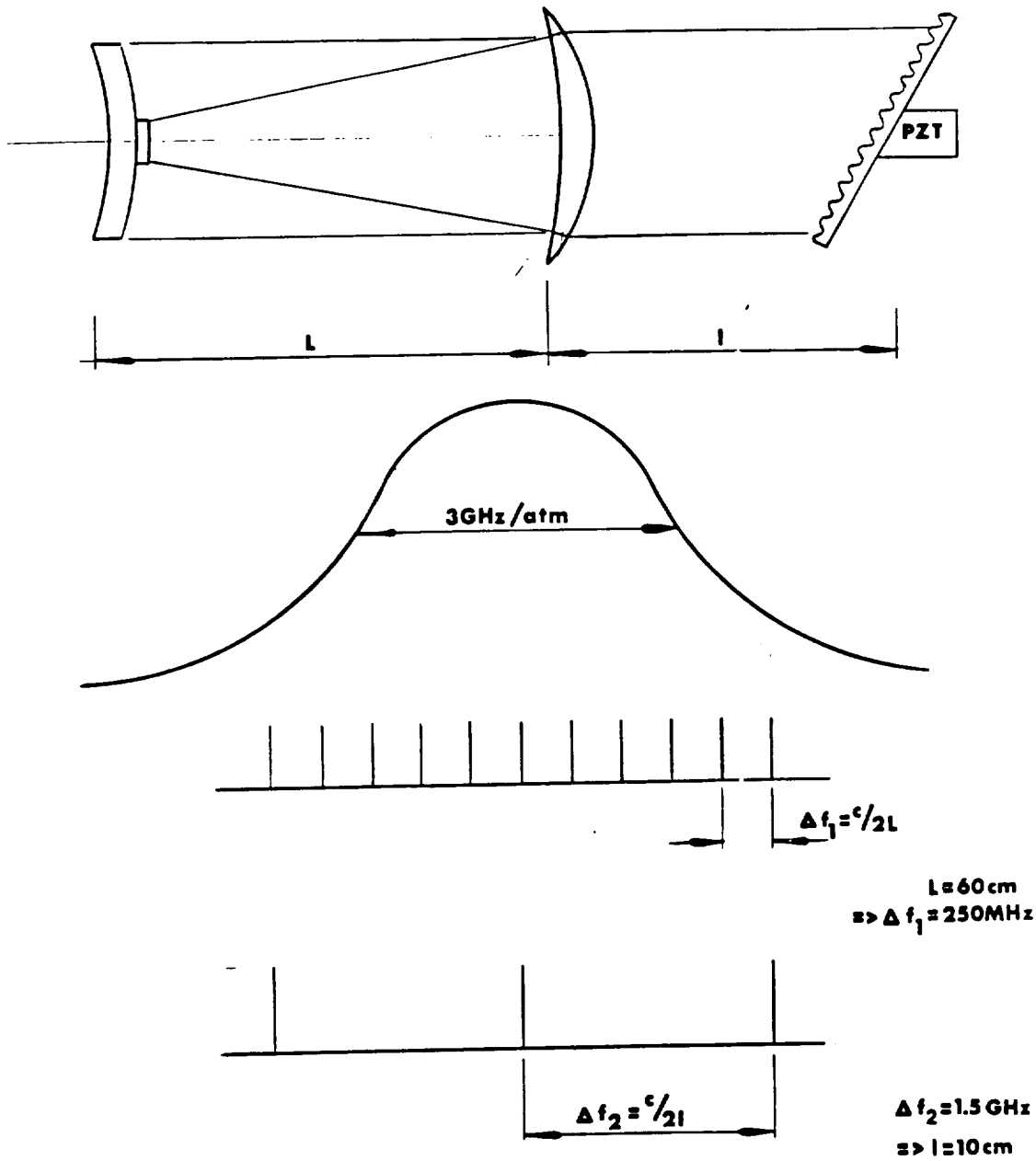

Figure 5-23. Baseline 3-Element Unstable Resonator

oscillator resonator length, this implies a requirement on the master oscillator that its frequency chirp be less than 100 MHz which is easily attainable.

Two options are available for injection seeding. These are the use of either a continuous wave or pulsed master oscillator. A continuous wave master oscillator will be more easily frequency stabilized with respect to the system local oscillator, but a pulsed master oscillator will be able to provide a greater energy density of seed radiation in the power oscillator. Although both types of master oscillator could be used to produce single longitudinal mode oscillation of the master oscillator, work at GEC Avionics, and elsewhere has indicated that the continuous wave master oscillator would not be able to produce single line output of the power oscillator without the need for dispersive optics on the power oscillator, which would introduce the problems discussed in the previous section. An investigation of injection seeding TEA CO_2 lasers to produce line tuned output from high energy unstable resonator power oscillator has shown that 30 mJ of injected energy was necessary to produce single line output at the 1 J level from the power oscillator. This work at GEC Avionics has concentrated on injection seeding short pulse high gain oscillators. Other work by Harrison et al. at Heriot-Watt University has investigated pulse seeding of a long pulse power oscillator using a TEA laser master oscillator. It was found to be possible to produce single line output from a non-dispersive unstable resonator power oscillator at low levels of injected radiation of order 10 mJ. That work has highlighted that the main requirement for efficient injection seeding producing single line output is the power level of the injected radiation.

The injection seeding process can be assisted, thus reducing the master oscillator power required, by increasing the intracavity loss for undesirable wavelengths. As previously mentioned, this could be achieved by coating the cavity optics for high reflectivity for R branch transitions of $C^{18}O_2$ and low reflectivity for P branch. The main intracavity competition in the power oscillator would be between the injected R20 wavelength and the highest gain line of the R branch which will not be too dissimilar in gain.

Master Oscillator. The master oscillator needs to provide enough injected power to enhance the radiation build-up in the power oscillator cavity on the required wavelength transition and longitudinal mode that it will dominate totally the laser output for the duration of the optical pulse.

Work undertaken at Heriot-Watt University on injection seeding a long pulse 3 J laser with a stable cavity has shown that it is possible to produce single line output for a number of lines in both the 9 μm and 10 μm bands of the $C^{16}O_2$ isotope using 10 to

20 mJ of injected energy from a reduced pressure TE CO_2 laser. For a 20 J power oscillator laser, it is estimated that it will be necessary to produce 100 mJ of line tuned single longitudinal mode energy from the master oscillator, as discussed in Section 5.2.1.2.1.11.

GEC Avionics has extensive previous experience of producing line tuned TEA laser oscillators at the 100 mJ energy level. From that work and a large knowledge base in mini-TEA lasers, a design outline of the master oscillator can be made.

As summarized in Section 5.2.1.2.1.3.6, using an injection seeded arrangement increases the LAWS laser efficiency from 7.3 percent for a dispersive cavity to 8.8 percent using an e-beam sustained discharge. After taking into account the input power needed for the master oscillator, the injection seeded approach has the additional advantage of greater overall efficiency.

The selected method of injection, and the relationship between the frequencies of the master oscillator, power oscillator, and local oscillator are described in Section 5.2.1.2.2.5.

5.2.1.2.1.8.5 Optical Cavity and Injection Technique

The optimum choice for the main laser resonator is to use an unstable cavity. This will provide inherent transverse mode selection and efficient energy extraction from the wide aperture discharge necessary to keep the intrapulse chirp due to LIMP within the required level. As discussed in Section 5.2.1.2.1.3.2, a hard-edged uniform reflectivity mirror (URM) unstable resonator will provide a better energy extraction from the laser gain medium than one employing Gaussian reflectivity mirrors (GRM). The effect of the transverse mode structure obtained from a URM unstable resonator on the overall LAWS system via the receiver heterodyne efficiency is discussed in Section 5.2.1.3.1.8.6, where it is seen that the URM resonator provides a higher figure of merit for the system as well as enhanced damage resistance. It is expected that the approximate "top-hat" radial profile of the URM unstable resonator will produce a lower chirp due to LIMP than a Gaussian profile, as the factor depending on the spatial variation of the gas heating rate across the cavity will be lower for the vast majority of the cavity area. All these aspects confirm the choice of a URM unstable resonator for the LAWS laser.

Following the discussion in Section 5.2.1.2.1.8.4, it was decided that the LAWS laser should be based on a master oscillator and power oscillator arrangement. This configu-

ration is expected to present the least technical risk at this stage while providing increased overall efficiency compared to a dispersive unstable resonator for which extra complexity is involved in producing a non-astigmatic beam.

The power oscillator will be based on a wide aperture unstable resonator mounted so as to be resistant to temperature and mechanical induced length variations. This oscillator will provide control of the transverse mode and intrapulse frequency chirp. The master oscillator, as described in Section 5.2.1.2.1.8.4, will be based on a stable or plane-plane cavity incorporating a grating for wavelength selection. A short cavity length will be used to ensure single longitudinal mode oscillation. The master oscillator will thus provide control of wavelength and longitudinal mode. Frequency control aspects are discussed in Section 5.2.1.2.2.5.

5.2.1.2.1.8.6 Local Oscillator Considerations

In the LAWS system, the back-scattered radiation from airborne aerosols will be mixed with the radiation from the local oscillator on a heterodyne detector. It is expected that the local oscillator will be a continuous wave CO_2 laser with a Gaussian output beam of diffraction limited divergence.

Tratt and Menzies (Ref. 6) have considered the heterodyne receiver efficiency for a diffuse distributed scatterer, as is applicable for the LAWS lidar. This has been achieved using the backward-propagated local oscillator (BPLO) approach. In this scheme, the local oscillator beam is projected out of the receiver optics and combined with the transmitter beam at a target plane in the far field. The heterodyne efficiency is then basically found from the overlap integral of the local oscillator and transmitter beams in the far field.

In the study, Tratt and Menzies compare the heterodyne efficiency for unstable cavities, employing both GRM and URM. They identify the optimum parameters for the GRM and find that for these conditions the heterodyne efficiency is approximately 45 percent, essentially independent of the cavity magnification factor M. For URM the efficiency increases with M reaching a value of 30 percent for M equals 2, which has been shown to give optimum performance for these cavities.

It is noted in their paper that this increased receiver detection efficiency of a GRM cavity is achieved at the expense of reduced damage resistance of the mirrors, an important factor in designing the long-life LAWS laser.

In deciding between the GRM and URM unstable resonators, the efficiency figures here must be considered in conjunction with the Spatial Mode Filling Factors, as discussed in Section 5.2.1.2.1.3.2. Following Tratt and Menzies, the Spatial Mode Filling Factors and the far-field receiver efficiency are multiplied together to give a comparative figure of merit for the two types of mirrors. The resultant figures of merit are given in Table 5-19.

Table 5-19. Mirror Type Figures of Merit

Mirror Type	Figure of Merit (M = 2)
Gaussian Reflectivity	0.14
Uniform Reflectivity	0.27

Thus, it is seen that overall the uniform reflectivity mirror unstable resonator is the optimum choice of cavity configuration for the LAWS system laser.

5.2.1.2.1.9 Foil Lifetime

Careful consideration must be given to the design of the foil and the foil support structure of the electron gun if an e-beam sustained discharge technology is chosen for the LAWS laser. A primary concern in these design considerations must be the necessity of obtaining a 109 pulse foil lifetime. This is an increase of 100 to 1000 times over currently reported foil lifetimes; however, it should be noted that long foil lifetimes were not a major design consideration of these prior systems.

At GEC Avionics, in ongoing catalyst characterization tests for an e-beam sustained laser, the foil currently in use has, to date, achieved a 4.0 x 106 pulse lifetime. This was for a discharge volume similar to the LAWS requirement and an operating pulse repetition frequency of 8 Hz.

In a well designed and operated laser, the foil will be well protected from the discharge by an adequate cathode mesh or grid electrode, and from arcs by a correct choice of operating parameters. Suitable quality control in the manufacture of the foil will remove failure modes due to weak points or micro-pores. Under these conditions, the main failure mode of the foil will be fatigue due to thermal and mechanical stress with each pulse.

The properties required by the foil material are

- High thermal conductivity
- Low electron absorption coefficient
- High ultimate tensile strength
- High endurance limit.

The main materials having these properties are aluminum and titanium, aluminum having a greater thermal conductivity and titanium being stronger. It is possible to combine the properties of the two materials by forming a composite Al:Ti foil. Indeed the longest foil lifetime reported to date of 10^7 pulses used such a composite. Other composites such as Kevlar:Al might be possible, combining strength and endurance with thermal and electrical conductivity. Such materials, as well as the use of other plastics such as mylar, should be investigated to assess their suitability for use.

Dr. D.V. Willetts at RSRE, Malvern has performed calculations investigating the thermal loading and mechanical stress effects on the foil lifetime. The following sections follow along the lines of his work.

5.2.1.2.1.9.1 Foil Geometry

In order to provide a basis for the following calculations, a standard foil geometry will be assumed, as illustrated in Figure 5-24. The foil is supported on carefully profiled parallel bars, spaced a distance of 2 b apart. The bars are assumed to be held at a constant temperature, Ts, throughout, either by internal cooling fluid flow or, as is probably more appropriate for an 8 Hz pulse repetition frequency, due to thermal conduction away from the e-beam area to a surrounding heat sink. The electron gun volume is taken to be essentially a vacuum, and the laser at presure, p, which will be near atmospheric. This pressure differential causes a center line sag of s between adjacent foil support bars.

The calculations will ignore the edge effects caused by the finite extent of the support bars and leading to two dimensional stress and thermal flows, and will treat the foil geometry as a one dimensional problem. The shape of the foil support for practical situations will be discussed below in reference to its effect on the foil lifetime.

5.2.1.2.1.9.2 Thermal Loading

During each pulse of the electron gun, there will be some absorption of the energy from the electrons passing through the foil. This will cause it to have a temperature increase.

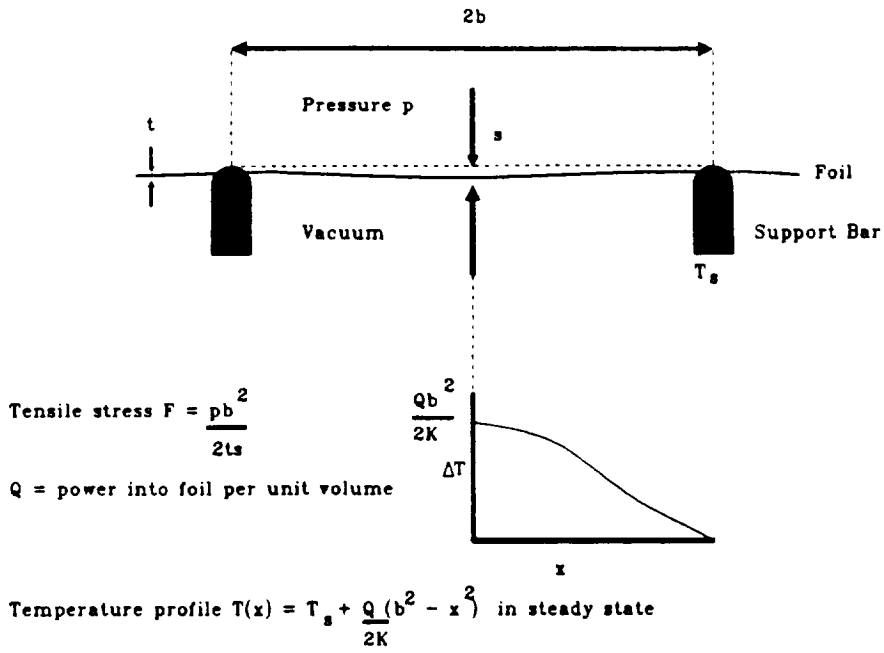

Figure 5-24. Foil Geometry

From the LAWS laser configuration data sheet for the e-beam sustained laser, it is seen that the electron gun current is 7.3 A over the same area as the cathode of 184 cm^2. For a 160 kV accelerating potential this corresponds to a power flux of 6.35 $kWcm^{-2}$. Taking the foil thickness as 25 μm and being made of aluminum having a transmission of 75 percent, the power deposited in unit volume of the foil will be 0.635 $MWcm^{-3}$ during an 8 μsec long pulse, giving an energy deposition per unit volume of 5.1 Jcm^{-3}. The specific heat capacity of aluminum is 0.9 J per gram per K, and its density is 2.7 gcm^{-3}. Thus the energy deposited of 1.9 J per gram will give a temperature rise of 2.1 °C every pulse. In the interpulse period, the heat will be conducted away from the heated regions giving rise to a lower mean temperature. This is illustrated in Figure 5-25.

For a titanium foil to have the same transmission as an aluminum one it must have half the thickness. This keeps the relative strengths of the foils constant as titanium has twice the tensile strength of aluminum. The specific heat capacity of titanium is 0.52 J per gram per K, and its density is 4.5 gcm^{-3}, so for a 13 μm thick foil the pulsed temperature rise will be 2.2 °C, very similar to that of the aluminum foil.

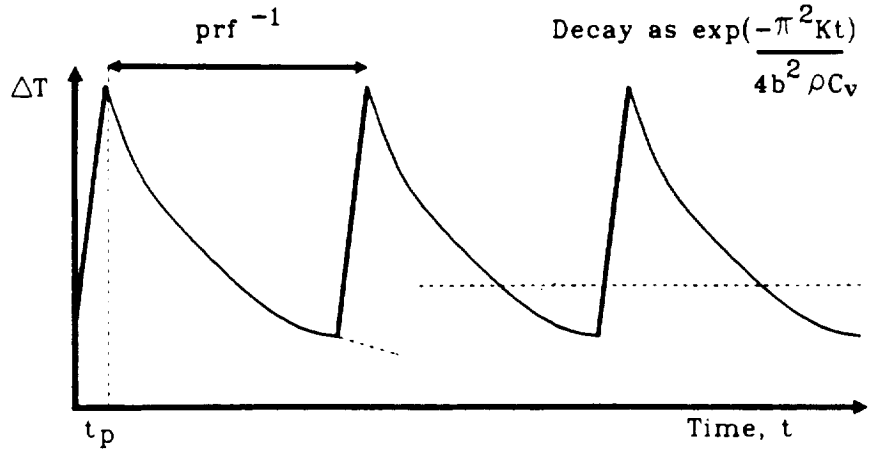

$$\Delta T_{max} = \frac{Qt_p}{\rho C_v} \qquad \Delta T_{mean} = \frac{Qb^2}{2K}$$

for t_p = 10μs, prf = 10Hz, b = 2.5mm
Aluminum gives ΔT_{max} = 5°C ΔT_{mean} = 1.5°C

Figure 5-25. Foil Centerline Temperature

The thermal conductivity problem of a heated rod held to constant temperature at both ends can easily be solved to give the sinusoidally varying temperature with length, as indicated in Figure 5-24, in the steady state when higher frequency Fourier components have decayed away. In the interpulse period, this temperature profile will decay with a characteristic time given by $4b^2\rho Cv/\pi^2 k$ as shown in Figure 5-25. The mean interpulse temperature can then be found approximately using the formula as shown. The mean temperature is seen to depend on the bar spacing, but taking a typical bar spacing of 5 mm and a pulse repetition frequency of 8 Hz gives a mean foil temperature change of 0.4 °C for aluminum and 1.7 °C for titanium with thermal conductivities of 236 $Wm^{-1}k^{-1}$ and 22 $Wm^{-1}k^{-1}$ respectively. Thus the temperature change of the foils will not be more than a few degrees. Referring to Figure 5-26 it can be seen that a temperature rise on this scale will have a negligible effect on the strength of the foil.

Therefore, it is not anticipated that thermal loading will adversely affect the foil lifetime. However, this assessment is based on a uniform heating of the foil. Care must be taken to keep the e-beam uniform and to avoid impurity/occlusion sites on the foil

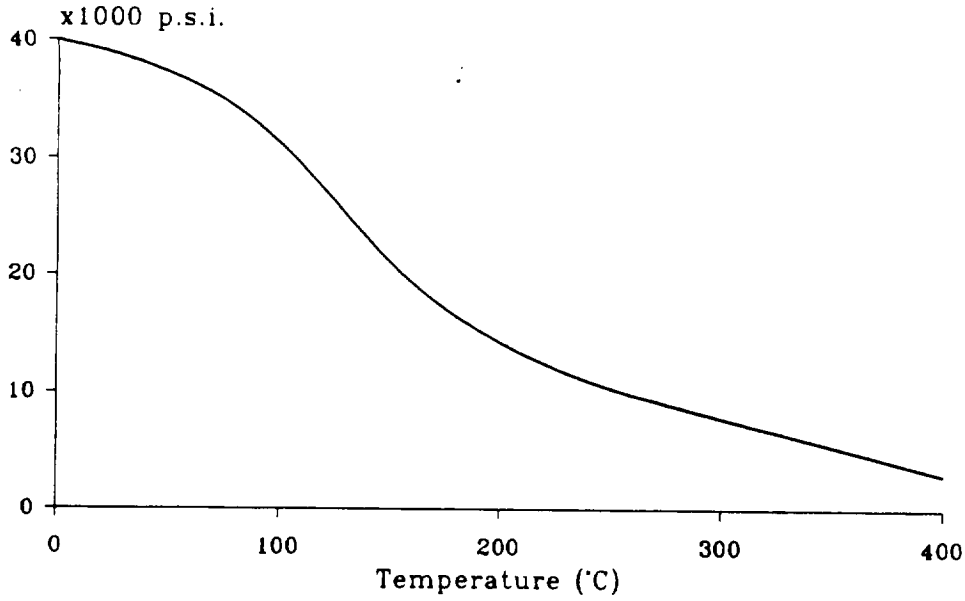

Figure 5-26. Yield Strength of Aluminum

which would locally absorb more energy from the e-beam. These local hot-spots will place a greater thermal stress on the foil.

5.2.1.2.1.9.3 Mechanical Stress

During each discharge pulse, heat is deposited in the gas on a timescale of a few μsec. This causes the temperature and pressure of the gas to increase at a constant volume. The gas will then expand adiabatically into the region surrounding the discharge volume during the interpulse period. The discharge volume gas pressure will then return to its initial value, but at an increased temperature. By equating the energy deposited in the discharge to the constant volume temperature rise, the pressure increase during the pulse can be found:

$$\Delta p = \frac{R}{C_v}\,\frac{E}{V} \quad (\,R = \text{gas constant},\ C_v = \text{specific heat}\,)$$

Inserting the values of 8.31 $Jmol^{-1}k^{-1}$ for R and 20 $Jmol^{-1}k^{-1}$ for Cv for a CO_2 laser gas mixture and taking a specific energy loading for the laser of 180 J/L gives a pulsed pressure rise of 0.7 atm. This pressure rise will appear almost instantaneously and then will be reduced in two steps as the rarefactions propagate in at the local speed of sound from the edge of the discharge volume.

From Figure 5-27, the Goodman diagram for aluminum at 20 °C, it can be seen that for typical conditions of the foil and a slightly greater pressure step than calculated above, the mechanical stress on the foil for each pulse is safely away from the failure limit. As can also be seen on this diagram, and by referring to the formula for tensile stress in Figure 5-24, the greater the foil sag between the support bars the less the stress on the foil. The fatigue failure criterion is presented in Figure 5-28 as a function of the number of times the foil is stressed to a certain level. It can be seen that failure would occur on the first cycle for a maximum stress equivalent to the ultimate tensile strength. However, if 10^9 cycles were required, it would be necessary to keep the maxiumum stress less than the endurance limit, which is approximately equivalent to one third of the ultimate tensile strength for aluminum. The maximum stress seen by the foil for a 1 mm sag is 3675 psi while the endurance limit is 13,000 psi. Thus the mechanical loading on the foil should not be a cause of foil failure for this simple analysis of the problem.

5.2.1.2.1.9.4 Support Structure Design Considerations

In the previous sections, it has been shown that the thermal loading and mechanical stress on the foil should not in themselves be a reason for its failure within the 10^9 pulse lifetime needed for the LAWS laser. There must therefore be other reasons for the foil failures experienced in existing e-beam sustained lasers. These could be due to weakness in the foil occurring during manufacture or from interaction with the high energy e-beam, causing defect sites in the crystal structure.

A major cause of weakness is due to the foil support structure. The finite extent of the suport bars has been ignored in the preceeding analysis, but where the bars meet their support frame, the foil will have a two dimensional curvature, which will tend to increase the stress on the foil. The profile of the foil supports themselves must be such that the foil will smoothly lie over them. Any sharp discontinuities, such as bends or creases, in the foil surface will cause a local increase in the stress and greater risk of foil failure.

The following methods could be used to improve the lifetime of the electron gun to the required number of pulses for the LAWS system.

Correct Design of the Foil Support Structure. Due to the low repetition rate of the LAWS system (8 Hz) it will not be necessary to individually cool each support member. Cooling of the edges of the support frame will maintain the required temperature of

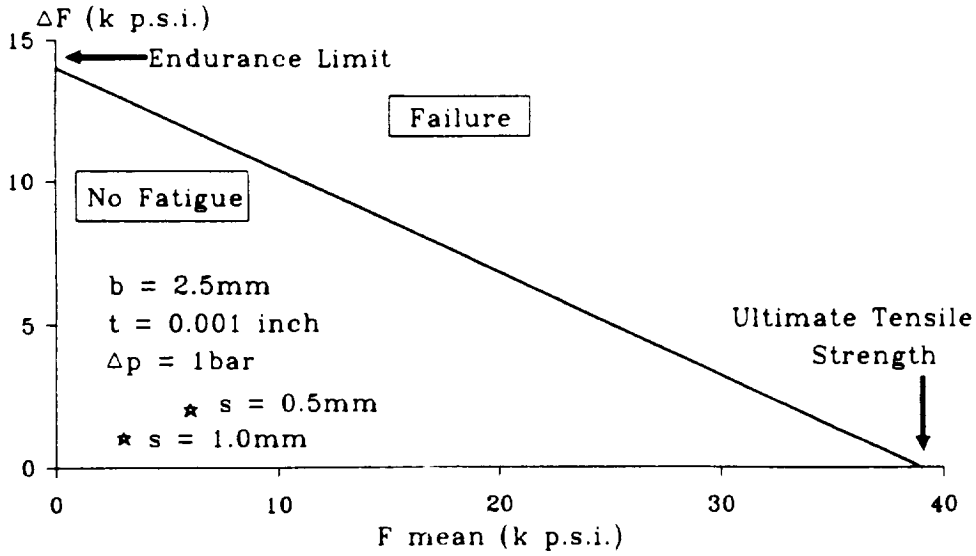

Figure 5-27. Goodman Diagram, Aluminum at 20 °C

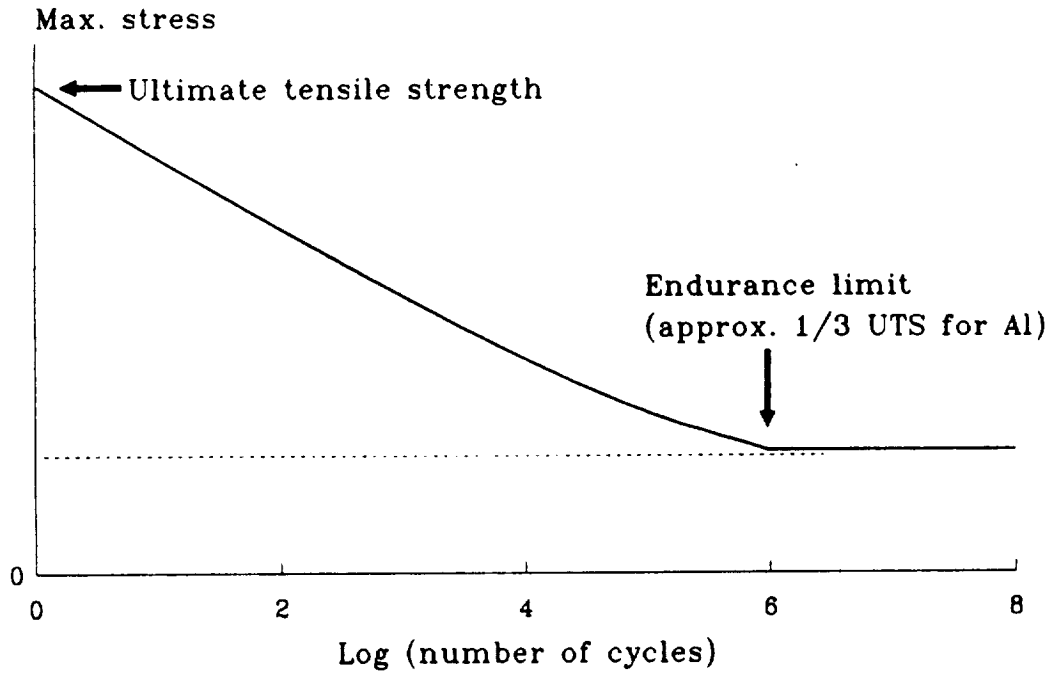

Figure 5-28. Fatigue: Ferrous-Like Material

each member. This will allow a greater flexibility of the design of the support structure. Further analysis might show that a departure from the standard bar arrangement to, for instance, a hexagonal grid would allow large transmission of the e-beam through the foil and support structure providing a uniform illumination of the discharge volume while giving improved support to the foil.

Correct Manufacture of the Foil Support Structure. As has been mentioned, anything causing the foil to deviate from a smooth profile will be detrimental. Therefore, the foil support must be finished to a high degree of smoothness, and there must be no sharp corners in its structure. It has been shown that a certain amount of sag in the foil between its support will reduce the stress caused by the pressure pulse. The foil supports must be profiled to match this sagging and thus smoothly support the foil as it passes over them.

Correct Mounting of the Foil. The foil must be mounted onto the support grid in such a way that no creases are formed in it, and an even tension is maintained over the whole foil area. Preforming of the foil over the support structure before mounting the assembly in the laser will help to facilitate the situation. A high degree of cleanliness in assembling the foil structure will be needed to prevent formation of possible hot-spot sites on the foil, as will careful inspection of foils for possible defects.

5.2.1.2.1.9.5 Foil Lifetime Conclusions

In the discussion above, a number of aspects affecting the lifetime of the foil which separates the high vacuum of the electron gun from the atmospheric pressure of the laser gas envelope have been briefly analyzed.

It has been found that the laser operating conditions do not inherently lead to foil failure in the required lifetime of the LAWS system. In designing the foil and its support structure for such a laser, a more detailed investigation of the aspects discussed above would need to be undertaken, but it seems that correct design of the components, with due regard to their mechanical and thermal properties, could extend the foil lifetime beyond currently reported values.

5.2.1.2.1.10 Radiation Issues

The current design for the LAWS laser proposed by GEC Avionics is an e-beam sustained laser. During the operation of such a laser, a 160 kV e-beam is generated, which then passes through a thin metal foil into the laser discharge region. Some of the electrons interact with the foil atoms, and X-rays are thus produced.

In this section, the X-ray dose that would be produced is determined, and it is ascertained that this will not adversely affect the space platform and its component parts if these have been properly designed to operate in the space environment.

5.2.1.2.1.10.1 X-Ray Production

The X-rays are produced as the electrons are accelerated (decelerated) by the Coulomb electric fields surrounding the atoms of the foil. This produces a continuum X-ray spectra (or Bremstrahlen) with a cut-off to short wavelengths given by the electron energy. For 160 kV electrons the shortest wavelength of the X-rays will be 7.8 pico-meters.

If the electrons are non-relatavistic, the X-rays are produced with an angular distribution:

$$I(\theta) \propto \mathrm{Sin}^2\theta$$

where θ is the angle between the direction of X-ray emission and the average direction of acceleration on the electrons, which is back along the direction of the e-beam. For relativistic electrons and at 160 kV the electrons are highly relativistic, the X-ray angular distribution is shifted in the forward direction of the e-beam, due to certain relativistic transformations.

The efficiency of X-ray production depends on the atomic number, Z, of the target material, and the energy, E, of the electrons, and is given by

$$\eta = 7 \times 105\ ZE$$

where E is in keV.

Standard foil materials are aluminum and titanium; taking the worst case of titanium foil (Z = 22) with 160 kV electrons, the theoretical X-ray production efficiency is η = 0.25 percent.

The current design for the laser has a 9.3 J pulse of electrons in the e-beam. Allowing for the variation of the LAWS laser pulse rate throughout its orbit, it is expected that the average pulse repetition frequency will be 5 Hz. This figure is also determined from a 2 kW average supply to the LAWS laser and a 5 percent efficiency with 20 J pulses. Therefore, the e-beam power is 46.5 W. As a typical transmission for the foil in an e-beam sustained laser is 75 percent, only 25 percent of this power is available to produce X-rays. Thus, the average X-ray power will be 0.03 W.

From the angular distribution of the X-rays, the maximum X-ray intensity can be found in terms of the X-ray power by integrating over all space. Thus, the X-ray intensity in the direction of the maxima of the angular distribution is

$$I \max (r) = \frac{3P}{8\pi r^2}$$

where P is the X-ray power, and the normal $1/r^2$ dependence of electromagnetic radiation is evident.

For the LAWS laser design parameters, the X-ray intensity is thus:

$$I \max (r) = \frac{0.003}{r^2} \ Wm^{-2}$$

To convert this to an X-ray dose rate, it is necessary to calculate the absorbed energy per unit mass of material.

The absorbtion of X-rays is governed by the differential equation:

$$\frac{dI}{dx} = -\mu I$$

where μ is the absorption coefficient.

To convert this figure to an absorption per unit mass, an X-ray beam incident on a cylinder of material of cross-section A, density and length x, and thus mass m, is given by:

$$m = \rho A x \ .$$

Thus, $$\frac{dm}{dx} = \rho A \ .$$

The rate of change of intensity as the beam travels through the material is then:

$$\frac{dI}{dm} = \frac{dI}{dx}\frac{dx}{dm} = \frac{-\mu I}{\rho A}$$

To find the absorbed power per unit mass, both sides need to be multiplied by the cross-sectional area, A. Then with power P given by P = IA, it is found that:

$$\frac{dP}{dm} = \frac{\mu}{\rho} \cdot I$$

where μ/ρ is known as the mass absorption coefficient. In SI units the dose rate will be in units of Wkg^{-1} or Gray sec^{-1}.

The value of the mass absorption coefficient depends on the energy of the X-rays. For a 160 kV e-beam, the Bremstrahlen radiation will peak with X-rays of approxi-

mately 100 keV photon energy, and so the mass absorption coefficient corresponding to radiation of this energy will be taken as representative.

Further, the mass absorption coefficient will vary with material as a fairly slow function of the material's atomic number, Z. To enable close comparisons with other figures, the absorption rate in aluminum (Z = 13) will be calculated. This will be close to the value for silicon (Z = 14) and for carbon (Z = 12), the basis of organic material. For 100 keV photon energy and for aluminum, the value of the mass absorption coefficient is 1.7 x 10–2 m2kg–1.

Thus, the dose rate for the LAWS laser is given as:

$$1.7 \times 10^{-2} \times \frac{0.003}{r^2} = \frac{5.9 \times 10^{-5}}{r^2} \text{ Gray/sec} = \frac{1.9 \times 10^{3}}{r^2} \text{ Gray/year}$$

5.2.1.2.1.10.2 Background Radiation Dose

Figure 5–29 shows the total dose expected for a satellite on a seven–year mission in a circular orbit at an altitude of 700 km. This information is courtesy of Ian McMillan, Marconi Space Systems. The orbit inclination of 65° to the equator is fairly close to the expected LAWS orbit, and this value will be used here.

From Figure 5–29 it can be seen that if there were no shielding around a component, it would receive a dose of 5 x 105 Gray for the seven–year mission, or 7 x 104 Gray/year. Thus, to not adversely affect the satellite modules, the X–ray dose rate outside of the electron gun and laser head enclosures must be less than this background level.

To find the required distance from the X–ray production site in the foil, the X–ray production dose is compared to the background level.

$$\text{Thus,} \qquad \frac{1.9 \times 10^{3}}{r^2} = 7 \times 10^{4} \text{ for } r = 0.16 \text{ m}$$

This will be the worst case along the direction of maximum X–ray intensity.

The closest that the edge of the laser enclosure will be to the foil is 230 mm in the present design configuration. Therefore, the expected dose rate outside the laser enclosure will be 3.5 x 104 Gray/year. This is half the background radiation level. The actual X–ray dose seen by other components outside the laser enclosure will probably be less than this calculated dose due to

- Shielding by components inside laser housing, e.g. electrodes
- Non–uniform angular distribution of X–rays

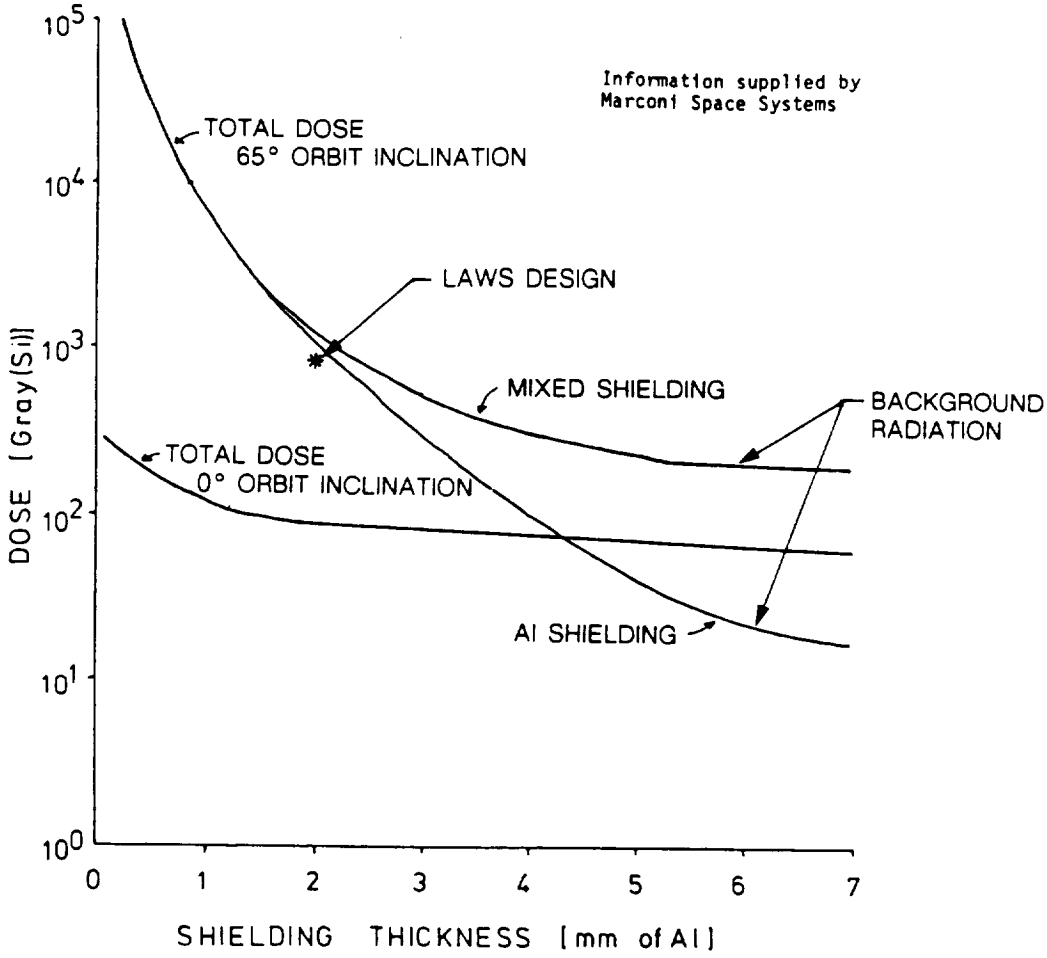

Figure 5-29. Dose/Depth Curve 7 Year Mission Circular Orbits (700 km at 0° and 65°)

- Many radiation sensitive components would be greater than the 0.23 m distance from the foil
- The laser gas envelope will provide a small level of shielding itself.

Thus, the radiation flux due to X-rays generated from the e-beam will be below the background level prevailing outside the laser enclosure due to cosmic radiation. The X-rays generated by the laser will also be "softer" than the cosmic radiation and thus more strongly absorbed by the shielding surrounding the other modules, having a correspondingly lower contribution to any radiation problems suffered by the components within those modules.

5.2.1.2.1.10.3 Experimental Determination of X-Ray Dose

The X-ray dose produced by an e-beam sustained laser built and operated by GEC Avionics Limited, Applied Physics Division, was measured. Using a radiation badge

placed 75 mm from the outside of the electron gun, a dose rate of 81.2 nSievert/pulse was measured. This corresponds to a yearly dose of 12.8 Sievert for a 5 Hz continuous pulse rate.

For this energy of X-rays, a dose of one Sievert can be considered equivalent to one Gray absorbed in silicon, and thus can be compared to the values used in the above sections.

Although this was taken at one point only, initial investigations with X-ray film surrounding the laser have shown that the radiation badge was not mounted in a position of anomalously low X-ray flux.

The case of the e-beam laser at GEC Avionics is 2 mm thick stainless steel, having a mass absorption coefficient of 2.1 x 10^{-1} m^2kg^{-1}, and a density of 7900 kgm^{-3}. Therefore, the walls of the laser envelope pass less than 4 percent of the X-ray intensity. The radiation badge was approximately 330 mm from the X-ray source point.

Therefore, allowing for the reduced laser envelope wall transmission, this figure implies a dose rate of 325 Sievert/year at the position of the film badge, compared to the value as calculated in the previous section, for a distance of 330 mm of 1.7 x 10^4 Gray/year, a factor of 50 lower. However, a reduction in intensity of 50 times could be caused by shielding which was equivalent of 2.3 mm of stainless steel. Due to the internal complexity of the e-beam sustained laser with the mounting structures for the foil etc., it is not unreasonable that this equivalent thickness of stainless steel is between the foil and the film badge position. It should be noted that as the film badge was not placed in the direction of expected maximum X-ray intensity, a discrepancy between the calculated and measured values is not unexpected.

However, this section has shown that the calculated dose is probably a pessimistic value, and yet in the previous section it was shown that even the calculated value could easily be tolerated. Therefore, the X-ray production by the e-beam sustained laser is not likely to pose a problem to the LAWS system.

5.2.1.2.1.11 Performance

A computerized performance model has been used to predict the behavior of the LAWS laser and validate the proposed laser design. The model solves the simultaneous rate equations describing the populations of the relevant CO_2 and N_2 vibrational levels and the intracavity photon density by numerical integration using a Runge-Kutta routine.

The electron pumping rates for CO_2 and N_2 are obtained from a knowledge of the discharge current as a function of time provided by the pulse forming network applicable to the laser type of interest.

The model was developed at GEC Avionics and has been employed for a number of years as a tool for the design and development of CO_2 lasers. For this study, the model was modified to include the effects of injection seeding of the laser. A parametric study was undertaken to determine the optimum conditions for the injection seeding of the power oscillator by the master oscillator. Some of the results of the computer modelling carried out by GEC Avionics are presented here.

In Figure 5-30 the result of running the computer model in the absence of any

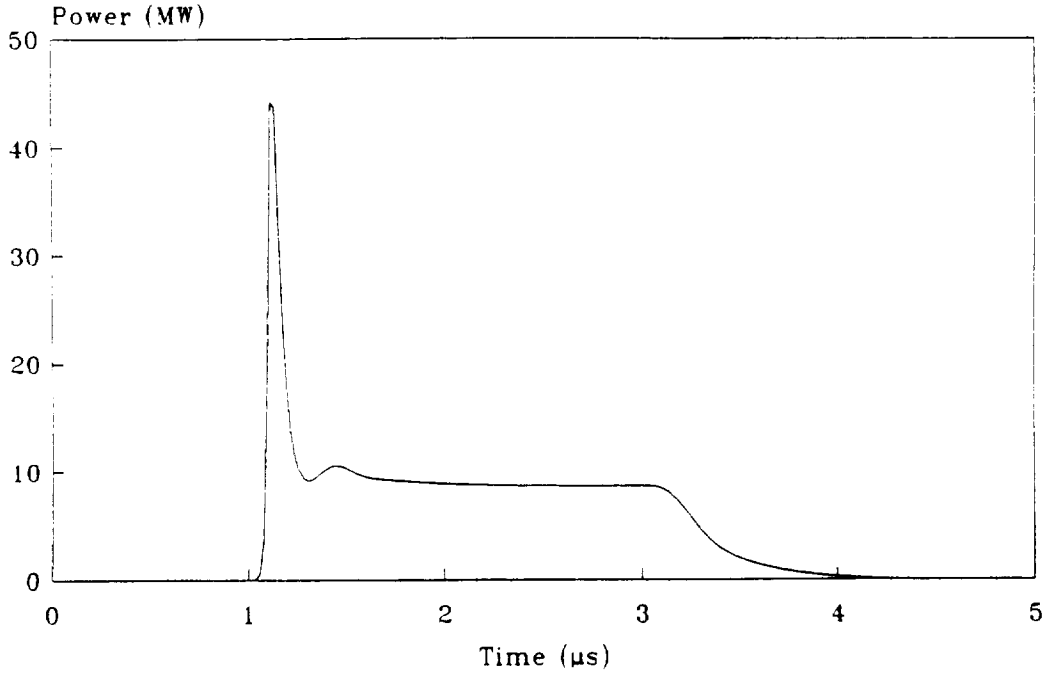

Figure 5-30. Power Oscillator Output Pulse, No Injection Pulse

seeding is shown. The laser dimensions employed are those of the baseline GEC Avionics LAWS laser employing an e-beam sustained discharge. The integrated area under the curve predicts a laser pulse energy of 24 J, as required by the LAWS system and allowing a safety margin. However, it can be seen that there is a large gain switched spike which would be detrimental to the operation of the LAWS system.

Figure 5-31 shows the effect of injection seeding with a 100 mJ 300 nsec long pulse as a function of the delay between the start of the power oscillator current pulse and the start of the injection pulse. It can be seen that the effect of the injected pulse is to

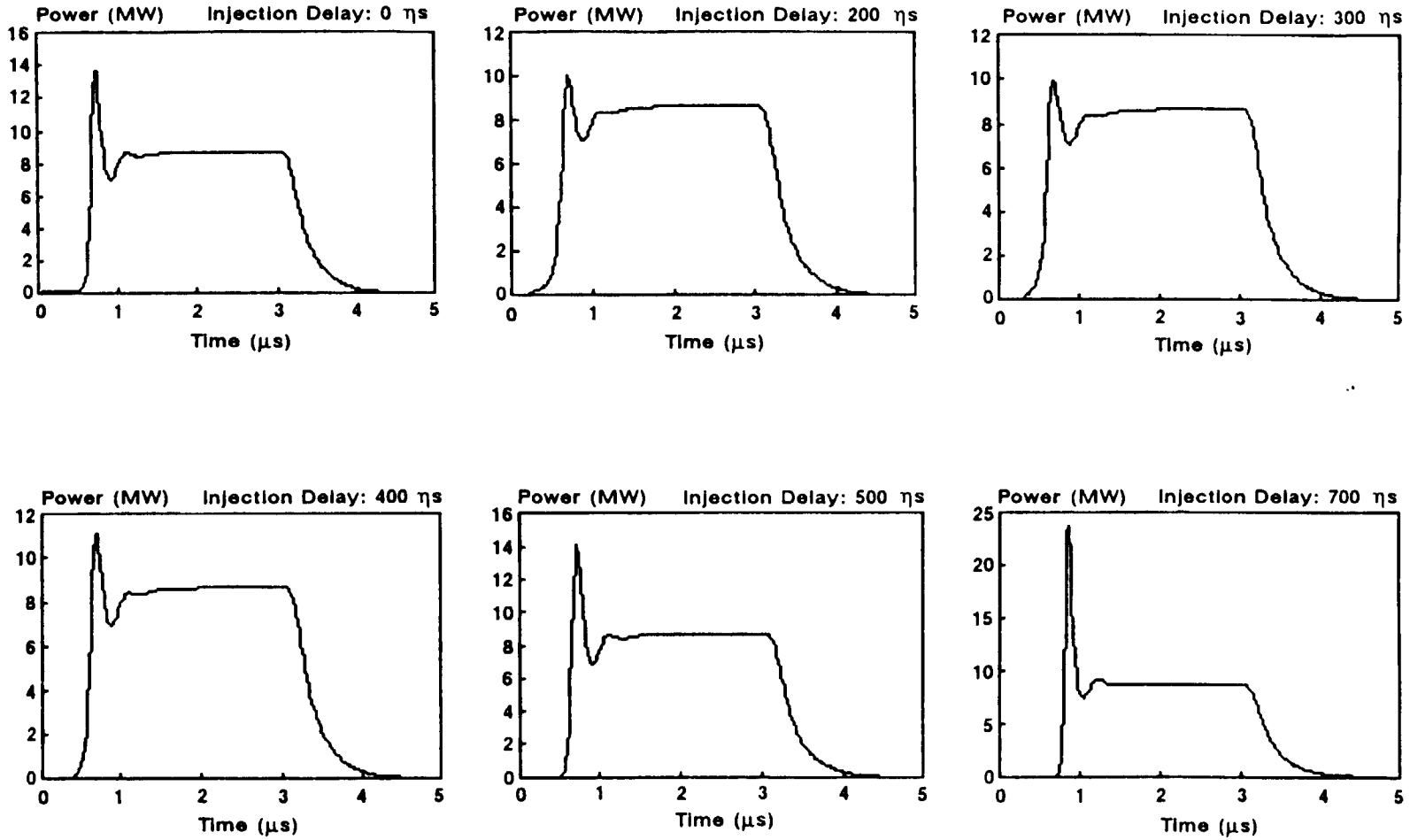

Figure 5-31. Pulse Shape versus Injection Delay

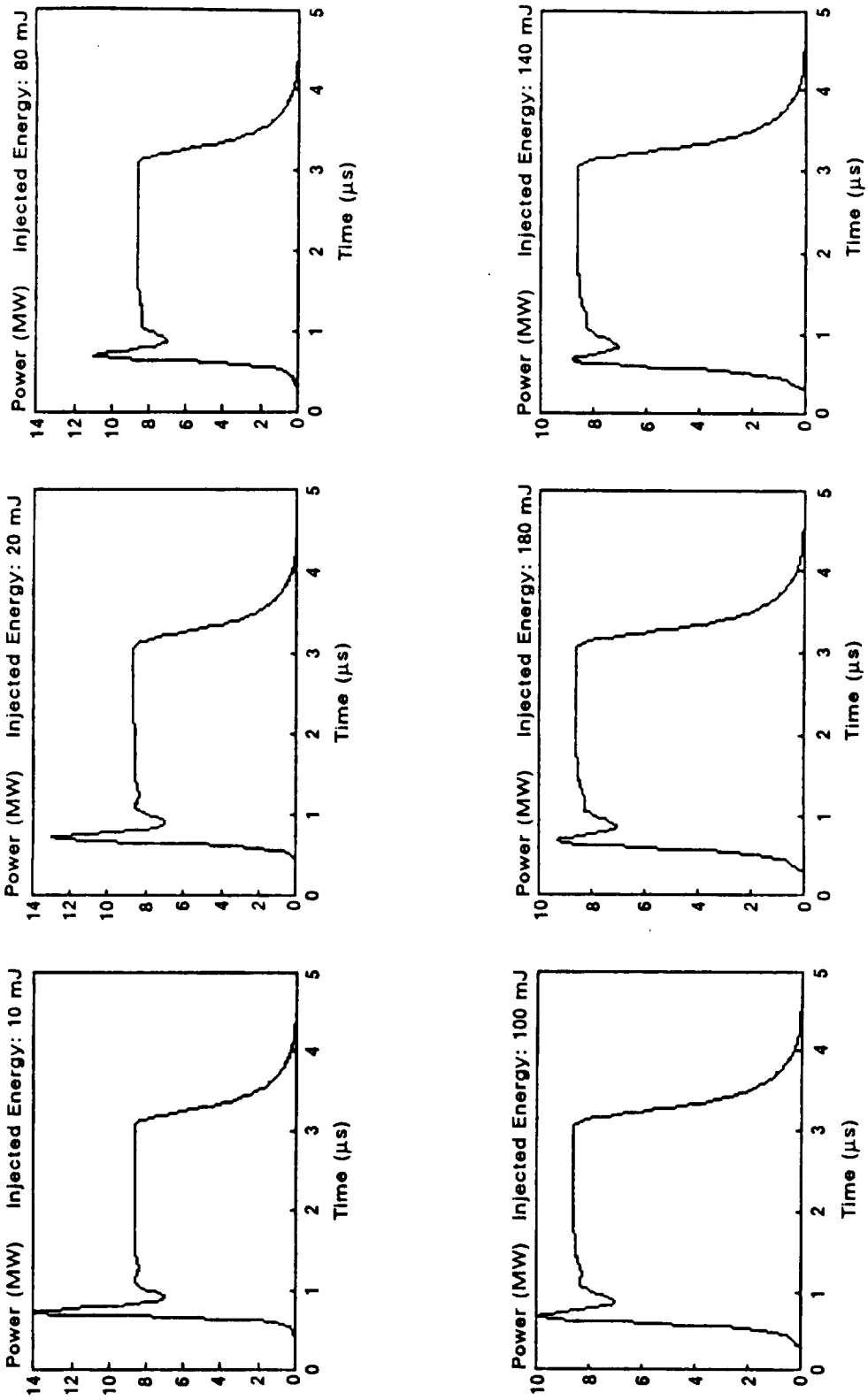

Figure 5-32. Pulse Shape versus Injected Energy

Table 5-20. Laser Performance Requirements

Weight	≤	175 kg
Pulse Energy	≥	20 J
Pulse Length	=	3 μsec (will consider 1 μsec)
Wavelength	=	9.11 μm single mode
Life	>	10^9 pulses
Pulse Rate	≤	8 Hz
Chirp	≤	200 kHz
Maximum Power	=	3200 W
Wall Plug Efficiency	>	5%

5.2.1.2.2.1.1 Weight Reduction Methods

Marconi Space Systems (MSS), another company within the GEC group, has considerable composites manufacturing capability, as well as a team of mechanical and design engineers experienced in the design of space systems. MSS has provided initial estimates of composite and honeycomb materials suitable for a variety of laser components. These have been used to provide weight estimates for major components and subsystems.

Other weight reduction techniques employed include the use of alternative light-weight materials for transformer cores, replacing heavy encapsulation around pulse forming network (PFN) components with pressurized gas in a sealed metal enclosure, and the use of a simple, light-weight electron gun design.

5.2.1.2.2.2 Laser Head

5.2.1.2.2.2.1 Principle of Operation

A high energy pulsed e-beam is injected into the laser medium to produce conductivity throughout a large volume between two electrodes. The main laser input energy can then be fed in at a voltage which is less than the breakdown potential, and which can be adjusted to obtain the optimum excitation of the relevant laser energy levels, and hence maximize efficiency. Thus, the e-beam laser reduces the problem of glow-to-arc transition, which is inherent in self-sustained lasers in which the electrode assembly

must be over-volted to produce a self-sustaining discharge at less efficient E/N levels. The e-beam laser has completely arc-free operation, provided the system is properly designed to ensure adequate distances from the high voltage electrode, and also provided that gas ratios within the laser are kept to a sufficiently constant level so that impedance matching is maintained between the laser and PFN. Small fluctuations of laser impedance can be monitored by current and/or voltage waveforms and a feedback system incorporated to adjust the laser supply voltage accordingly. Thus, provided the laser is properly designed and set up, there will be no arcs whatsoever to the foil between the laser and electron gun, which means that the only foil life limiting factors will be pressure and temperature effects.

5.2.1.2.2.2.2 Laser Design

A gas envelope is used to enclose the electrode assembly, circulating fan, catalyst, a heat exchanger, optical resonator, and internal ducting. This generic scheme has been widely used at GEC Avionics and has proved very successful for lasers with repetition rates up to 200 Hz. It has weight and size advantages over a widely used scheme with an external duct loop which requires large quantities of metalwork.

5.2.1.2.2.3 Electron Gun

The electron gun design is based on a device recently built and tested by M. Harris, RSRE Malvern. Previous electron guns in use at RSRE and GEC Avionics, developed by GEC Hirst Research Center, provide satisfactory performance but do not readily lend themselves to ultra-high vacuum construction. Such construction is a pre-requisite if guns are to be developed for sealed operation, dispensing with the need for bulky pumps and gas supplies. Sealed operation is an essential requirement if lasers are to be built to perform in the field or to meet the needs of space based applications, such as LAWS. A further problem with the existing gun design is that large areas of the gun envelope are pulsed to voltages up to 150 kV making compact construction of laser systems impossible without resorting to encapsulation.

5.2.1.2.2.3.1 Design

The electron gun proposed for LAWS is a simple, ultra-high vacuum design in which the complete envelope is metal held at 0 V. The gas envelope is a composite structure comprising carbon fiber material and an internal metal coating. Additional screening may possibly be required for EMI and X-ray containment. The cathode is of

aluminum alloy and is supported on a ceramic high voltage feedthrough. The nickel auxiliary electrode in the field-free drift tube is carried on ceramic-metal hard sealed feedthroughs with knife edge/copper gasket seals.

5.2.1.2.2.3.2 Principle of Operation

E-Beam Generation. A continuous low current (5 to 50 mA) dc discharge at a few hundred volts is maintained in the drift section by virtue of the auxiliary electrode. When a high voltage pulse, typically 150 kV, is applied to the cathode, positive ions extracted from the auxiliary discharge are accelerated down the gun to bombard the cathode. Bombardment of the cathode liberates electrons which are accelerated up the gun to form the e-beam. The beam dimensions are determined by an aperture in the wall separating the drift and accelerator sections.

High Voltage Insulation. The device operates in He over a pressure range of 1 to 10 Pa, to the left of the minimum of the Paschen curve, where long path breakdown is favored. Hence, high voltage hold-off is achieved by keeping paths short. This means that the gun dimensions are minimized; the walls of the gun only needing to exceed the beam dimensions sufficiently to allow radiusing of the cathode edges and adequate tracking length over the insulated high voltage feedthrough.

5.2.1.2.2.4 Electrical System

5.2.1.2.2.4.1 Laser Pulse Forming Network

The laser pulse forming network produces a nominally square pulse of 6 μsec pulse width. This is achieved using a five mesh network, each mesh consisting of an equal value of inductance and capacitance. At the two ends, a slightly larger inductance may be used to avoid mis-match and smooth out ripples. The total inductance is 48.4 μH and the capacitance 0.19 μF. The discharge current is 1532 A and the charging voltage 49 kV. These figures were used to determine the weight and size of the capacitors and inductors.

The laser PFN is discharged by the laser itself responding to electrons from the electron gun.

5.2.1.2.2.4.2 Gun Pulse Forming Network

The electron gun pulse forming network produces a nominally square pulse of 8 μsec pulse width. This is achieved using a five mesh network. The total inductance

for the gun PFN is 877 μH and the capacitance 18 nF. The discharge current is 7.3 A and the charging voltage 32 kV. These figures were used to determine the weight and size of the inductors and capacitors.

The gun PFN is discharged by the thyratron switch, described in Section 5.2.1.2.2.4.3, and discharges into the pulse transformer, described in Section 5.2.1.2.2.4.4.

5.2.1.2.2.4.3 Switch

Thyratrons have been used for many years for PFN switches. They have the capability to withstand high voltages (in excess of 240 kV with multi-gap devices), can pass very high surge currents (up to 15,000 A), have fast turn-on times (typically 0.1 to 0.5 μsec), and are designed to run at high frequency and thus have a long life. They also have good jitter characteristics (typically 5 nsec).

Their major disadvantages are in size and supporting circuitry such as heater transformers.

For this type of application, a heater current of 25 A is required at 6.3 V. The grid drives require a voltage of +125 V on one grid and a pulse of +600 Volts with a standing level of -125 V on the other grid. The pulsed voltage can be supplied by small ferrite toroids and the +125 V produced by a bipolar transformer/rectifier circuit, as very little current is required.

5.2.1.2.2.4.4 Pulse Transformer

Requirements. The pulse transformer is required to step up the voltage from 16 kV to the necessary 160 kV for the electron gun, as it is difficult to switch this level of voltage otherwise.

Due to the high flux density required, a large cross-sectional area is needed. Also, the windings are long, due to the high voltages involved, the need to keep the winding away from the edges of the core, and the need to allow the high voltage winding to be spread out to ensure good turn-to-turn insulation. Thus, the limbs of the core need to be long to accommodate the coil assembly.

Further considerations are associated with the stray inductances and capacitances which are related to the distance between the layers, length of winding, number of turns, cross-sectional area of winding, and the voltage. The stray inductances and capaci-

tances determine the shape of the waveform, in particular, the rise time, amount of ripple, overshoot, and droop.

Previously, good results have been obtained with the primary winding sandwiched between the two halves of the secondary winding. This keeps the interwinding capacitance low and gives a uniform magnetic field. The first method, previously used, would be recommended for use for this application. This method is recommended. However, the transformer would not be placed in oil, but in a suitable gas mixture which it shares with the rest of the equipment.

Weight Considerations. The coil assembly is heavy, due to the amount of resin used, but it would be unwise to reduce this insulation as it would undoubtedly have an adverse effect on reliability because of the increased likelihood of an electrical breakdown occurring. Having extra secondary layers would add to the capacitance of the transformer and affect the pulse characteristics.

The optimum choice of core material is cobalt-iron due to its high flux density, hence small cross-sectional area, and thus low weight.

5.2.1.2.2.4.5 High Voltage Power Supplies

Laser PFN Supply. Assuming a total capacitance of 0.19 μF has to be charged to 49 kV at a repetition rate of 8 Hz, a power supply of approximately 1.8 kW is required.

The power supply is assumed to be 85 percent efficient, which could be achieved using a resonant switch mode supply with a switching frequency of approximately 100 kHz. To achieve these figures, a system supply of 300 Vdc is assumed.

Gun PFN Supply. A total capacitance of 0.018 μF is charged to 32 kV at a repetition rate of 8 Hz; therefore, a power supply of 75 W is required. The same assumptions are made as for the laser PFN supply, but obviously this supply is much smaller.

Gun Auxiliary Supply. This supply is required to provide a 15 kV initial peak to the auxiliary electrode in the gun prior to it striking and 500 V after striking. A supply of 12.5 W is required.

Diagnostic and Control. The diagnostic and control circuitry operates at low voltage and consists of (1) the interface to the satellite control system; (2) the thyratron drive control circuit; (3) safety interlocks; (4) controls for purging the gas in the laser head (if required); (5) drive circuits for the piezo electric transducers in the laser head and master oscillator (if used); (6) interface to the detector circuit, and (7) an impedance

compensating circuit which monitors the current and drives the PFN voltage and gas mixture, thus maintaining a steady current in the load. Built-in test circuits are included (where appropriate) to check supply voltages, temperatures at critical points, and other important parameters. The bulk of this circuitry is mounted on printed circuit boards.

5.2.1.2.2.5 Frequency Control and Master Oscillator

In this section the integration scheme for the laser modules of the LAWS system is considered. In particular, the following topics are addressed: relative frequency stability of local oscillator and power oscillator output laser radiation, frequency matching of power oscillator and master oscillator laser radiation, and injecting of the master oscillator pulse into the power oscillator.

5.2.1.2.2.5.1 Frequency Control of Local Oscillator

The LAWS system will use coherent detection of the return radiation, by mixing it on a detector with radiation from the local oscillator. There is thus a requirement that the return radiation and local oscillator remain coherent throughout the mixing period. The laser output pulse from the power oscillator will have an intrapulse frequency stability of 200 kHz giving it a coherence time of 5 μsec, greater than its 3 μsec pulse length. The return pulse will have a length of order 100 μsec due to scattering from the altitude intervals from 20 km to the ground. The local oscillator needs to be coherent over this period giving a frequency stability requirement of less than 10 kHz in 100 μsec. The local oscillator will be a continuous wave CO_2 laser operating on single line and single mode, and this short term frequency stability must be met by proper control of the driving circuit and correct design of the local oscillator resonator mounting. Any tendency to longer term slow drifts of the local oscillator frequency can be actively stabilized, using a scheme as discussed below.

The Doppler shift due to atmospheric aerosol velocities will be superimposed on a large Doppler shift (up to 1.4 GHz) due to the satellite motion. The magnitude of this large shift must be known to determine the wind velocity. It can either be found from an accurate knowledge of the satellite's velocity relative to the ground obtained from an external source, or by a measurement of the frequency of the ground return component of the incoming signal. This latter signal might not always be present due to cloud cover, but if it is utilized there is no need to accurately know the relative frequency of the local oscillator and power oscillator as any frequency difference produces a constant offset in the beat frequency of the local oscillator and the return pulse, which would be

included in the ground return component and thus automatically removed from all wind velocity components. However, if the former scheme is to be used, the relative offset of local oscillator and power oscillator output must be known so that the frequency shift it produces on the Doppler frequency can be accounted for in the post detector processing. A facility to measure the power oscillator to local oscillator offset has been included in the scheme presented here. In this case, the requirement on the frequency stability of the local oscillator is that its frequency must not change during the transmitter pulse time of flight by an amount that would affect the velocity measurement accuracy. A one m/sec velocity accuracy requires measurement of frequency to 180 kHz. The time of flight from satellite to ground and back will be 7.5 msec. Thus the local oscillator must have a frequency stability of 180 kHz over 7.5 msec. This is more stringent than the frequency stability required for coherent detection, as discussed above, and is equivalent to a frequency stability of 24 MHz/sec during the time of flight period.

A block diagram of a proposed scheme for controlling and measuring the freqeuncy offset of the local oscillator and power oscillator is shown in Figure 5-33. Some of the power oscillator output and local oscillator output are mixed in a detector. The power oscillator portion could come from a high transmission beam splitter, as shown, or possibly from low level reflections off other optical components in its beam path to the LAWS telescope. From the detector the electrical signal passes into a discriminator (probably with a 10 to 20 MHz bandwidth) which produces an analogue voltage proportional to the beat frequency of the local oscillator and power oscillator. This output is held in a triggered sample and hold. This voltage, as a measure of the frequency offset, would then be available to the post-detector processing system if required. Dependent on the relative frequency offset, a correction voltage can be applied to the HV amplifier driving the PZT controlling the local oscillator cavity length. It is expected that the power oscillator and local oscillator frequency would be stabilized to a 40 to 50 MHz offset with a time constant of a few seconds.

5.2.1.2.2.5.2 Frequency Control of Power Oscillator

At present, it is not envisaged that any active stabilization will be applied to the power oscillator cavity. The current design of the power oscillator provides for an intrapulse frequency stability of 200 kHz. The resonator mirors will be mounted on a rigid optical frame, whose spacing is controlled by ultra low expansion carbon fiber tubes. Using a figure for the longitudinal expansivity, α, of these tubes of 0.02 x

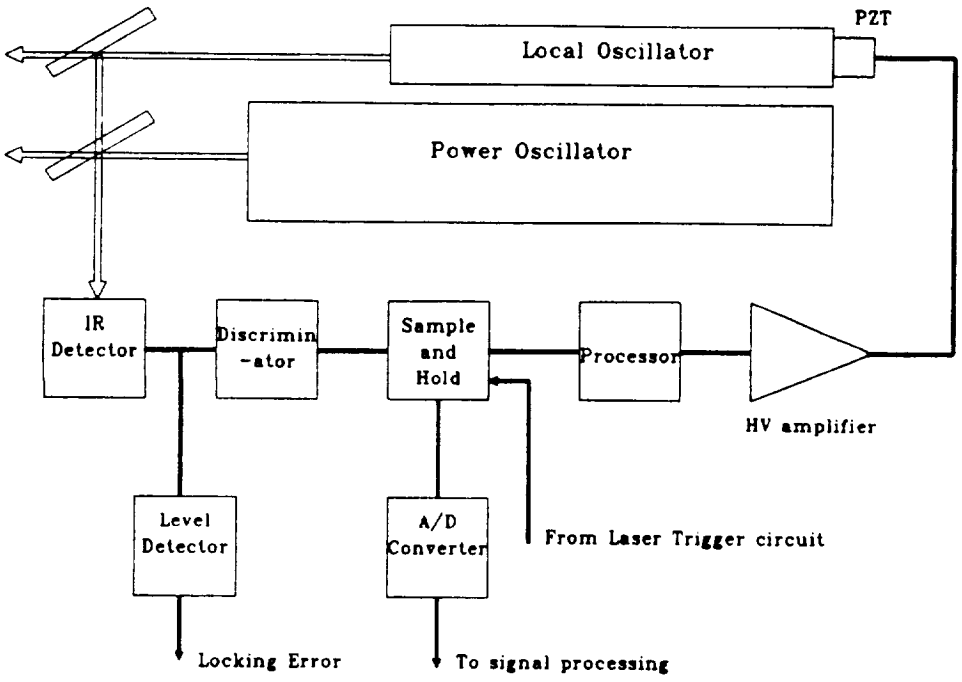

Figure 5-33. LO/PO Frequency Stabilization

$10\text{-}6K^{-1}$, a cavity length of 535 mm and a laser frequency of 3.28 x 10^{13} Hz (9.11 μm), then from combining the equations for thermal expansion and variation of cavity mode frequency with length, the frequency change with temperature as given by

$$\Delta\nu = \alpha\nu\Delta T$$

is $$\Delta\nu/\Delta T = 0.66 \text{ MHz } K^{-1} .$$

For a 535 mm cavity the mode spacing is approximately 280 MHz. Thus, it is seen that even a temperature change of 100 K, well outside that expected in normal operating conditions, would produce a frequency change of only 66 MHz, much less than the mode spacing. This result justifies the current design principle of not actively stabilizing the power oscillator cavity.

5.2.1.2.2.5.3 Frequency Control of Master Oscillator

The current design calls for a master oscillator cavity length of 143 mm, giving a longitudinal mode spacing of 1050 MHz. The master oscillator will oscillate on a single

line and single mode, and it is required to maintain the master oscillator mode frequency close to that of one power oscillator mode close to line center. Once this mode has been selected during the initial start-up phase of the laser operation, the discussion in Section 5.2.1.2.2.5.2 has shown that the power oscillator mode frequency will not vary greatly, and the master oscillator cavity length must be stabilized to enable the master oscillator frequency to track the small power oscillator frequency variations.

The master oscillator is used to injection seed the power oscillator. That is it provides initial photons in one of the power oscillator cavity modes, which then preferentially reaches lasing threshold thus causing the power oscillator to have a single mode output. In this scheme, it is not necessary for the power oscillator and master oscillator to have exactly the same frequency. Work at Advanced Technology Laboratory, Marconi Defence Systems has verified that a 10 to 20 MHz offset will provide the required injection seeding of the power oscillator. Such an offset is advantageous in allowing the master oscillator and power oscillator frequencies to be locked together; as a zero offset cannot be verified using heterodyne detection techniques.

A similar scheme to that discussed above, shown in Figure 5-34, would be used to measure the relative frequency of the master oscillator and power oscillator on a shot by shot basis and to provide a correction to the PZT controlling the master oscillator cavity to correct for any frequency drift, with a time constant of approximately one second.

It is possible that using a suitably stable resonator mounting for the master oscillator, as discussed for the power oscillator, it may not be necessary to actively stabilize the master oscillator cavity length due to the very low thermal drifts in cavity lengths. This is an issue that will be addressed during the breadboard laser investigations.

5.2.1.2.2.5.4 Injection Scheme

There are a number of schemes available to achieve injection of the master oscillator output into the power oscillator, and two options are described here.

Hole in Cavity Mirror. The master oscillator beam is directed through a small hole of a few millimeters diameter, in the rear cavity mirror of the power oscillator. This method had been successfully used at GEC Avionics, though not for a frequency stable laser. There is some evidence that the cavity transverse mode structure can be distorted in this scheme. An additional problem is power oscillator laser radiation escaping through the hole and causing frequency pulling of the master oscillator, or damaging its optics. An

isolation device would probably be needed between the master oscillator and power oscillator to prevent this.

Off-Axis Injection. It has been shown that it is possible to injection seed a multijoule laser using radiation not injected exactly along the laser cavity axis. Experiments at Heriot-Watt University have shown that as long as the injected radiation makes a single pass through the gain medium it will injection seed the laser cavity. This scheme, with the master oscillator not aligned with the power oscillator cavity, removes the need for an isolation device between the two oscillators, as no high energy laser radiation will be coupled into the master oscillator. A schematic diagram of this injection method is shown in Figure 5-35. This method forms the baseline scheme for the injection of the master oscillator radiation into the power oscillator cavity.

With the current baseline optical arrangement for the LAWS system, it is not necessary to have a polarized output from the power oscillator in order to separate the laser transmitted and return beams. However, the power oscillator output is expected to have a reasonably high degree of polarization in any case; the master oscillator is polarized

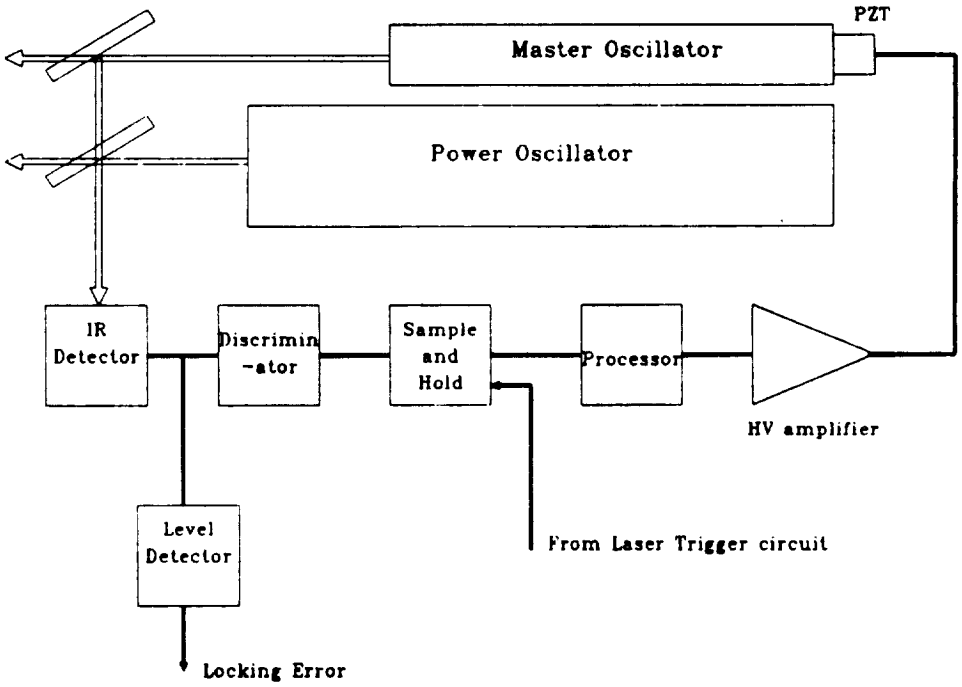

Figure 5-34. MO/PO Frequency Stablization

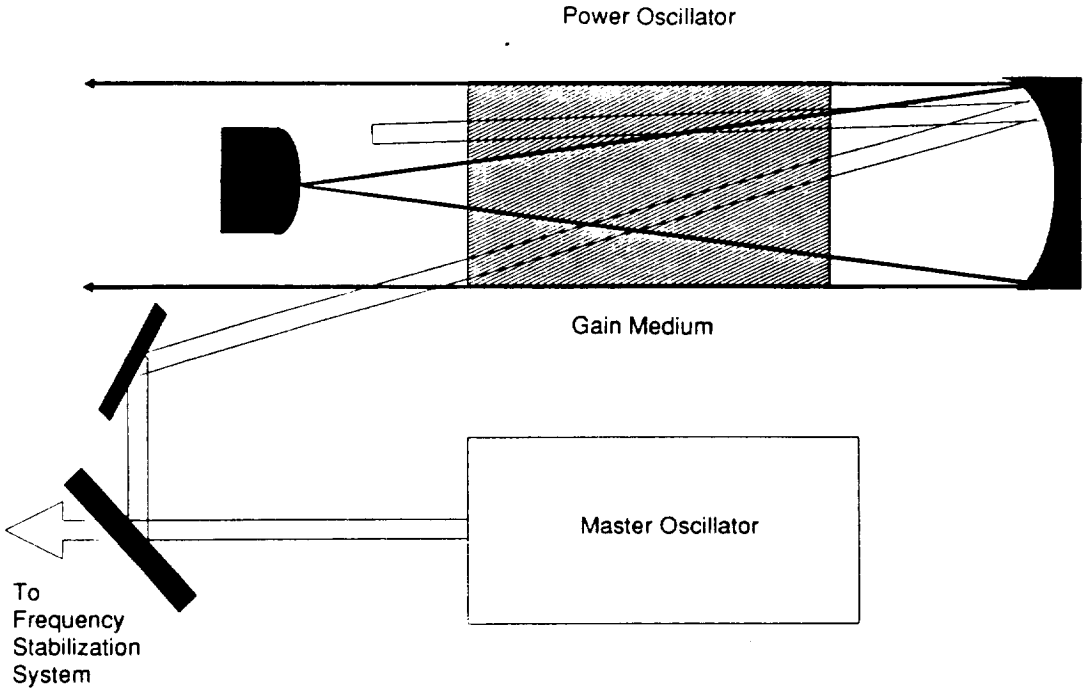

Figure 5-35. MO/PO Injection Scheme

by the diffraction grating, and it is anticipated that the gain build-up of the power oscillator will follow this polarization characteristic. If there were a firm requirement for a polarized laser output, this aspect would be investigated further.

In this section the proposed method for introducing the injection seeding radiation into the power oscillator has been shown. The power oscillator will operate on a single longitudinal mode and on a single line. The method for controlling the relative frequency of master oscillator and power oscillator has been outlined. A scheme has been presented to determine the local oscillator frequency offset relative to the power oscillator, and to stabilize this parameter. Thus, the important frequency stability aspects necessary for the accurate operation of the coherent laser radar have been addressed.

5.2.1.2.2.6 Laser Subsystem Design

The weight, volumes and power requirements of all individual modules have been estimated, in most cases by analyzing the design to component level.

The modules have then been arranged to form a compact laser subsystem, following sound design principles based on GEC Avionics' experience of CO laser system design. These design guidelines are summarized in Table 5-21.

Table 5-21. GEC Laser Subsystem Design Guidelines

- All high voltage connections are bulkhead to bulkhead plug/sockets to minimize EMI emissions. This eliminates high voltage wires between modules.
- Each module is an individually screened metal enclosure.
- No current passes through the outside of enclosures.
- Both laser electrodes are isolated from the laser enclosure.
- Modules will to be kept close together to minimize laser current loop and hence radiated magnetic fields.
- Electron gun is positioned immediately above the laser to permit entry of electrons. Some currents will flow around the foil and drift tube area.
- The electron gun vacuum chamber, therefore, should be covered with an insulator outside while there is another metal enclosure to provide EMI screening. The screening is also adequate to reduce emitted X-ray radiation to below the background level for orbits passing polar regions.
- Transformer size can be obtained by combining the core and coil which overlap.
- Position transformer immediately next to gun to prevent any wires carrying 160 kV.
- Master oscillator laser head should be near large laser to minimize length of laser beam connection. Master oscillator pulse forming network near to laser head for minimum inductance and EMI screening.
- Pulse forming network should be the opposite end from the laser output to allow space for high voltage leadthroughs.
- The master oscillator and electron gun both operate at 32 kV so they can use the same high voltage power supply. They may also be able to use the same switch. This is a high risk option at present as the delay between the two lasers would be fixed. Two switches have therefore been included.
- Master oscillator switch should be adjacent to pulse forming network for EMI containment.
- Electron gun PFN is adjacent to transformer to minimize lead lengths.
- Electron gun switch next to gun PFN.
- Electron gun high voltage power supply unit is adjacent to gun switch or gun PFN.

Table 5-21. GEC Laser Subsystem Design Guidelines (Concluded)

- Electron gun high voltage power supply unit is adjacent to master oscillator switch of PFN.
- Thyratron power supply is adjacent to both switches to prevent power losses in high current lines, and to minimize weight of thick wires.
- Auxiliary discharge power supply is adjacent to electron gun.
- Spare space at output end of laser transmitter used for control/diagnostics and connectors to LAWS Instrument.
- EMI shielding/housing around modules.
- There will be a high tolerance on the output beam stability with respect to the laser mounting face; therefore, the number of components between the mounting face and the optical resonator should be minimized.
- Laser head is mounted directly on laser subsystem mounting face.

A block diagram of the laser subsystem is shown in Figure 5-36; the modular arrangement is shown in Figure 5-37(a), and an outside view is shown in Figure 5-37(b). An artist's cutaway concept of the laser head is provided in Figure 5-38.

System power and weight summaries are shown in Tables 5-22 and 5-23; interface requirements and a summary of laser characteristics are shown in Tables 5-24 and 5-25.

5.2.1.2.3 Risk Reduction

During the course of the LAWS Phase One Study, a number of areas have been identified as potential risk issues which require experimental work in order to assess fully. These issues could largely be addressed by a LAWS laser breadboard build. They are listed in Table 5.26.

5.2.1.2.4 Conclusions

A thorough and objective study has been carried out on laser technology for LAWS by looking at all possible options at the outset with no pre-conceived notions. The trades studies carried out have enabled a selection of the optimum LAWS laser configuration, and a laser design has been evolved which meets all the requirements.

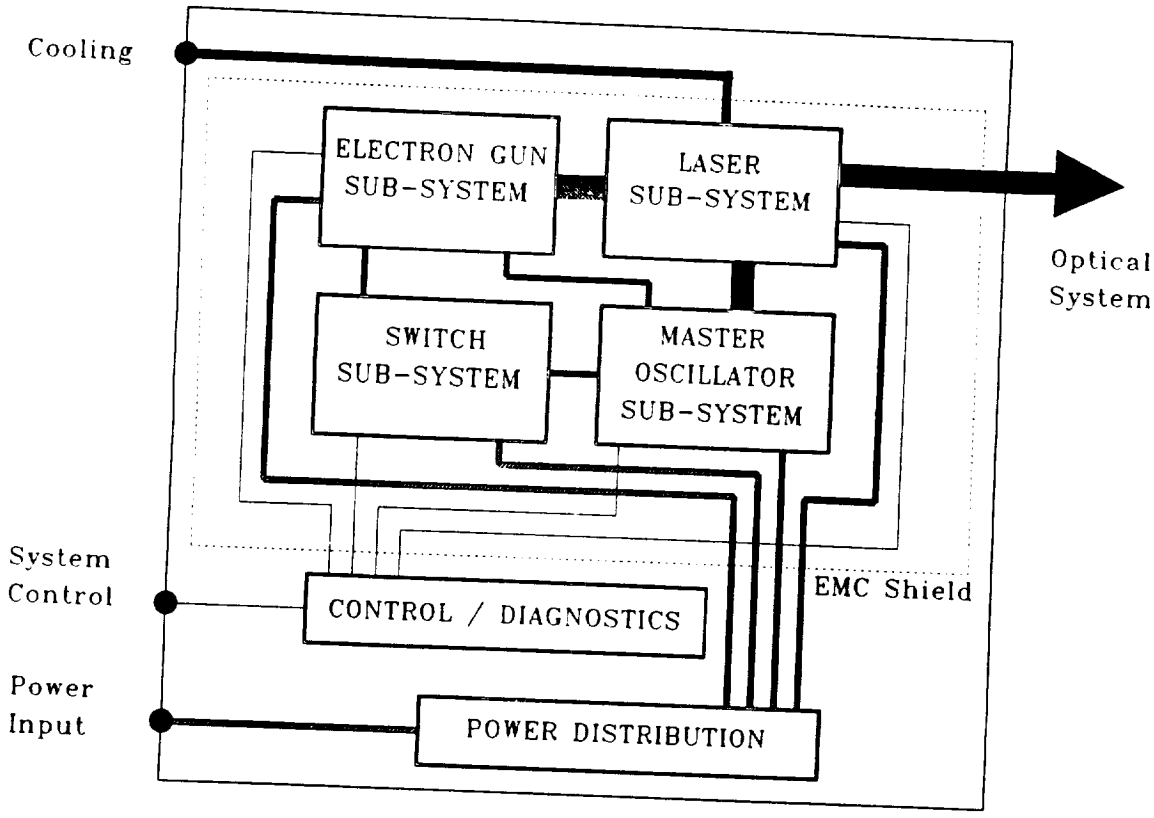

Figure 5-36. LAWS Laser System Block Diagram

In establishing the choice of configuration, and details of operating parameters, appropriate design margins have been included in order to ensure good discharge stability and high reliability for the required laser lifetime.

The considerable experience of GEC Avionics in designing reliable, well-engineered lasers for field use, augmented by the space expertise of Marconi Space Systems, places GEC in an optimum position for undertaking a breadboard and space qualified laser build with a high level of confidence that the initial engineering estimates of weight and performance will be achieved.

5.2.1.3 Requirements for Laser Breadboard

From the above discussion of both Avco and GEC laser designs, it can be seen that experimentation is required to solve several laser issues. These issues are outlined in Figure 5-39 for both the corona pre-ionized (Avco preferred) and e-beam sustained (GEC preferred) approaches. The principal issue for the e-beam laser is foil lifetime; for the pre-ionized laser it is the pre-ionizer lifetime. Most of the other issues apply to either laser approach. A number of the issues will essentially require technology

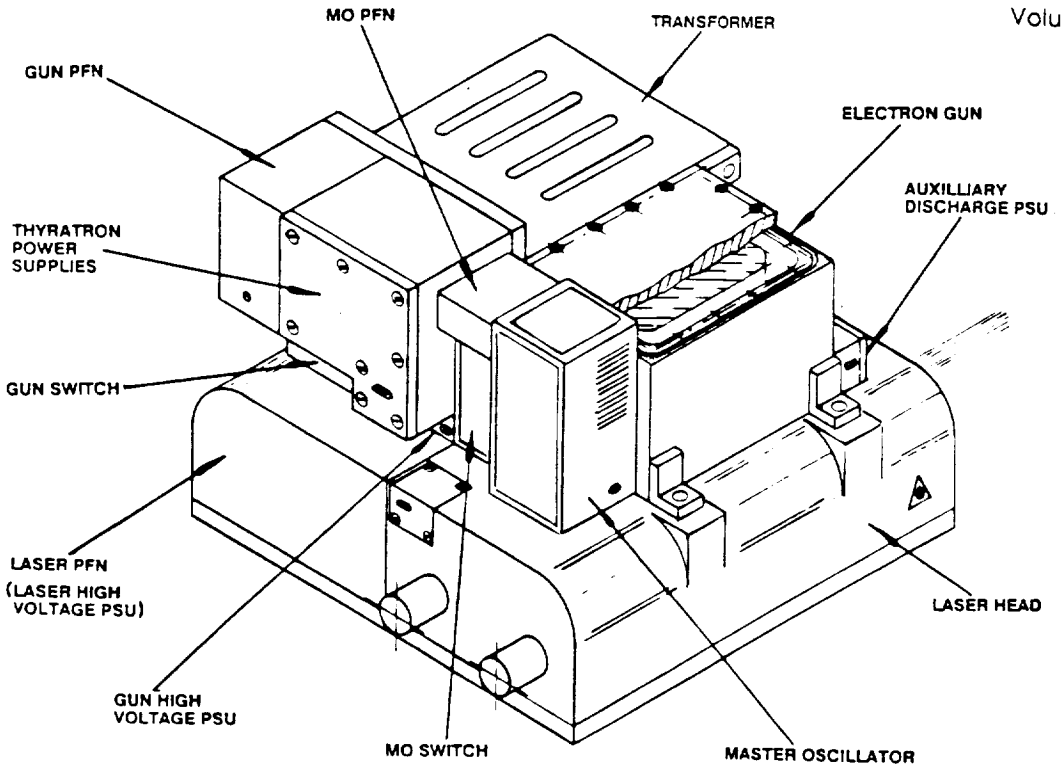

(a) Modular Arrangement

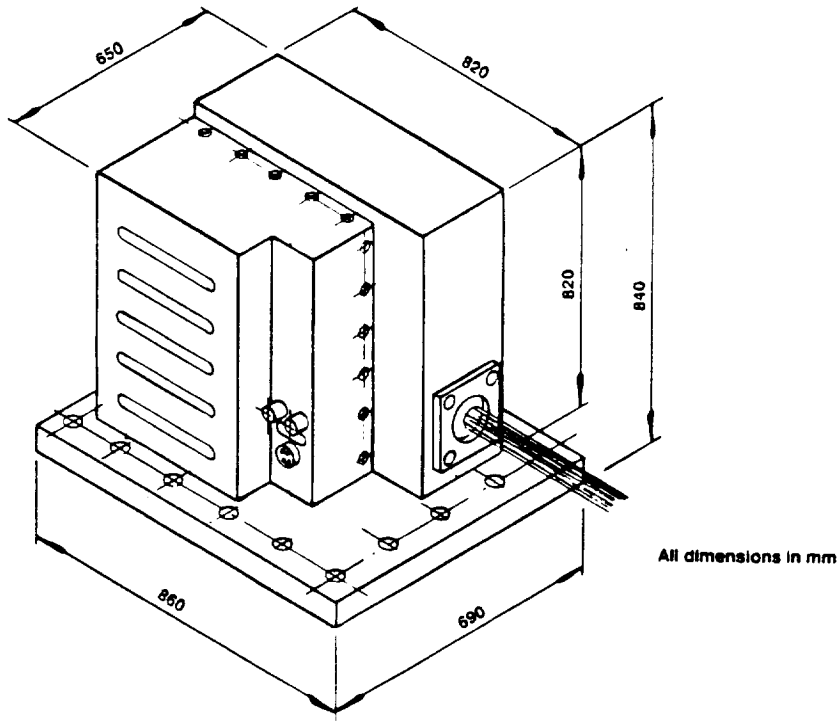

(b) External View

Figure 5-37. Laser Subsystem

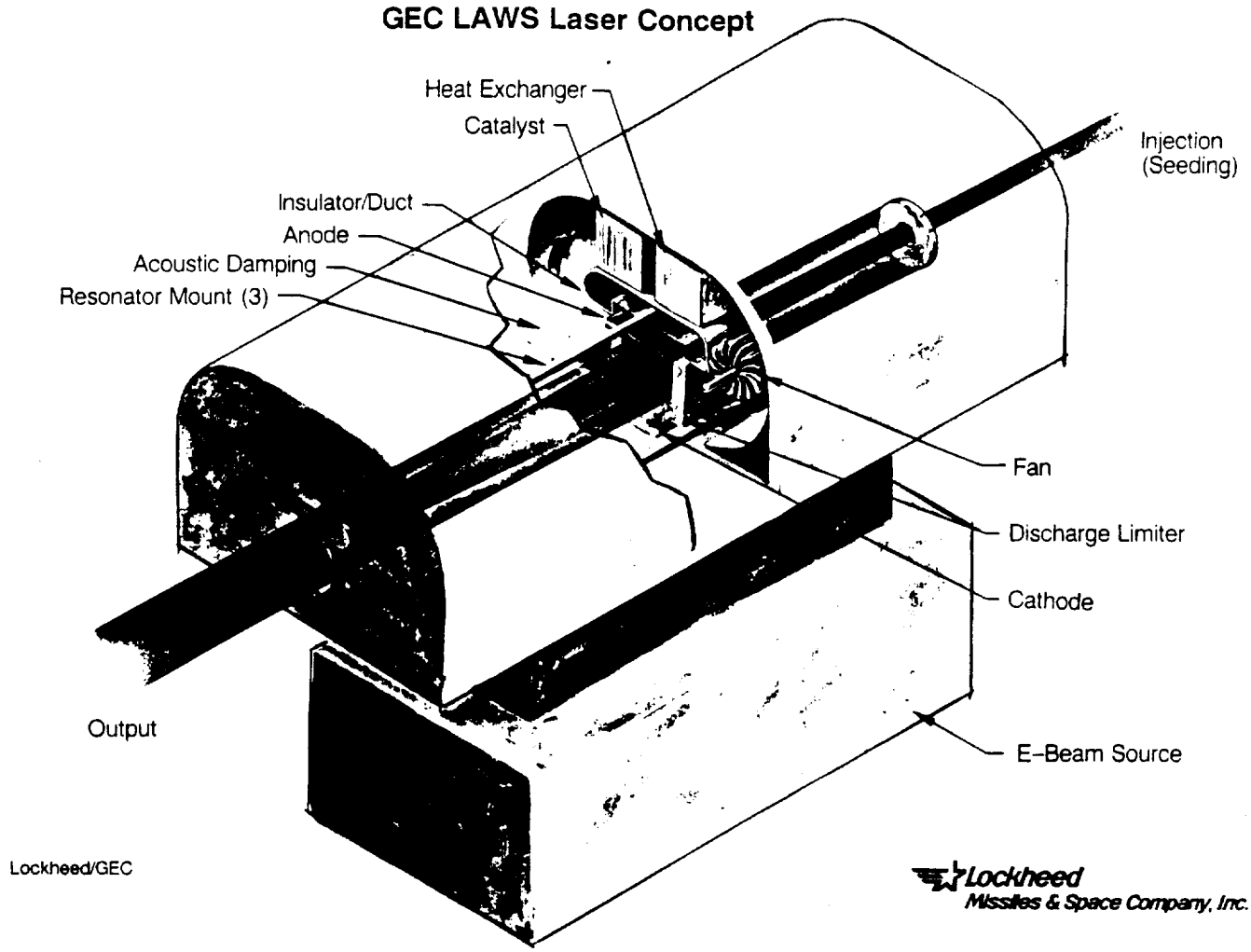

Figure 5-38. GEC LAWS Laser Head Concept

development or demonstration to prove the capability. Other of the issues can be readily solved using known engineering principles.

Figure 5-40 addresses which issues should be solved at the component level and which require a system breadboard to resolve. Electrical and mechanical issues can basically be resolved at the component breadboard test level. However, such issues as laser output, pulse characteristics, and laser system lifetime issues will require testing at the repetitively pulsed laser breadboard level including cavity, flow loop, and gas control mechanisms. The catalyst is being addressed internally by NASA. However, eventually the laser system must be operated with the chosen gas isotope and catalyst to demonstrate long-term operation with minimal performance degradation.

Table 5-22. Power Summary (W)

Laser power	2139
Electron gun	88
Auxiliary discharge	15
Thyratron heater	378
Fan motor	40
Master oscillator	47
Diagnostics and control	10
Total power	2717
Wall-plug efficiency (%)	5.9

Table 5-23. Weight Summary (kg)

Laser head	25.9
Electron gun	5.3
Laser PFN	45.1
Laser HVPSU	14.2
Electron gun PFN	3.0
Electron gun HVPSU	0.6
Switches	6.0
Thyratron heater PSU	7.7
HV transformer	26.5
master oscillator and PFN	8.8
Miscellaneous	15.1
Sub-total	153.5
Contingency (%)	10
Total weight	168.9

Table 5-24. Interface Requirements

DC supply voltage	300 Vdc
Liquid cooling capacity	1818 W
Radiative cooling required	738 W
Optical interface	TBD
Control and command signals	TBD
Mounting platform	TBD

Table 5-25. Laser Characteristics

Weight	174 kg
Pulse energy	20 J
Pulse length	3 μsec
Wavelength	9.11 um single mode
Life	10^9 pulses
Pulse rate	< 8 Hz
Chirp	< 200 kHz
Maximum power	2716 W
Wall-plug efficiency	5.9%
Volume	409 liters

Table 5-26. GEC Risk Reduction Issues

- Lifetime of foil, design of foil assembly, materials choice
- Lifetime of laser gas and catalyst; isotopic scrambling
- Pulsed injection techniques and full characterization
- Single longitudinal and single transverse mode control
- Lifetime of electrical components, in particular the electron gun transformer
- Wall-plug efficiency of laser subsystem for LAWS type outputs
- Frequency stability; agreement with theory
- Pulse energy, pulse length, and pulse shape
- Space qualification issues.

LASER TECHNOLOGY / DEVELOPMENT REQUIREMENTS / ISSUES	CORONA PRE-IONIZED LASER		ELECTRON BEAM SUSTAINED LASER	
	ENGINEERING USING KNOWN PRINCIPLES	REQUIRES TECHNOLOGY DEVELOPMENT/ DEMONSTRATION	ENGINEERING USING KNOWN PRINCIPLES	REQUIRES TECHNOLOGY DEVELOPMENT/ DEMONSTRATION
LIFETIME				
Components				
Foil				●
E Beam Source			●	
Pre-ionizer		●		
Optics	●		●	
Mechanical (fans, etc.)	●		●	
Pulse Forming Network	●		●	
Deposition Upon Optics		●		●
Lasing Medium				
Catalyst - O_{18} isotope		●		●
Catalyst - Other		●		●
Gas Mixture, Pressure	●		●	
Gas Poisoning	●		●	
OUTPUT PARAMETERS				
Pulse Temporal (Amplitude) Shape	●		●	
Pulse Mode Purity (SLM & STM)		●		●
Intrapulse Frequency Stability		●		●
Interpulse Frequency Stability		●		●
Pulse Long Term Stability		●		●
EFFICIENCY (WALL PLUG >5%)		●		●
ACCEPTABLE MASS	●		●	

LAWS 5-39

Figure 5-39. Transmitter Laser Technology Issues

TECHNOLOGY DEVELOPMENT REQUIREMENTS / ISSUES	RESOLVABLE FROM REQUIRED COMPONENT BB TEST	REQUIRES SYSTEM BB TO RESOLVE
LIFETIME		
Components		
Foil	●	
Pre-ionizer	●	
Optics		●
Mechanical (fans, etc.)	●	
Pulse Forming Network	●	
Deposition Upon Optics		●
Lasing Medium		
Catalyst - O_{18} isotope	NASA	●
Catalyst - Other	NASA	●
Gas Mixture, Pressure	●	
Gas Poisoning		●
Laser Head Overall		●
OUTPUT PARAMETERS		
Pulse Temporal (Amplitude) Shape		●
Pulse Mode Purity (SLM & STM)		●
Intrapulse Frequency Stability		●
Interpulse Frequency Stability		●
Pulse Long Term Stability		●
EFFICIENCY (WALL PLUG >5%)		●

LAWS 5-40

Figure 5-40. Requirements for Transmitter Laser Development

5.2.1.4 REFERENCES

1. R.T. Menzies, Appl Opt. 25, 15, p. 2547.
2. G.M. Ancellet, R.T. Menzies, and D.M. Tratt, Appl. Opt. 27, 23, p. 4907, 1988.
3. J.D. Wood and P.R. Pearson, Journal de Physique 41, 11, C9-351-C9-357.
4. V.G. Roper, H.M. Lamberton, E.W. Parcell, and A.W. Manley, Opt. Comm. 25, 2, pp. 235-240, 1978.
5. A. Parent, N. McCarthy, and P. Lavigne, IEEE Jour. Quart. Electron, QE-232, pp. 222-227, 1987.
6. D.M. Tratt and R.T. Menzies, Appl. Opt. 27, 17, pp. 3645-3649, 1988.
7. C.E. Hamilton, A.L. Pendroh, T.R. Lawrence, and C.H. Fisher, Proc. Fifth Conference on Coherent Laser Radar P. III 9 (5-9 June, Munich, FRG), 1989.
8. A. Javan, J. Quantum Elect. 8, 11, pp. 827-832, 1972.
9. V. Hasson, G. Theophanis, H. Chow, and D.P. Pacheco, SPIE Vol. 783, Laser Radar II, pp. 9-16, 1987.
10. A. Chakrabarti, and J. Reid, J. Appl. Phys. 66 (1), pp. 37-42, 1989.
11. H.T. Price and S.R. Shaw, NASA C.P. 2456, pp. 77-84, 1987.
12. M.J. Brown, S.R. Shaw, M.H. Evans, J.M. Smith, and W.E. Holman, NASA C.P. (to be published).
13. P.M. Schwarzenberger and X. Matzangou, NASA C.P. (to be published).
14. D.V. Willets and M.R. Harris, IEEE Jour. Quant. Electron QE-19, 5, pp. 810-814, 1983.
15. D.V. Willetts and M.R. Harris, J. Phys. D, 15, pp. 51-67, 1982.
16. D.V. Willetts and M.R. Harris, Opt. Comm. 49, 2, pp. 151-154, 1984.
17. D.V. Willetts and M.R. Harris, IEEE Jour. Quant. Electron QE-21, 3, pp. 188-191, 1985.
18. V.P. Avtonomov, E.T. Antropov, N.N. Soboler, and Y.V. Troitskii, Sov. Journ Quant. Electron 2, 3, pp. 300-302,1972.
19. J.S. Leune, Appl. Phys. Lett. 22, 3, pp. 55-57.
20. R.J. Tough and D.V. Willetts, Journ. Phys. D, 15, pp. 2433-2442, 1982.

5.2.2 Optical Subsystem

5.2.2.1 Introduction

The LAWS optical system fundamentally operates in two modes, transmit and receive. While in the transmit mode the optical system couples a pulsed laser to a telescope which transmits the beam approximately 1200 km to the earth's atmosphere which then scatters the light. Some of this light is scattered back in the direction of the transmitted pulse and collected by the LAWS optical system, which in the mean time, has been switched into its receive mode. In this mode the telescope collects the backscattered light and combines it with a local oscillator laser beam at the heterodyne receiver.

As the LAWS platform orbits the earth, the optical system samples only a narrow swath on the atmosphere, unless some mechanism for scanning the beam is included in the system. Studies that predate this effort have determined that the best scanning method is to point the telescope off of nadir and then rotate the whole telescope about the nadir axis, thus producing a conical scan. Scanning at substantial angular rates coupled with large slant ranges causes the return beam to lag behind the telescope by up to 8 mrad. This lag angle must be compensated in real time to a precision of less than 1.5 μrad. The 1.5 μrad requirement comes about because of the necessity to align the wavefronts of the return beam and the local oscillator to maximize the heterodyne detection efficiency.

Finally, the return beam is combined with the local oscillator beam by the interferometer assembly and focused on the heterodyne receiver. The need to maximize the efficiency of this process drives the majority of the system performance specifications.

5.2.2.2 Laws

The top level LAWS optical system requirements, shown in Figure 5-41, were used to determine the design specification of Figure 5-42. The following paragraphs explain the origins of and the rationale for the design specifications.

The first of these specifications is a result of the need to couple the collimated transmitter laser output into the atmosphere which is a large distance away. An afocal beam expander is the result of the large distance of the target. This means that the optical system magnifies a narrow collimated input .

The second item results from the lag angle created by the conical scanning pattern. For the baseline 6.8 rpm rotation rate and the maximum nadir angle of 60 deg, a full

Weight	≤ 225 kg
Diameter	≥ 1.67 m
Lag Angle Compensation @ 6.8 RPM	1200 km at 7 km/sec orbital velocity
Pointing Accuracy	≤ 3 μrad (2σ)
Variable Nadir Angle	$30^{\circ} \leq x \leq 60^{\circ}$
Size compatible with JPOP and Shuttle	

LAWS 5-41

Figure 5-41. LAWS Optical System Requirements

Afocal Telescope	
Full Field of View	1°
Wavelength	9.11 μm
Magnification	-42X
Performance (λ = 9.11 μm)	0.07 λ rms
Obscuration	< 7% area
Accessible Pupil	Low Distortion

LAWS 5-42

Figure 5-42. Telescope Flowdown Requirements

field of view of 16 mrad (- 1.0 deg) is necessary. This value is proportional to both the scanning rate and the nadir angle, since the change in the field position of the transmitted and received pulse is proportional to these quantities. Therefore, increases in these values will result in an increase in the full field of view. To compound the problem, the field must remain flat over the entire field of view so as not to adversely affect the heterodyne detection, or else the heterodyne efficiency is decreased due to the focus aberration.

The requirement for an operational wavelength of 9.11 μm is a NASA implied specification and was determined based on signal maximization laser technology, and eye safety issues.

As was stated previously, the afocal system increases the diameter of the input transmitter laser. The amount that this system increases the diameter by is defined as the system magnification. With a 4 cm x 4 cm transmitter laser output and a 1.67 m diameter telescope (for S/N considerations) the required system magnification is 42 x.

The requirement for an accessible pupil comes from the need to very accurately align the return beam with the local oscillator. The only way to make the return and the local oscillator beam collinear while matching the wavefront tilts of each beam using only one mirror, is to locate that mirror at a pupil image. Other techniques require two mirrors working simultaneously to perform this same function; one redirects the beam toward the optical axis while the second redirects the beam on to the optical axis. The creation of an accessible pupil in the telescope forms an intermediate image which is beneficial for system alignment but in high energy laser testing could pose a problem because of dielectric breakdown of the air. The simplicity of using one mirror at a pupil, versus the complex coordination of two mirrors, outweighs the draw back of high energy testing in air. If it is necessary to test the transmit laser at full power in air, it is possible to place either an evacuated cell at the internal focus or just simply place the entire system in a vacuum chamber for this test. Since we are doing the lag angle compensation at a pupil, the pupil distortion as a function of the field of view must be small because pupil distortion appears as a change in the magnification as a function of the field angle. Excessive pupil distortion will mitigate aligning the two beams precisely.

5.2.2.3 Optical Efficiency

The following factors determine the overall S/N performance of the LAWS transceiver:

a. The loss of energy due to obscuration of the transmitter by the telescope optics
b. Optical losses including polarization mismatch in the transmit and receive paths of the transceiver
c. Detector quantum efficiency
d. The wavefront error in the transceiver optics
e. Pointing error
f. Transmitter illumination pattern
g. Heterodyne efficiency.

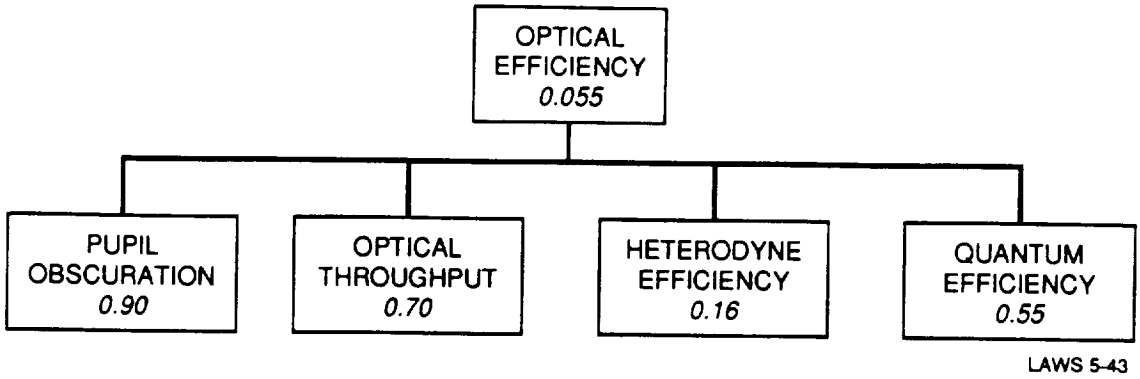

Figure 5-43. Optical System Efficiency

0.07 λ's rms, and a pointing error of 1.5 μrad is 0.16. (For the wide-area distributed aerosol scatterers, the maximum theoretically achievable heterodyne efficiency is somewhat less than 50 percent because of the angular distribution of backscattered signals.)

The quantum efficiency used for this calculation of overall efficiency is 55 percent. This represents what would be achievable for a detector with moderate BW in a system that uses some degree of Doppler compensation in the receive local oscillator. The product of these efficiencies is 0.05.

The SNRs which depend directly on the overall optical efficiency factors determine the probability of obtaining a meaningful velocity measurement and the error bounds on the velocity measurement. The achievable accuracy of the velocity measurement also depends on the time waveform of the transmitter. For example, the correlation time of the transmitter gain-switched spike is shorter than the correlation time of the main pulse, and the measurement time interval or measurement window to achieve the best performance is closer to the overall pulse width. The returns from the narrow gain-switched spike will decorrelate several times during this measurement window, and the contribution to the velocity measurement by the gain-switched spike will be relatively less than the energy contained in this spike. This form of degradation must be considered in the signal processing to determine the overall system performance.

5.2.2.4 LAWS Optical System Baseline

The LAWS optical system is composed of a telescope supported by a gimbal which rotates the telescope and transfers the transmitted and return beams to and from the optical bench. The following section provides a description of the baseline design and the rationale for the choices made.

The optical design of the LAWS system, Figures 5-44 and 5-45, is divided into two assemblies, the telescope and the relay optics. This choice was made because a system that meets all of the performance requirements using only a three mirror telescope design could not be produced. The problem is that there are not enough degrees of freedom with only three mirrors to produce a system that is diffraction limited over a 1 deg field of view with the telescope providing the total system magnification. The problem is compounded when the requirements for a well corrected pupil and a flat field are also included. To simplify the problem the system is split into two parts, allowing a reduction of the magnification of the telescope (which produces a workable telescope design) followed by the relay optics yielding the remaining magnification.

The LAWS optical system has been configured to maximize wavefront quality over the field of view and to minimize pupil distortion. The need for wavefront quality is easily recognized in that the heterodyne efficiency decreases with the variance (rms^2) of the wavefront error. The need for good pupil imagery is more subtle. If the pupil image moves, then the beam from the local oscillator and the return beam do not overlap in collimated light space (efficiency reducing tilt fringes are produced at the focus on the detector). The nonoverlapped beams lower the heterodyne efficiency proportional to the degree of nonoverlap.

Good wavefront quality and minimum pupil distortion tend to be mutually exclusive requirements for an optical system. The ability of an optical system to meet both requirements is increased by minimizing the afocal magnification.

Thus our optical configuration shares the total required magnification of 42 X between the telescope and the optical bench. The telescope produces a magnification of 12 X and the bench a magnification of 3.5 X. The wavefront quality can be met at the same time keeping the pupil distortion to less than 2 percent. (If the whole magnification were put into the telescope, the pupil distortion would rise to 8 percent with an attendant 8 percent reduction in efficiency.) The penalty for sharing the magnification between the bench and the telescope is the need for three beam reducing mirrors in the bench. These mirrors are parabolas that are well within the state-of-the-art. Another benefit of

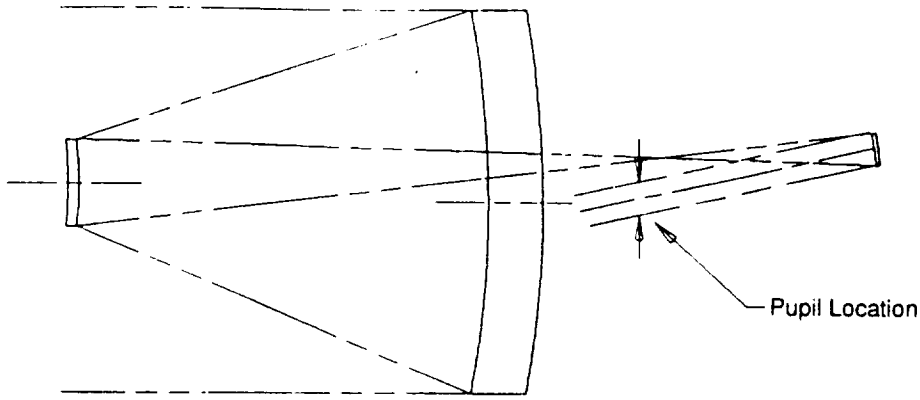

		Surface Specifications:	
Field of View	1 ° Circular	Primary	Parabola
Wavelength	9.11 μm	Secondary	Hyperbola
Magnification	12X	Tertiary	Ellipse
Obscuration	7%		

LAWS 5-44

Figure 5-44. Afocal Eccentric Lens Design Telescope

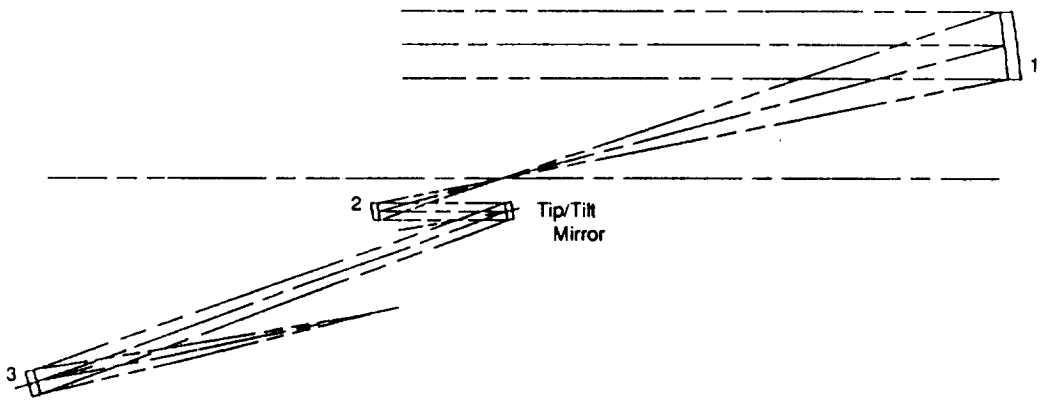

		Surface Specifications:	
Field of View	1 mrad Circular	Mirror #1	Parabola
Wavelength	9.11μm	Mirror #2	Parabola
Magnification	3.5X	Mirror #3	Parabola
Wavefront Error	≤0.01 λrms		
Obscuration	Unobscured		

LAWS 5-45

Figure 5-45. Afocal Eccentric Lens Design Relay Optics

sharing the magnification is that the misalignment sensitivities of the telescope are minimized by a factor of approximately five.

In summary, our optical configuration represents an optimal compromise between heterodyne efficiency and complexity as determined by the number of optical components.

The baseline optical design of the telescope, Figure 5-44, is a three mirror eccentric afocal Cassegrain with a 12 X magnification that produces a 14 cm diameter beam at the pupil image. The baseline design is an eccentric in field three mirror Cassegrain. This means that the intermediate image created over the full 1 deg field of view is displaced slightly above the center line of the telescope aperture, as can been seen in Figure 5-44. This has two primary effects; the first is to slightly decenter the secondary, and the second is to form a pupil image slightly below the aperture center line. The first effect has little or no impact on the heterodyne efficiency, and the second provides an accessible pupil where the lag angle compensator can be placed without obscuring the beam. This design is preferable to a concentric design because a concentric design would locate the pupil and the lag angle compensator in the middle of the converging beam creating a very large obscuration.

The trade study performed to choose this optical form is summarized in Figures 5-46 and 5-47, which show the different optical forms that were looked at and the reasons they were eliminated. The options in Figure 5-46 were disregarded early in the trade study because they did not satisfy all of the design requirements, leaving the three options of Figure 5-47 to be investigated. The choice of the afocal eccentric field design over the others was influenced purely by Itek's experience designing and manufacturing all three types, showing that the baseline design is the simplest of the three.

The relay optics of Figure 5-45 form the second part of the total optical system giving us the full 42 x magnification. This design uses three parabolas to reduce the beam diameter from 14 cm exiting the telescope down to the final 4 cm diameter and then focus the beam on to the heterodyne detector/receiver. Like the telescope, there is an accessible pupil where a tip/tilt mirror is used to remove the residual lag angle which is expected to be on the order of 1 mrad. (Most of the lag angle is corrected with a rotating polygon, located at the telescope pupil described in the mechanism section.)

For this baseline configuration, both the transmitter beam and the return beam are transferred between the relay optics and the telescope through a Coudē path. This path takes the beams through the gimbal structure and is used so that changes in the

elevation angle and the rotation angle do not cause the beam to deflect. More information concerning the Coudé path will be provided during later discussions of the gimbal assembly.

The structural design of the LAWS optical system is shown in Figures 5-48 through 5-50. The telescope assembly of Figure 5-48 and the gimbal assembly of Figure 5-49 are interfaced with each other. The telescope assembly is a graphite epoxy shell supporting ULE optical elements, the largest of which is the 1.67 m diameter light weighted ULE primary mirror. The trade study that resulted in the baseline design is summarized in Figure 5-51. This study considered three basic structural concepts: a shell, an athermalized truss, and a tripod; each of which was evaluated for both Beryllium and graphite epoxy. All of the concepts were assessed according to their wavefront performance, their line-of-sight stability performance, their thermal control requirements, and their weight. To aid in the determination of an adequate structure, the wavefront and line-of-sight error budgets of Figures 5-52 and 5-53 were generated by taking the requirements of Figures 5-41 and 5-42 and flowing them down to the component level. The athermalized truss was ruled out because of its high cost and difficulty of manufacturing, while Beryllium as a possible material was disregarded because of the excessive wavefront error in the remaining concepts. The shell was chosen over the tripod because a shell is a very simple structure which will be easier to manufacture and assemble.

Having chosen the structural material, the choice of the optical materials was made. Three materials were evaluated: ULE, Beryllium, and Silicon Carbide. Because of the mismatch between the thermal coefficients of expansion for graphite epoxy and Beryllium, the choice of materials was narrowed to ULE and Silicon Carbide. ULE was chosen over Silicon Carbide because of Itek's experience with the manufacturing of large light weight ULE optics.

The Coudé path mentioned earlier is shown in Figure 5-48. The mirror to the left of the pupil image is used to direct the beams through the elevation bearing toward the fold mirror located inside the gimbal portion of the elevation bearing seen in Figure 5-49. In Figure 5-49, two more mirrors direct the beam through the gimbal and then up through the azimuth bearing, which is then folded by another mirror toward the optical bench. As well as housing the Coudé path, the gimbal assembly provides the functions of scanning the telescope and varying the elevation angle. This structure is manufactured of Beryllium for the purpose of achieving the highest structural frequency for the lowest

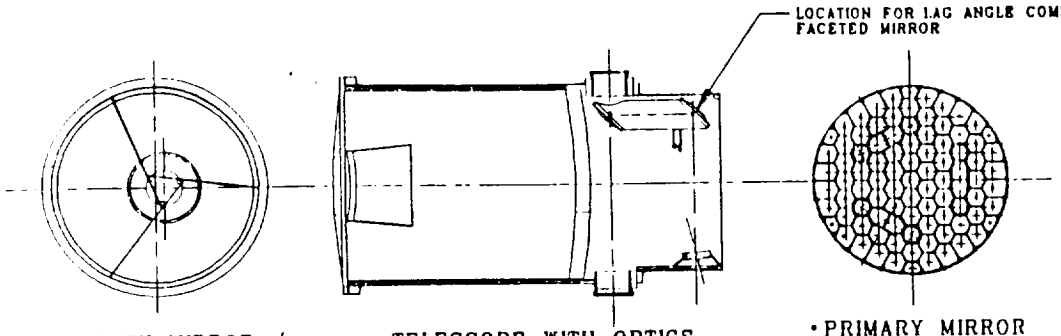

DESIGN REQUIREMENTS / SPECIFICATIONS

- Allowable WFE ~ 0.07 λrms operational; λ0.014 rms fab/align
- Thermal control power 110 watts; weight 2 kg
- Weight 107 kg; frequency 200 Hz
- Modular design / limited space envelope
- Launch dynamics; 30 g - quasi static load; Telescope locked during launch
- ULE Optics, graphite epoxy metering structure
- Trunnion mounted, center of gravity to within 2 mm of AZ/EL axes

Figure 5-48. Telescope Assembly

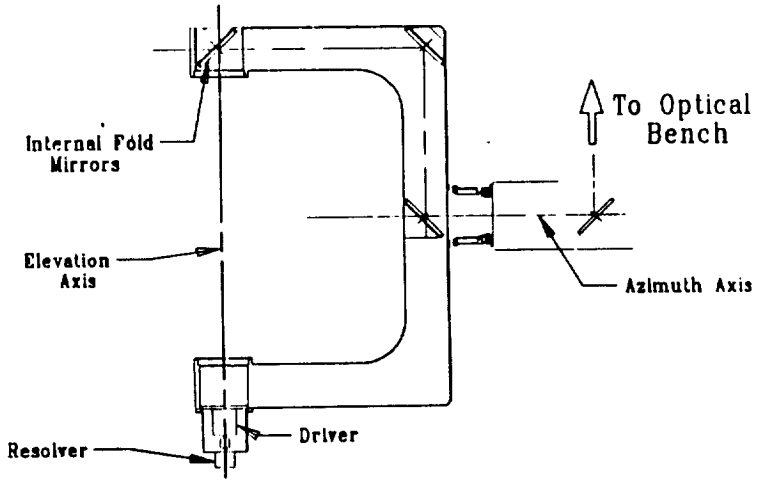

DESIGN REQUIREMENTS/SPECIFICATIONS

- Elevation angle range 30 - 60 set and hold / elevation drive
- Azimuth Scan - continuous rotation at 6.8 rpm / azimuth drive
- 0.6 μrad allowable tiip/tilt
- Weight 26 kg; frequency 50 Hz
- Material - Beryllium
- Power consumption - 4 watts

Figure 5-49. Gimbal Assembly

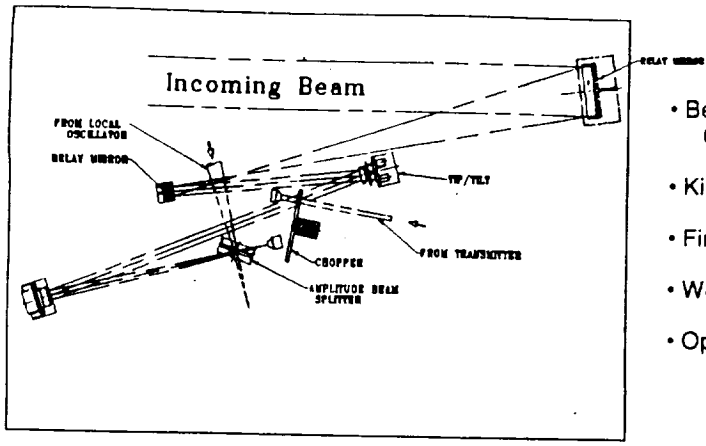

- Beryllium, egg crate structure 0.9 m x 1.27 m x 15 cm deep
- Kinematically mounted to platform
- First bending frequency 200 Hz
- Weight, including thermal control 41 kg
- Optics modularly mounted to surface

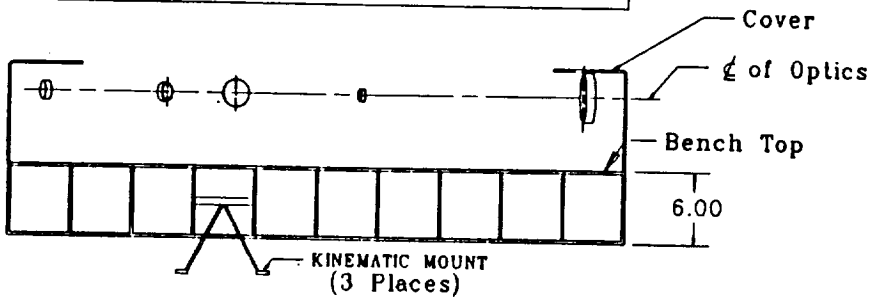

Figure 5-50. Optical Bench Assembly

	SHELL		ATHERMALIZED TRUSS		TRIPOD	
	Gr/Ep	Be w/ULE Rods	Gr/Gr	Be/Gr	Gr/Ep	Be
WFE λ_{rms}**	.015	.047	.008	.010	.018	.10
Weight (lbs)	62	65*	50	48	30	18
Thermal Control Weight	7.8	8.0	11	11	9.0	9.0
Power (Watts)	110	115	85	83	64	64
Fn (Hz)	200	335	200	200	200	200
Soak/Gradient	20°C/2°C	20°C/2°C	20°C/1°C	20°C/1°C	20°C/3°C	20°C/3°C
Comments		Excessive WFE due to Tip of Secondary	Accessibility high cost		Accessibility	Excessive WFE

* Based on Minimum Be thickness

** 0.015λ allocated to structure

Candidate concepts evaluated for performance, weight, power consumption, and stiffness.
Conclusion: Select graphite epoxy designs based on performance and weight - recommend detailed analysis to finalize selection.

Figure 5-51. Metering Structure Concepts Trades

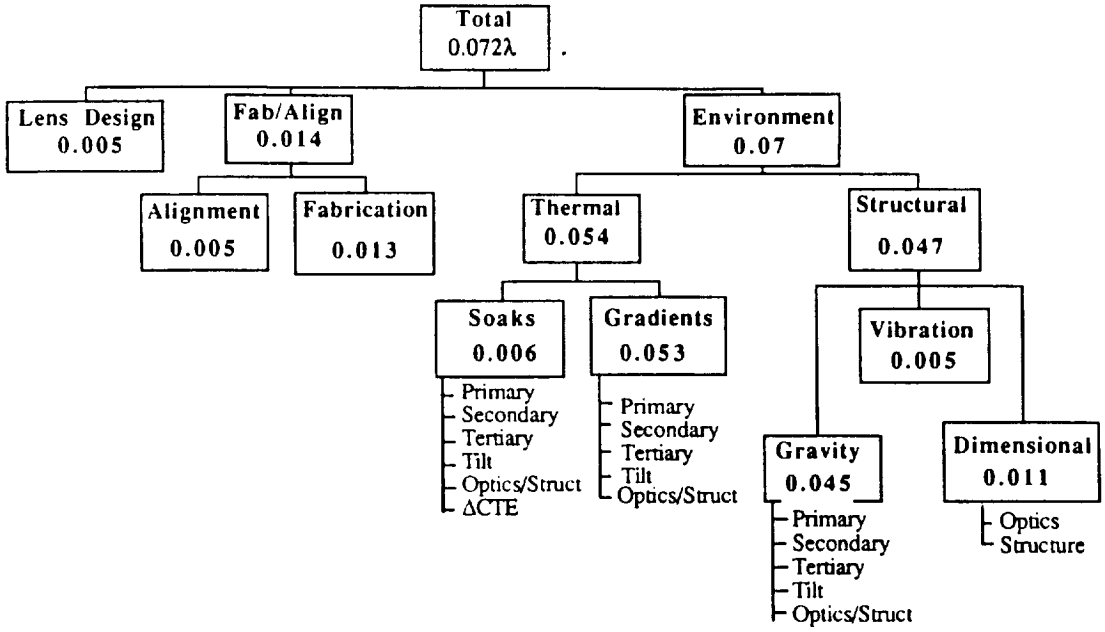

Figure 5-52. LAWS Optical System Wavefront Error Budget λ = 9.11 μm

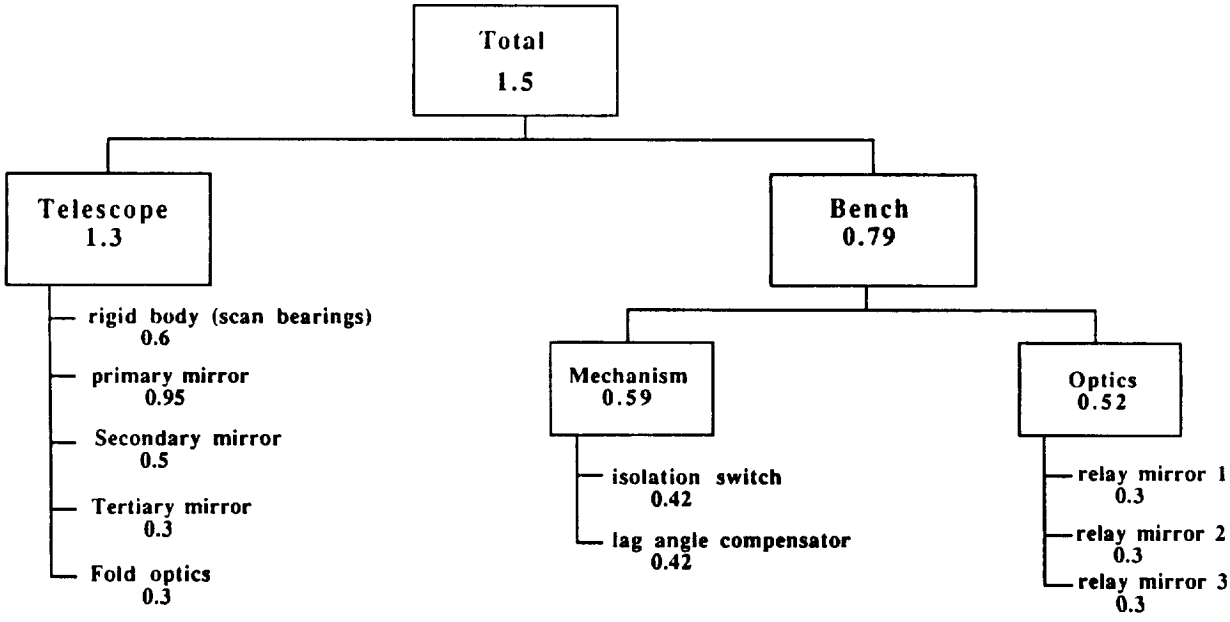

Figure 5-53. LAWS Optical System Line-of-Sight Error Bugdet μrad

weight. As in the telescope, the structural requirements for the gimbal are derived from the line-of-sight error budget.

Attached to the gimbal is the beam scanner assembly of Figure 5-54. This assembly must allow the beams to pass through unaffected while rotating the telescope and gimbal assemblies. Allowable bearing runout of 0.6 μrad was determined from the line-of-sight error budget. The 6.8 rpm requirement results in an assembly that weighs 15 kg and consumes 10 W of power.

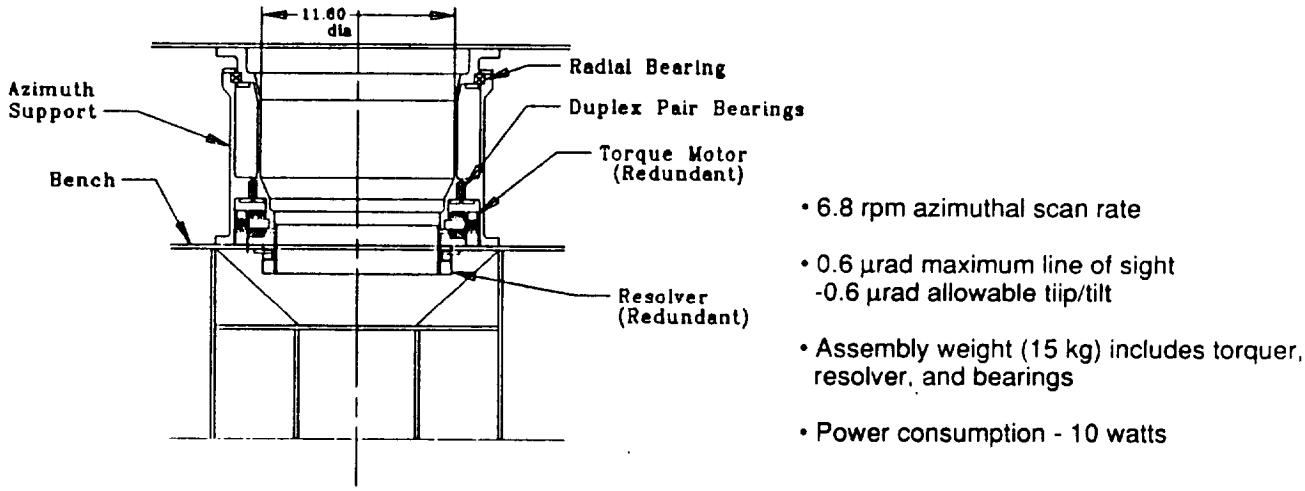

Figure 5-54. Beam Scanner Assembly

The final structure to be discussed is that which holds the relay optics; this optical bench assembly can be seen in Figure 5-50. This bench not only holds the relay optics but also the isolation switch and the interferometer assembly. The location of the optical bench relative to the telescope and gimbal is dependent on the design of the vehicle with which the LAWS system will interface. Lack of information with regard to the platform is not a drawback at this time since the laser beams entering and leaving the telescope are both collimated beams going through a Coudé path, resulting in some

flexibility as to where the bench can be located. Structurally the bench is a 0.9 m x 1.27 m x 15 cm Beryllium egg crate. The choice of Beryllium was driven by stiffness to weight ratio since all the elements must be held rigidly in place.

The optical bench assembly also holds the interferometer assembly . This assembly performs the function of combining the local oscillator with the return beam. This is performed using a simple amplitude beam splitter that reflects 96 percent of the return beam off the front surface toward the receiver and transmits 4 percent of the local oscillator beam toward the receiver.

In summary, the LAWS optical system is a three mirror eccentric afocal telescope which is supported by a graphite epoxy structure, itself supported and rotated by a Beryllium gimbal. The light that is directed to and from the telescope passes through a Coudé path inside the gimbal toward the Beryllium optical bench which supports the isolation switch, relay optics, and the interferometer assemblies. Lag angle compensation is performed by a rotating polygon at the telescope's exit pupil, and the residual lag angle is removed by a tip/tilt mirror located on the bench.

5.2.2.5 Mechanisms

The major mechanisms are the lag angle compensation, isolation switch, and alignment assembly. The function of the lag angle compensation is to undo the effect of the scanning of the telescope, and the function of the isolation switch is to couple the transmitter beam into the system and then allow the received (return) beam back through to the interferometer. Maintaining the alignment of the the return beam with the local oscillator is an important function of the system; therefore, a system that measures the angular position of the optical system in real time is necessary. The effects of each of these mechanisms on the line-of-sight error are kept within the line-of-sight error budget.

The isolation switch assembly of Figure 5-55 is composed of a 15 cm diameter disk which is rotated at a rate determined by the maximum pulse repetition frequency (PRF) of the laser ($\approx$ 2400 rpm). When the laser is fired, the disk is rotated into the 100° sector that reflects the laser pulse out through the telescope. This sector is sized to allow for variation of the PRF. By the time the backscattered laser pulse has returned, the wheel has rotated into a position where a slot in the disk allows the return beam to pass through and toward the interferometer assembly. The fact that there is a slot cut into the wheel requires that the wheel be dynamically balanced since tipping of the

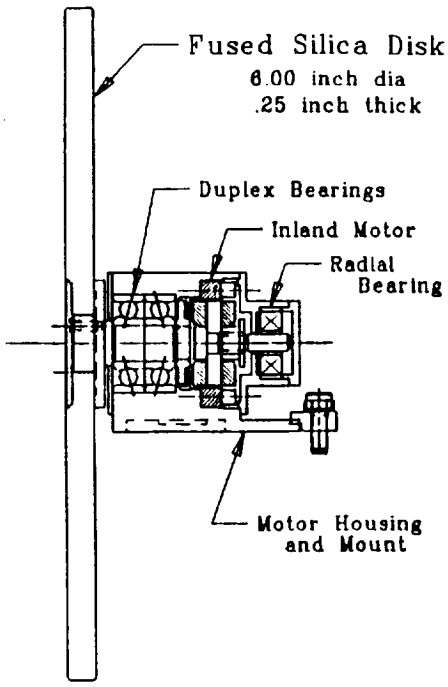

- Switch rotational speed ~2400 rpm
- Laser pulse diameter 1 cm
- Laser pulse duration 3×10^{-3} sec
- Receive beam time 8×10^{-3} sec
- Reflective sector 100^{0}
- Assembly weight ~2 kg
- Allowable TIR ~2 micrometers
- Power consumption 2 watts

Figure 5-55. Isolation Switch Assembly

wheel will cause misalignments of the return and local oscillator beams. The motor is designed such that there is positive control of wobble, due to bearing runout, using duplex bearings in combination with the radial bearings shown in Figure 5-55. These considerations result in an assembly that weighs 2 kg and consumes 2 W.

The most critical part of the LAWS optical system is the lag angle compensation assembly since this function has to be performed precisely. The baseline approach is to use a spinning multifaceted mirror that rotates a facet into place such that the pulse is sent out centered on the optical axis. By the time the backscattered pulse has returned, the faceted mirror has rotated the appropriate amount (to correct for the lag angle) redirecting the return beam back on the optical axis. Any second order and residual uncompensated lag angle, due to non-linear and cross-axis effects, will be corrected at the tip/tilt mirror located on the optical bench. This tip/tilt mirror is a standard flat mirror mounted to voice coil linear actuators through flexures. The magnitude of the expected residual lag angle that this mirror will have to correct is estimated to be on the order of 1 mrad at a bandwidth consistent with the rotation of the system.

The results of an analysis performed to determine the first order design parameters of a spinning multi-faceted mirror are plotted in Figure 5-56. Figure 5-56 is a plot of

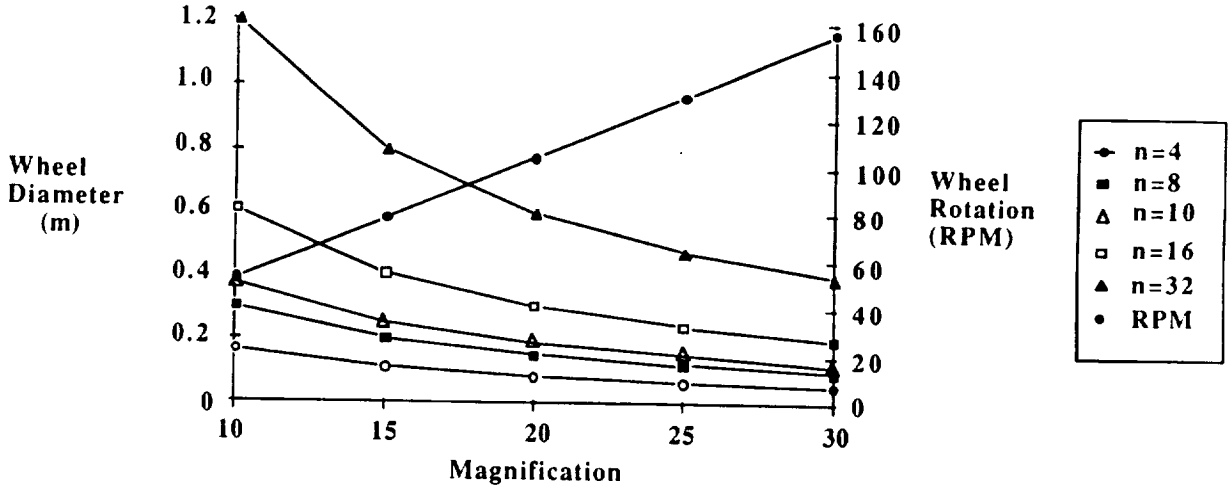

Figure 5-56. Lag Angle Compensation Design Trade

the resulting wheel diameter as a function of the telescope magnification and a plot of the required rotational rate versus the telescope magnification. From this it was determined that a telescope with a magnification of 12 x requires a 30 cm diameter wheel with 9 facets to be rotated at approximately 60 rpm.

Although the alignment assembly does not appear on the telescope subsystem structure, it is nevertheless an important aspect of the system design. This assembly, in conjunction with rotary encoders on the beam scanner assembly, provides a real time estimate of where the telescope is pointing. This is necessary due to the very tight alignment requirements between the return beam and the local oscillator beam (1.5 μrad), and the present understanding that the proposed platforms (Space Station and JPOP) roll on the order of 20 times our alignment requirement. In order to perform the lag angle compensation adequately with this level of error, some measure of the line-of-sight pointing has to be produced. Depending on the platform to provide the information is not good because of the complicated structural interactions between the LAWS system and the platform that may cause significant errors. The baseline approach is to have an inertial reference unit updated periodically by star sensors . Location of the inertial reference unit and the star trackers will be determined at a later

date when more information concerning the platform is known so that star viewing angles and the structural connections between the inertial reference unit and the optical system can be determined. The effect of dynamic disturbances other than rigid body rolling of the platform will be dealt with by designing the structures so that they are dynamically stiff enough to effectively damp these errors.

5.2.2.6 System Weight Summary

Using the baseline system as previously described, a summary of the weight of each of the elements is provided in Figure 5-57.

5.2.2.7 Possible Improvements

Improvements should be considered to reduce the number of mechanisms in the system. A potential subject for improvement is the isolation switch assembly. One improvement to consider for the isolation switch would be to change to a system where the field of view of the telescope is split in half rather than transmitting and receiving down the center of the optical axis. One half would be for the transmitter, and the other would be for the receiver. This would also have the effect of reducing our lag behind angle because we would be in effect pointing ahead. A possible drawback to this

ITEM	WEIGHT (kg)
1. Primary	50 (90%)
2. Secondary	2
3. Tertiary	2
4. Tip/Tilt	8
5. Bench Optics	23
6. Telescope Structure	53
7. Gimbal Structure (3 bearings)	26
8. Optical Bench (Beryllium)	18
9. Thermal Control/Shroud	9
10. Mounts/Hardware	9
11. Drive Motors/Tachometers/Controls	23
Total	223

Figure 5-57. System Weight

approach is that it could make the optical system more difficult to manufacture. The increased difficulty will not be known until a lens design study is performed.

5.2.2.8 Summary

The LAWS optical system meets all the performance requirements of Figure 5-41 and all the derived requirements described throughout this report. The system meets these requirements using low risk technologies which provide a high degree of confidence in the manufacturability of this system.

5.2.3 Receiver/Processor Subsystem

The Receiver/Processor Subsystem baseline design is summarized as follows:

- Quad HgCdTe photovoltaic detector array with 55 percent quantum efficiency at 300 MHz BW
- Signal aligned on central element of array with exterior elements for alignment monitoring
- Two-stage phased-electro optical modulator local oscillator to reduce detected bandwidth from 1.35 GHz to 0.3 GHz
- Local oscillator beam tailored for shot noise limited operation with phase front matched to signal beam
- Split Stirling Cycle cryogenic cooler to optimize detector operating temperature
- Bias supply and preamplifiers space-qualified versions of standard units
- 12 bit 50 MHz analog to digital converter for adequate frequency response and dynamic range
- Optional on-board FFT processor for real-time velocity data.

The LAWS Receiver/Processor Subsystem consists of a moderate bandwidth photo detector array, active cooling for the photo detector, bias circuitry, preamplifiers, and on-board signal processing electronics. For each of these components, several options were considered. These options will be outlined below along with the logic for selection of the baseline Receiver/Processor Subsystem components.

Figure 5-58 is the Receiver/Processor Subsystem block diagram. The local oscillator optical source (upper left hand corner of figure) from the master oscillator is fed into the modulator where it is up/down shifted before being focused on the photo detector. The Doppler signal is received from the telescope and optical train, superimposed on the local oscillator, and directed toward and focused on the photo detector array. Cooling is

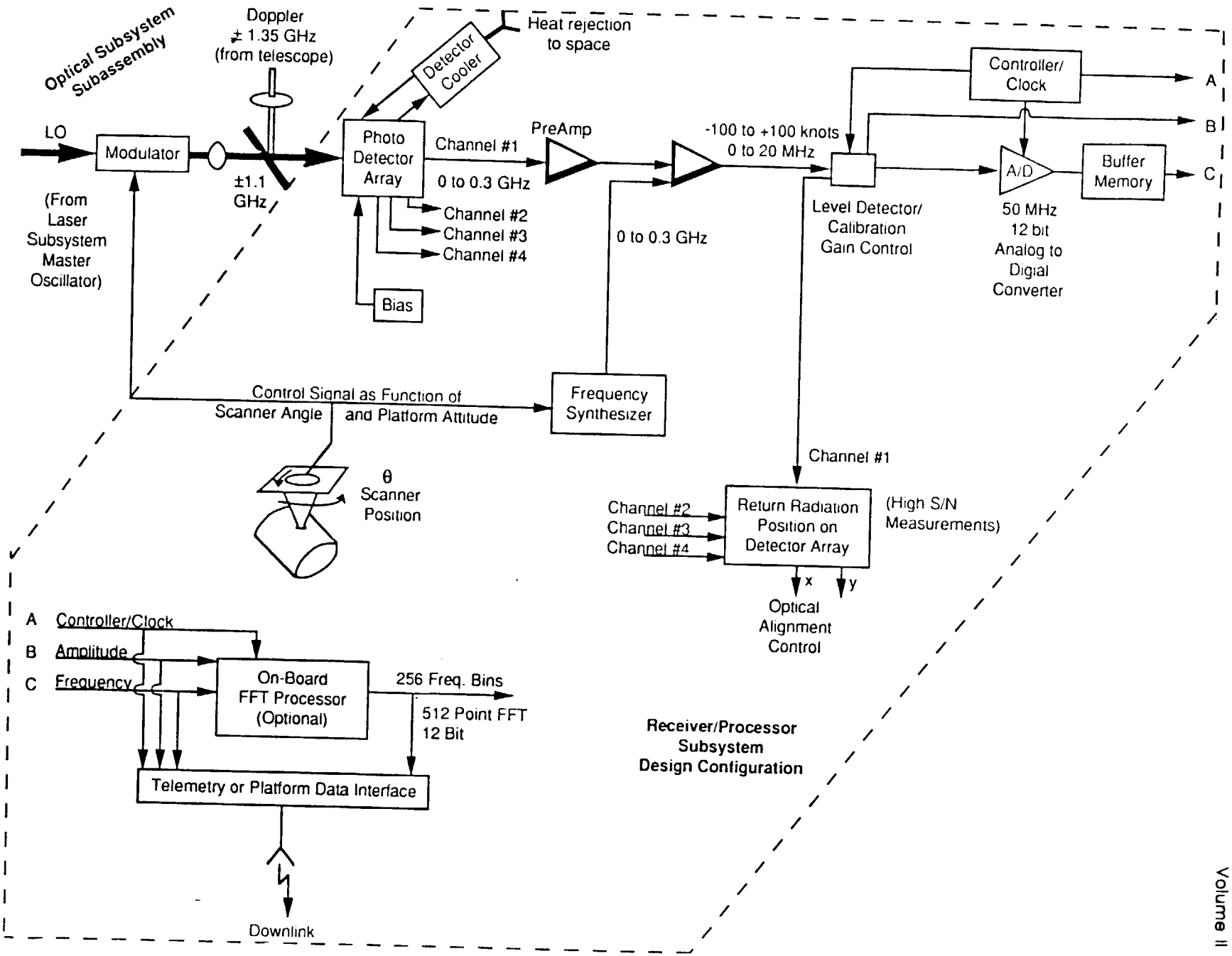

Figure 5-58. LAWS Receiver/Processor Block Diagram

provided for the detectors. Outputs from the detectors are amplified and frequency shifted to the frequency/amplitude range of the analog-to-digital (A/D) converter. The "zero" Doppler (relative to the ground) is set for the center of the 0 to 20 MHz baseband to minimize fold over. The levels of each channel from the detector array are measured to monitor the received optical signal spot location upon the small detector array for optimal alignment. The output of the A/D is buffered and telemetered to the platform data interface or (optionally) directly to earth. On-board FFT processing can also be provided to obtain real time velocity spectra.

5.2.3.1 Photo Detector

The LAWS photo detector is a critical element of the overall system. The detector detects the returned signal (Doppler shifted radiation) which is mixed with the local oscillator (LO) radiation at a controlled frequency to produce the Doppler shifted beat signal.

The line-of-sight Doppler signal of the tropospheric winds as measured from the orbiting satellite will vary from $+2/\lambda(V_s \pm 1V_w)\text{Sin}\ \alpha$ to $-2/\lambda(V_s \pm 1V_w)\text{Sin}\ \alpha$. As the LAWS telescope traverses through the conical scan, the satellite velocity either adds to or subtracts from the wind velocity component. For a cone half angle (α) of 45°, a laser wavelength (λ) of 9.11 x 10-6 m and a satellite velocity (V_s) of 7.5 km/sec, this satellite velocity bias varies from approximately 5.3 km/sec to -5.3 km/sec or $\pm$ 1.16 x 10^9 Hz. (The wind velocity adds only $\pm$10 MHz to this number for $\pm$100 kn winds.) Thus, if the detector sees a purely homodyned signal with no LO offset, it must be capable of efficiently detecting signals with a bandwidth of approximately $\pm$1.2 GHz (1.35 GHz for a 55° cone half angle).

Single element detectors have been built and tested with 50 percent to 70 percent quantum efficiency for bandwidths (BW) of less than 0.3 GHz, 35 to 45 percent for BW up to 1 GHz, and 15 to 25 percent for BWs up to 2 GHz. Quantum efficiencies for arrays are typically less than those for single element devices. But single elements within the array can have quantum efficiencies that approach the best achievable with individual detectors. Optical preamplifiers can lead to increasing these efficiencies as has been demonstrated with low pressure, low BW optical preamplifiers for low BW requirements. However, for the above GHz BWs, the optical preamplifier requires a high pressure low electrical efficiency design, and is thus not included in this baseline.

Quantum efficiency is stressed here because a 1dB improvement in receiver efficiency is equivalent to 26 percent increase in laser power or telescope aperture area. The

highest quantum efficiency can be achieved via heterodyning with a controllable local oscillator signal, i.e., an LO which can be programmed to provide a known frequency output as a function of conical scanner position to compensate for the gross Doppler shift due to the satellite velocity. The following two methods accomplish offset of the local oscillator frequency:

1. Shift the frequency of the LO laser with cavity length tuning
2. Externally modulate the frequency with either an acusto-optical or electro-optical (EO) modulator. (The EO modulator approach is the LAWS Baseline.)

The desired frequency shift of the LO is a controlled +1.1 GHz to -1.1 GHz for the 55 deg cone half angle (or $\pm$0.9 GHz for the 45 deg cone half angle). The resulting beat signal of the optical signal on the detector is below $\pm$0.3 GHz. This bandwidth reduction eases the detector design and allows us to maximize its performance and the receiver efficiency.

Shifting of an LO through intracavity length change has been performed to 0.5 GHz without major reduction of the laser output amplitude. However, $\pm$0.9 GHz (much less $\pm$1.1 GHz) is beyond the bandwidth (i.e., usable linewidth) of frequency stable lasers operating in the 9 to 12 μm region. This approach has been rejected for the baseline configuration. The selected baseline approach is the external modulator approach.

Acousto-optical modulators are used with tactical coherent ladars/lidars to obtain an offset LO. However, these offsets are typically 24 to 48 MHz, much less than the LAWS requirement. Electro-optical modulators have much wider bandwidth capabilities. These devices are currently being used by MIT/LL on the Firepond laser to modulate the 20 kW signal after it has been chopped into 30 μsec (i.e., 600 mJ) pulses. For the Firepond application, multiple phase matched EO modulators have been arranged in series to overcome the normally rapid amplitude dropoff (efficiency) of the individual device outputs as a function of frequency. Firepond results indicate that a two-stage device will provide a 1.77 GHz BW with a 50 percent throughput in the intensity of the sideband at either side of the center frequency. For the LAWS LO application, where little laser power is required for detector shot noise limited operation, the modulators are frequency shifters with no requirements on instantaneous bandwidth. These designs with low drive power can be used to provide the required frequency shift.

Thus the LAWS detector baseline configuration requires a moderate BW detector with a dual EO modulator shifted LO (controlled as a function of scanner position) to bring the Doppler shifted optical signal into the detector operating range. Fifty percent

quantum efficiency of the detector array is achievable with this configuration baseline. The modulator will also be used to maintain constant LO power on the detector.

A two dimensional (quad) detector array of elements is selected over a single element to simplify system alignment. Matched optics are used to optimize LO distribution upon the detector elements. Typical detector arrays have some losses due to physical (line width) separation between the elements; optimal performance is achieved when all of the signal is directed to a single element. The elements will be physically arranged to allow optical alignment of all received signal upon a single element. Ground returns will be used to aid in this alignment process.

5.2.3.2 Detector Cooling

Photo detectors operating in the 9 to 12 μm range have optimum performance when cooled to approximately 77 K. For long-term satellite operation, two types of cooling are potentially available to achieve operation at these temperatures: passive or active.

Passive cooling is practical on satellites for low energy heat loads where free-space look angles are available to the detector cold finger. The cold finger must be kept short in length to minimize heat leaks into the detector which would raise its temperature. This approach is typically used for spacecraft dedicated to a particular mission (such as LAWS) rather than for spacecraft dedicated to a group of instruments or missions (such as JPOP or SS). Thus the passive cooler will not be considered for LAWS Baseline, but will be considered as an option until the platform configuration is defined.

The active thermal cooler proposed for many of the other EOS Facility payloads is adequate and is selected for the LAWS Baseline. Lifetime of the cooler is a consideration and is being tested/enhanced for these other programs. Vibration is a consideration which is probably more important with the LAWS Instrument than for the other Facility instruments. However, LAWS team members have routinely used both mechanical coolers and Joule-Thompson coolers with coherent Doppler lidar systems with no measurable degrading effects. Care must be taken in designing the mechanical fixtures and providing vibration isolation where required. Information on the British Aerospace Split Stirling Cycle Cooler being considered by many EOS Facility Instruments is included in Figure 5-58. We propose this device in our baseline design.

5.2.3.3 Bias and Preamplifiers

Bias and preamplifiers for the LAWS receiver will be very similar to those used for conventional coherent lidar systems, but the LAWS device must be space-qualified.

The bias circuit will be well shielded. The preamplifiers, one for each detector element, must be low noise with adequate bandwidth and dynamic range to accommodate the detected lidar signal with β varying over 4 orders of magnitude. Design trades will be made with respect to cooling the preamplifiers located in the dewar with the detector chip, or mounted separately and operated at higher temperatures. For the baseline configuration the preamplifiers are mounted separately to reduce the detector cooling load.

5.2.3.4 Signal Processor

The signal processor receives the preamplified signal from the preamplifiers, provides gain to the signal appropriately for input into the analog-to-digital converter, and performs any required additional on-board signal processing. A signal amplitude detector (i.e., a sample and hold level detector) is required for each detector element for alignment purposes under conditions of strong returns. For the baseline configuration, a frequency synthesizer is used to mix the 0 to 300 MHz signal into a 0 to 20 MHz signal BW. The 0 to 20 MHz will allow measurement of line-of-sight wind velocities from -100 to +100 kn or over any selected 200 kn span (e.g., from -50 to +150 kn).

The level-detector/gain control device will be preprogrammed to prevent calibration returns through the square law heterodyne detector from saturating the analog-to-digital converter. We are specifying a 12 bit, 50 MHz A/D to allow over 7 decades (72 dB) of dynamic range of the received hetrodyne signal to accommodate a wide range of β and ground return values. The 50 MHz includes a Nyguist sampling factor of 2.5 for the A/D. This is within today's A/D state-of-the-art (e.g., we have on hand a 10 MHz/12 bit device). A/D state-of-the-art is expected to advance significantly within the LAWS development time frame. An optional 100 MHz 12 bit device should be available to accommodate ±200 kn winds. One 50 MHz device is required for each detector element. For our baseline design with one detector element for data and three elements for alignment, a single analog-to-digital converter is required.

Discussions of the science team have revealed a potential requirement for real time wind velocity (frequency spectra) data to be downlinked directly from the LAWS platform. To meet this requirement, an optional on-board FFT processor is baselined. To provide ±100 kn winds with 1m/sec resolution (- 0.2 MHz), a 512 point FFT processor is selected for 256 point frequency resolution. This will be a miniaturized version of the unit we have operating in the laboratory today.

5.2.4 Command, Communication, and Control Subsystem

The Command, Communication, and Control Subsystem baseline design is summarized as follows:

- Hardware implementation
  - Flight computer
  - Communication links
  - Transceiver
- Software modules
  - System management
  - Shot management
  - Communication management.

At this stage of the LAWS Instrument definition process, the emphasis for defining the command, communication, and control of the system is placed on requirements analysis and definition of the associated functions to be implemented and their interrelationships. The Command, Communication, and Control Subsystem encompasses all functions associated with system control, data processing, and communication control. The system operation concept described in Sections 5. and 5.1 shows how this subsystem provides the control and communication management. The functions allocated to this subsystem are those that control system operation and communicate data and commands (see Figure 5-1 for the location of these in the system functional hierarchy). In operation, the function of the Command, Communication, and Control Subsystem is to provide the control of the LAWS Instrument operation, and control communication between LAWS subsystems and between the LAWS Instrument and the host platform. The logic required to implement these functions will be incorporated in the flight computer identified in Figure 5-3. Before proceeding to the flight software, definition requirements allocated to this subsystem must be examined.

5.2.4.1 Requirements Analysis

The following system requirements govern this subsystem design:

1. Provide continuous on-board operation
2. Provide a control system
3. Provide adjustable telescope elevation angle

4. Employ shot managemet to conserve laser life and obtain dual measurements of the wind vector components
5. Monitor and report instrument health and status
6. Report measured wind data in Level 0 format
7. Append platform ephemeris data, ground calibration data and time to level 0 to create Level 1A data
8. Perform calibration and alignment checks
9. Accept commands from ground control
10. Provide safing control.

Requirement (1) dictates that the LAWS operation be in real-time. Requirement (2) is an all encompassing requirement that says a separate and distinct control be provided. Requirements (3) and (4) are based on analysis conducted in Phase I. Requirements (5) through (9) are derived from analysis of the "LAWS Data System Preliminary Requirements Review," dated 6 December 1989. The creation of level 1A data is included as an option. The requirement for safing is applicable for Space Station operation.

5.2.4.2 Flight Software Definition

Figure 5-59 identifies the functions to satisfy the operations described in Section 5.1 and the system requirements identified above. These functions have been classified as related to system management, shot management, and communication management. All system management functions are associated with control and implementation of the system operations. Shot management controls the laser pulse operation. Attitude/position determination is a function that supports shot management. It provides instrument attitude and position data required to correctly fire the laser for a given beam location during a telescope scan. The timing of each laser pulse will be derived from logic based determination of attitude, time position in space, and position in the scan. Communication management is concerned with communication between the LAWS instrument and its host platform and between the LAWS hardware components. All communications (i.e., commands received from the ground or data transmitted) to and from the ground station are assumed to be handled by the host platform. Therefore, the LAWS design assumes a communication interface between the instrument and the host platform.

5.2.4.2.1 Control of/and Data Flow from Subsystems. Both hardware and software are required to implement the functions identified in Figure 5-59. Figures 5-2 and 5-3

look at the LAWS Instrument from a top level systems viewpoint and show the first level of allocations to the hardware components. Figure 5-4 also indicates the overall flow of signals through the instrument. Figure 5-6 takes this process one step lower and shows a more detailed flow of data, information, and signals through the system. The form of this chart is an N2 diagram. The diagram shows the hardware components in solid boxes along the diagonal. Boldface enclosures denote a subsystem. Information at the vertical and horizontal intersections denote data, signals, etc. The output of one block is the input of another, and the output/inputs are shown at the intersections from each block. All inputs are shown in the horizontal direction, and all outputs are shown in the vertical direction.

The configuration baseline has nine separate data/information flow paths through the system that are associated with functional implementation. These are denoted by the

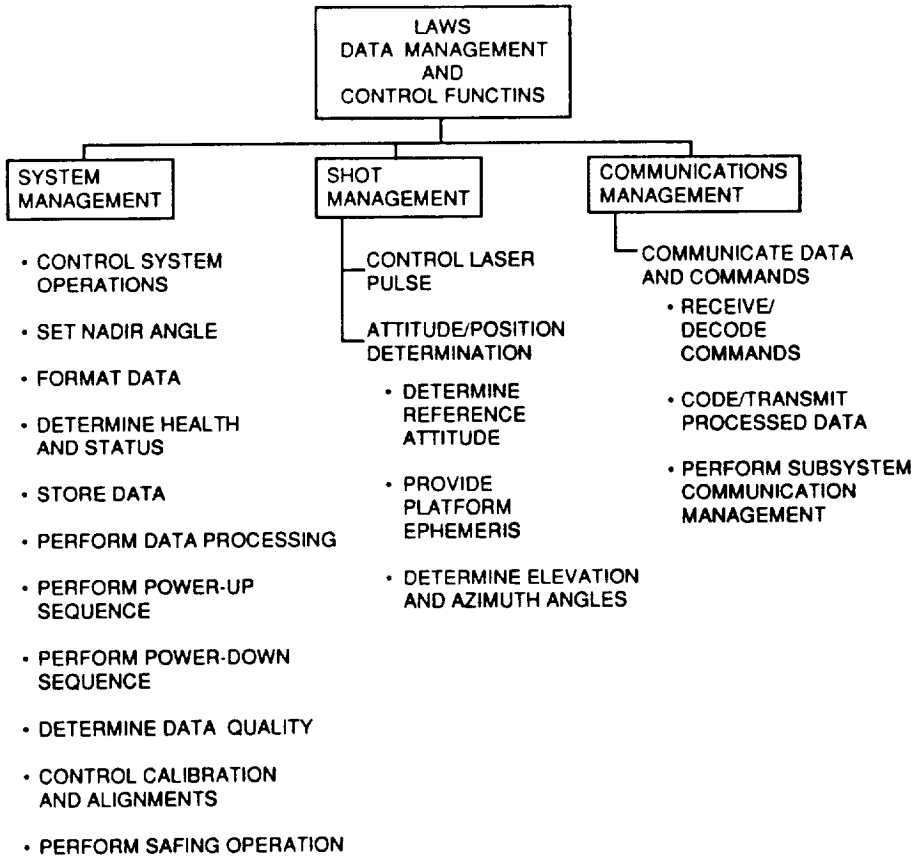

Figure 5-59. LAWS Flight Data Management Functional Hierarchy

numbers in parenthesis on Figure 5-60. Each path is briefly described below and can be traced within the system by following the input/output flow of Figure 5-60.

Path 1, Power Application. This path is associated with the power-up and power-down sequences and includes the operations for stowing and deploying the instrument. The power-up command is issued via the host platform. The flight computer then controls the hardware component power-up sequence via a junction box located in the Electrical Power Subsystem (EPS). A ready status will be issued to the ground when the power-up sequence has been completed. Power-down will be accomplished in a similar fashion. The command to power down is issued from the ground except in emergency situations when it is automatically issued from the platform. Logic incorporated in the flight computer will then control the power down sequence i.e., the sequence of component deactivation.

Deployment is a special case of the power-up sequence. During instrument deployment or instrument dormant periods, power will be applied to selected hardware components until system power is applied to initiate instrument operation. Stowing covers the special case for retrieval from the Space Station. The power-down sequence will include retracting the telescope and locking in the stowed position. Provisions will be made for power to be applied to specified hardware components during instrument dormant periods.

Path 2, Laser Beam Output. This is the optical path from the transmitter through the beam scanner assembly to direct the laser beam to a specified location.

Path 3, Beam Reference Signal. This is the optical path to direct the reference signal from the laser subsystem master oscillator through the interferometer located in the optical subsystem to the receiver/processor subsystem.

Path 4, Beam Reflection. This is the primary path for the return signal from the atmosphere or ground through the instrument. The reflected signal is collected by the telescope and directed through the interferometer to the receiver where the doppler frequency shift is detected. The doppler signal is then amplified and digitized by the signal processor. The digitized data is then formatted as Level 0 data for transmission to the ground. Provisions are also made for appending time tags, platform ephemeris, and reference attitude data to create Level 1A data. Level 1A data is included as an option at this stage of the system development. Likewise spectrally processed data is also provided as an option for direct broadcast from the platform.

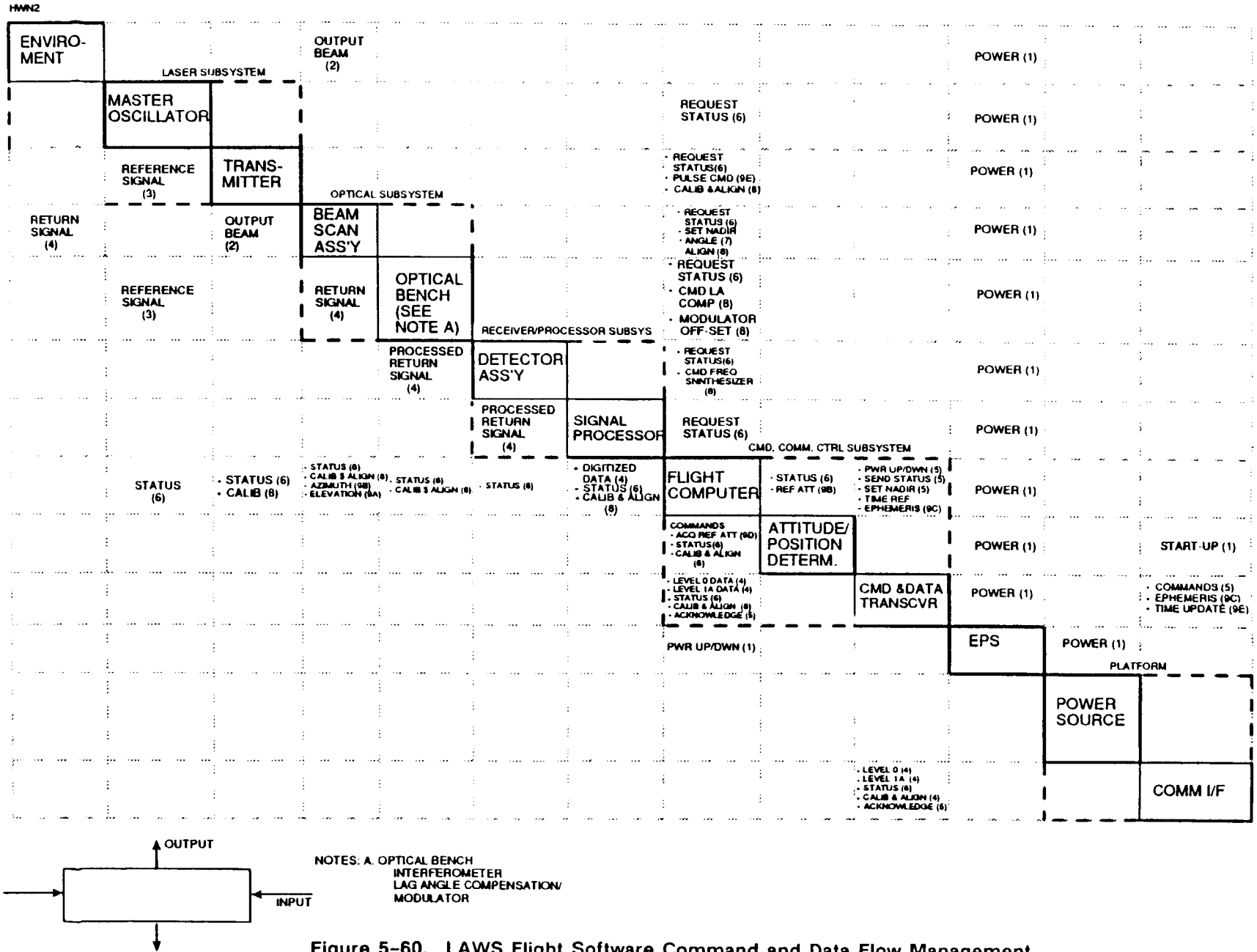

Figure 5-60. LAWS Flight Software Command and Data Flow Management

Path 5, Ground Generated Commands. Provisions are made to receive, process, and implement commands received from the ground. These commands are request for instrument status, select one of three nadir angle, power-up or power-down, and perform calibration and alignment procedures. The receipt of a command will be acknowledged. The completion of command implementation will be acknowledged. These acknowledgements may be either in near real time or delayed for many minutes (or several hours) depending upon communication channel availability.

Path 6, Status Determination. Provisions are made to determine the health and status of the system via self tests of the respective hardware components. This is controlled via logic incorporated in the flight computer software. The process will be accomplished on a scheduled basis or on command from the ground. Status commands will be issued from the flight computer to the components with self-test sensors. The status of each component will be returned to the flight computer for processing and formatting for transmission to the ground via the host platform.

Path 7, Select Nadir Angle. Provisions are made to select one of three nadir angle settings. A default nadir angle of 45 deg will be incorporated in the flight instrument. This will be the nadir angle when the telescope is locked in place from the stowed position. The command to change the nadir angle setting will originate from the ground. Control logic incorporated in the flight computer will manage the change to the new angle. Once the new nadir is set, calibration and alignment procedures will be performed.

Path 8, Calibration and Alignment. Operations on this path are concerned with any procedures to calibrate or align any hardware component. The baseline design makes provisions for said procedures in the transmitter laser assembly, the beam scanner assembly, the interferometer, the receiver/signal processor, and the attitude/position determination assembly. All calibration and alignment data will automatically be appended to digitized data stream being transmitted to the ground as Level 0 data.

Path 9, Shot Management. Operations along this path are concerned with acquisition and processing of data required for the shot management logic and the implementation of shot management commands. Each shot requires input of the telescope line of sight azimuth (scan) angle values, previous shot position, reference attitude with respect to the telescope off-nadir angle, platform attitude, system time, and the platform ephemeris. Telescope gimbal data (azimuth and elevation) is obtained from the beam scanner assembly; the reference attitude is obtained from the attitude determination

system (likely a star tracker); the ephemeris data is obtained from the host platform, and the time is obtained from a system clock. The ephemeris data is obtained on a periodic basis. Provisions are made to update the attitude determination system reference. This process is labeled acquire reference attitude (ACQ REF ATT) on Figure 5-60. The system time is maintained in the flight computer and updated periodically from the host platform to maintain accuracy.

5.2.4.2.2 Flight Computer Functions

The flight computer will implement all functions associated with system management, shot management, and communication management. The actual functional implementation is via the flight software identified in Figure 5-61. It is assumed the flight software will be a single configuration end item. Operation of the software elements and the information flow between each is shown in Figure 5-62. As shown in Figure 5-61, the flight software configuration end item will consist of three subelements: the system management module, shot management module, and communication management module. Each is identified by bold lines in Figure 5-62. A brief description of the major modules and submodules follows.

System Management Module. The system management module provides the overall control for operation of the LAWS instrument. This module is activated at system start-up and operates continuously until the instrument is powered down. The clock provides the system time. Provisions are included to update the time from either the host platform or the ground. The time accuracy is currently TBD. Data storage is provided to store system control parameters, platform ephemeris, and temporary data storage for ancillary data and processed data.

System Executive. This module is the system real-time monitor and schedules the activation of other modules to execute the appropriate function. The system executive module will accept ground commands for instrument status determinination. A status message will be generated for transmission to the ground receiving station.

Power Management. This module has two functions: (1) initiate and manage the instrument power-up sequence, and (2) initiate and manage the instrument power-down sequence.

The module will execute via a preprogramed sequence for each mode (i.e., power up or power down). When power-up is complete, a ready status flag will be generated to indicate that the instrument is ready for operation. During the instrument deployment

component. Figure 5-62 defines several of the hardware components for which status will be maintained.

Data Formatting Management. This function generates two data strings: Level 0 data, and Level 1A data. All data strings will be encoded with the proper "hand shaking" for transmission. Level 0 data includes all instrument data, which is the digitized data stream, instrument performance data, and status information. The status information to the Level 0 data is a status indicator. The status indicator will denote the nature of the malfunction. Instrument health and status will be send to the ground both routinely and upon command.

Calibration and Alignment Management. This module initiates and controls calibration and alignment checks performed by various hardware elements. Several of these elements are identified on Figure 5-60.

Nadir Angle Management. This module initiates and manages the setting of a specific off-nadir angle. When the operation is complete, which includes calibration and realignment of the optical train, a ready status will be generated.

Attitude/Position Determination. This module provides the current attitude and position. The reference attitude is obtained from the attitude & position determination system (see Figure 5-60). The platform ephemeris is obtained from the host platform and stored for use. The telescope elevation and azimuth angle is obtained from the beam scanner assembly.

Laser Pulse Manager. This module contains the logic to compute the timing sequence necessary to correctly generate a laser pulse at the appropriate times.

5.2.4.3 Other LAWS Software

Figure 5-61 identifies three catagories of software required for the LAWS instrument: flight support software, flight software, and support software. Flight software has been discussed above. System support software is both GSE and airborne servicing software. GSE software is any software that will be developed for the ground support equipment. Airborne servicing software is any software required for orbital servicing operations. Support software is any software required to support development of the flight, GSE, or airborne servicing software or support mission operations. Development support software is primarily the set of case tools used in design of the flight software. Operations support are data bases and software used in instrument performance evaluation. System simulation is any software used in simulating the instrument or orbital

servicing operations. Mission support software is any software developed by the prime contractor to support mission operations. Test support software is all software used to checkout and verify the flight, GSE, and airborne servicing software.

5.2.4.4 LAWS Computer Hardware

The computer subsystem will be sized from a detailed analysis of the required computational, interface, and storage functions. Interface functions have been delineated above. The computational functional requirement is quite sensitive to the degree of shot management required. The above scenario describes the shot management function for a fire-on-position/attitude command requirement to provide a near intersection of the lines-of-sight of dual laser shots. A simpler shot management such as a strictly latitude dependent shot management would decrease the computational load. The computer memory requirement is dependent upon the above stated requirements to acquire and store data from such sources as the ephemeris and also to reformat from Level 0 to 1A. (This function could optionally be performed on the ground.) If the option is selected by the LAWS team to broadcast frequency spectra data direct from the platform, the storage requirement could potentially increase by orders of magnitude. If the LAWS Instrument instead of the platform is required to provide data storage for down link to NOAA facilities (as was discussed at the Configuration Review), the data storage requirement increases from fractions of a second to tens of minutes. These items affecting LAWS instrument computer hardware requirements (options) must be resolved before the final configuration can be fully designed.

5.2.5 Electrical Power Subsystem

The Electrical Power Subsystem baseline design is summarized as follows:

- Interfaces with platform prime power and provides circuit protection/filtering to/from prime power source
- Provides power at appropriate level to all subsystems via distribution box, circuit breakers, and shielded cables
- Provides emergency stand-by power
- Controls electromagnetic interference to/from platform via shielding and ground system

The baseline Electrical Power Subsystem consists of the connectors to platform power, the power distribution box, the circuit protection assembly, the power conditioning assembly, and the power distribution cables (see Figure 5-63). The Electrical Power

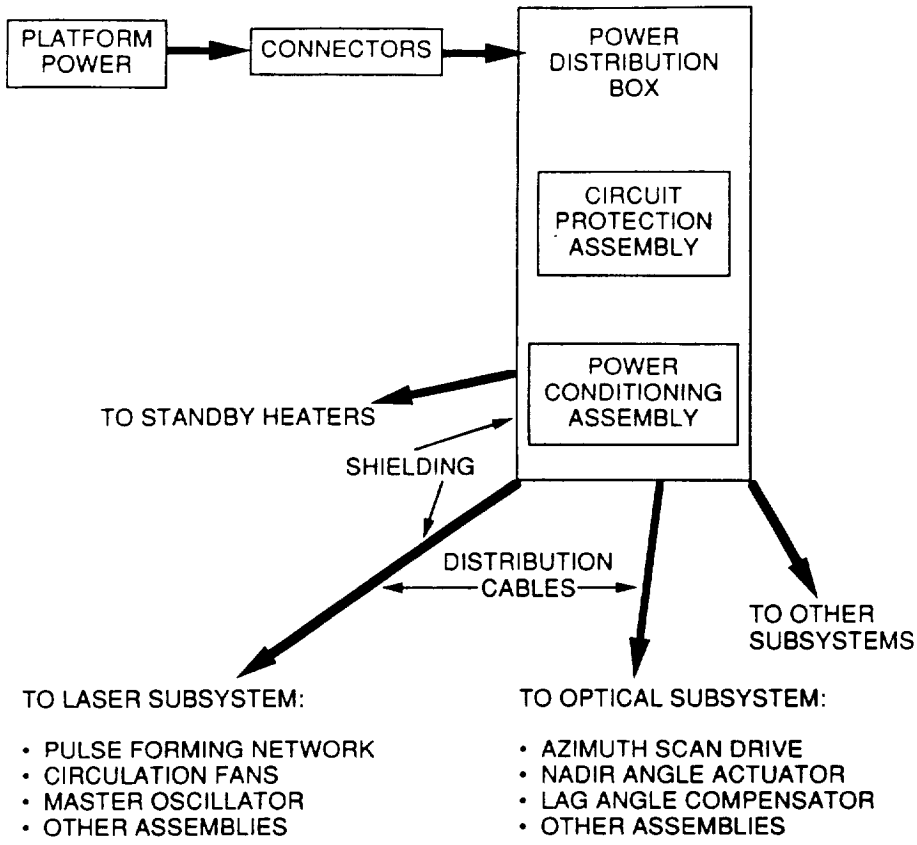

Figure 5-63. Baseline Electrical Power Subsystem Configuration

Subsystem receives power from the platform solar cells/batteries and conditions/distributes the power to other LAWS subsystems with provisions for circuit protection and stand-by emergency power. Circuit protection is designed to prevent catastrophic failure from accidental shorts during assembly and deployment. Circuit protection will protect the LAWS Instrument from power surges potentially introduced by faults from other platform payloads and will likewise limit LAWS Instrument effects upon the platform prime power. Emergency power is in the form of stand-by power and heating when subsystem components are in a nonoperating mode and prevents of freezing of fluids and joints.

The power distribution box will contain the circuit protection assembly as well as the power conditioning assembly. The power conditioning assembly will accept platform prime power, filter to prevent power surges (both in platform prime power to LAWS and in feedback to the platform), and provide the voltage amplitudes required by the various

subsystems. Cables from this box will be routed to the various subsystems with appropriate connectors. Shielding will be used to maintain acceptable levels of electromagnetic interference (EMI) both from the platform upon LAWS and from LAWS upon the other platform instrumentation.

If the LAWS host platform is in near-equatorial orbit (for SS) or in a near-noon crossing orbit (projected for JPOP), the available output from platform solar cells is as depicted in Figure 5-64. During approximately 50 percent of the (- 100 min) orbit, the solar cells are in earth shadow and are not providing output. If the panels are articulated for maximum sun angle, the output function will be trapezoidal, as depicted in the figure; if they are fixed, the output will be more sinusoidal. The platform batteries will charge during solar cell sun exposure and discharge while in earth shadow. (Another possible polar orbit, although not projected for the LAWS POP, is the twilight orbit where solar cells are typically in sunlight for the entire orbit.)

Concern has been expressed about shot management, i.e., intermittent operation of the laser, requiring additional storage batteries. If the shot management is operated to maintain an energy balance over each orbit as we propose in our baseline configuration, then no additional storage batteries are required. The batteries will be charged while the solar cells have sun exposure and will discharge while in the shade. Shot management will only distribute the discharge function over the total orbit.

The original LAWS SOW indicates 3 kW of average power is available for LAWS. For the Concept Review, Lockheed presented a system allowing a maximum power of 4.2 kW for higher laser pulse repetition rate (and thus higher average power) during a specified period. The 4.2 kW peak power requirement will be offset with a much less than 3 kW power requirement (e.g., 0.6 kW) to provide a net average power over the orbit of 3 kw. If the platform power availability is less than 3 kW (2 kW has been discussed for JPOP), the global shot density must be decreased accordingly, or the energy per pulse must be decreased. This in turn degrades overall LAWS performance, but not to the point of greatly reducing mission viability.

5.2.6 Mechanical Support Subsystem

The Mechanical Support Subsystem baseline is summarized as follows:

- A base platform constructed of structural edge beams with rib stiffened panels and major structural cross members serves as the mechanical interface to the space platforms and the launch vechicles

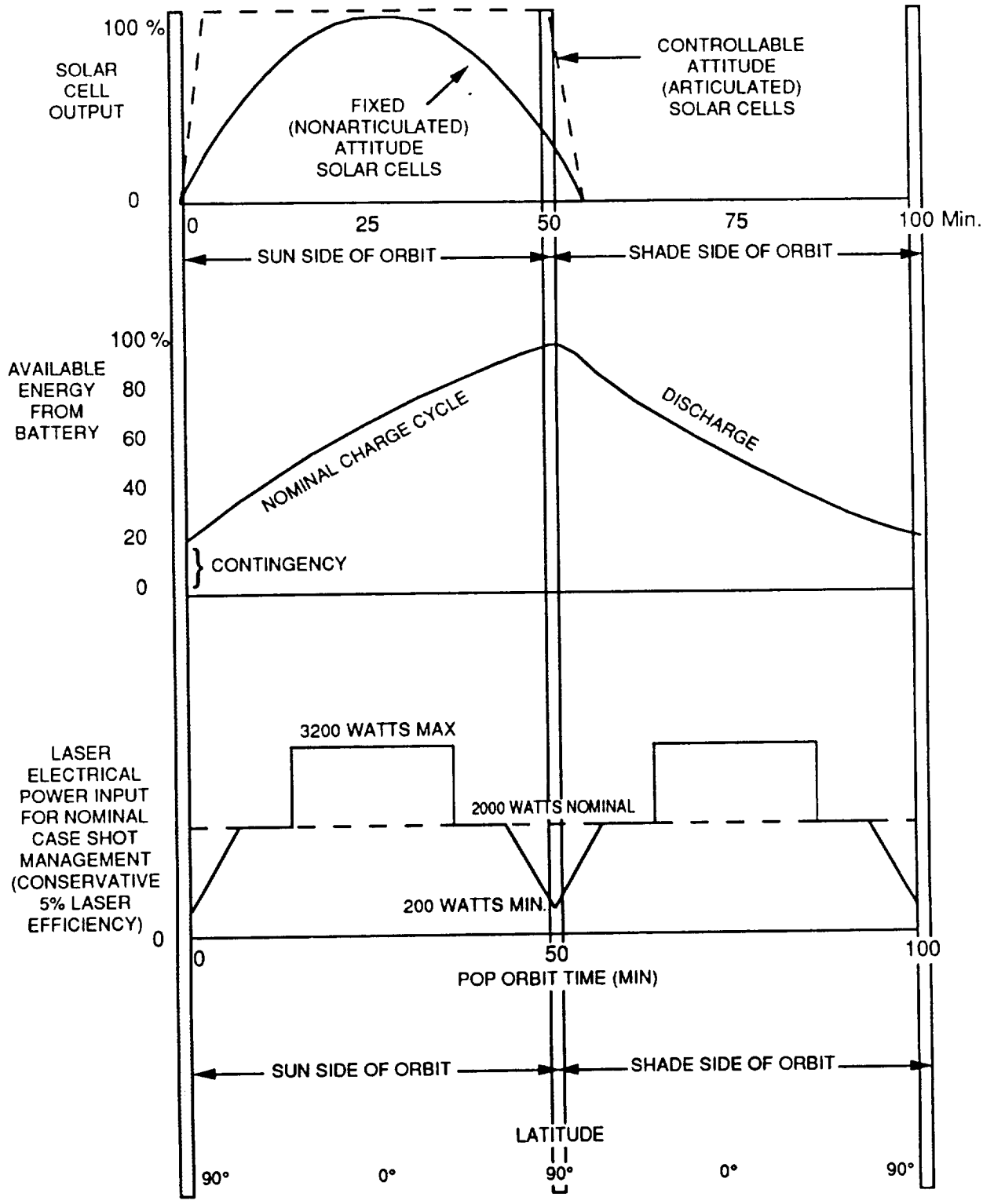

Figure 5-64. Electrical Parameters as Function of Position in POP Orbit for Typical 100 Minute Orbit

- A grapple fixture for RMS or telecoperator handling
- A thermal control system with cold plate interface to space platform thermal system or with a space radiator if the JPOP has no cooling loop available
- A $C_{18}H_{38}$ phase change wax thermal reservoir to support varying thermal loads due to shot management.

The Mechanical Support Subsystem consists of the base platform to which the LAWS subsystems are attached, the grapple fixture for in space positioning, attachments for both launch vehicle and/or space platform accommodation, and the thermal control system. Baseline design of the platform is an aluminum skinned structure with aluminum ribs and beams covered with a multilayer thermal protection system. Detail thermal, optical, and structural analyses will be performed during Phase II to ensure that (1) optical misalignment due to structural distortion from thermal and mechanical loads are within system tolerances, and (2) overall LAWS weight stays within system requirements.

Initial sizing indicates the aluminum base structure is within the total LAWS weight budget. Composite structures will be investigated in Phase II for weight savings and minimization of structural distortion.

The grapple fixture for LAWS baseline is located on the aft corner for ease of manipulation of the LAWS package from the delivery vehicle to SSF for installation at the station interface assembly (SAI). Attachment to the SAI attachment point is via the payload interface adapter (PIA). Provision will be made in the LAWS interface to the PIA, in order to compensate for the negative pitch angle of the operational SSF which is dependent upon final station design. For the JPOP operations, the LAWS Instrument will be integrated to the JPOP on the ground prior to launch. Mechanical and interface attachment will be through this base platform.

Thermal control of major portions of the LAWS Instrument will be through the thermal control unit of the Mechanical Support Subsystem; radiation cooling of individual components along with multilayer insulation of the instrument platform will also contribute to LAWS thermal control) For the SSF, the LAWS Mechanical Support Subsystem will interface directly to SSF cold plates to provide a heat sink for LAWS. For the JPOP, we have assumed no cold plate is available and have designed a deployable radiator into the LAWS Instrument. The radiator has been sized at 9.6 m^2 total exposure area (4.8 m^2 per side) with controlled edge orientation toward both the sun and earth for maximum radiator efficiency. The radiator will be positioned away from the JPOP to minimize radiation effects from the spacecraft.

In addition to the radiator or cold plate, the baseline mechanical support subsystem will contain a thermal reservoir with provisions to circulate a liquid coolant through critical components of the LAWS Instrument such as the laser. Figure 5-65 depicts this baseline thermal control assembly. A major element of the thermal control assembly is the reservoir/heat exchanger. The thermal reservoir/heat exchanger allows for non-uniform thermal loads (such as those created by laser shot management). It allows these non uniform thermal loads to be averaged over a period of time (see Figure 5-66). For the LAWS baseline we have selected one-half orbit (- 50 min) as the time period over which these thermal loads will be averaged. For a worst case with the laser being operated at 2 x average power for 1/4 orbit, 16 kg of $C_{18}H_{38}$ phase change wax will be required (or optionally 75 kg of liquid alcohol). For the wax reservoir case, the wax will melt during the laser-operating cycle and refreeze during the laser-off cycle with less than 1 °C change in temperature throughout the wax. (For the alcohol case, the alcohol would rise 20 °C during the laser operating cycle and recool to nominal during the laser off cycle). Figure 5-65 shows heat pipes transferring heat from the reservoir to the radiator because of their inherent reliability. For the SSF, direct interface of the reservoir to the SSF cold plate will likely delete the heat pipe requirement. Heat pipes will also be considered as an option during Phase II for the liquid heat transfer loop to and from the laser heat exchanger. Also, as part of the thermal control system, heat strips will be attached to critical elements to provide emergency or stand-by heating and to prevent system freezing.

In summary our baseline mechanical support subsystem provides a platform for mounting the LAWS subsystems, interfacing it to either SSF or JPOP, and controlling LAWS operating temperature within acceptable bounds. The mechanical base plate also provides mechanical interfaces with the flight support structure for launch/flight/return on the STS.

To meet the tele-operator accommodation requirement for the JPOP vehicle, the grapple fixture could be replaced with a drogue mating fixture. This would provide for a mechanical interface with an OMV or satellite servicer for LAWS component changeout. Robotic manipulators would be used to perform the actual component replacement.

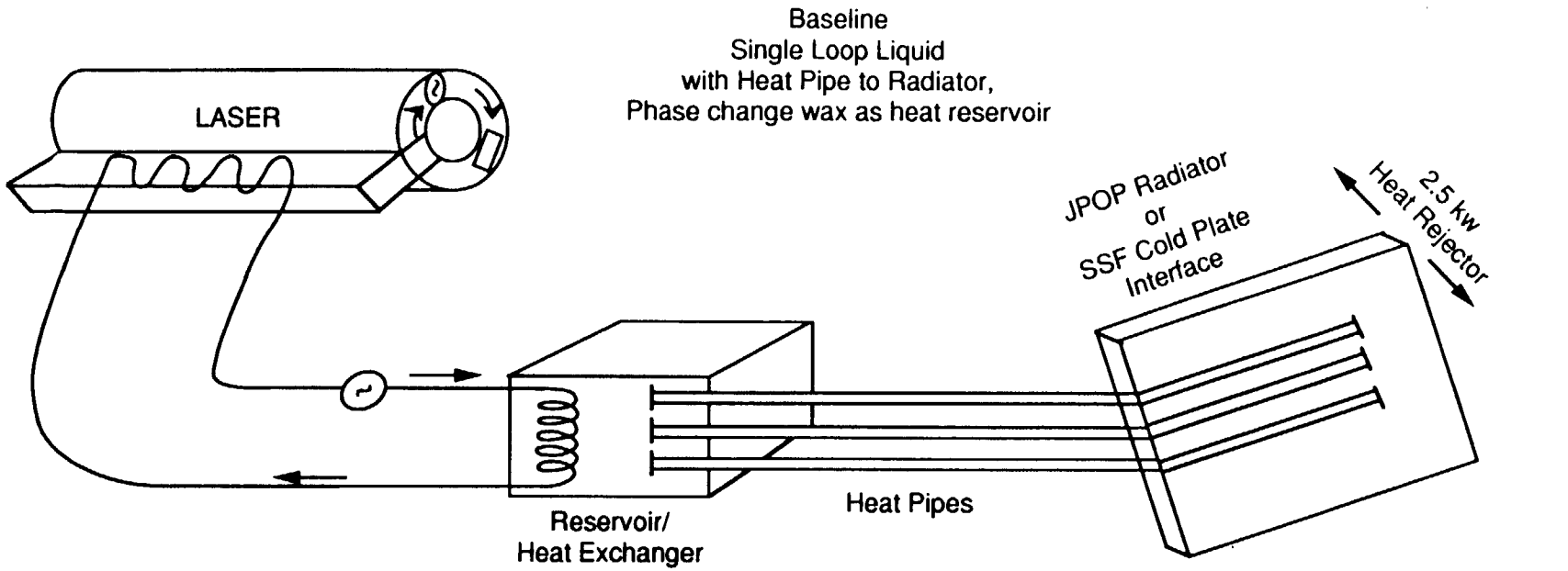

Max Thermal Storage (worst case)
Assumes laser operates at 2 x nominal rate for 1/4 orbit and is off for next 1/4 orbit, and radiator operates at an approximately constant (2.5 kw rejection) rate.

2.5 kw x 1 x 1/4 orbit =
2.5 kw x 1 x 25 min = 63 kwmin
= 1 kwhr
= 75 kg 20°CΔT/Alcohol or
16 kg 1°CΔT Phase Change Wax* ($C_{18}H_{38}$ for example)

*Baseline Selection

Figure 5-65. Thermal Control Assembly

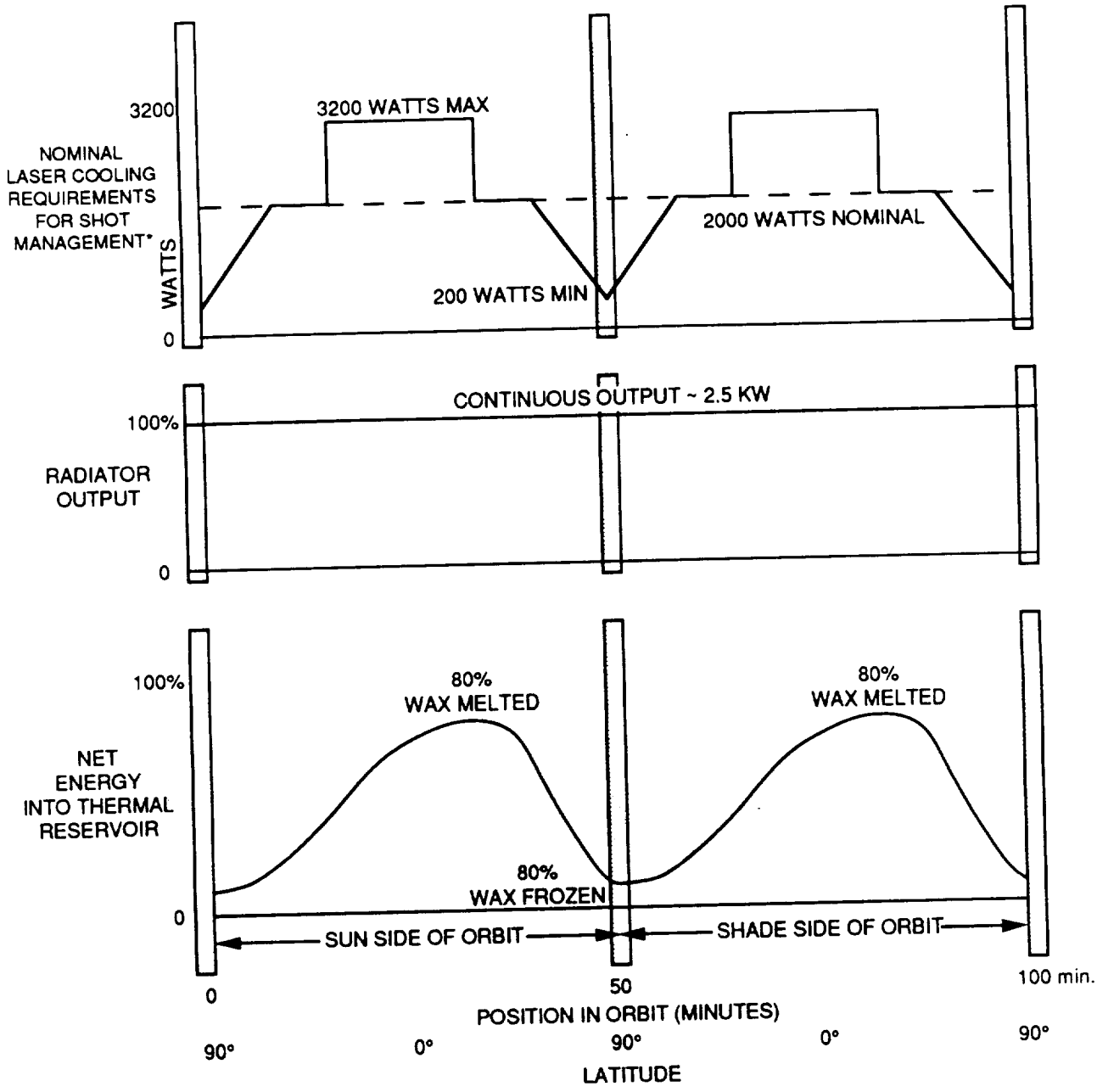

Figure 5-66. Thermal Parameters as Function of Position in POP Orbit for Typical 100 Minute Orbit

5.3 LAWS BASELINE CONFIGURATION

Lockheed's baseline LAWS Instrument design is shown in Figure 5-67. This baseline configuration accommodates either the Avco or GEC laser subsystem with minimum impact on the basic configuration. All subsystems, excluding the telescope, are packaged within an approximately 2 m x 2 m area. This facilitates installation, minimum cable/plumbing lengths for subsystem interfaces, and EVA servicing. The tapered, contoured telescope yoke provides a minimum rotational clearance envelope, leading to maximum utilization of the platform area. The forward platform area is beveled for weight reduction. A grapple fixture is included to assist on-orbit servicing and positioning which uses the RMS, or tele-operator systems. All RMS clearance envelope requirements for accessing the grapple fixture are accounted for in the design layout. The baseline configuration is contained in a maximum volume of 3.9 m x 2 m x 2.3 m.

The baseline design's mass, c.g., and power characteristics are presented in Table 5-27. All system parameters are well below those specified.

Mounted on a base strut, the LAWS telescope is driven by an electric motor at a nominal 6 rpm. The telescope pivots around the yoke attach points to provide the proper off-nadir viewing angle through a full 360 deg sweep, as shown in Figure 5-68. The telescope can be positioned, at one of three predetermined off-nadir angles, to provide the desired conical sweep area for data collection. For launch load environments, the telescope is constrained with its longitudinal axis parallel to the base structure by the yoke in a locked position, and by a forward attach point to the base platform. Once on-orbit, in the operational/checkout mode, the telescope rotates around the yoke pivot points to the desired off-nadir angle, and then it can sweep through the full 360 deg field of view. A pivot drive motor is located in the yoke at the pivot point to rotate and position the telescope. An off-nadir angle range of 0 to 60 deg can be accommodated and still maintain proper telescope clearance of the other subsystems.

Due to lack of configuration and interface system data for the JPOP, a self-contained thermal control system with panel radiator was developed for LAWS, as shown in Figure 5-69. If radiators are provided by the JPOP, as they are for the Space Station installation, the LAWS radiators can be deleted. This will provide a 68 kg weight saving. This radiator has a planform area of 4.8 m^2 and is positioned, when deployed, with edges perpendicular to earth and sun and both sides viewing deep space. Total exposed radiation area is 9.6 m^2, sufficient to maintain all LAWS subsystems

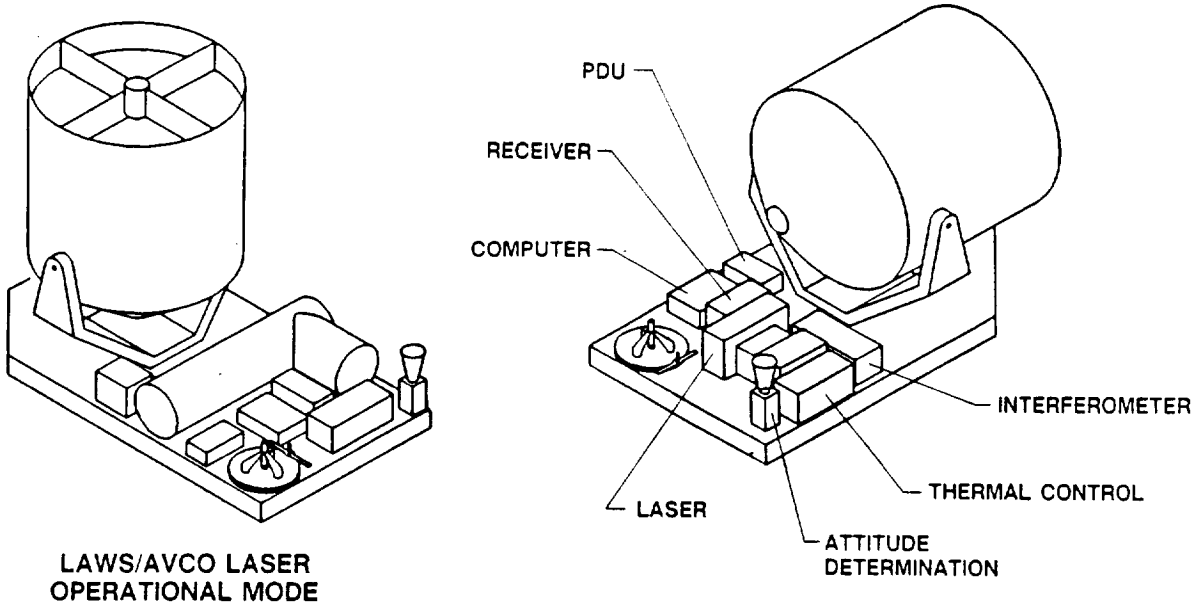

LAWS/AVCO LASER
OPERATIONAL MODE

LAWS/GEC LASER
LAUNCH CONFIGURATION

Figure 5-67. LAWS Baseline Configurations

Table 5-27. LAWS Baseline Parameters

Configuration	Weight (kg)	Envelope Dimensions (m)	Power (watts)	Data Communication Rate	Thermal Control Requirement (watts)
Budget	800	Accommodate H-II/Titan ELVs and Space Shuttle (STS)	3000 Avg. (4200 Peak with Shot Management	Compatible with TDRSS	Space Bus Compatibility or Integral System
LAWS/AVCO Laser	763	3.9 x 2 x 2.31	3323 (Peak)	Temporary Data Storage for Transfer to Platform/TDRSS	2922
LAWS/GEC Laser	743	3.5 x 2 x 2.31	3227 (Peak)	Temporary Data Storage for Transfer to Platform/TDRSS	2088

LAWS 3-1

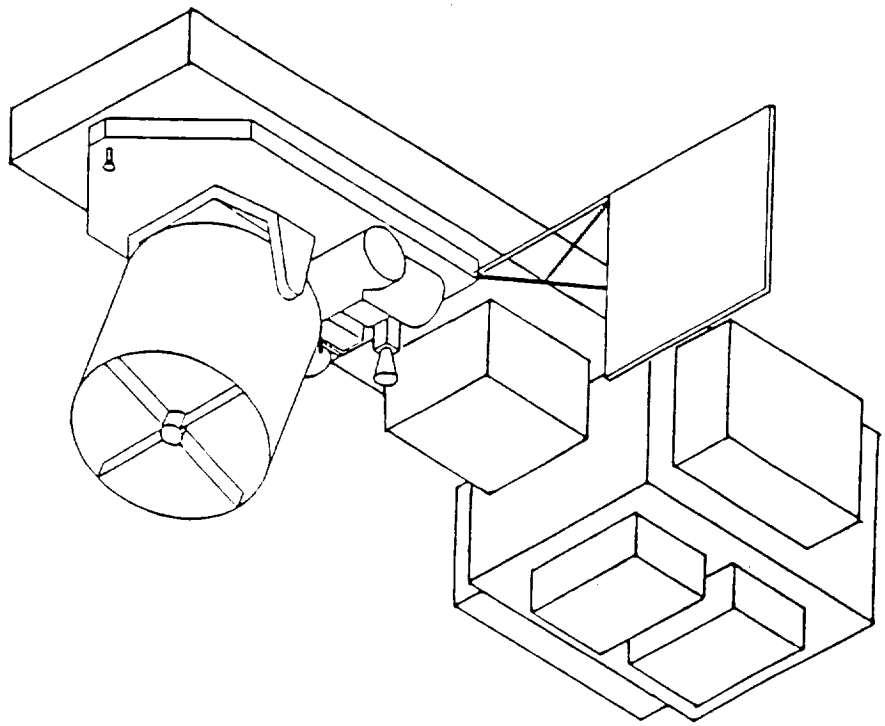

Figure 5-68. Typical Laws/POP Configuration

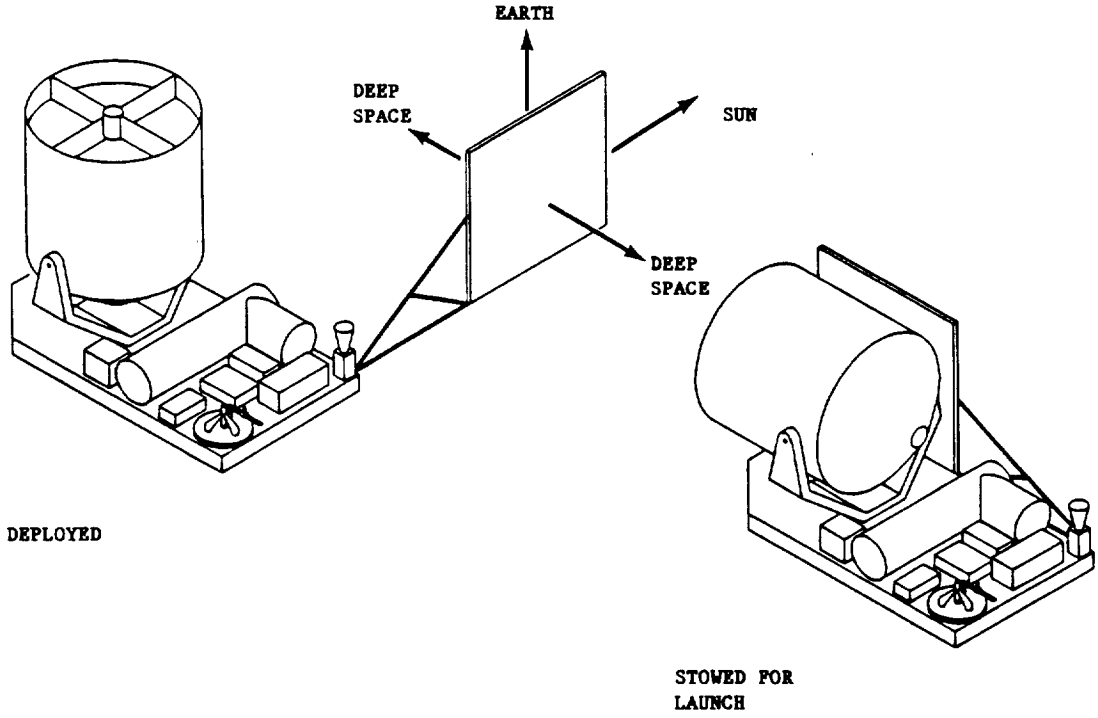

Figure 5-69. LAWS with Radiator

within their normal operating temperatures. The radiator attaches to the telescope yoke and base structure for launch environment, then pivots and rolls to position on-orbit.

The resultant force and moment imparted to the base structure due to the telescope/ yoke assembly rotation were determined. Rotation was assumed to be at 6 rpm (0.628 rad/sec) with the telescope positioned at 45 deg off-Nadir. Total mass for the telescope/ yoke assembly is 178 kg, and the assembly is dynamically balanced. The resultant force and moment are:

F = 3.856 N (0.867 lbf)
M = 6.088 NM (4.49 ft x lbf).

5.3.1 LAWS Configuration with AVCO Laser

Three view drawings and an isometric view with all subsystem components identified, are shown in Figures 5-70 and 5-71, respectively, for the baseline configuration with the Avco laser installed. Overall dimensions of the configuration are 3.9 m x 2 m x 2.31 m. Subsystem weight, c.g. location, and power characteristics are given in Table 5-28. The origin of the coordinate system for all configurations shown is at the intersection of the telescope mounting strut centerline and the top surface of the base structure. A right hand coordinate system is used with +X-axis perpendicular to the base plate toward the telescope, and +Z-axis toward the telescope forward launch attach point. The LAWS c.g. is -0.82 m aft of the telescope strut and +0.27 m above the face plate. This X-location is 0.47 m from the interface of the LAWS Instrument to either the JPOP or Space Station structure. Deletion of the radiator from the design brings the Y-axis coordinate to +0.06 m with minimal changes in the X and Z coordinates.

5.3.2 LAWS Configuration with GEC Laser

Three view drawings and an isometric view with all subsystem components identified are shown in Figures 5-72 and 5-73, respectively, for the baseline configuration with the GEC laser installed. Overall dimensions of the configuration are 3.5 m x 2 m x 2.31 m. Subsystem weight, c.g. location, and power characteristics are given in Table 5-29. The LAWS c.g. is -0.65 m aft of the telescope strut and +0.27 m above the face plate. This X-location is 0.47 m from the interface of the LAWS Instrument to the JPOP or Space Station structure. Deletion of the radiator from the design brings the Y-axis coordinate to +0.05 m with minimal changes in the X and Z coordinates.

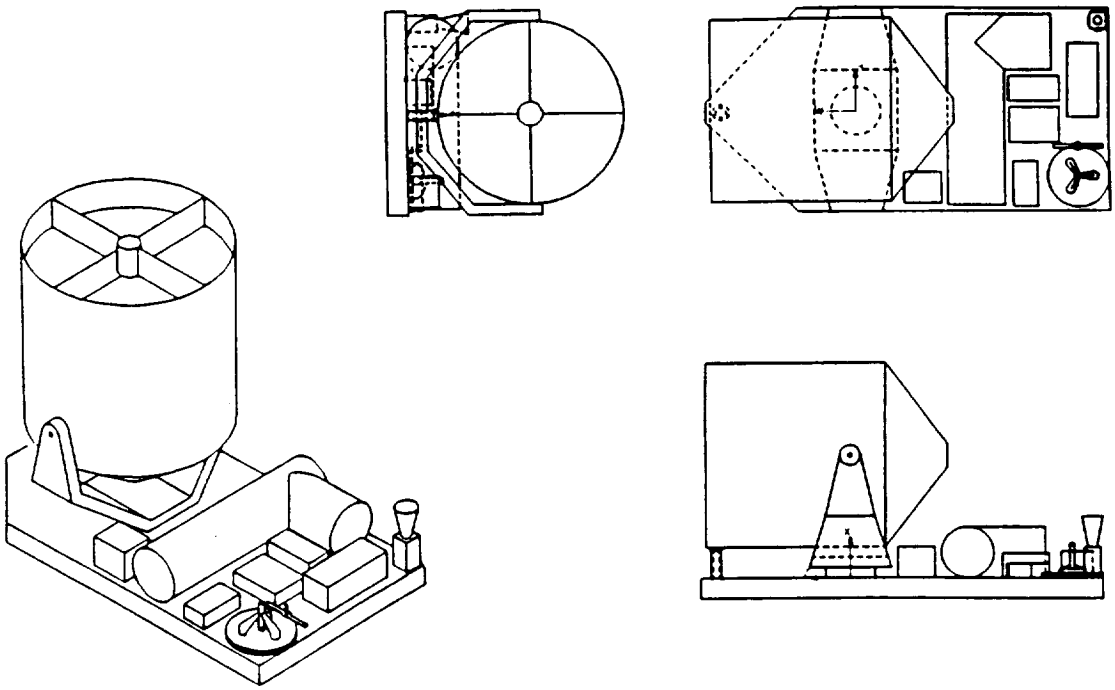

Figure 5-70. LAWS/Avco Laser

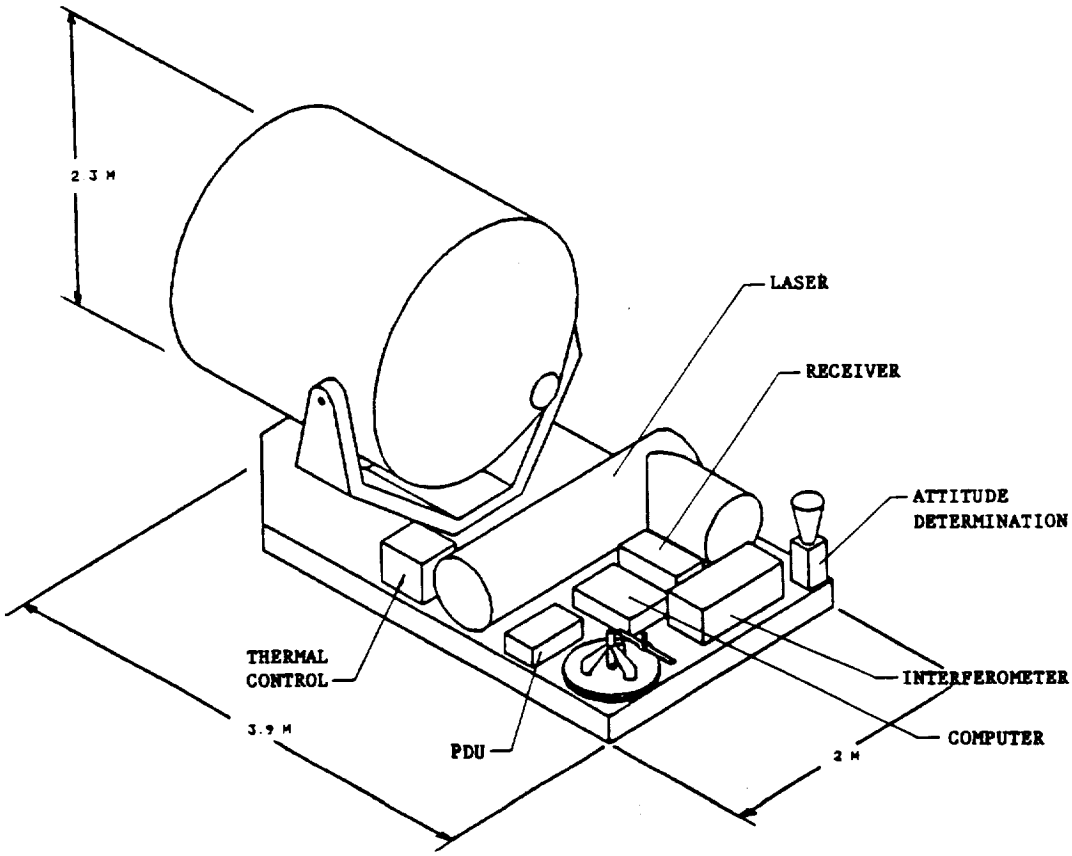

Figure 5-71. LAWS/Avco Laser

Table 5-28. Baseline Configuration/Avco Laser

Item	Weight (kg)	CG Location (M) X	Y	Z	Power Required (watts)	Active Thermal Control Requirement (watts)
Optical Telescope	93	+1.20	0.0	0.0		
Yoke/Gimbal Mechanism	85	+0.24	0.0	0.0	221	Internal In System
Interferometer	45	+.12	+.28	-2.2		
Laser	171	+.25	+.22	-1.33	2812 (Peak)	2652
Flight Computer	18	+.07	-.16	-1.72	20	20
Attitude Determination	8	+.09	+0.81	-2.36		
Power Distribution Unit	13	+.07	-.74	-1.64	20	-
Receiver	10	+.13	+.22	-1.72	50	50
Grapple Fixture	13	+.04	-.68	-2.17	-	-
Base Structure	221	-.10	0.0	-.54	-	-
Radiator w/Support Structure -		68	+.65	+1.0	-.76	-
Thermal Control	18	+.16	+.62	-.70	200	200
Total System	763 kg	+.27M	+.15M	-.82M	3323 (Peak)	2922

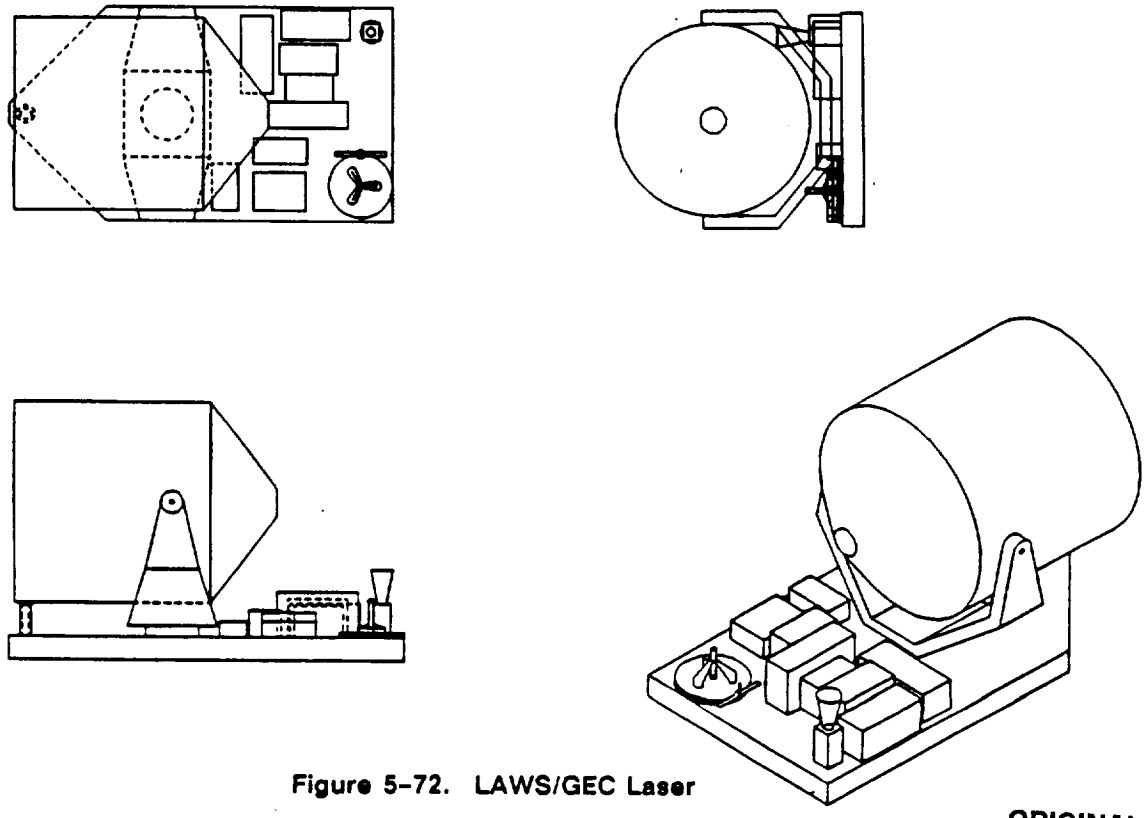

Figure 5-72. LAWS/GEC Laser

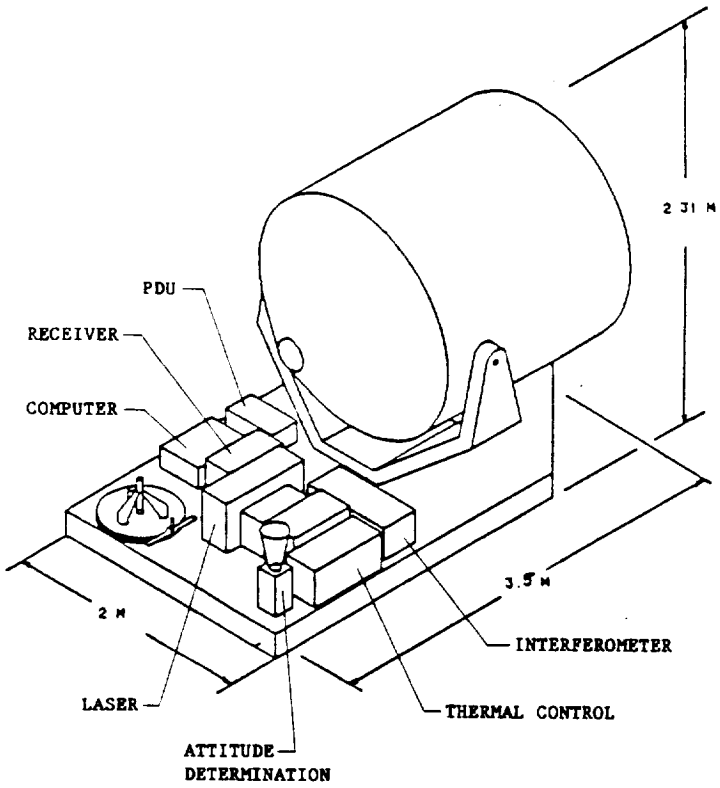

Figure 5-73. LAWS/GEC Laser

Table 5-29. Baseline Configuration/GEC Laser

Item	Weight (kg)	CG Location (M) X	Y	Z	Power Required (watts)	Active Thermal Control Requirement (watts)
Optical Telescope	93	+1.20	0.0	0.0		Internal In System
Yoke/Gimbal Mechanism	85	+0.24	0.0	0.0	221	
Interferometer	45	+.12	+.56	-.85		
Laser	167	+.20	+.20	-1.32	2716 (Peak)	1818
Flight Computer	18	+.07	-.72	-1.08	20	20
Attitude Determination System	8	+.09	+0.84	-1.90		
Power Distribution Unit	13	+.07	-.68	-0.58	20	-
Receiver	10	+.13	-.34	-1.08	50	50
Grapple Fixture	13	+.04	-.70	-1.80	-	-
Base Structure	205	-.10	0.0	-.37	-	-
Radiator w/Support Structure	68	+.65	+1.0	-.67	-	-
Thermal Control	18	+.14	+.84	-1.44	200	200
Total System	743 kg	+.27M	+.15M	-.65M	3227 (Peak)	2088

5.4 LAWS ACCOMMODATION

The Lockheed LAWS configuration is designed to accommodate installation on polar orbiting platforms and/or SSF. Launch-to-orbit can be by Space Shuttle or unmanned expendable launch vehicles, such as H-II or Titan. Servicing can most economically be performed at SSF by astronauts during EVA. All components, except the telescope, can be replaced on-orbit using standard NASA inventory EVA tools. Component changeout procedures will be used that have been developed and validated through many hours of 1-g and neutral buoyance simulations on Lockheed's HST, AXAF, and Space Station Freedom contracts and development work.

Figure 5-74 shows LAWS installation on a typical polar orbiting platform. LAWS installation could be rotated 180 deg to position the radiator and grapple fixture end away from the other POP instruments/experiments, if so desired. This would provide maximum clearance for RMS, or tele-operator system access to the grapple fixture and minimum shielding or reflection of the POP body on the radiator.

SSF/LAWS installation is shown in Figure 5-75. Installation is directly to the payload interface adapter (PIA), mounted on the station interface adapter (SIA). The LAWS thermal control system will interface with the station thermal control system cold plate the PIA. This will delete the requirement for the LAWS radiator from the configuration, providing a 68 kg weight reduction. Depending on final station design, the LAWS interface structure that mates with the PIA can be biased to compensate for the negative pitch angle of the operational SSF.

The length of the LAWS/Avco laser configuration is 3.9 m, matching the octagon dimension of the SIA. The length of the LAWS/GEC laser configuration is shorter, 3.5 m, due to the difference in the laser configuration. The longer configuration is shown in Figure 5-75.

The baseline LAWS is easily accommodated for launch using either expendable launch vehicles or the space shuttle (STS). Figure 5-76 shows the POP/LAWS configuration in the 3.65 m diameter fairing for the Japanese H-II launch vehicle. The base end of the POP would interface with the boost vehicle for launch/flight load reaction. A similar configuration would be used for the Titan launch vehicle.

STS/LAWS launch configuration is shown in Figure 5-77. The Hubble Space Telescope Orbital Replacement Unit Carrier (ORU carrier) design developed for the HST maintenance and refurbishment missions would be utilized. This ORU carrier is based

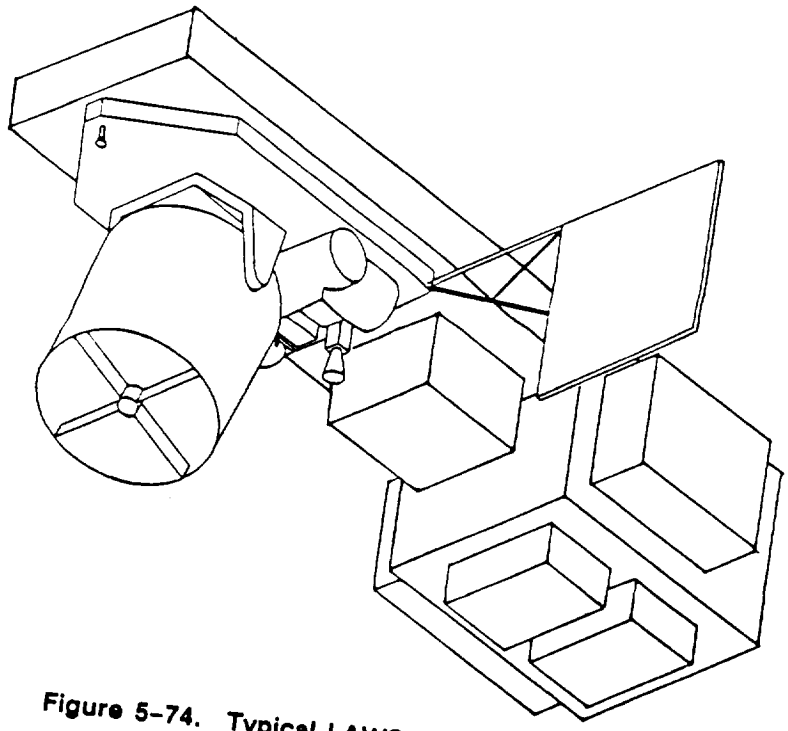

Figure 5-74. Typical LAWS/POP Installation

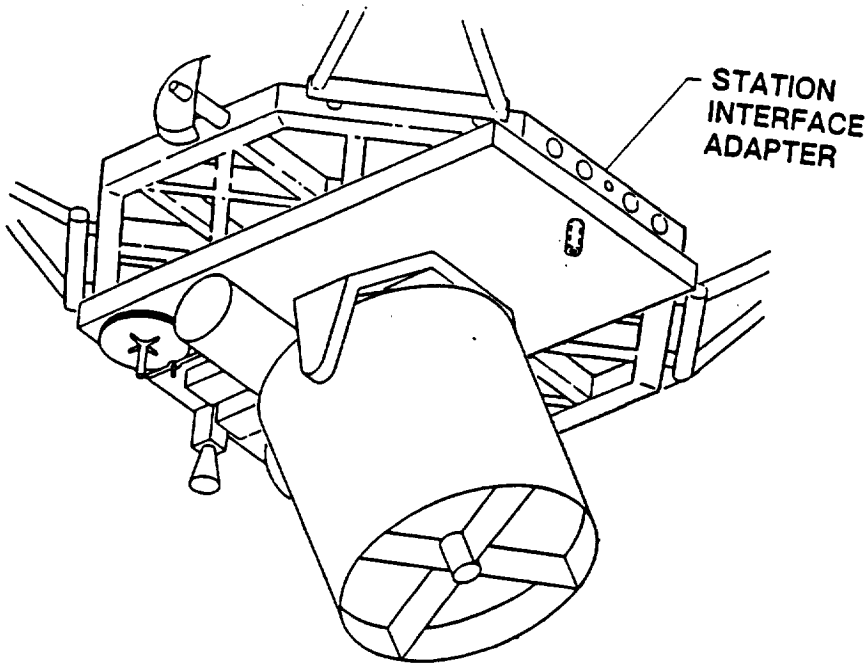

Figure 5-75. Space Station Installation

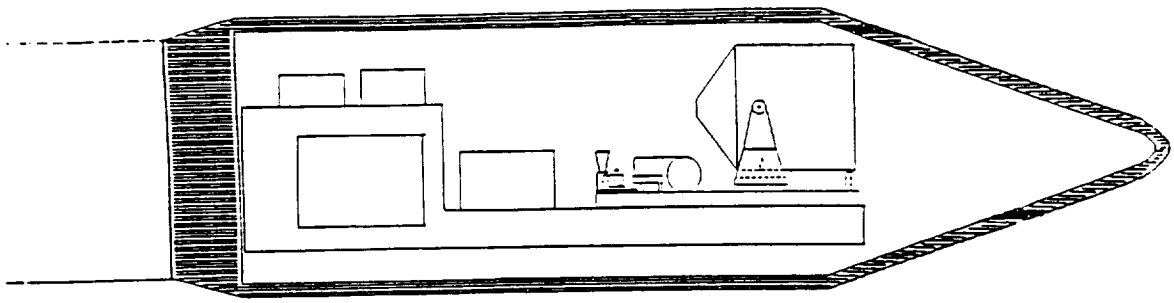

POP/LAWS CONCEPT

Figure 5-76. H-II Launch Configuration

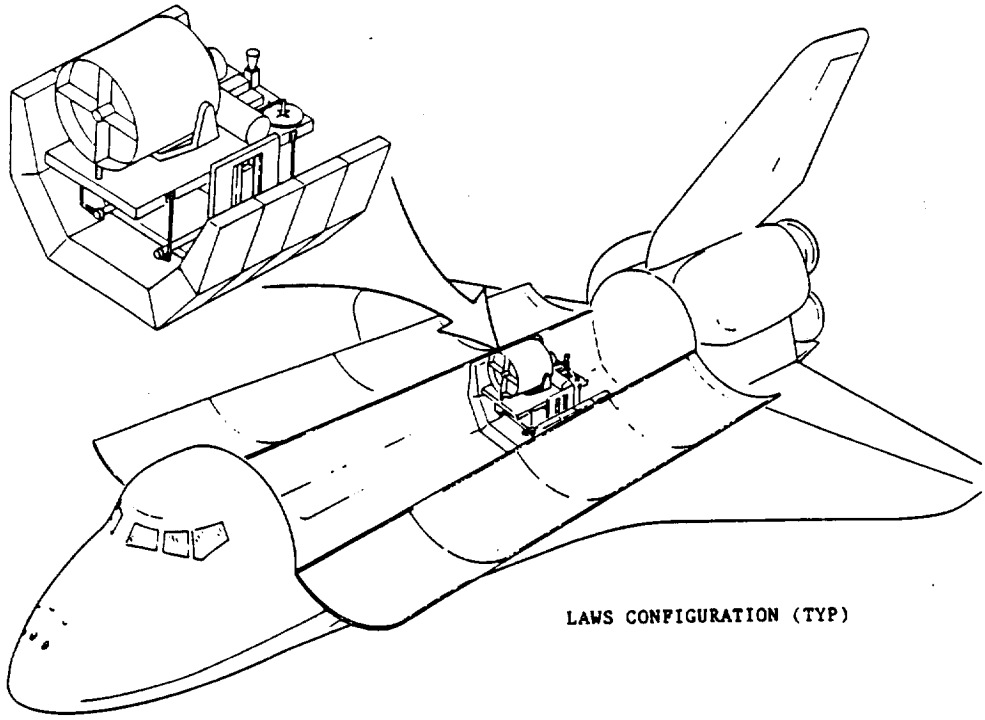

Figure 5-77. Shuttle Launch Configuration

on a standard Spacelab pallet. It was designed by MSFC and fabricated/assembled/verified by Lockheed-Huntsville. The HST ORU carrier has a load isolation system (LIS) to attenuate the harsh loads that the replacement HST instruments would experience during STS launch/landing environments. This LIS system was space flight qualified, for maximum payloads up to 1451 kg, well above our maximum LAWS weight of 763 kg. The Y-dimension between the LIS/payload interface attach points matches the 2 m width of the LAWS base structure. LAWS would be removed from the ORU carrier/STS cargo bay by the RMS using the LAWS grapple fixture for transfer to the Space Station SIA.

Based on the maintenance mission schedule of the HST, the ORU carrier could be borrowed for the LAWS launch mission. To prevent possible schedule conflicts, a duplicate LIS could be fabricated from the existing MSFC design and installed on a Spacelab pallet for the LAWS mission at minimum cost.

5.5 LAWS SERVICING

If required, the LAWS layout is configured for ease of maintenance by EVA or tele-operator systems. With the exception of the telescope, all components can be accessed for removal by an astronaut performing EVA, or by a tele-operator robotic system and a replacement unit installed. If the telescope fails, the LAWS could be returned to earth from the Space Station for repairs. On a POP, the LAWS could be released and transferred by the OMV to SSF or an orbiter for return to earth.

The LAWS was designed with a grapple fixture to facilitate on-orbit positioning and movement by RMS. For orbital transfer from Space Station to POP, the grapple fixture would be replaced by a drogue mating system to accommodate an orbital maneuvering vehicle (OMV). The drogue system would also be used during module replacement on POP maintenance missions. The manipulator satellite servicing system of the OMV would be used to perform module changeout.

If the requirement for LAWS servicing on the POP is deleted, the subsystem interface designs can be greatly simplified to allow space station changeout by astronauts during EVA. Procedures, techniques, and special design features to allow on-orbit changeout of components for the Hubble Space Telescope have been developed by Lockheed with NASA. These require minimum impact on standard component design. All LAWS components will be designed with handles, self-captive quick disconnect fasteners, tether loops, and connectors with large shells and winged flanges to allow easy

handling by an astronaut in a space suit. Hand holds and portable foot restraint receptacals are designed into the LAWS base structure for EVA use. All of these orbital maintenance design features have been incorporated and verified on the HST during many hours of 1-g and neutral buoyancy testing at both the MSFC NBS, and the JSC WETF.

5.6 ALTERNATE LAWS CONFIGURATION

The Japanese National Space Development Agency (NASDA) personnel presented a very preliminary sketch of a potential JPOP/LAWS configuration at the August 1989 Quarterly Review (see Figure 5-78). This concept shows the LAWS cantilevered off the front of a T-shaped JPOP structure. This configuration would restrict the LAWS telescope to an arc survey sweep only instead of the desired full 360 deg field of view. JPOP would have to be positioned in a gravity gradient mode for this configuration to allow a full 360 deg sweep. Gravity gradient positioning would inhibit the viewing by other JPOP EOS experiments. The L-shaped POP configuration, previously shown in Figure 5-68, is the desired design.

In the event that the T-shaped JPOP design were chosen, an "Alternate LAWS" configuration was developed, as shown in Figure 5-79. LAWS is packaged around a box base structure which interfaces with the leg structure of JPOP. Various viewing angles can be accommodated by tilting the telescope.

The Alternate LAWS configuration with the Avco laser is shown in Figures 5-80 and 5-81. A trapezoidal base structure is used to minimize weight. LAWS is contained within a cylindrical envelope of 2.92 m diameter x 3.7 m high in launch configuration. A thermal control radiator can be accommodated within this volume. Other configuration parameters are given in Table 5-30. The coordinate system centroid is the intersection of the centerline of the telescope strut with the top face of the base structure. Positive X-axis is out through the telescope. The base structure is fabricated from typical aluminum cross sections and sheet materials.

The Alternate LAWS configuration with the GEC laser is shown in Figure 5-82 and 5-83. The subsystems are mounted on a rectangular base structure. Total cyclindrical volume envelope for the configuration is 2.76 m diameter x 3.6 m high. If a LAWS thermal control radiator is required, the maximum volume diameter is 2.96 m. Other configuration parameters are given in Table 5-31.

Figure 5-84 shows an Alternate LAWS configuration with a thermal control radiator. Once on-orbit, the radiator is released from the telescope yoke structure, rotated

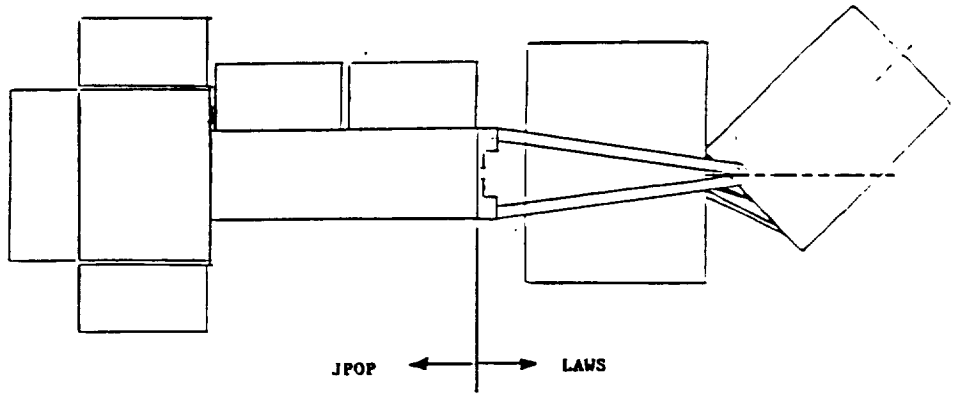

PRELIMINARY CONCEPTS

- Telescope restricted to arc survey sweep
- Gravity gradient mode necessary for full 360 conical survey

NASDA

Figure 5-78. Preliminary Japanese JPOP/LAWS Concept

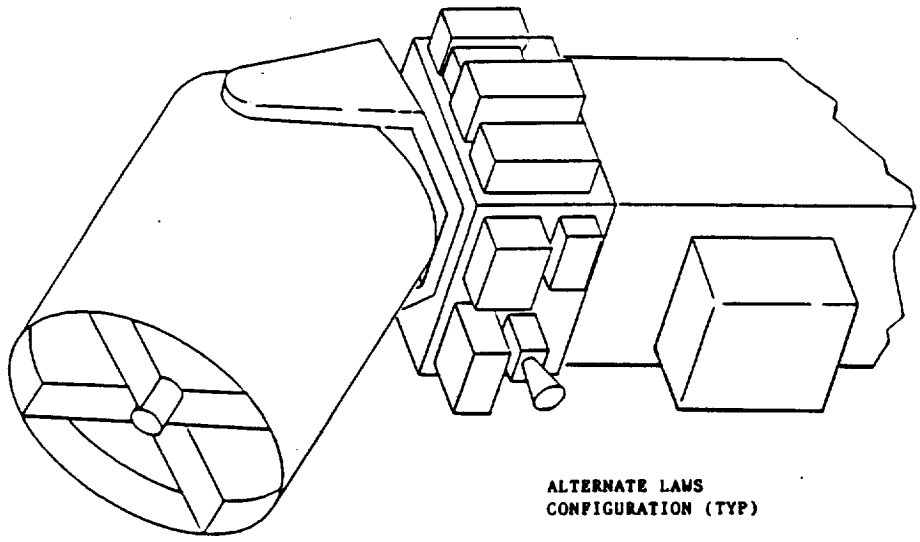

Figure 5-79. JPOP/LAWS Installation

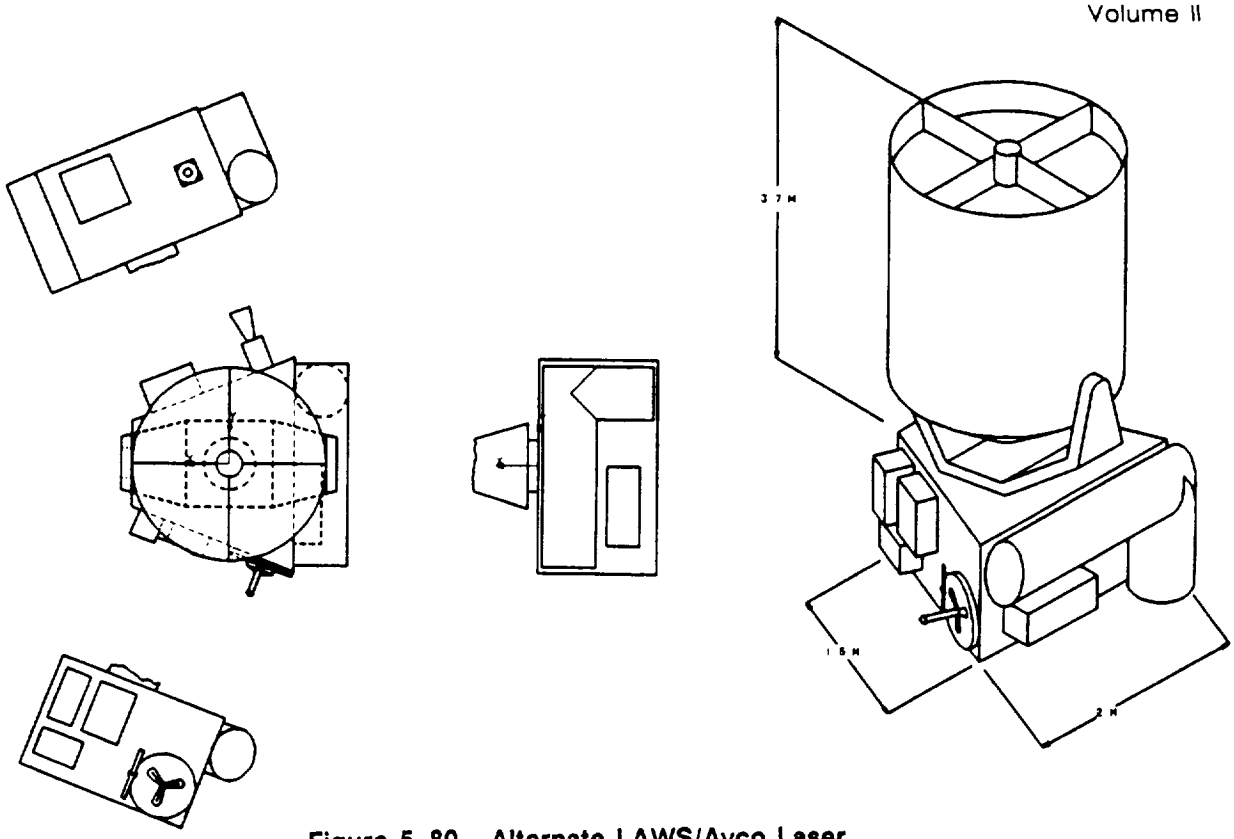

Figure 5-80. Alternate LAWS/Avco Laser

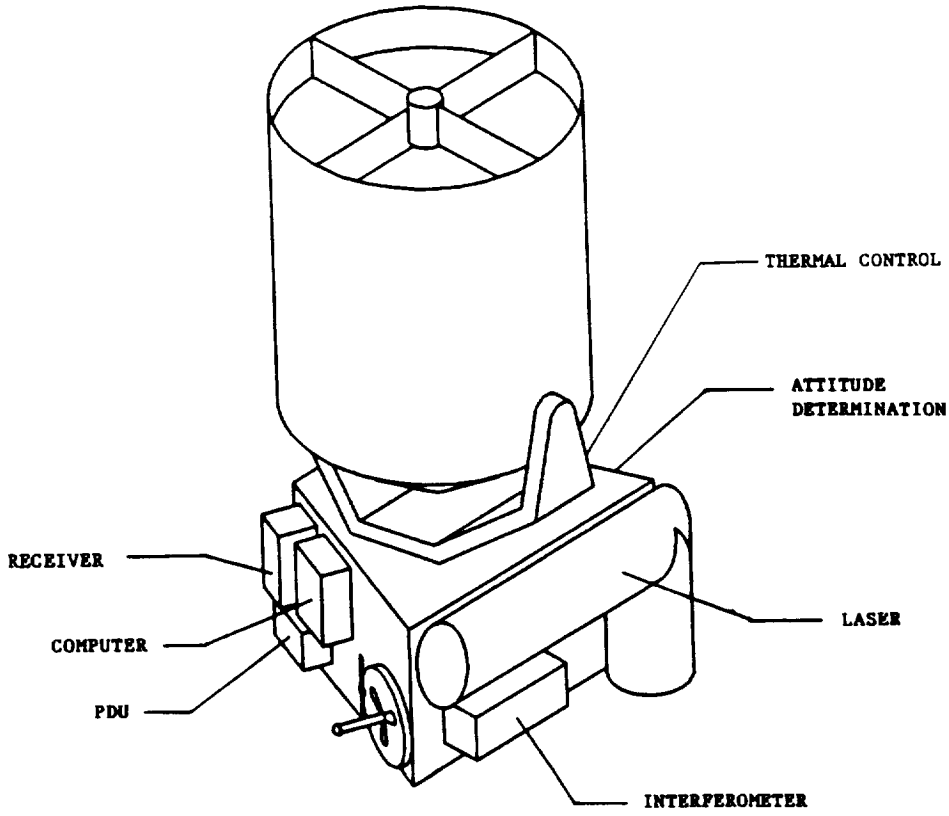

Figure 5-81. Alternate LAWS/Avco Laser

Table 5-30. Alternate Configuration/Avco Laser

Item	Weight (kg)	CG Location (M) X	Y	Z
Optical	93	+1.20	0.0	0.0
Yoke/Gimbal Mechanism	101	+0.10	0.0	0.0
Interferometer	45	-.80	-.40	-.74
Laser	171	-.43	+.23	-.88
Flight Computer	18	-.35	-.67	+.40
Power Distribution Unit	13	-.84	-.56	+.68
Receiver	10	-.35	-.56	+.80
Attitude Determination	8	-.54	+1.03	-.22
Grapple Fixture	13	-.80	-.92	-.32
Radiator w/Support Structure	61	+.44	0.0	+1.23
Base Structure	128	-.55	0.0	+.04
Thermal Control	18	-.74	+.65	+.55
Total System	679 kg	-.13M	-.03M	-.17M

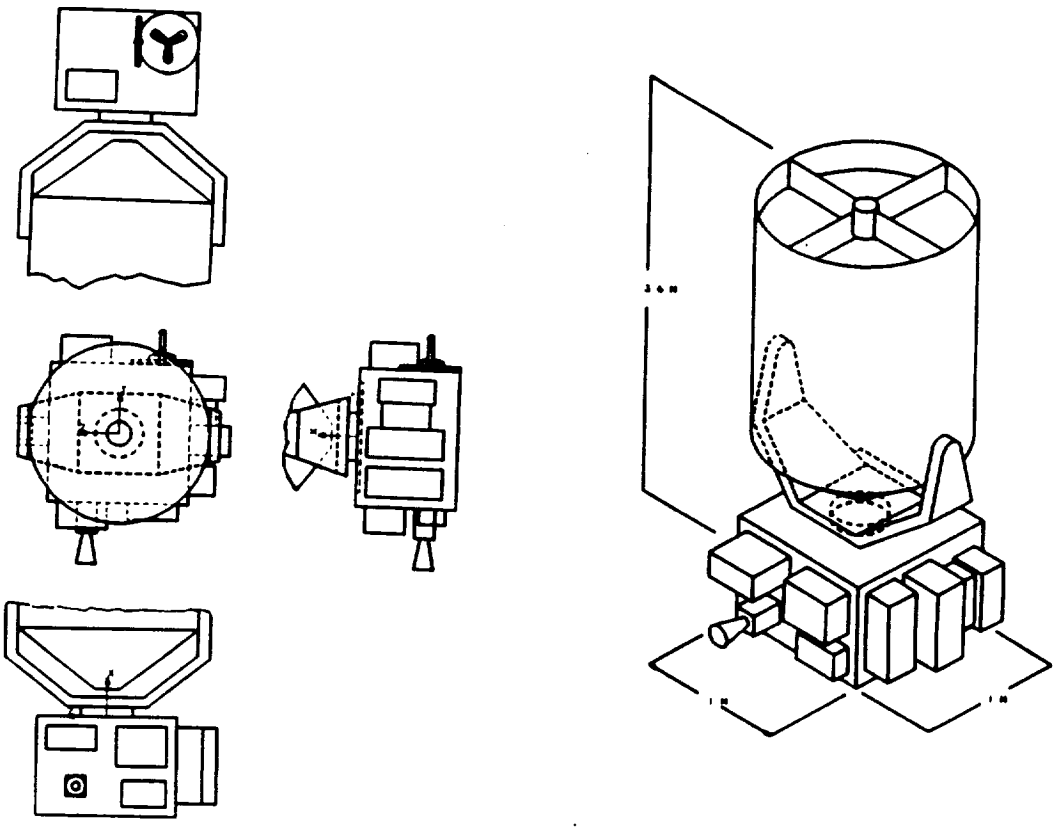

Figure 5-82. Alternate LAWS/GEC Laser

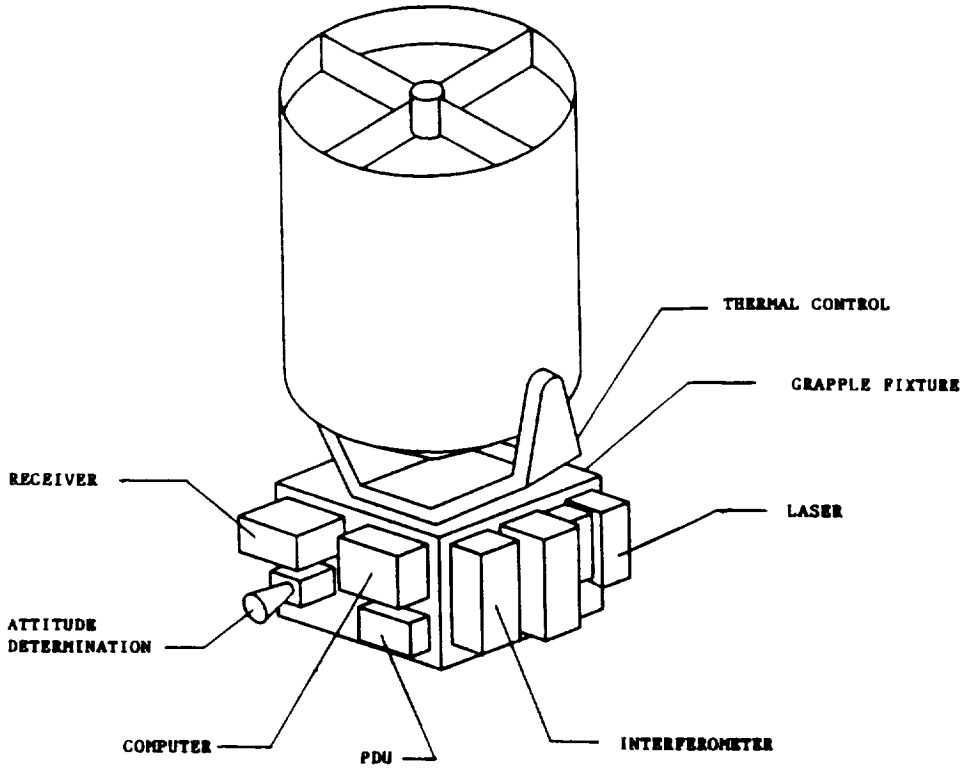

Figure 5-83. Alternate LAWS/GEC Laser

Table 5-31. Alternate Configuration/GEC Laser

Item	Weight (kg)	CG Location (M) X	Y	Z
Optical Telescope	93	+1.20	0.0	0.0
Yoke/Gimbal Mechanism	99	+0.12	0.0	0.0
Interferometer	45	-.50	-.44	-.84
Laser	167	-.72	+.12	-.90
Flight Computer	18	-.30	-.78	-.35
Power Distribution Unit	13	-.76	-.78	-.38
Receiver	10	-.24	-.84	+.34
Attitude Determination	8	-.70	-.86	+.30
Grapple Fixture	13	-.70	+.74	-.40
Radiator w/Support Structure	61	+.44	0.0	+1.23
Base Assembly	120	-.50	0.0	0.0
Thermal Control	18	-.36	+.82	+.35
Total System	665 kg	-.05M	-.02M	-.18M

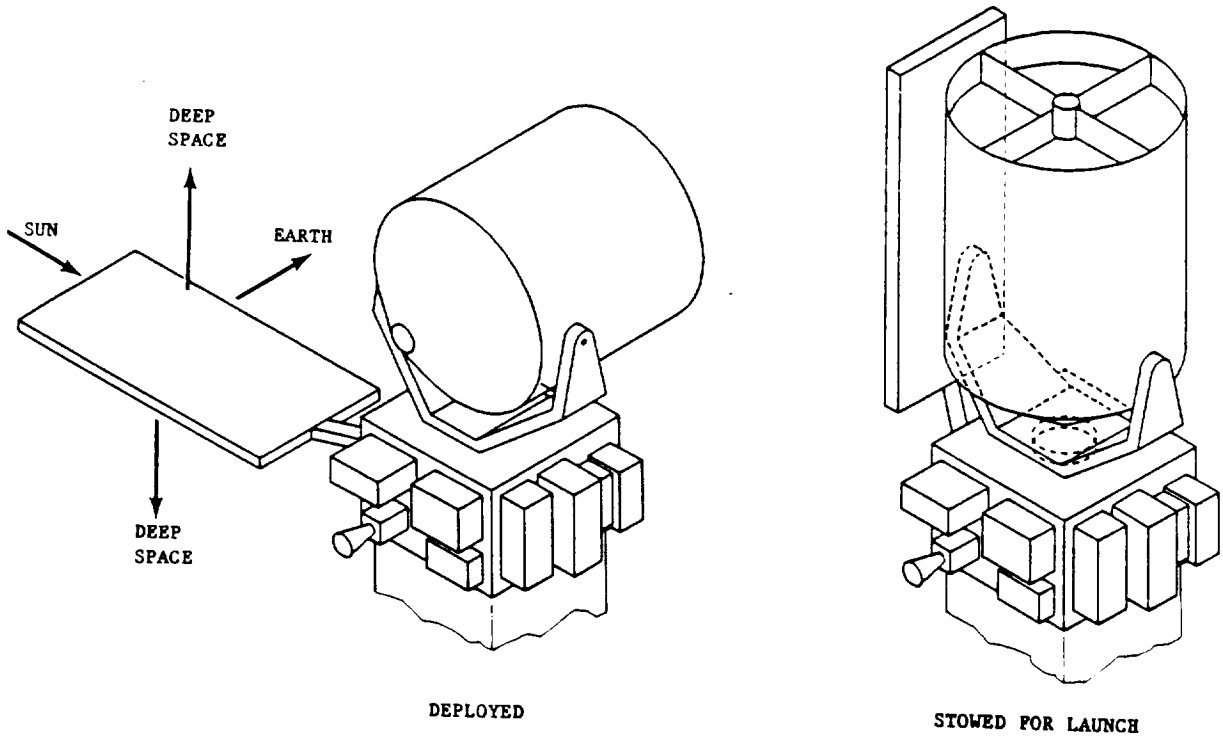

Figure 5-84. Alternate LAWS with Radiator

90 deg, then pivoted to position the radiator edges to earth and sun with the panel faces to deep space. A total radiator exposed area of 9.6 m^2 is provided by this design to produce the same thermal control capabilities as the LAWS Baseline design.

The Alternate LAWS configuration can be easily accommodated in the 3.65 m diameter fairing specified for the H-II launch vehicle, Figure 5-85.

Typical Alternate LAWS design is shown attached to the SSF in Figure 5-86 using the deck carrier assembly. The deck carrier would also be used for LAWS launch by the STS, Figure 5-87. To save weight the Alternate LAWS configuration can mount and interface directly to the Space Station PIA/SIA without the deck carrier. The LAWS grapple fixture would be used to assist the transfer of LAWS from the orbiter to the Space Station by RMS.

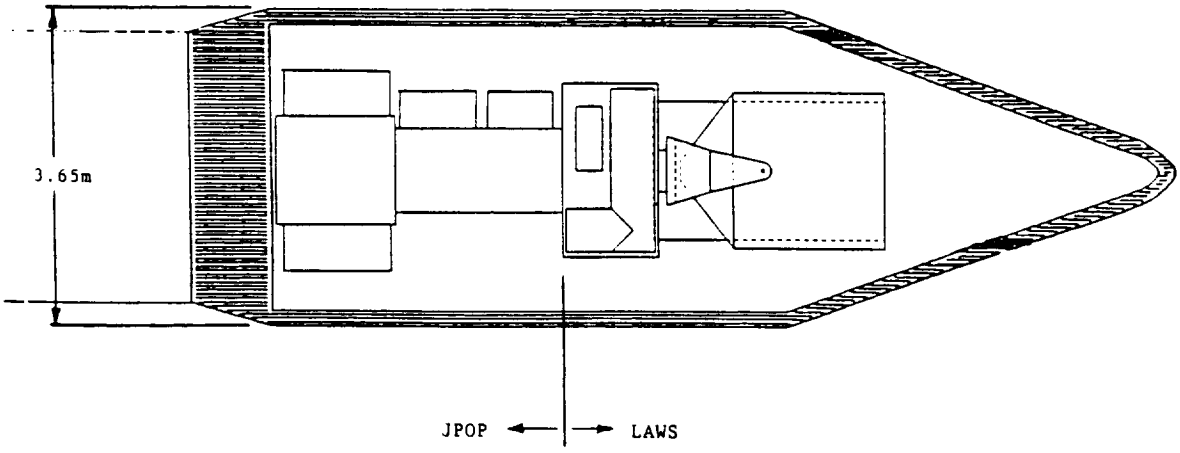

JPOP/ALTERNATE LAWS CONFIGURATION (TYP)

Figure 5-85. H-II Launch Configuration

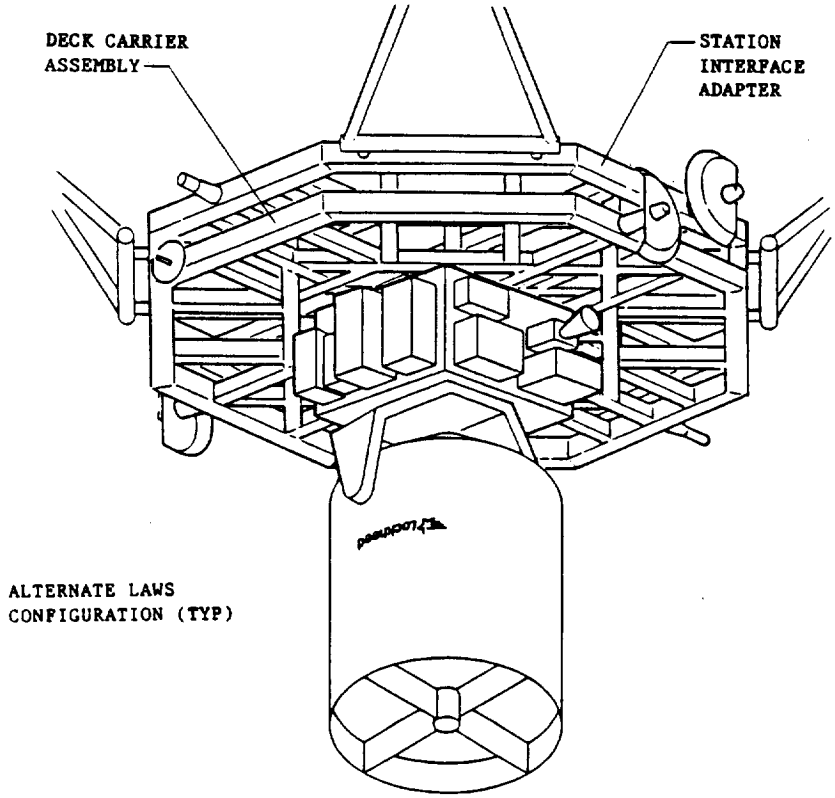

Figure 5-86. Space Station Installation

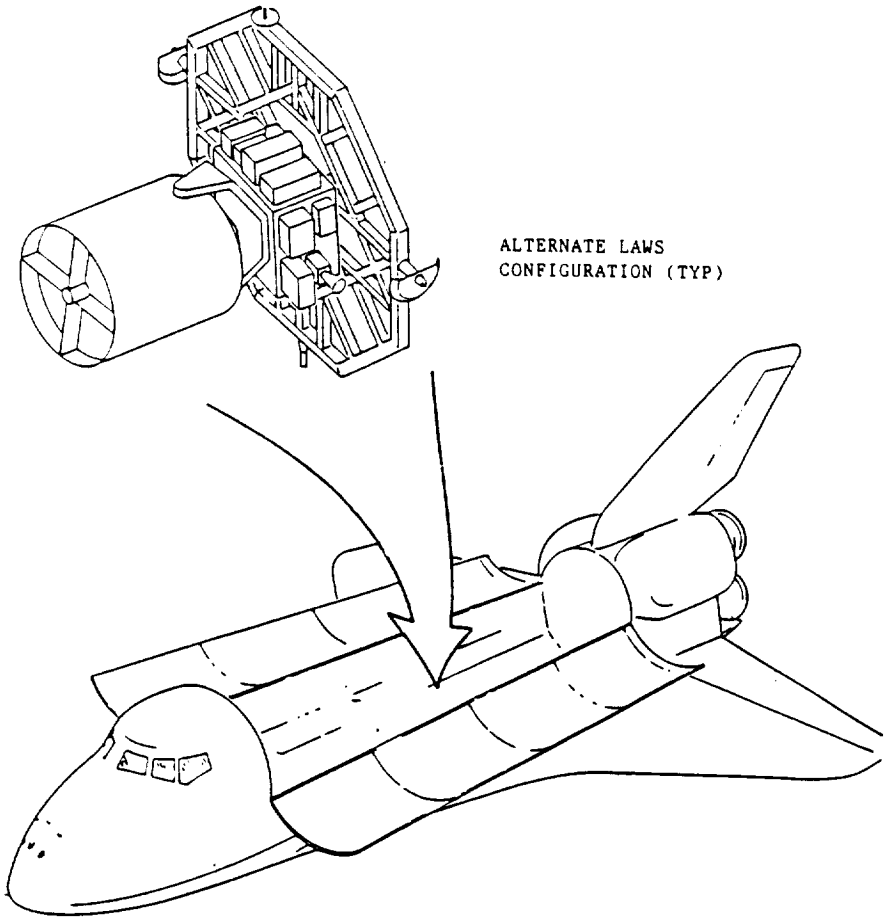

Figure 5-87. Shuttle Launch Configuration

SECTION 6. Work Breakdown Structure (WBS)

The basic objective of the Phase I and Phase II WBS related development activities is to define the Phase C/D project effort. The instructions provided in the LAWS SOW, other LMSC requirements documents, and the guidelines contained in NHB 5610.1 Handbook for "Preparation of Work Breakdown Structures" were used as the basis for constructing the successive levels and subdivisions of the project effort work/cost elements. Guidelines contained in MM 8020.6A, "MSFC Cost/Schedule Performance Criteria," and MM 8020.8A, MSFC Technical Performance Criteria," were used to categorize descriptions of the effort presented in DR-5, Draft WBS, and WBS Dictionary. The end product will be a WBS and WBS Dictionary that can be incorporated in a Request for Proposal (RFP) for the LAWS Phase C/D Project.

Normally the top three levels of the contractor's WBS are included in the RFP. The offerers should be instructed to extend the WBS to as many levels as necessary to structure the work effort to achieve the LAWS project objectives with effective cost control.

Before the WBS tasks and associated schedules discussed in the next section can be defined, the project contract end items and major milestones must be ascertained. For the Phase I and Phase II definition process the LAWS phase C/D Contract End Items (CEIs) have been assumed to be the following:

1. One assembled and verified LAWS Instrument flight article
2. Data Items (i.e., DRs)
3. Spares
4. System support equipment (mechanical and electrical)
5. Software end items.

System support equipment includes all components required to support the development and servicing of the flight hardware. It is actually divided into two major categories: ground support equipment (GSE), and airborne support equipment (ASE). Ground support equipment includes mechanical and electrical support equipment. Mechanical support equipment includes jigs, fixtures, mockups, dollies, shipping containers, optical alignment benches, etc. Electrical support equipment includes anything used to check out the flight hardware article. This can range from specialized black boxes to general purpose computers. Airborne support equipment is any item associated with orbital servicing of the flight hardware.

Software end items include the flight software, software required for system support equipment, and simulation software. System support equipment includes all ground

support equipment (electrical and mechanical) and space support equipment which may be required to support orbital deployment and servicing. Required milestones are a Project Requirements Review (PRR), Preliminary Design Review (PDR), Critical Design Review (CDR), Configuration Inspection (CI), Flight Readiness Review (FRR), and a Launch Readiness Review (LRR). The basic assumption used in the development of the WBS is that a baseline LAWS Instrument will be designed for the POP. Where necessary, specific WBS elements have been added to reflect specific efforts applicable to the Space Station. Where similar work for both the POP and the Space Station are contained in a given element, separate allocations are made for each.

The WBS presented in DR-5 and depicted in Figure 6-1 is end item oriented for the hardware and software to be produced, services to be performed (project management, systems engineering, verification, etc.), and data to be submitted to NASA/MSFC during the Phase C/D contract activities. It was prepared to Level III, except for software development and orbital servicing task descriptions. The software WBS (WBS Element 2.3.2) has been extended to Level IV to clearly delineate the flight, ground, mission, and simulation software. The orbital servicing tasks encompassed in WBS Element 2.8 comply with the requirement of the LAWS SOW dated March 15, 1988, for servicing and maintenance of the LAWS Instruments on both the POP and the Space Station. Orbital servicing tasks have been extended to level IV to delineate the various elements to develop the mission servicing equipment and verify the orbital servicing procedures and/or the equipment developed for servicing the LAWS Instrument. The task descriptions for both are presented in DR-5. The Level II WBS elements are summarized below.

The LAWS Instrument development effort is divided into eight Level II elements. These elements cover the effort to: (1) provide project and technical management; (2) derive and maintain system technical and interface requirements and configurations; (3)study, analyze, design, and support the development and fabrication of all flight and ground hardware and all software; (4) assemble and verify all flight and ground hardware, and (5) support all operational aspects of the LAWS Instrument.

WBS Element 2.1, Project Management This element includes business management (i.e., program planning, performance measurement, reporting, and controls), configuration management, information management, procurement management, and management of GFE items.

WBS Element 2.2, Systems Engineering and Integration. This element includes the performance of all activities necessary to ensure compliance with contractual require-

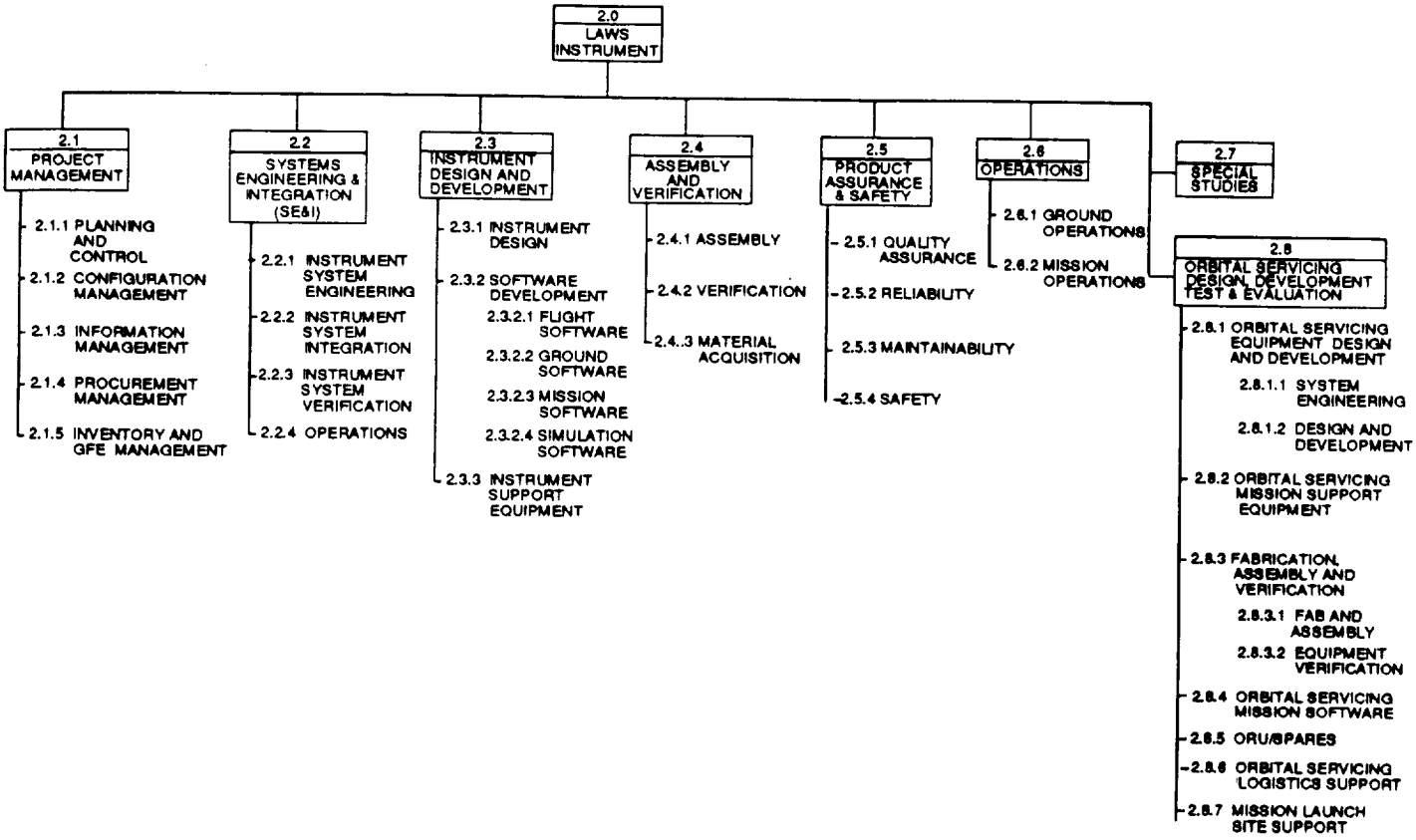

Figure 6-1. LAWS Project Work Breakdown Structure

ments through the establishment of detailed technical requirements and the use of system specifications to ensure LAWS performance and maintainability. This is accomplished through system and interface requirements analysis and definition, system performance and functional analysis and allocations, configuration definition, performance audits, technical performance measurement, system verification, and system operations requirements and planning analyses.

WBS Element 2.3, Instrument Design and Development. This element includes all design and development efforts for the LAWS Instrument, subsystems, and required system support equipment. The engineering effort includes optical engineering, laser support, structures and mass properties, electromagnetic compatibility, thermodynamics, environmental compatibility to include contamination, space debris vunerability assessment, electromagnetic interference/electromagnetic contol, eye safety, and electronics engineering. Software development includes all efforts to design, develop, code, integrate, verify/validate, and document the development and maintenance of the software. This element also includes the design and support of all LAWS Instrument support to

include ground and orbital servicing equipment WBS Element 2.4, Instrument Assembly and Verification. This element covers the efforts to (1) provide manufacturing support to design engineering, (2) plan and control manufacturing operations, (3) procure, fabricate, process, assemble, and checkout flight and ground support equipment, (4) construct mockups and test articles, and (5) plan the verification program, define test procedures, and perform developmental and environmental verification tests on the flight hardware. All costs associated with hardware acquisition are included in this element.

WBS Element 2.5, Product Assurance and Safety. This element covers all efforts to establish, implement, and maintain a Product Assurance and Safety Program and addresses all hardware and software elements. Product assurance covers quality assurance, reliability, and maintainability. Safety addresses the efforts to establish, implement, and maintain a LAWS safety program which meets project requirements and which complies with the safety requirements of the transportation system and host platform.

WBS Element 2.6, Operations. The two major elements are ground operations and mission operations. Ground operations includes planning for and supporting preflight integration into the launch vehicle, logistics, and packaging and shipping. Mission operations covers mission planning, training of mission operations personnel, support of mission operations, and orbital verification.

WBS Element 2.7, Special Studies. This element includes all work effort on special studies or tasks related to design, development, or operation of the LAWS Instrument and support equipment.

WBS Element 2.8, Orbital Servicing Space Support Equipment Design and Development. This element includes the system engineering and engineering effort to design and develop LAWS orbital airborne support equipment for servicing the LAWS Instrument on the Space Station or the POP. It includes ground support equipment, mockups, and other training support equipment required to support development of orbital servicing.

SECTION 7. PROJECT SCHEDULES

The project schedules presented in this section assume the LAWS Baseline is the instrument designed for the POP. A separate schedule will be required for the delivery of the Space Station instrument. This will be developed during the Phase II studies.

The NASA/MSFC master schedules (Figure 7-1) and the constraints discussed below provided the basis for preliminary Phase C/D schedule definition. Phase C/D project constraints were assumed to be the following:

1. Contract Authority to Proceed (ATP) occurs at the beginning of FY 1993.
2. LAWS Flight hardware is to be delivered at the end of the third quarter in FY 1996.
3. A PRR is to be held within three months after ATP.
4. The remaining major reviews are scheduled by agreement between the contractor and MSFC.
5. The launch integration phase is 21 months in duration.

Items (3) and (4) comply with the requirements of NASA/MSFC 8010.5, "MSFC Baseline Design Reviews." The basis for Phase I and Phase II planning activities is to develop a network and master schedule. A top level logic network and master schedule have been formulated. These will be extended to the subsystem hardware level in Phase II. The rationale for this approach is that insufficient definition is currently known about the subsystem assemblies to realistically develop schedules to that level.

7.1 SOURCE DATA

The LAWS Phase C/D logic networks and schedules are based on three sources: (1) Contract End Items and associated schedules; (2) major milestones; and (3) tasks to be performed. For the Phase I study, the Contract End Items were assumed to be:

1. One assembled and verified LAWS Instrument flight article
2. Data items
3. Spares
4. System support equipment
5. Software end items.

The data items are simply the documentation required by MSFC to support the design disclosure and acceptance process. To support the task definition process and

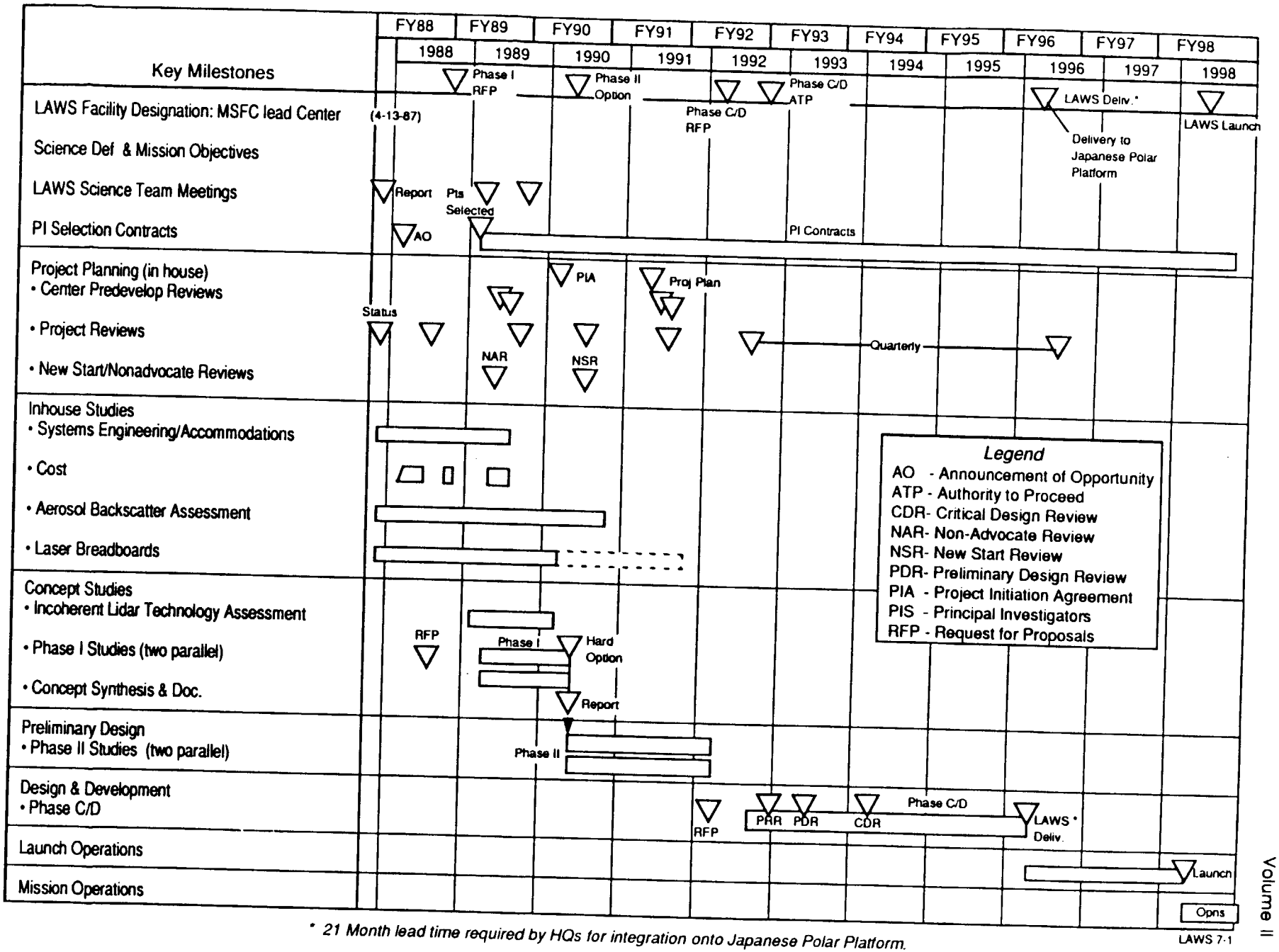

* 21 Month lead time required by HQs for integration onto Japanese Polar Platform.

Figure 7-1. LAWS Master Schedule

development of the logic network and master schedule a "straw man" set of Data Requirements (DRs) was identified. These also support the cost estimating activities described in Volume III of this final report. A summary of the "straw man" set of DRs and the major milestones that each supports are presented in Figure 7-2.

It should be noted that DRs addressing System Support Equipment (SSE) cover both GSE and ASE. Space support equipment has been included to comply with the POP and Space Station servicing requirements of the LAWS SOW, para. 4.0, Item (5).

The major project milestones are listed in Table 7-1.

It was assumed that the CI and Design Certification Review can be held concurrently because collectively these reviews demonstrate that the LAWS Instrument is built to the released engineering drawings; the Instrument has been verified to an approved test plan and procedures; and the acceptance data package is in order. The FRR addresses both flight and ground elements to ensure that all elements taken as a system are ready to support the launch and mission, and that safety and interface compatibility has been demonstrated. An LRR has been scheduled at month 64 to ascertain readiness to launch. An Orbital Readiness Review (ORR) has been scheduled three months after launch to verify that a successful on-orbit condition has been achieved, and that the LAWS Instrument is functioning properly.

The LAWS documentation tree presented in Figure 7-3 shows the hierarchy of the documentation and the distribution by major categories. The flight hardware and software are shown at equal levels because the assumption was made that these are separate deliverables and require separate and distinct documentation. The tree also shows the flow down from the deliverables to the lower level documentation used to control the project. For example, separate CEIs will be prepared for major hardware components procured from outside vendors, and separate specifications will be prepared for GSE hardware components. Supporting DRs under the column labeled "Flight Hardware" are engineering design DRs such as SE05, SE06, SE07, SE09, SE15, SE16, SE18, SE30, etc., identified in Figure 7-2. Similarly, the DRs under "Operations" are those directly applicable to operations. DRs applicable to Ground Operations are concerned with the logistics of transporting and handling the LAWS Instrument and supporting integration at the launch site. DRs applicable to Mission Operations are concerned with support of the LAWS Instrument during orbital operations. This includes operations in ground facilities, orbital verification, and evaluation of the Instrument's performance. The analysis has assumed the LAWS Instrument contractor will not be responsible for evalu-

DR#	TYPE	DR TITLE	MAJOR MILESTONES: PROP	60 DAC	PRR	PDR	CDR	TST	CV DCR	FRR	LR	ORR
CONFIGURATION MANAGEMENT (CM)												
CM01	1	Plan,Configuration Management	X		X							
CM02	1	Specification, Contract End Item (CEI)	X		X		X					
CM03	1	Specification, Ground Support Eqmt (GSE)			X	X	X					
CM04	1	Documents, Interface Reqmts (IRD)			X	X						
CM05	1	Documentation, Major Reviews			X	X	X		X	X	X	X
CM06	1	Data Package, Acceptance						X				
CM07	1	Documents, Interface Control			X	X	X					
CM08	1	Specification, Space Support Equipment				X	X					
CM09	3	Reports, Change Status & Accounting	per event									
CM10	1	Inputs, LAWS Flight Element ICDs				X	X					
DATA MANAGEMENT (DM)												
DM01	1	Plan, Software Development			X							
DM02	1	Specification, Software Requirements			X	X						
DM03	3	Specification, software Design				X	X					
DM04	3	Reports, Software Problem				monthly						
DM05	3	Manual, Software Users							X			
DM06	3	Plan, Software Test				X						
DM07	3	Procedures, Software Verification Test						X				
DM08	3	Procedures, Software Validation Test						X				
DM09	3	Procedures, Software/System Acceptance					X					
DM10	3	Reports, Software Verification Tests						X				
DM11	3	Reports, Software Validation Test						X	X			
DM12	3	Reports, Software/System Acceptance Test						X				
DM13	1	Analysis, S/W Fault Tolerance & Fail Modes Effect			X	X	X					
LOGISTICS (LS)												
LS01	1	Plan, Logistics			X							
LS02	3	List Spares					X		X			
LS03	1	Plan, Gov't Furnished Eqm t Mgmt			X							
LS04	3	Document, Transportation and Handling			per shipment							
MISSION OPERATIONS (OP)												
OP01	1	Planning and Analysis, Mission					X			X		
OP02	2	Document, LAWS Simulator Requirements			X							
OP03	3	Procedures, Systems					X					
OP04	3	Handbook, Operations Data				X						
OP05	1	Requirements, Operations Ground System					X					
OP06	3	Document, Support Instrumentation Reqmts (SIRD)			X	-						
OP07	1	System Operations & Requirements Document				X						
OP08	1	Systems Operations Reqmts Doc (SORD)				X						
OP09	2	Plan, Ground Systems Operations Testing & Verif.					X					
OP10	2	Inputs, Compatibility Test					X					
OP11		Procedures, Operations										
OP12	2	Plan, Training & Certification				X	X					
OP13	2	Plan, Simulation			X							
OP14	1	Requirements, Orbital Activity Verification				X						
OP15	1	Timeline, Orbital Verification				X						
OP16	1	Data Base, Operations			semi annually							
OP17	1	Plans, Operations Data Base Management				X	X					
OP18	1	Plan, Operations Support				X	X					
OP19	3	Plan, LAWS Orbital Verification Support					X					
OP20	1	Document, LAWS Orbital Verification Support Reqmts					X					

Figure 7-2. LAWS "Strawman" Data Requirements

DR#	TYPE	DR TITLE	MAJOR MILESTONES: PROP	60 DAC	PRR	PDR	CDR	TST	CI/ DCR	FRR	LR	ORR
SERVICING (OS)												
OS01	3	Analysis, Integrated Systems				X	X					
OS02	3	Characteristics, Orbital Replaceable Units (ORUs)				X	X					
OS03	3	Assessment, Maintainability/Servicing				X	X					
OS04		Plan, LAWS Mock-up Hardware Simulation				X	X					
OS05	2	Plan, Servicing Maintenance & Refurbish. Logistics				X	X					
OS06	3	Plan, Orbital Servicing Contamination Control				X	X					
OS07	3	Plan, ORU Inventory Control/Quality Maintenance				X	X					
OS08	3	Plan, Servicing GSE/STE Storage				X	X					
OS09	3	Analysis, ORU Support Requirements (SRAs)				X	X					
PRODUCT ASSURANCE (PA)												
PA01	1	Plan, Quality Assurance	X		X							
PA02	2	Analysis, Failure Mode and Effect (FEMA)				X	X					
PA03	2	List, Critical Items (CIL)				X	X					
PA04	1	Plan, Maintainability Program				X						
PA05	1	Plan, Reliability			X							
PA06	2	List, Limited Life Items					X					
PA07	1	Plan, EEE Parts Program			X							
PA08	2	List, EEE Parts				X	X					
PA09	1	Request, Nonstandard Parts Approval (NSPAR)			per event							
PA10	2	Document, NASA ALERT System			per event							
PA11	3	Reports, Nonconformance and Resolution			per event							
PA12	3	Reports, Nonconformance Summary			per event							
PA13	2	Analysis, Maintenance Concept				X	X					
PA14	1	Plan, Software Quality Assurance			X							
PA15	1	Certificate of Qualification (COQ)						X				
PA16	2	Analysis, Reliability Predictions				X						
PROJECT MANAGEMENT (PM)												
PM01	1	Plan, Project Management		X								
PM02	1	Plan, Performance Measurement		X								
PM03	3	Report, Monthly Cost and Schedule Performance			monthly							
PM04	1	Plan, Make or Buy	X									
PM05	3	Report, New Technology			annually							
PM06	2	Report, Project Schedule		X								
PM07	2	Structure, WBS & WBS Dictionary	X	X		-						
PM08	3	Report, Financial Management (533)			monthly							
SAFETY (SA)												
SA01	2	Data, Safety Compliance				X	X				X	
SA02	3	Report, Accident/Incident/Mishap			per event							
SA03	1	Plan, Safety	X									
SA04	2	Analysis, Systems Hazard				X	X	X				
SA05	2	Summary, Risk Management				X	X	X				
SYSTEM ENGINEERING (SE)												
SE01	2	Plan, System Engineering	X	X								
SE02	1	Plan, Mass Properties Control		X		X	X					
SE03	1	Plan, Electrical Power Control			X							
SE04	1	Plan, Materials and Processes Control			X							
SE05	2	List, Material and Process Specification (MPSL)				X						
SE06	2	List, Material Identification and Usage				X						

Figure 7-2. LAWS "Strawman" Data Requirements (Continued)

DR#	TYPE	DR TITLE	MAJOR MILESTONES									
			PROP	60 DAC	PRR	PDR	CDR	TST	CV DCR	FRR	LR	ORR
SE07	1	Agreement, Material Usage (MUA)										
SE08	2	Doc, LAWS Verif Reqmts & Spec (VSRD) Reqmts					X	X	X			
SE09	3	Report, Mass Properties		X		X	X					
SE10	3	Report, Electrical Power and Energy Status		X		X	X					
SE11	3	Analyses and Models, Sys and Subsys Technical				X	X					
SE12	3	Lists, Eng Dwgs/Doc, Specs and Standards				X	X					
SE13	3	Drawings			as released							
SE14	3	Diagrams, Schematics, and Lists, Electrical				X	X					
SE15	3	Handbook, Description				X	X					
SE16	3	Log Book, Equipment				-			X		X	
SE17	1	List, Instrumentation Progm & Command (IP&CL)			X	X	X					
SE18	3	Document, Design Reference Mission (DRM)			X	X	X					
SE19	1	Plan, Electromagnetic Cocmpatibility Control			X							
SE20	2	Inputs, Launch Site Support Plan			X	X	X					
SE21	3	Procedures, Special Handling and Storage							X			
SE22	1	Plan, Launch Site Contingency			X		X					
SE23	1	Plan and Report, Oribital Verification								X		
SE24	1	Requirements, LAWS Launch Site Operations				X	X					
SE25	2	Description, Cmd & Data Mgmt Subsys Fnct (C&DMS)				X	X					
SE26	2	Analysis, EEE Parts Application					X					
SE27	2	Matrix, LAWS Level I-IV Requirements						X				
SE28	3	Plan, Contamination Control & Implementation, CCIP					X					
SE29	3	Plan, LAWS System Alignment				X	X					
SE30	3	Error Budgets and Analysis, LAWS System			X	X	X		X			
SE31	3	Analysis, LAWS Systems Performance Prediction			X	X	X					
SE32	3	Plans and Procedures, Fracture Control				X	X					
SE34	3	Anal and Rept, Space Enviro Effct on Matl & Sys				X	X					
SE35	3	Document, Equations Definition			X							
SE36	3	Documentation, Elect Ground Support Eqmt (EGSE)				X	X					
SE37	3	Documentation, Mech Ground Support Eqmt (MGSE)					X					
SE38	1	Plans and Courses, Tech Support Persnl Training					X					
SE39	3	Space Debris Vulnerability Analysis										
VERIFICATION (VR)												
VR01	2	Plan, Manufacturing and Assembly	X	X								
VR02	1	Plan, Verification			X	X	X					
VR03	1	Document,Verif Reqmts & Specif (VRSD)			X	X	X					
VR04	2	Procedures, Verification Test						X				
VR05	2	Reports, Verification Test				-		X				

Figure 7-2. LAWS "Strawman" Data Requirements (Concluded)

Table 7-1. LAWS Major Project Milestones

Event	Occurrence	Purpose
ATP	Contract-go-ahead	Initiate Contract Activities
PRR	ATP + 3 Months	Establish Project Requirements Baseline
PDR	ATP + 9 Months	Establish and Approve Design Requirements Baseline
CDR	ATP + 18 Months	Establish and Approve Drawing Baseline
CI	ATP + 40 Months	Establish and Approve the Configuration Baseline
DCR	ATP + 40 Months	Certify qualification
FRR	ATP + 43 Months	Certify flight worthiness
Ship	ATP + 45 Months	Transport to Launch Site
Launch	ATP + 64 Months	Attain on-orbit configuration

ating data acquired by the LAWS Instrument. It was assumed the LAWS Instrument contractor would be responsible for evaluating and verifying performance of the Instrument, and that NASA would be responsible for evaluation of the data acquired by the Instrument.

The WBS tasks required to accomplish project objectives were summarized in Section 7 of this Volume and presented in some detail in DR-5, "Draft WBS and WBS Dictionary". This part of the project definition looks at the time phasing of the WBS tasks implementation to accomplish project deliverables and meet milestones.

7.2 LAWS PHASE C/D LOGIC NETWORK

Once the project deliverables and associated tasks have been defined, the next part of the planning process is to determine how the project will be accomplished. The planning tool for this is a logic network. The preliminary LAWS Phase C/D Logic Network is presented in Figure 7-4. It reflects the interrelationships of the key

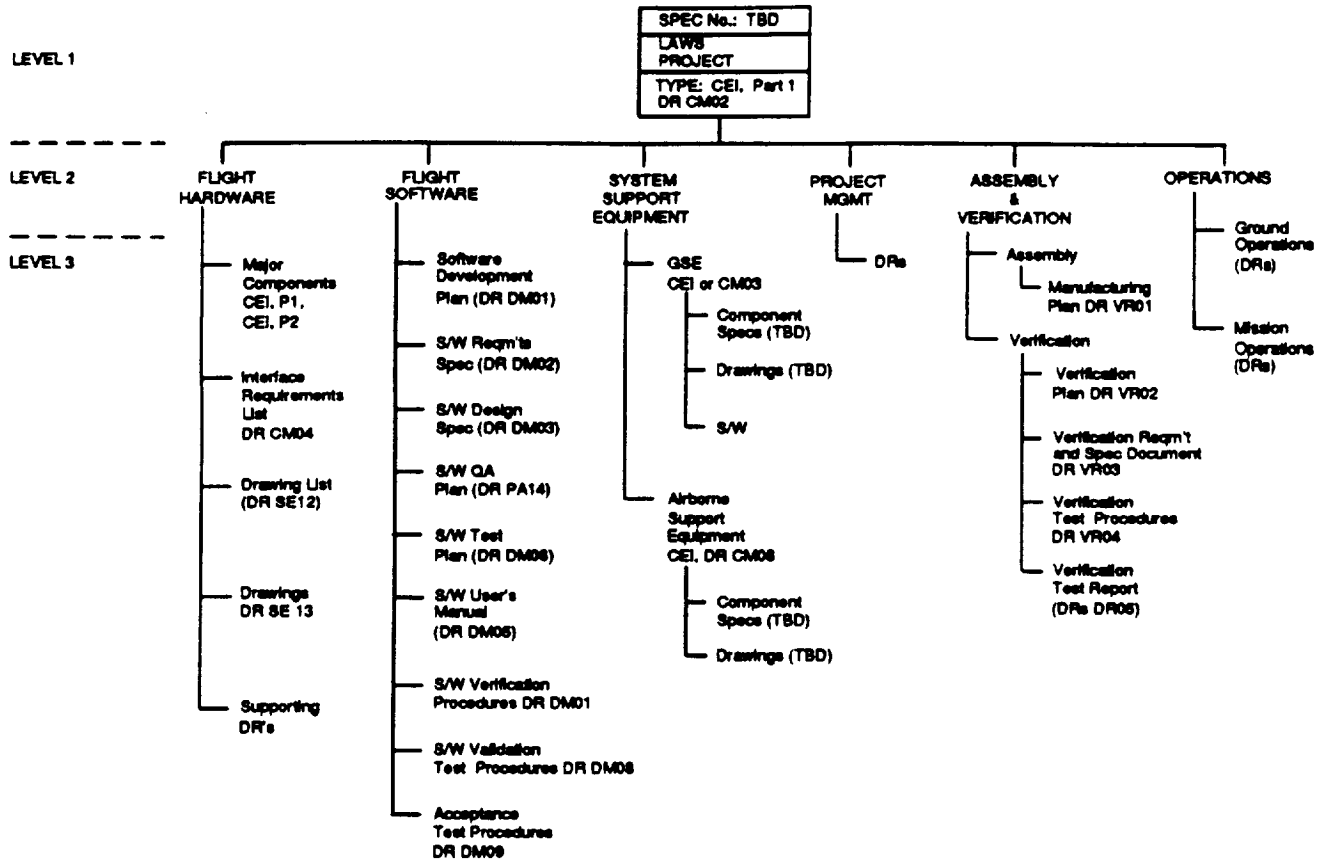

Figure 7-3. LAWS Phase C/D Documentation Tree

milestones discussed above, major events, and those activities necessary to meet the projects deliverable requirements.

The proposal process prior to submission of the formal proposal for evaluation is an important part of the initial planning for Phase C/D implementation. Items that are customarily included in a proposal for a Phase C/D project are the preliminary contract end item specifications, the Software Development Plan, the Product Assurance plans (e.g., quality and safety), the Manufacturing and Assembly Plan, and the Project Management plans. Project management plans cover configuration management, scheduling, make or buy, and the WBS Dictionary. In essence, the above items define the approach the prime contractor intends to implement, and the method he will pursue to implement it. During the time between ATP and PRR, the project plans are updated, new ones written where required, and the LAWS project requirements reviewed. The milestones associated with this phase of the project are those identified as 60 DAC in Figure 7-2. The objectives are to finalize the project plans and establish a requirement baseline.

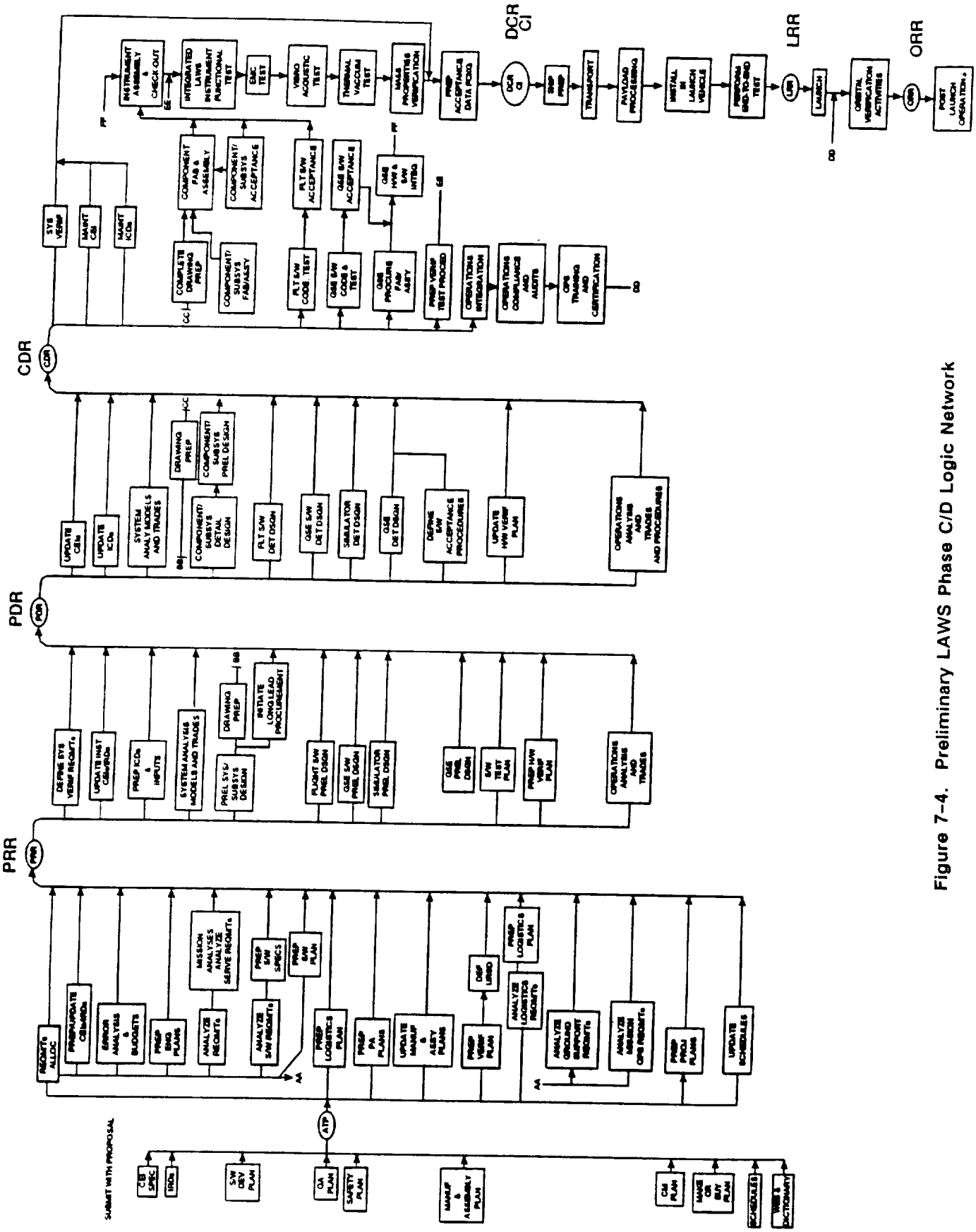

Figure 7-4. Preliminary LAWS Phase C/D Logic Network

After the PRR, system engineering activities will begin to address verification requirements and prepare/release contract end item specifications. In the Phase I analysis activities the flight hardware design activities are simply identified as system/subsystem design activities. These will be expanded in detail as the subsystem definition matures. It should be noted that the software and GSE PDRs and CDRs may not be held concurrently with the flight hardware design reviews. This is primarily because much of the GSE and GSE software will be required to support the integration and assembly of the flight hardware. Review dates for these activities will be recommended as the system definition matures. Concurrently with the hardware and software design activities, the contractor will be required to define the LAWS Instrument verification plan and associated procedures for the verification, and define the operational aspects of the projects. Operations covers both ground operations and mission operations. Ground operations as used in this project definition is concerned with the logistics, transportation, and launch site integration. Mission operations is concerned with those activities required to support the definition of flight operations. During the PDR phase, ground operations activities will address inputs to the launch site integration plan and planning for shipping. Mission operations activities will begin to address the ground facility mission requirements, orbital timelines, verification, and training.

After the CDR activities are complete, the project will proceed with the completion of drawings and release of the hardware items (flight and SSE) to procurement and fabrication. At the same time, the software will be coded and tested. It should be remembered that separate PDRs and CDRs may be utilized. Concurrently with these activities verification procedures will be prepared for the Instrument verification test program. Operation activities will be directed toward supporting definition of the mission timelines, supporting the determination of ground based facilities requirements, defining training, and preparing documentation for the mission team. This includes training material, procedures, timelines, and verification procedures. It was assumed that the verification tests would include functional test of the LAWS flight hardware, environmental tests, and mass properties verification. After launch, orbital verification has been included to verify that the Instrument is functioning properly after deployment in orbit.

7.3 LAWS PHASE C/D MASTER SCHEDULE

The preliminary LAWS Phase C/D master schedule is presented in Figure 7-5. It has been constructed to correspond to the WBS elements in Section 6 and time phases

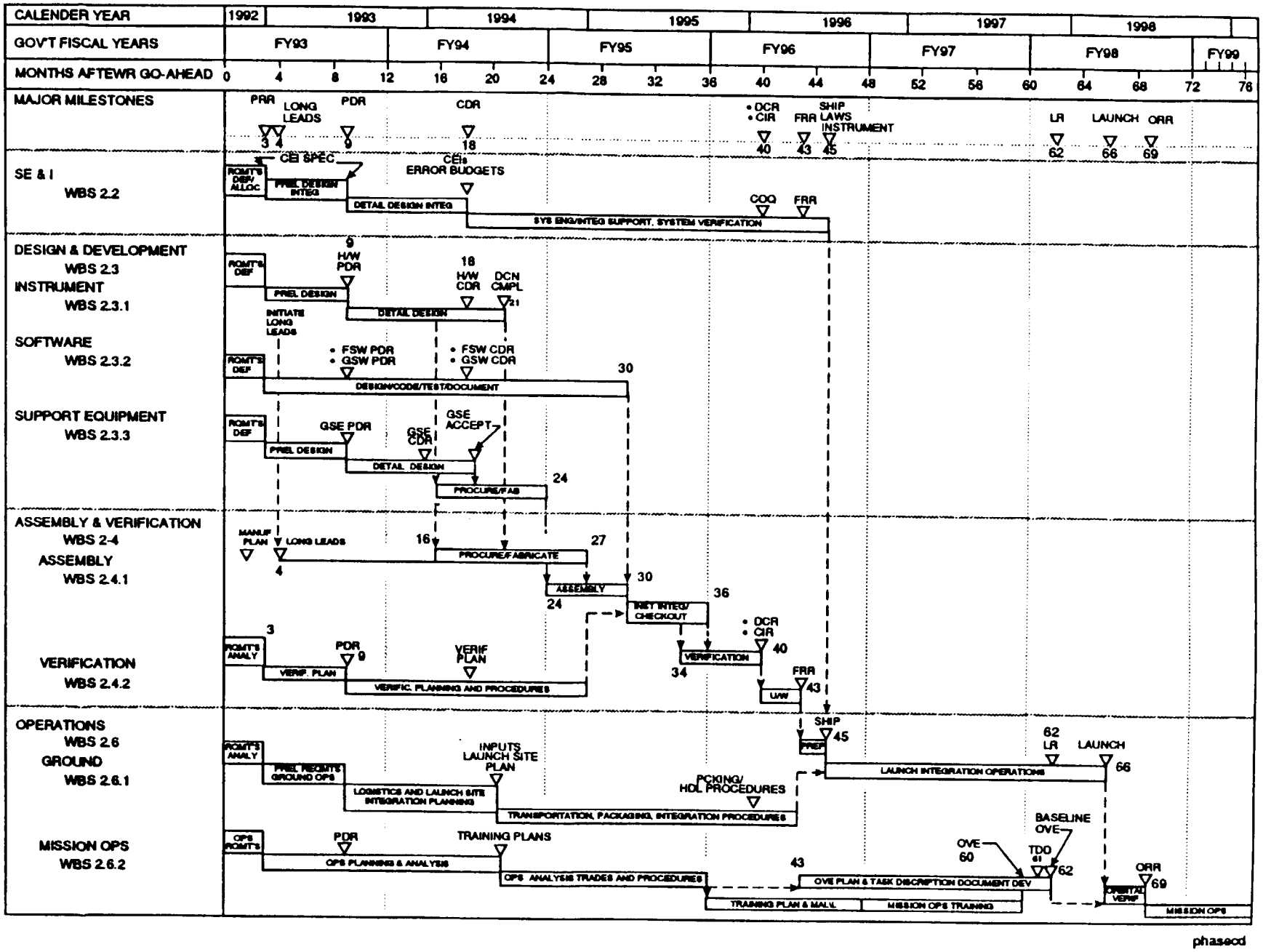

Figure 7-5. Preliminary LAWS Master Schedule for JPOP Phase C/D

the logic network presented in Figure 7-4. From ATP through orbital verification the project spans 69 months. A PRR has been scheduled three months after ATP. The intent of this review is to finalize the requirements defined and documented in Phases I and II and to approve the project plans.

After the CDRs (i.e., hardware, software, and GSE), drawing release activities will be completed, and the assembly and integration process initiated. Analysis indicates that the Instrument integration and checkout will be initiated about 24 months after ATP. This is based on estimated delivery of the laser and telescope 24 months after placement of subcontracts for these items. Laser and telescope delivery would then occur at about 28 months after ATP. These items are considered to be long lead items. Instrument assembly is scheduled to be complete by month 36 with Instrument verification complete by month 40. Verification of the LAWS includes Instrument integrated functional tests, environmental tests, electromagnetic compatibility tests, thermal vacuum tests, and mass properties verification. The CI and Design Certification Reviews (DCR) should be conducted about month 40, and the certification for flight readiness completed by month 43. At the present time, 3 months of unscheduled work are indicated to correct any deficiencies noted in the CI, DCR, and FRR activities. Shipment is scheduled at about month 45 after ATP.

Because of the fairly long launch integration time, most of the mission training and flight operation certification activities are scheduled between 36 and 62 months after ATP. This period is just over two years and includes developing training procedures and materials, preparing an Orbital Verification and Evaluation (OVE) plan, and conducting mission simulation and training exercises. The result of these activities will be a baseline OVE at about 62 months after ATP and a Task Description Document at about 61 months after ATP. The LRR should then be held at about month 64 with launch occurring at 66 months after ATP.

The current schedule calls for the first three months of the mission to be devoted to orbital verification. This is an evaluation period to verify that the Instrument is functioning properly, and that the mission operations facility is also functioning properly. An Operational Readiness Review (ORR) is scheduled 69 months after ATP. After successfully completing this review, the experiment is scheduled for operation for the next 57 months.

Appendix A

LAWS SYSTEM AND SUBSYSTEMS DESIGN TRADE STUDIES SUMMARY

LAWS DESIGN ENHANCEMENTS

NASA Strawman LAWS System	Lockheed LAWS System
Coherent Lidar • Pulsed Transmitter (CO_2) • 9.11 μm Wavelength • 3 μsec Pulse Length • 10 Hz PRF • 10 Joules/Pulse • 5% Wallplug Efficiency • 10^9 Shots Lifetime **Telescope** • 1.5 m Aperture • 6 rpm Scan Rate • 45 deg Nadir Angle	**Coherent Lidar** • Pulsed Transmitter (CO_2) • 9.11 μm Wavelength (11.2 μm being Considered) • 1 μsec - 3 μsec • 1 - 10 Hz on Demand • 20 Joules/Pulse • 5% Wallplug Efficiency • 10^9 Shots Lifetime **Telescope** • 1.67 m Aperture • 6.6 rpm • 35, 45, 55 deg Nadir Angles

LAWS - 10

LAWS
NASA\MSFC

LAWS SYSTEM DIAGRAM

Lockheed
Huntsville

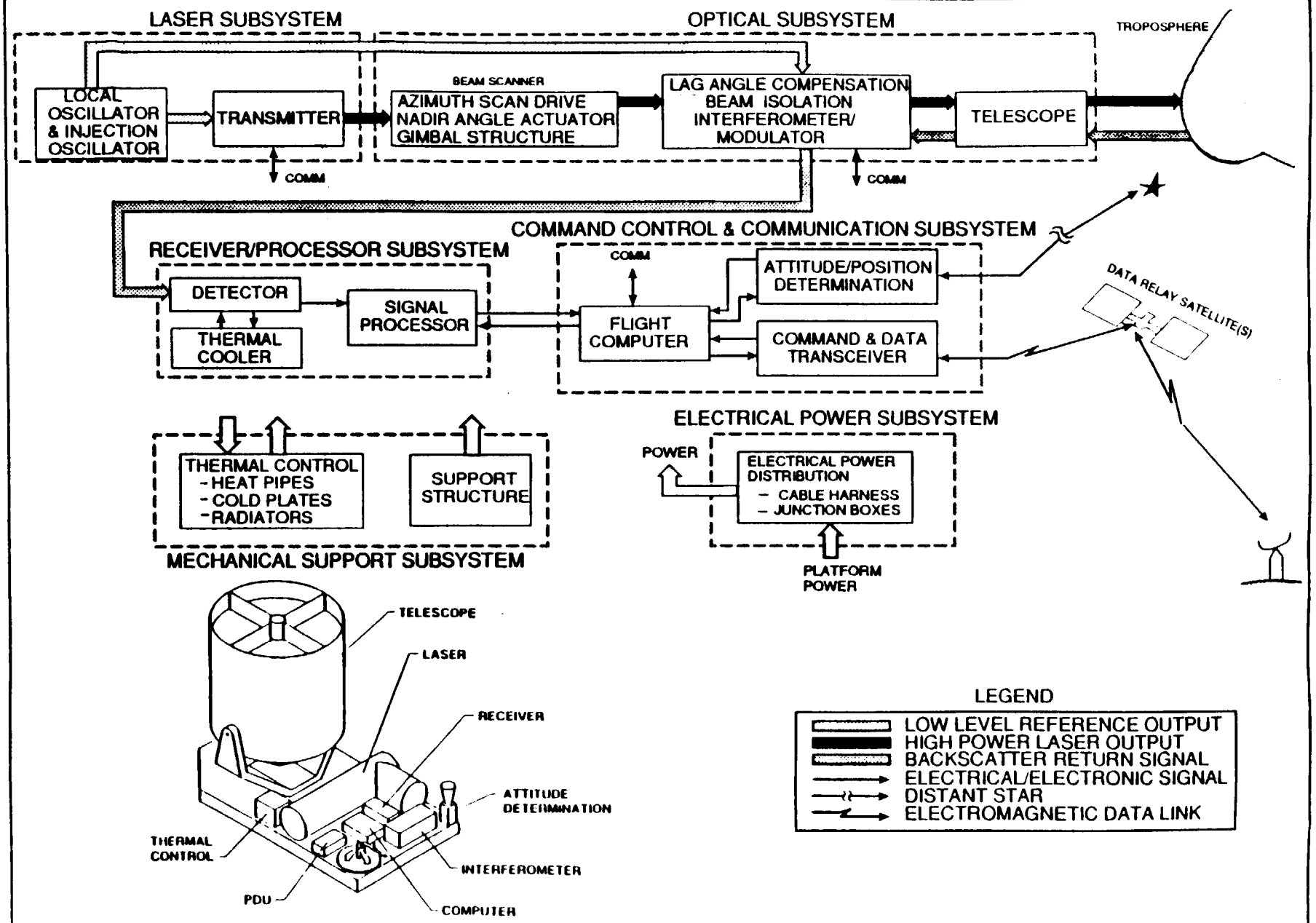

CONCEPT SELECTION

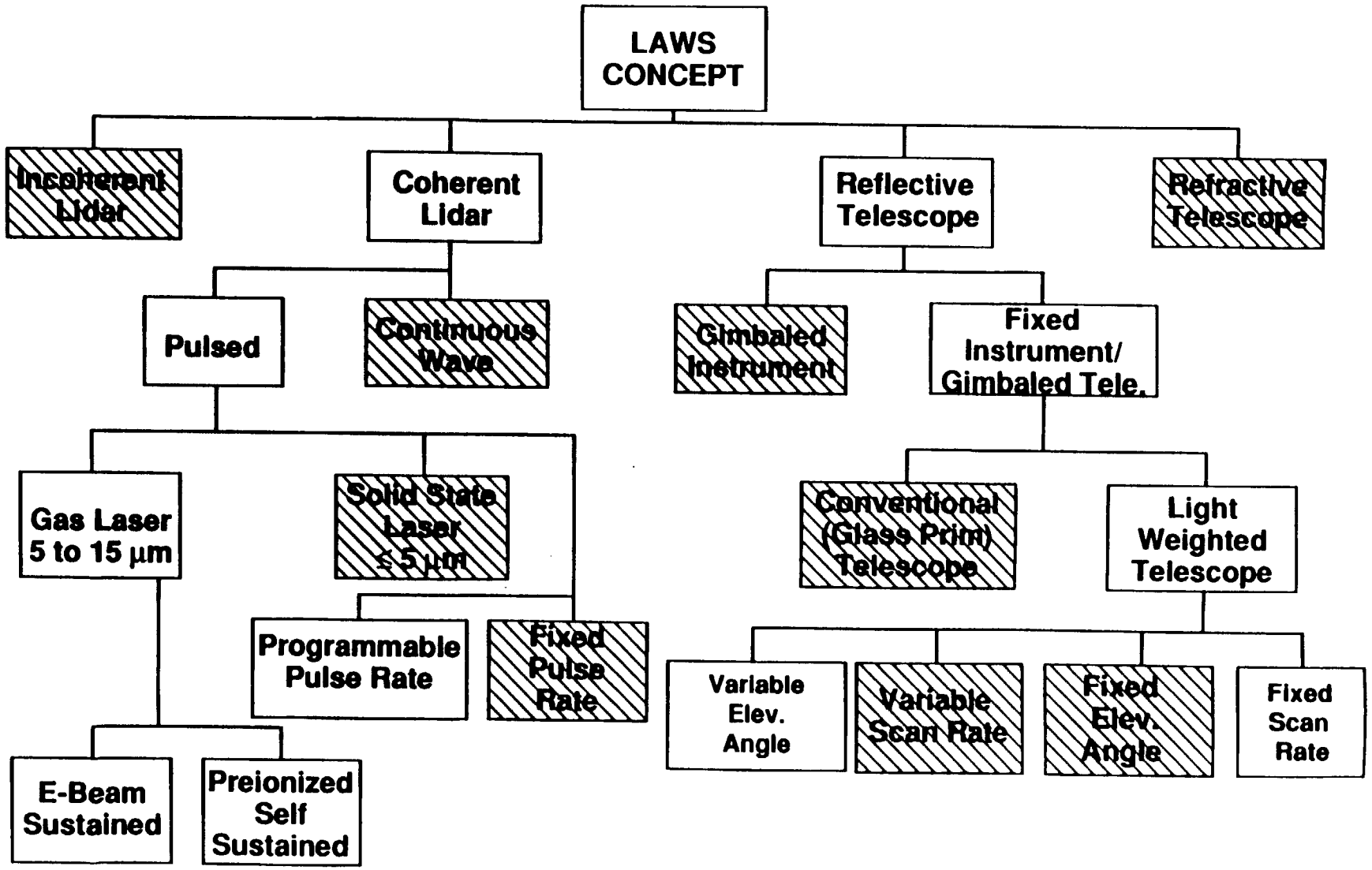

LAWS
NASA\MSFC

SYSTEM LEVEL TRADES

Lockheed
Huntsville

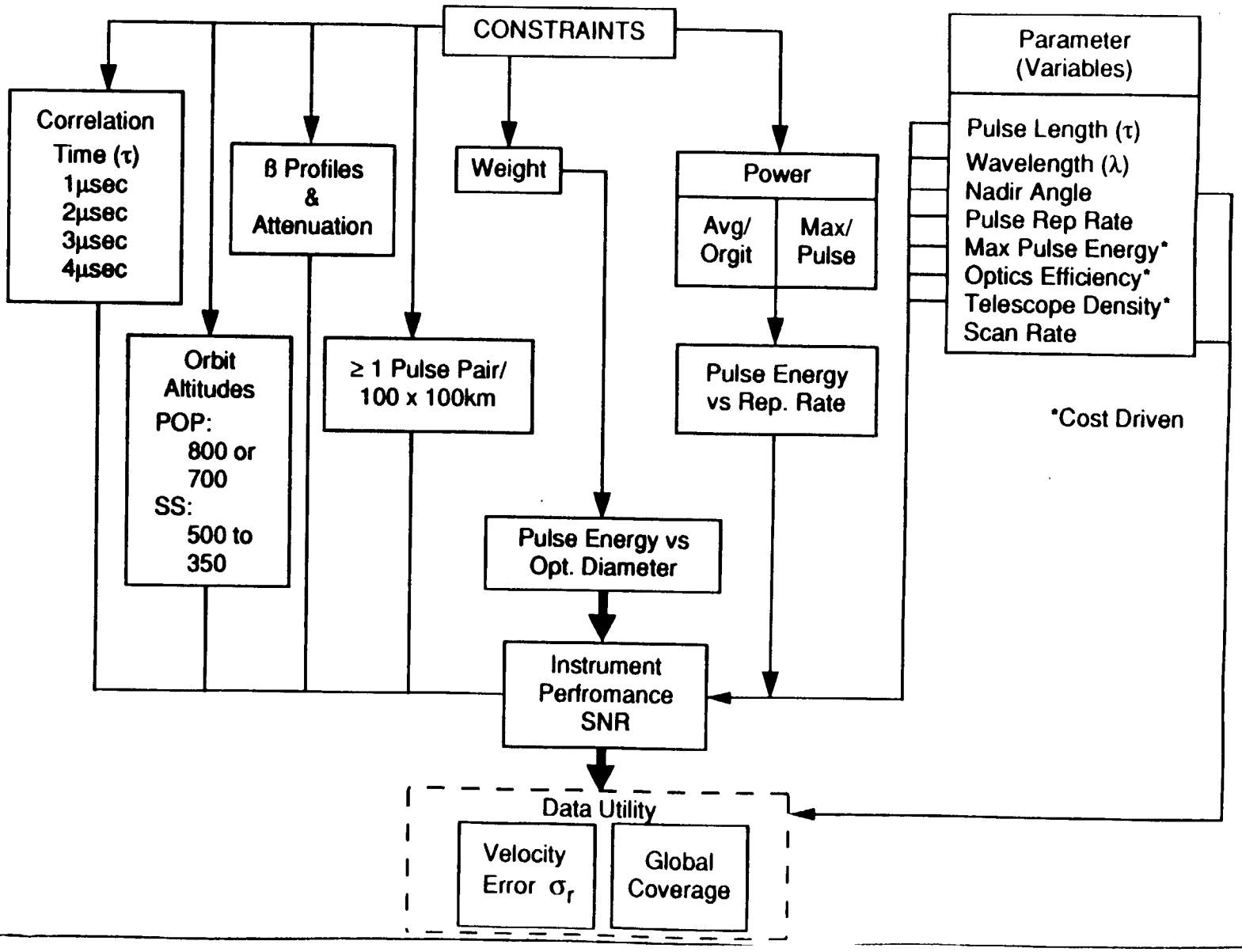

sys level trades.djw

LAWS
NASA\MSFC

400KG COMBINED LASER/TELESCOPE/ MOTOR/BEARING CONCEPT TRADES

Lockheed
Huntsville

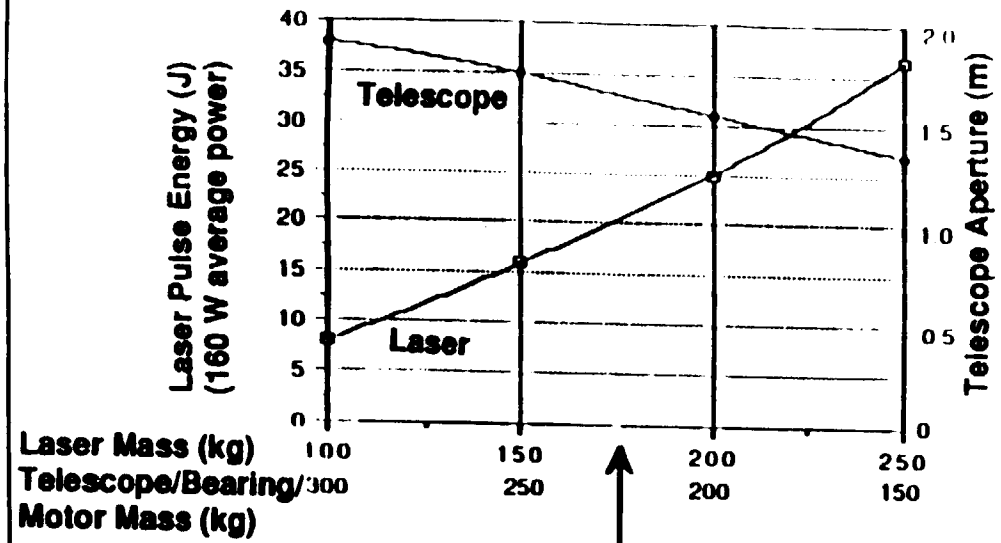

Nominal Design Concept

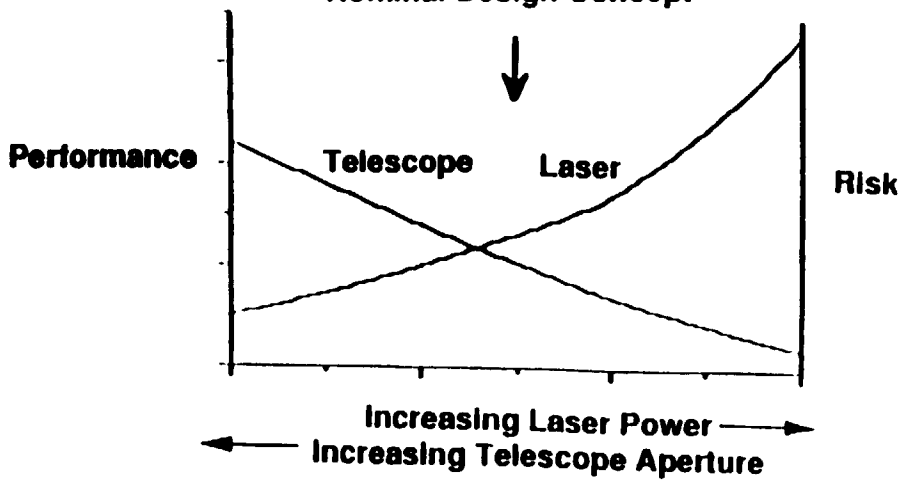

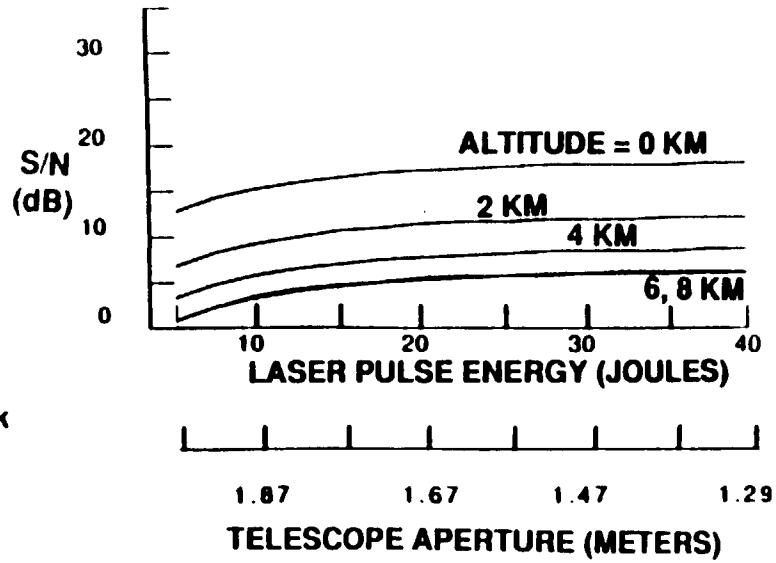

LAWS
NASA\MSFC

SHOT MANAGEMENT PLOT/COVERAGE

Lockheed
Huntsville

SATELLITE ALTITUDE = 800 KM
NADIR = 45 DEG

SCAN RATE = 6.7 SCANS/MIN

RAPID PULSE RATE = 8 HZ
LASER POWER = 3200 W

MODERATE PULSE RATE = 5 HZ
LASER POWER = 2000 W

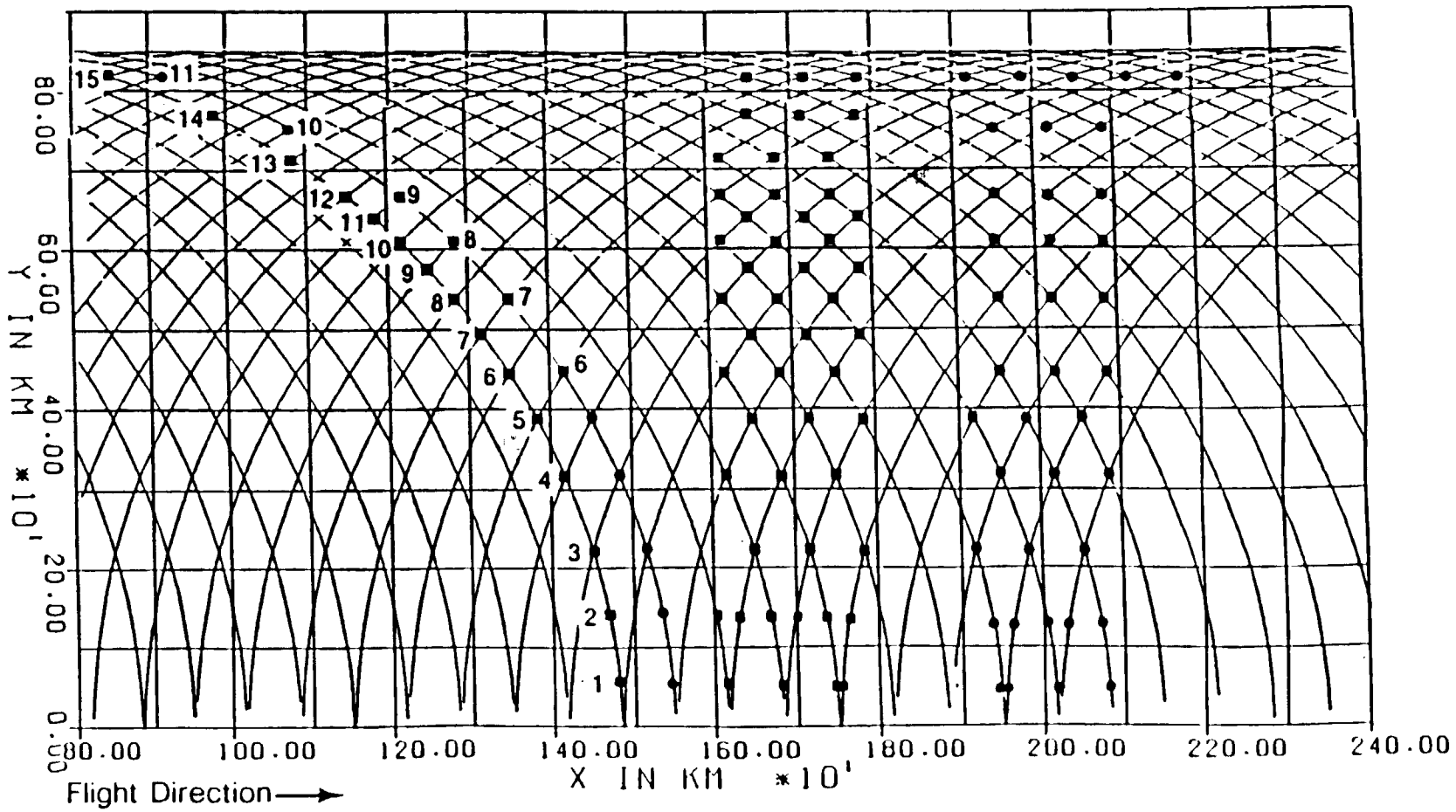

LASER REQUIREMENTS

Performance Requirements

- ≤ 175 kg Weight
- ≥20 Joules/Pulse
- 3 Microsec Pulse Length
  (will also consider 1 μsec)
- ≥10^9 Pulse Lifetime
- Controllable Pulse Rate up to 8 Hz
  (≥125 ms between pulses)
- ≤200 KHz Chirp
- Max. Average Input Power of 3200 watts
- >5% Wall Plug Efficiency at Max. Power

FEATURES OF GEC TRANSMITTER

- E BEAM SUSTAINED DISCHARGE FOR HIGH EFFICIENCY, GOOD FREQUENCY CONTROL, LOW CO_2 DISSOCIATION AND TOP HAT PULSE SHAPE
- POWER OSCILLATOR FOR REDUCED WEIGHT & VOLUME
- LARGE APERTURE FOR TRANSFORM LIMITED CHIRP
- UNSTABLE RESONATOR FOR SINGLE TRANSVERSE MODE OPERATIONS
- OFF-AXIS PULSED INJECTION SEEDING FOR LONGITUDINAL MODE AND WAVELENGTH CONTROL
- EMITTED RADIATION BELOW BACKGROUND LEVEL FOR JPOP ORBIT

GEC LAWS LASER SYSTEM

- CONFIGURATION SELECTION HAS BEEN COMPLETED
- ELECTRON BEAM SUSTAINED LASER SELECTED BY GEC
- UNSTABLE RESONATOR OPTICAL CAVITY
- PULSED INJECTION CONTROL OF MODE & WAVELENGTH
- LAWS LASER CONSISTS OF FOUR MAJOR SUB-SYSTEMS:
  - ELECTRON GUN
  - LASER (POWER OSCILLATOR)
  - SWITCH
  - INJECTION OSCILLATOR

Energy per Pulse	20 J
Pulse Width	3 μs
PRF	8 Hz
Weight	174 kg
Chirp	<200 k Hz
Average Input Power	2720 W
Lifetime	10^9 shots
Wall-Plug Efficiency	5.9%

GEC LAWS Laser Concept

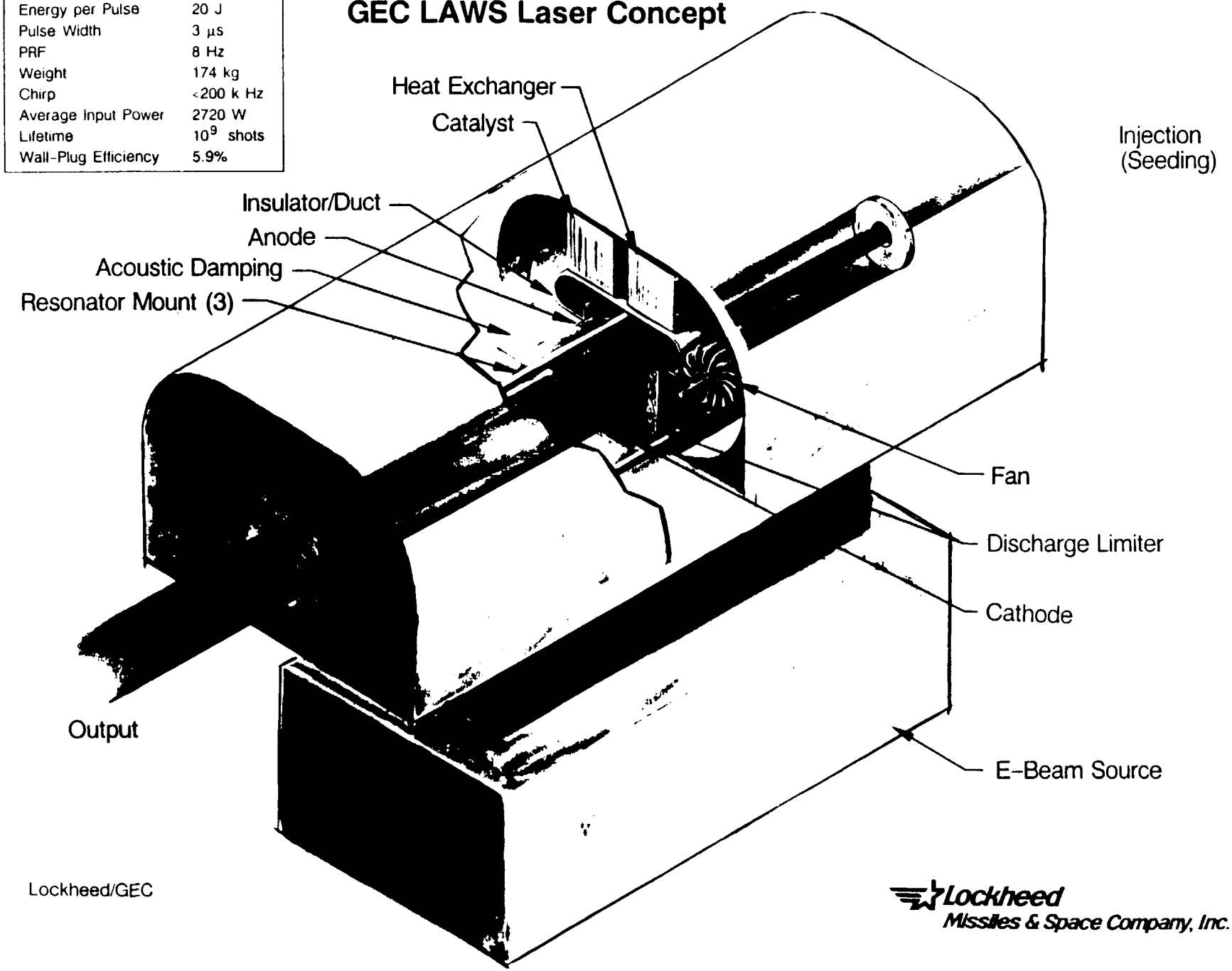

Lockheed/GEC

Lockheed
Missiles & Space Company, Inc.

AVCO LAWS Laser Concept

Energy per Pulse	20 J
Pulse Width	1-3 μs
PRF	8 Hz
Weight	171 kg
Chirp	<200 k Hz
Average Input Power	2800 W
Lifetime	10^9 shots
Wall-Plug Efficiency	5.7%

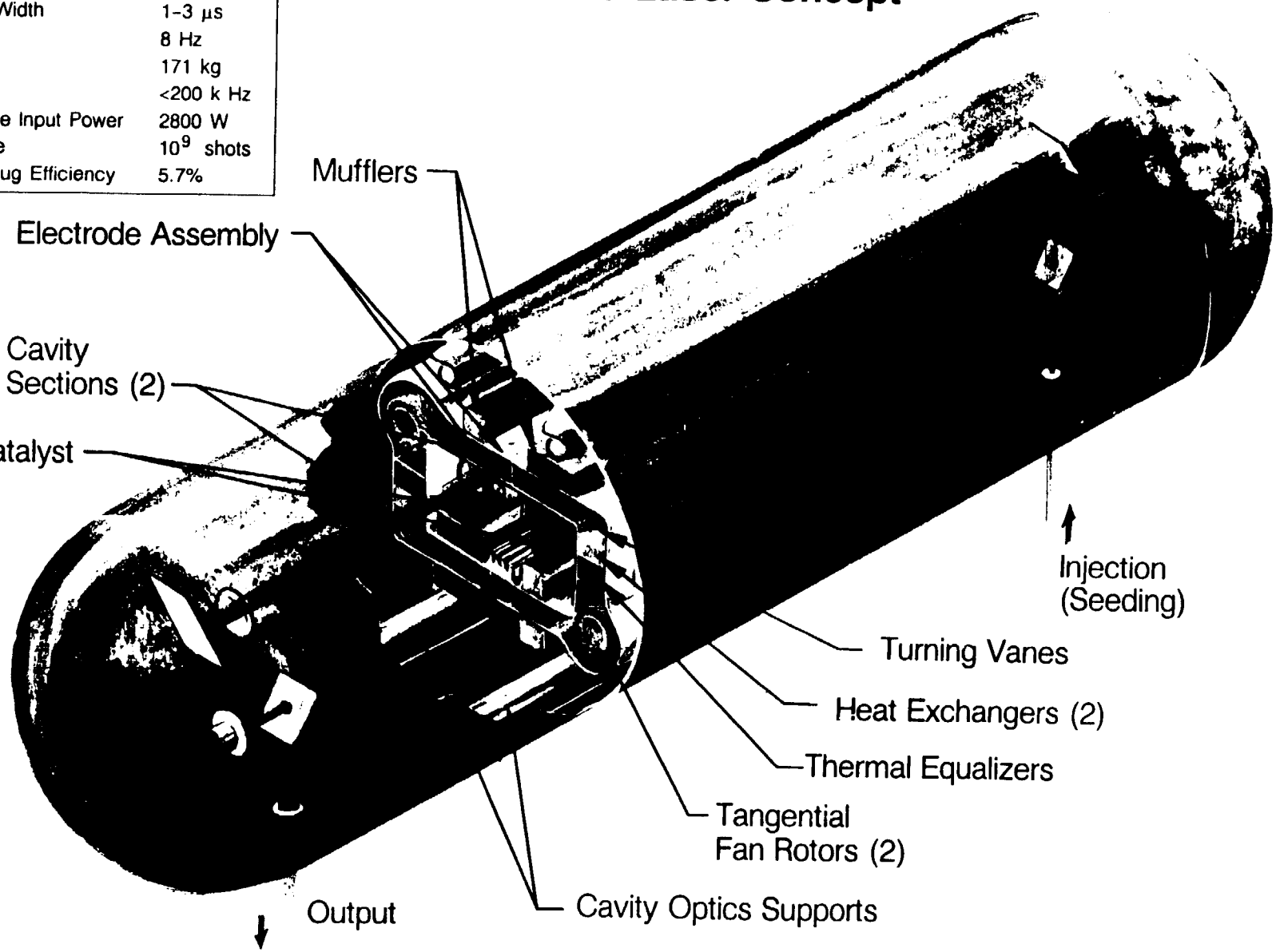

Lockheed/AVCO

Lockheed Missiles & Space Company, Inc.

LAWS PHASE I TRADES LEAD TO OPTIMUM SYSTEM

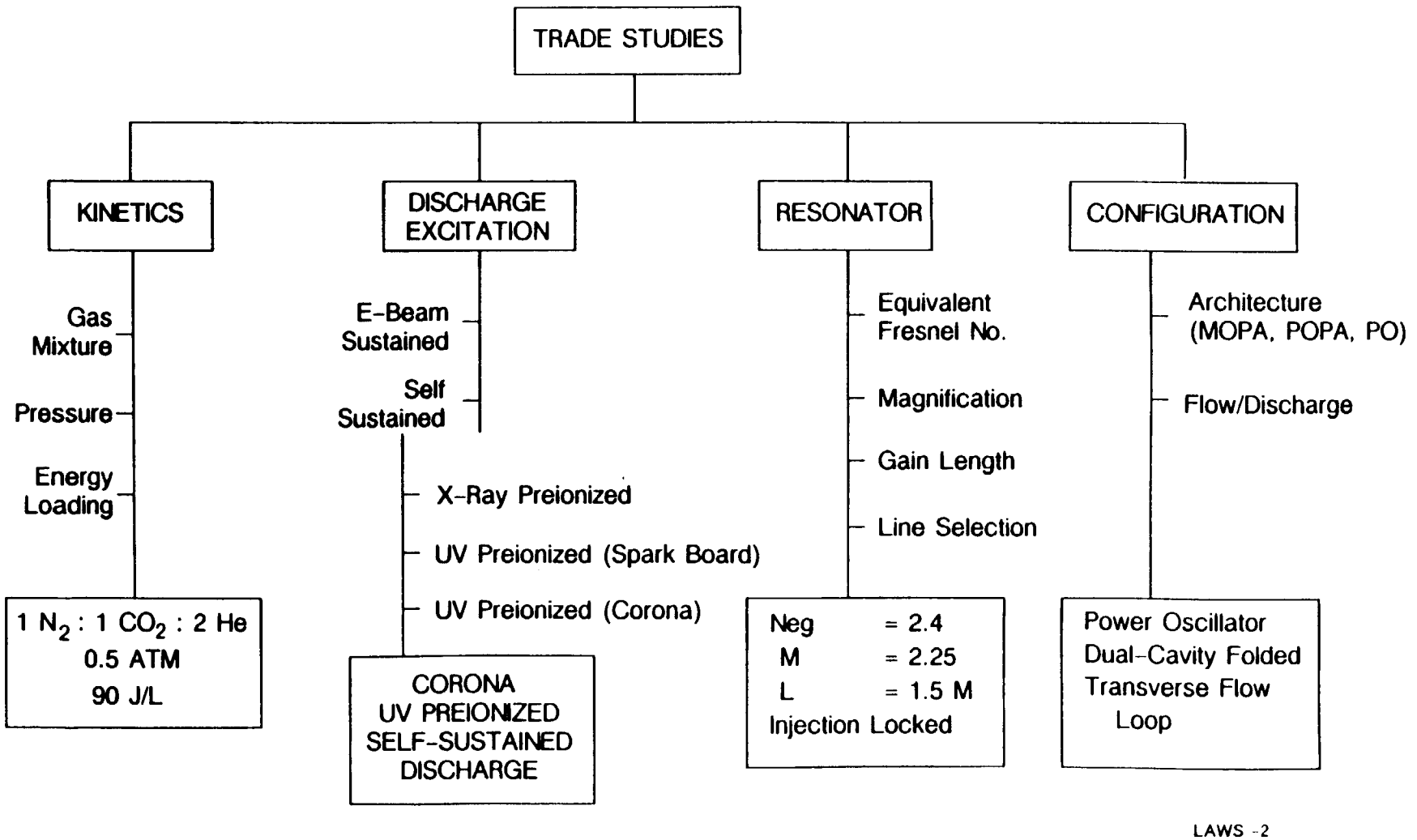

BASELINE TRANSMITTER SYSTEM BLOCK DIAGRAM

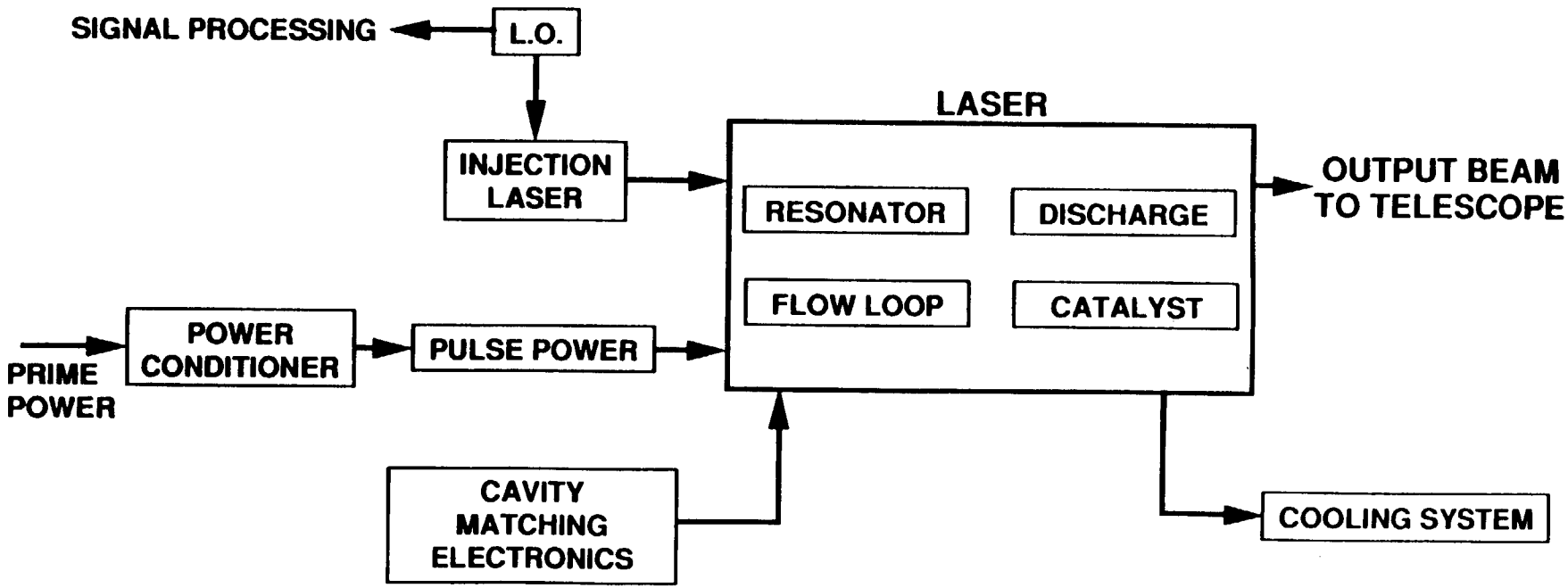

LAWS
NASA \ MSFC

SALIENT FEATURES OF THE BASELINE TRANSMITTER

Lockheed Huntsville
Avco Research TEXTRON

- POWER OSCILLATOR FOR LOW WEIGHT AND VOLUME
- MODE SELECTION BY INJECTION LOCKING
- RELIABLE TRANSVERSE MODE CONTROL ENSURED THROUGH ARL DEMONSTRATED PROCEDURE FOR FULL APERTURE EXTRACTION AND APPROPRIATE FRESNEL NUMBER SELECTION
- TRANSVERSE FLOW LOOP WITH DUAL DISCHARGE CAVITY FOR COMPACTING
- CORONA PREIONIZED SELF SUSTAINED DISCHARGE WITH LOW SPECIFIC ENERGY LOADING FOR MAXIMUM LONG TERM RELIABILITY
- FLEXIBLE PACKAGE INCORPORATING A MODULAR DESIGN FOR BOTH LASER AND PULSE POWER

LAWS
NASA \ MSFC

DUAL-CAVITY TRANSVERSE FLOW LOOP FOR MINIMUM SIZE AND WEIGHT

Lockheed Huntsville
Avco Research TEXTRON

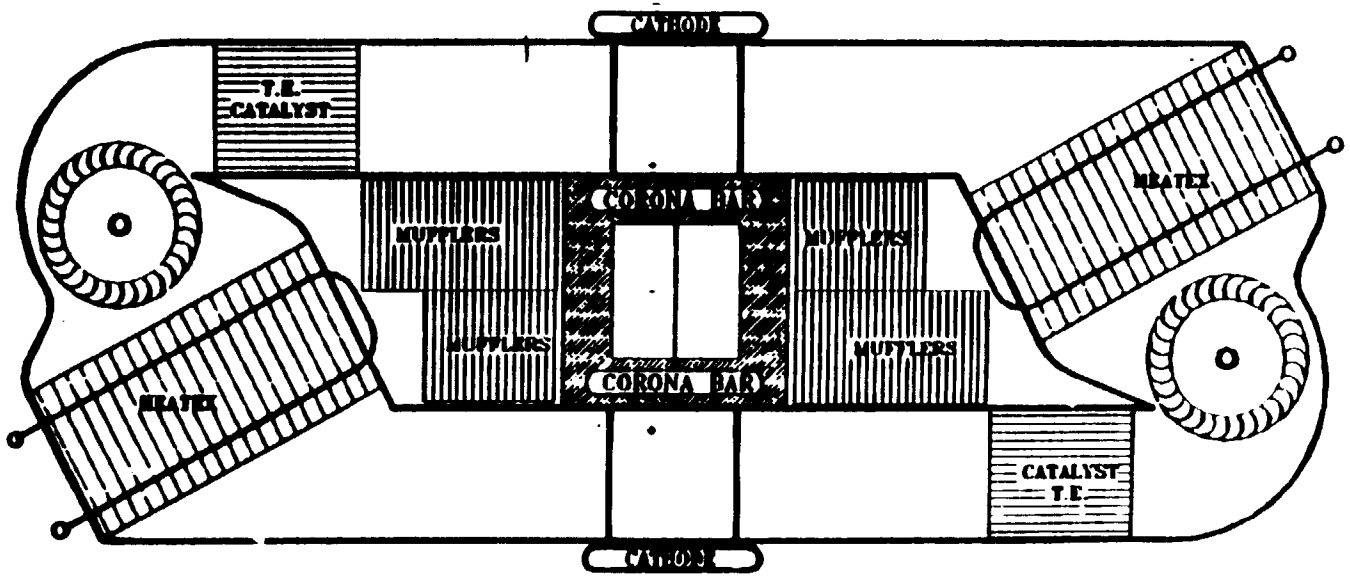

KEY FEATURES

- PACKAGE SIZE AND WEIGHT MINIMIZED
- LOOP LOSSES, THUS POWER CONSUMPTION, MINIMIZED
- GOOD THERMAL MANAGEMENT & FLOW DISTRIBUTION
- ADEQUATE ACOUSTICAL CONTROL
- ADEQUATE ELECTRICAL TRACKING DISTANCES

LAWS
NASA \ MSFC

OUTSTANDING DESIGN ISSUES ARE MAINLY LIFETIME RELATED

Lockheed Huntsville
Avco Research TEXTRON

- **DISCHARGE**
  - PREIONIZER DIELECTRIC FAILURE
  - ELECTRODE EROSION
- **FLOW LOOP**
  - FERRO FLUIDIC SEAL LIFETIME - FLUID LOSS, SEAL FAILURE
  - GAS CONTAMINATION - MATERIALS DAMAGE
- **CATALYTIC CONVERTER**
  - REDUCTION IN CATALYST EFFICIENCY
  - ISOTOPE SCRAMBLING
- **GAS COMPOSITION**
  - OXYGEN BUILD-UP
  - LOSS OF CO_2
  - NOX FORMATION
  - CONTAMINATION DUE TO OUTGASSING
- **PULSE POWER**
  - CAPACITOR
  - HV SWITCH

LAWS
NASA \ MSFC

LAWS LASER SUMMARY AND RECOMMENDATIONS

Lockheed Huntsville
Avco Research TEXTRON

- ARL BASELINE DESIGN ADDRESSES ALL THE PERFORMANCE REQUIREMENTS OF THE LAWS TRANSMITTER
- ARL DESIGN IS BASED ON INDIVIDUAL PERFORMANCE PARAMETERS DEMONSTRATED IN THE LABORATORY AND ALSO FIELDED DEVICES
- DESIGN PARAMETERS HAVE BEEN CHOSEN CONSERVATIVELY TO ADDRESS THE 10^9 - SHOT LIFETIME ISSUE
- A DEMONSTRATION OF ALL THE PERFORMANCE PARAMETERS IN AN INTEGRATED DEVICE SHOULD BE MADE A HIGH PRIORITY SINCE SUCH HIGH POWER LIDAR QUALITY TRANSMITTERS OF THE LAWS TYPE ARE YET TO BE DEMONSTRATED
- LASER LIFETIME ISSUES HAVE BEEN IDENTIFIED AND RISK REDUCTION EXPERIMENTS HAVE TO BE PERFORMED TO ACHIEVE THE DESIRED GOAL

LAWS
NASA\MSFC

LAWS OPTICAL SYSTEM

Lockheed
Litton Huntsville
Itek Optical Systems

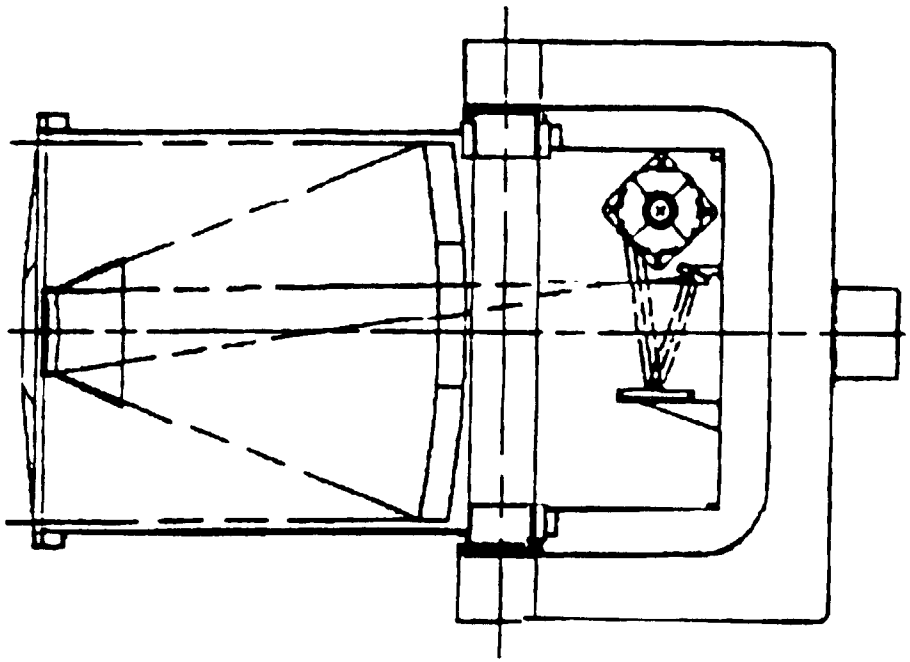

REQUIREMENTS

- **1.67m clear aperture**
- **Weight 223kg**
- **6.8 RPM rotation azimuth**
- **35°, 45° and 55° selectable Nadir angle**
- **Average power <221 watts**
- **Meets optical and packaging requirements**

OPTICAL SUBSYSTEM ABBREVIATED RAY TRACE

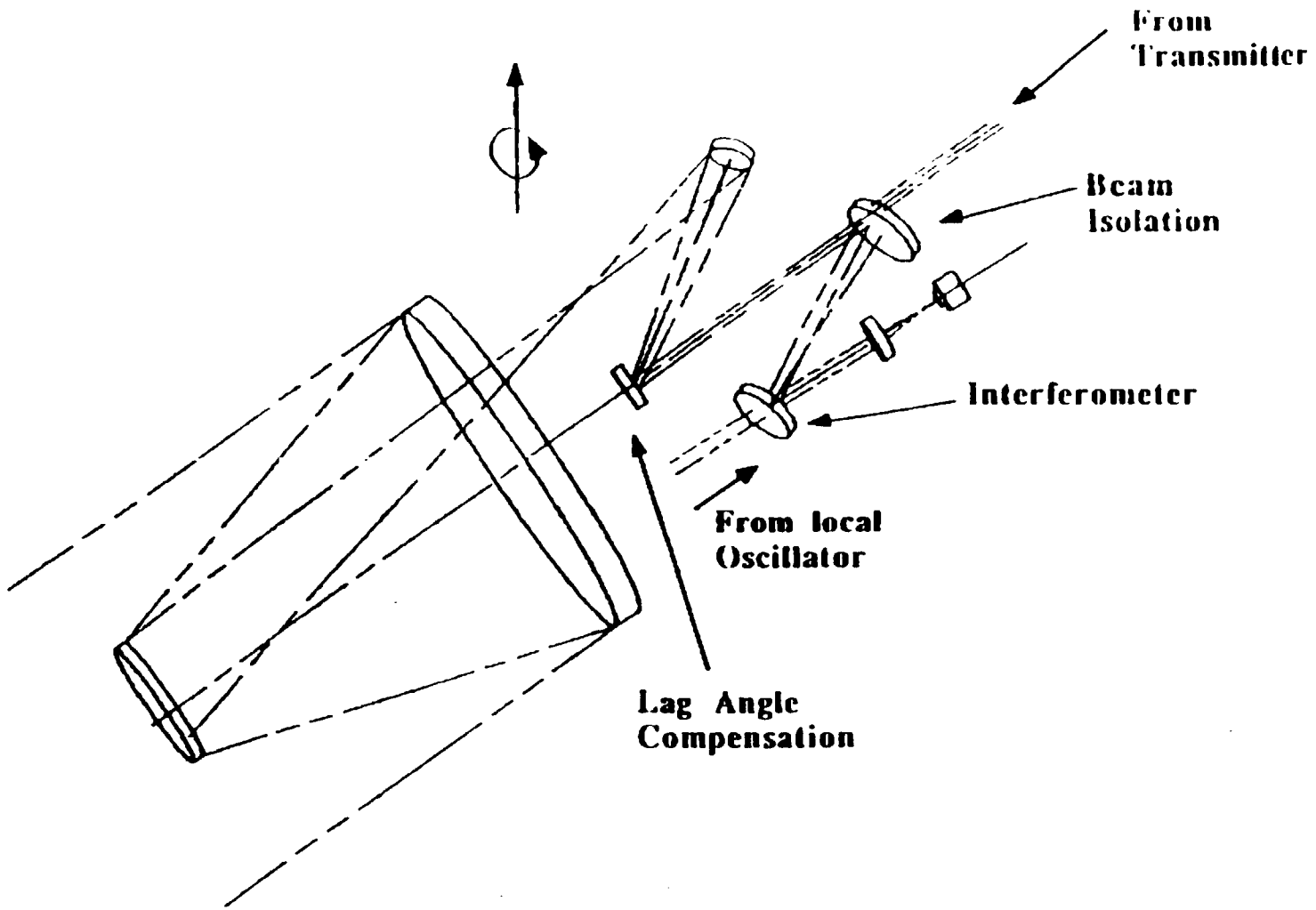

LAWS TRADE MATRIX

	Optical System	Real Pupil	Flat Field	<0.05 λrms Wavefront Error	Obscuration <7% Area	Mfg & Align Difficulty	Comments	
Afocal Cassegrain	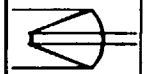	No	No	No	No	Low	No real pupil, Unacceptable image quality	UNACCEPTABLE
Afocal Gregorian	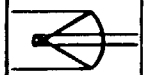	Yes	No	No	Possible, not likely	Low	Unacceptable image quality	
Three Mirror Afocal-on-axis		Yes	Yes	Yes (up to 10X Magnification)	No	Low	Unacceptable Obscuration	
Three Mirror Afocal eccentric in Field	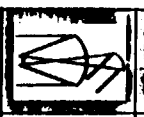	Yes	Yes	Yes (<12X Magnification)	Yes	Moderate	Baseline Concept	ACCEPTABLE
Three Mirror Afocal eccentric in Pupil		Yes	Yes	Yes (<8X Magnification)	No obscuration	High	Requires fast primary mirror (F/5) Large Volume	
Three Mirror Afocal Unusual Surface 3-D Geometry	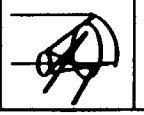	Yes	Yes	Under Investigation	No obscuration	High	Can be made extremely compact	

	SHELL		ATHERMALIZED TRUSS		TRIPOD	
	Gr/Ep	Be w/BLE Rods	Gr/Gr	Be/Gr	Gr/Ep	Be
WFE λ_{rms}**	.015	.047	.008	.010	.018	.10
Weight (lbs)	62	65*	50	48	30	18
Thermal Control Weight	7.8	8.0	11	11	9.0	9.0
Power (Watts)	110	115	85	83	64	64
Fo (Hz)	200	335	200	200	200	200
Soak/Gradient	20°C/2°C	20°C/2°C	20°C/1°C	20°C/1°C	20°C/3°C	20°C/1°C
Comments		Excessive WFE due to Tip of Secondary	Accessibility high cost		Accessibility	Excessive WFE

* Based on Minimum Be thickness

** 0.015λ allocated to structure

Itek Optical Systems

LAWS
NASA\MSFC

RECEIVER SUBSYSTEM

Lockheed
Huntsville

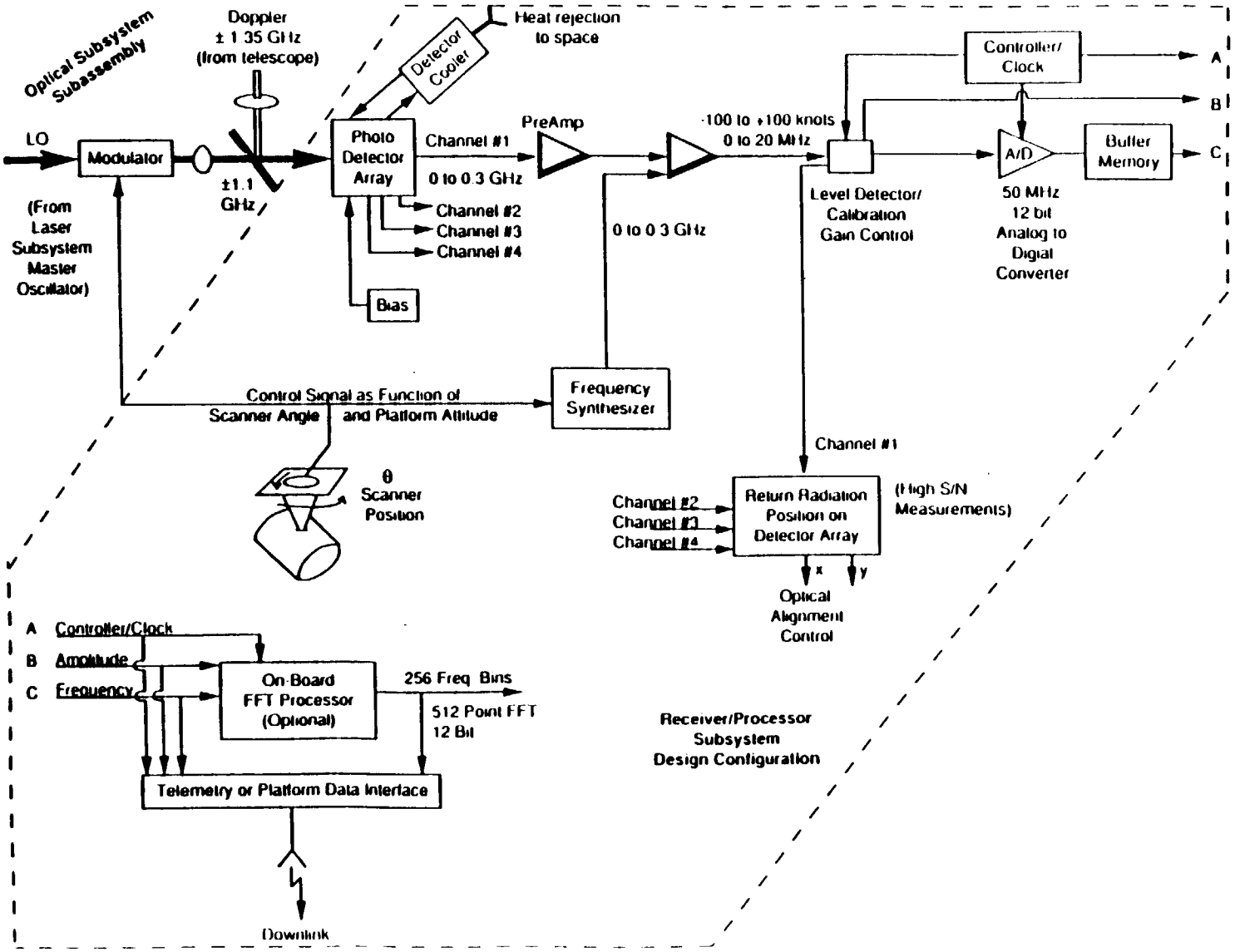

RECEIVER TRADES

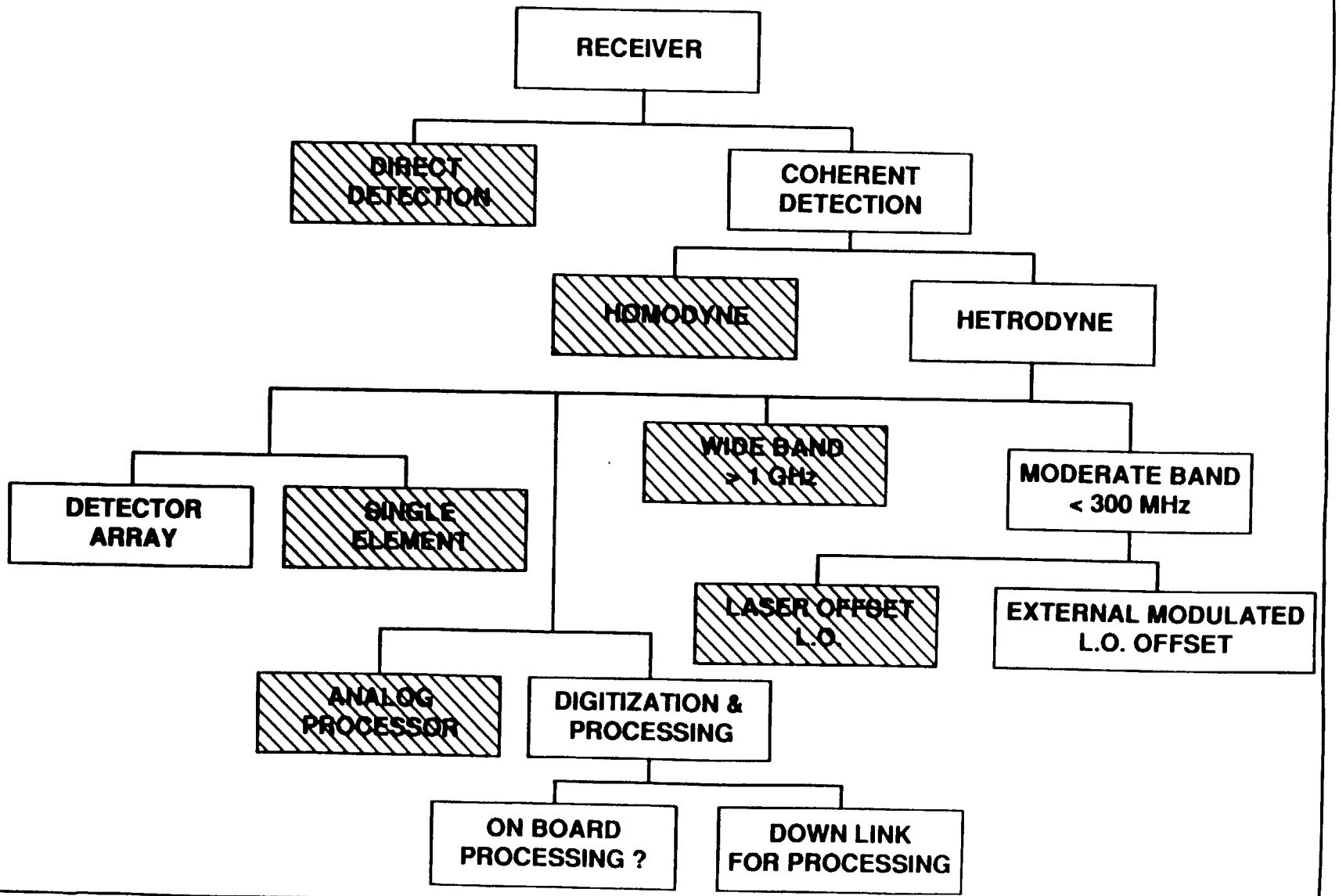

receiver trades

LAWS
NASA\MSFC

LAWS INSTRUMENT MANAGEMENT AND CONTROL

Lockheed
Huntsville

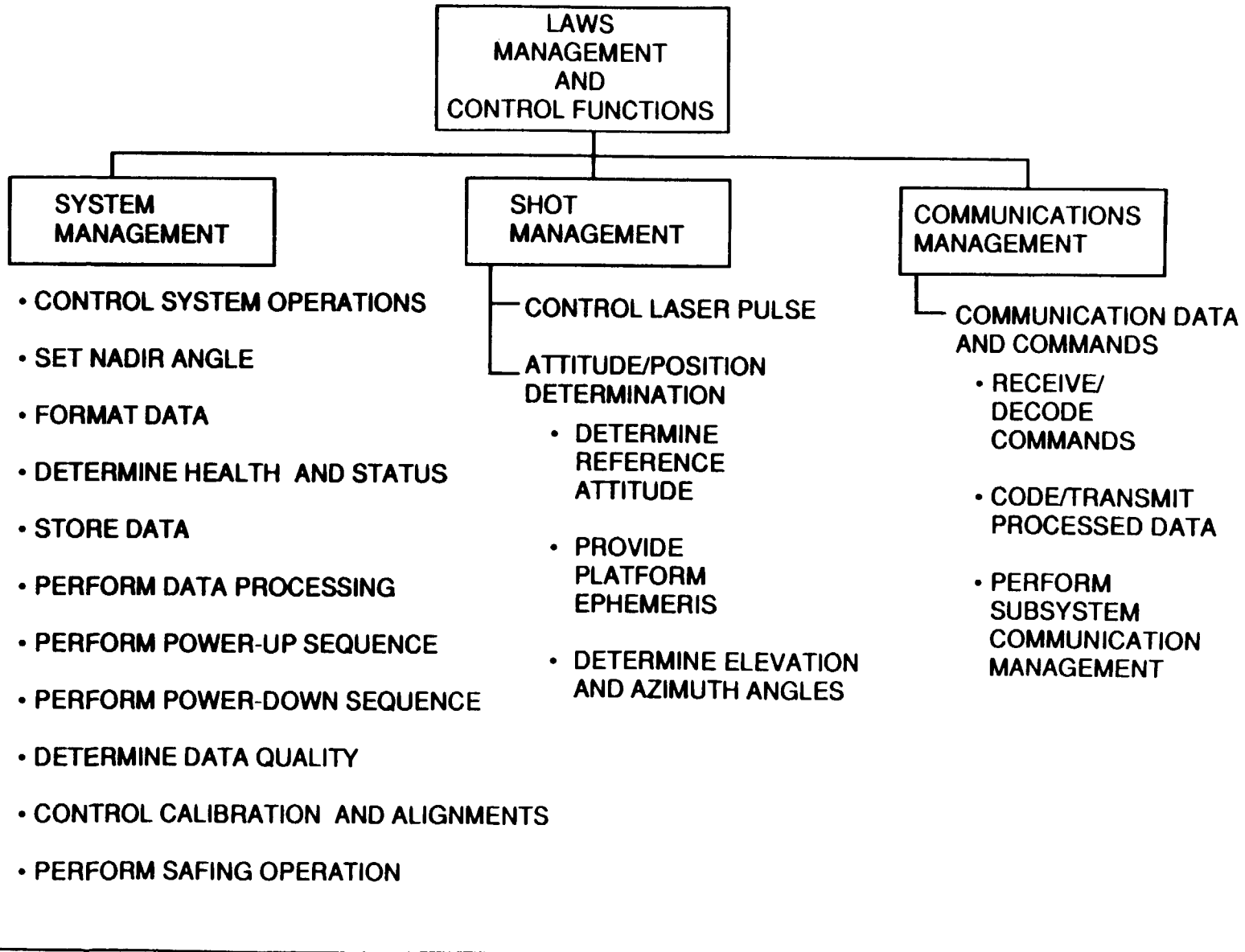

laws inst man